Comparative functional analysis of the atypical Notch ligands DLK1 and DLK2 in vertebrate development

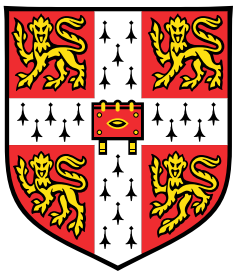

Alexandra Svarrer Ashcroft

Department of Genetics
University of Cambridge

This dissertation is submitted for the degree of
Master of Science

Downing College December 2018

Declaration

I hereby declare that dissertation is the result of my own work and includes nothing which is the outcome of work done in collaboration with others, except as specified in the text, acknowledgements, and technical support. It is not substantially the same as any that I have submitted, or, is being concurrently submitted for a degree or diploma or other qualification at the University of Cambridge or any other University or similar institution except as declared in the Preface and specified in the text. I further state that no substantial part of my dissertation has already been submitted, or, is being concurrently submitted for any such degree, diploma or other qualification at the University of Cambridge or any other University or similar institution except as declared in the Preface and specified in the text. It does not exceed the prescribed word limit for the relevant Degree Committee.

Alexandra Svarrer Ashcroft
December 2018

Abstract

Comparative functional analysis of the atypical Notch ligands DLK1 and DLK2 in vertebrate development

Alexandra Svarrer Ashcroft

DLK1 and DLK2 are vertebrate specific non-canonical Notch ligands. Dlk1 is imprinted throughout murine development [76] but selectively loses its imprint in the postnatal neurogenic niche by an unknown mechanism [78]. Possessing both secreted and membrane-tethered isoforms[212, 211], DLK1 plays critical roles in a wide range of developmental processes and is implicated in several diseases, including obesity and cancer[35, 241].Apart from a few exceptions[78], in the majority of processes, the precise roles and relative contributions of membrane-bound and secreted DLK1 are unknown . DLK2 is a related gene with homology to DLK1 [108, 49]; however virtually nothing is known about it. Preliminary data from the Ferguson-Smith lab suggests that it is involved in neurogenesis in the Zebrafish. This project investigates the role that DLK2 plays in wild-type mice and compares the gene to DLK1.

Technical Support

During the duration of this project I was plagued with ill health that made the execution of experiments, including pipetting, physically challenging. I am extremely grateful to the following people for the technical assistance they provided me during my experiments. Jennifer Corish maintained the *Dlk1*-/- mouse line and assisted me with mouse dissections and parts of various other experiments including RNA extraction, cDNA synthesis, and *in situ* hybridisations. Frances Dearden also assisted me with dissections and overall maintenance of the *Dlk2* mutant colonies, including Schedule 1, ear notching, and occasionally helping with postnatal weight acquisitions. Dr. Celia Delahaye designed and synthesised the gRNAs used in the second CRISPR attempt. She also genotyped the founder animals. Dr. Carol Edwards calculated the Ka/Ks values and evolutionary distances for DLK1 and DLK2 used in the bioinformatic analysis. Dr. Mitsu Ito assisted with the genotyping of the first CRISPR mutants. Erin Slatery also assisted with genotyping. Finally, William Watkinson also provided me with much assistance: he helped me with dissections and genotyping, including cutting the bands out of agarose gels. He also assisted me with qPCR and with maintaining the *Dlk2* mutant mouse colonies, including Schedule 1, ear notching, and occasionally helping with postnatal weight acquisitions.

Acknowledgements

I am extremely grateful for all of the help and support given to me for the duration of this project. My supervisor, advisor, programme coordinators, colleges, and family members created a fantastic network without which I do not believe this project would have been possible.

My supervisor, Professor Anne Ferguson-Smith, has provided extensive supportive, both pastorally and intellectually. She has always had my best interests at heart and I am extremely grateful for her patience and kindness, especially regarding management of my physical and mental health. Professor Steve Russell and Dr Clare Baker, my advisor and programme coordinator respectively, have also provided a lot of pastoral support. I am very grateful for their assistance in finding the best way to achieve my academic goals.

As I outlined in the technical support section, I have received a large amount of help with the technical aspects of the experiments made challenging by the illness I developed. The Ferguson-Smith laboratory is a fantastic place to work as everyone is extremely supportive, generous, and kind. Beyond the technical support I have received a significant amount of teaching from various lab members; notably Dr. Carol Edwards, Dr. Mitsu Ito, Dr. Nozomi Takahashi, and Dionne Gray. I am very grateful for their patience and time.

Finally, I owe a great deal of thanks to my family. My husband, Eric Seckler, parents, Marianne and Charles Ashcroft, and aunt, Frances Ashcroft, have been particularly great. They have always been there with kind words, encouragement, and fantastic hugs.

Table of contents

List of figures

List of tables

Nomenclature

$18s$	18s ribosomal RNA
$2900026A02-RIK$	2900026A02 RIKEN cDNA
μg	Microgram
μl	Microlitre
aa	Amino acid
$ADAM10$	Metallopeptidase Domain 10
$ADAMTS13$	ADAM metallopeptidase with thrombospondin type 1 motif 13
AFS	Anne Ferguson Smith
AKT	RAC-alpha serine/threonine-protein inase
Amp	Ampicillin
$ANOVA$	Analysis of Variance
ATP	Adenosine triphosphate
BAC	Bacterial Artificial Chromosome
$BLAST$	Basic Local Alignment Search Tool
$BLAT$	BLAST-like alignment tool
bp	base pair
BSA	Bovine Serum Albumin
C	Cytosine
$CAVIN2$	Caveolae-associated protein 2
$cDNA$	Complementary Deoxyribonucleic Acid

CFR	Cysteine-rich FGF Receptor
ClustalO	Clustal Omega
*CRB*1	Crumbs 1, Cell Polarity Complex Component
CRISPR	Clustered regularly interspaced short palindromic repeats
*CYR*61	Cysteine Rich Angiogenic Inducer 61
DelA	*Delta A*
DelD	*Delta D*
DEPC	Diethylpyrocarbonate
DEXA	Dual Energy X-ray Absorptiometry
DIG	Digoxigenin
*DIO*3	Iodothyronine Deiodinase 3
*DK*13	13bp deletion in exon 5 of *Dlk2*
*DK*16	16bp deletion in exon 3 of *Dlk2*
*DK*1*C*	Insertion of 1C into exon 3 of *Dlk2*
*DK*1*G*	Insertion of IG into exon 3 of *Dlk2*
*DK*73	73bp deletion in exon 5 of *Dlk2*
*DLK*1	Delta like homolog 1
*DLK*1	Delta like homolog 1
$DLK1-Fc$	DLK1-Fc chimeric fusion protein
*DLK*2	Delta-like homologue 2
*DLL*1	Delta like 1
DNA	Deoxyribonucleic Acid
DNase	Deoxyribonuclease
DOS	Delta and OSM-11

dpf	days post fertilization
DPX	Distyrene, plasticizer, and xylene
DSL	Delta-Serrate-Lag2
E	Embryonic day (of mouse development)
EDTA	Ethylenediamine Tetraacetic Acid
EGF	Epidermal Growth Factor like repeat
ENCODE	Encyclopedia of DNA Elements
ERK	Extracellular Signalregulated Kinases
F	Generation
*FANTOM*5	Functional Annotation of the Mammalian Genome
*FBXO*44	F-Box Protein 44
*FBXO*6	F-Box Protein 6
*FGF*18	Fibroblast Growth Factor 18
FSH	Follicle Stimulating Hormone
G	Guanine
g	Gram
GDP	Guanosine diphosphate
GFAP	Glial Fibrillary Acidic Protein
GH	Growth hormone
*GM*128	Predicted gene 128
GnRG	Gonadotrophin Releasing Hormone
gRNA	Guide Ribonucleic Acid
GT	Genotyping
*GTL*2	Maternally expressed 3

GWAS	Genome Wide Association Study
h.p.f	Hours post fertilization
*HES*5	Class B Basic Helix-Loop-Helix Protein 38
IG − DMR	Intergenic differentially methylated region
*IGF*1	Insulin Like Growth Factor 1
*ILDR*2	Immunoglobulin Like Domain Containing Receptor 2
INDEL	Insertion and deletion
*IRAK*1	Interleukin-1 Receptor-associated Kinase 1
ISH	*In situ* hybridization
Ka	The number of nonsynonymous substitutions per non-synonymous site
*KAP*1	Tripartite motif-containing 28
kb	Kilobase
KCl	Potassium Chloride
*KDM*4*D*	Lysine Demethylase 4D
KI	Knock-in
*KLF*4	gut-enriched Kruppel-like factor
KO	Knockout
Ks	The number of synonymous substitutions per synonymous site
L	Litres
LB	Lysogeny broth
LH	Luteinizing Hormone
*LNX*2	Ligand Of Numb-Protein X 2
*LRRC*24	Leucine Rich Repeat Containing 24
M	Molar

$M-DLK1$	Membrane bound delta like homolog 1
MAP	Mitogen-activated protein
$MARCKSL1$	MARCKS Like 1
MAT	Maternally inherited chromosome
MF	Myofibers
mg	Milligrams
$MgCl2$	Magnesium Chloride
$mi-RNA$	Micro Ribonucleic Acid
$miR-126-5p$	miRNA 126-5p
$MIRG$	Maternally expressed 9
ml	Millilitres
MM	Mismatches
mM	Milli Molar
MNB	Mindbomb
MRC	Medical research council
MRI	Magnetic Resonance Imaging
$mRNA$	Messenger Ribonucleic Acid
MS	Multiple Sclerosis
$mUPD14$	Maternal Uniparental Disomy of chromosome 14
N	Generation backcrossed (mouse)
$NaCl$	Sodium Chloride
$NaOH$	Sodium Hydroxide
$NARFL$	Cytosolic Fe-S cluster assembly factor NARFL
$NBP/BCIP$	Nitro-blue tetrazolium chloride/5-bromo-4-chloro-3-indolylphosphate

NCBI	National Center for Biotechnology Information
NFκ*B*	Nuclear Factor Kappa-light-chain-enhancer of activated B cells
NFASC	Neurofascin
ng	Nanograms
NTMT	NaCl, Tris-HCl, MgCl2, Tween-20
NTP	Nucleotide
p	Postnatal day (of mouse development)
PAM	Protospacer adjacent motif
PAT	Paternally inherited chromosome
PBS	Phosphate Buffered Saline
PCR	Polymerase Chain Reaction
PFA	Paraformaldehyde
PLVB	Primordium of the lumbar vertebral body
*POGLUT*1	Protein O-Glucosyltransferase 1
qPCR	Quantitative Polymerase Chain Reaction
RNA	Ribonucleic Acid
$RNA-seq$	RNA sequencing
RNase	Ribonuclease
*RTL*1	Retrotransposon like 1
rtPCR	Reverse Transcriptase Polymerase Chain Reaction
$S-DLK1$	Soluble delta like homolog 1
*SCAMP*4	Secretory Carrier Membrane Protein 4
*SCL*17*A*7	Vesicular glutamate transporter 1
SD	Standard deviation

*SENP*6	SUMO Specific Peptidase 6
SLY	*Sytherin*
snoRNA	Small nucleolar Ribonucleic Acid
SNP	Single nucleotide polymorphism
SOC	Super Optimal broth with Catabolite repression
*Sox*9	Transcription factor Sox-9-A
*SpCas*9	*Streptococcus pyogenes* Cas9
SPTMP	Single pass type I membrane protein
SSC	Saline-Sodium Citrate
STRING	Search Tool for the Retrieval of Interacting Genes/Proteins
*SYNE*2	Nesprin-2
SYNM	Synemin
TACE	Tumour necrosis factor-alpha converting enzyme
Taq	Thermostable DNA (polymerase)
TBE	Tris/Borate/EDTA
TBP	TATA box binding protein
TM	Transmembrane
tRNA	Transfer ribonucleic acid
UCSC	University of California, Santa Cruz
UV	Ultraviolet
V	Version (software)
VIVO	Verification of *In Vivo* Off-targets
*WNT*10*b*	Wingless/Integrated 10b
WT	Wild type

1 Introduction

1.1 Protein structures of DLK1 and DLK2

Protein delta-like homolog 1 (*Dlk1*) was discovered three independent times in 1993 [106, 129, 213] and is a vertebrate-specific member of the Jagged/Delta/Serrate family of NOTCH ligands [129]. Less is known about protein delta-like homolog 2 (*Dlk2*), first sequenced in 1998 [108], despite relatively high (protein) sequence conservation between the genes across multiple species.

The overall folded structure of both genes is still unknown; no structural studies have been carried out on DLK2 and despite a preliminary analysis of the structure of DLK1 [127], it has yet to be purified. Although the protein model portal provides homology models for both genes, the models are based on experimentally verified structures with less than 60% sequence homology [91]. These probably unreliable structures compound the challenge of elucidating the genes' already complicated signalling mechanisms (section 1.6). Nevertheless, key domains can be inferred from the gene sequences (table 1.1), emphasising the similarity between the two proteins.

Structural component	**DLK1**	**DLK2**	**References**
Chromosome	12	17	[113]
Protein length (aa)	385	382	[227]
Mass (Da)	41320	40404	[227]
Protein type	SPTMP	SPTMP	[227]
EGF domains	6	6	[207, 212, 211, 247]
Cleavage domain	Exc. isoforms C, C2, D & D2	e.u.	[113, 207]
Calcium binding domains	n.p.	2	[207, 227]
Motifs	Asn-Xaa-Cys	n.p.	[127, 227]

Table 1.1 (continued)

Structural component	DLK1	DLK2	References
N-linked glycoslyation (at)	100, 165 (p), 174 (a), 295 (pd)	157	[127]
O-linked glycosylation	94, 126, 224, 258, 267 (p), 271	n.p.	[227]
Predicted phosphorylation (at aa)	262, 264, 357	47, 316	[25]
Disulphide bonds	18	17	[207, 227]

Table 1.1 **Comparison of structural domains present in DLK1 and DLK2 in mice**

Acronyms used: *a — atypical, aa — amino acid, EGF — epidermal groth factor like repeat, e.u. — experimentally unvalidated, Exc. — excluding, n.p. — none predicted, p — partial, pd — predicted, SPTMP — single pass type I membrane protein*

DLK1 and DLK2 are transmembrane proteins. As is typical of proteins in the Delta family, they contain a series of Epidermal Growth Factor (EGF)-like repeats (figure 1.1). Although both DLK1 and DLK2 contain six of these tandemly repeated EGF-like motifs in mice, they lack the conserved residues thought to be required for binding to EGF receptors [129]. Instead, the two most N-terminal EGF-like repeats of the DLK genes are a conserved DOS Delta and OSM-11 motif, shared by classical Notch ligands [122]. Crucially both genes also have short intracellular domains and lack Delta/Serrate/LAG-2 (DSL) domains, present in canonical Notch ligands [122]. Notch ligands are believed to activate Notch through the DSL domain [65]. The absence of a DSL domain suggests that DLK genes interact with Notch in an atypical manner (section 1.6).

Both DLK1 and DLK2 contain a juxtamembrane motif (figure 1.1), in all species except zebrafish that lacks the cleavage domain in *Dlk1*. Experiments on cell lines demonstrated that tumour necrosis factor-alpha converting enzyme (TACE) can cleave the juxtamembrane domain of DLK1 to produce a soluble protein (S-DLK1) [247]. Reports of S-DLK1 *in vivo* [95] suggest that cleavage of DLK1, probably by TACE, is a real, physiologically relevant phenomenon. However, there is no experimental evidence to support or refute cleavage of DLK2. Indeed, whether the cleavage domain is contained in the final mRNA transcript of any species is still unverified. Immunohistological experiments in zebrafish, the only model organism in which DLK2 protein has been characterised, cannot determine whether a soluble

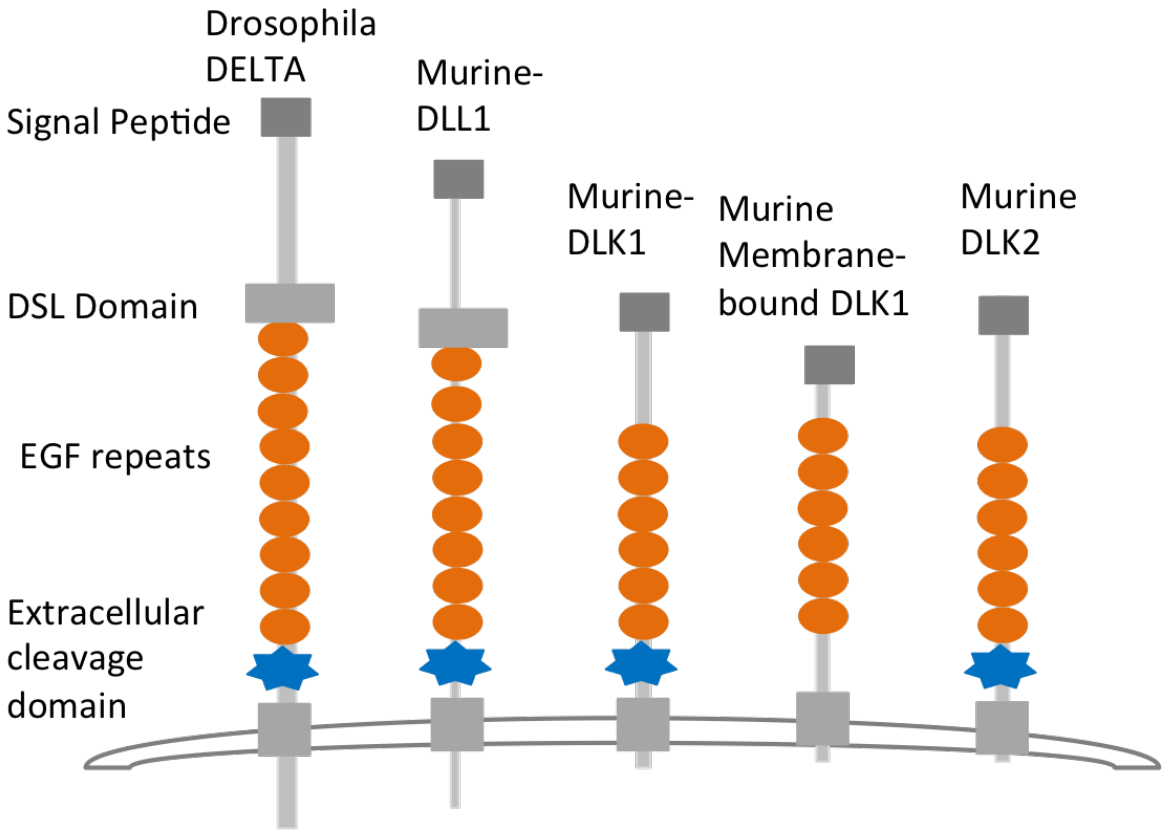

Fig. 1.1 **Structures of murine DLK1, DLK2, and DLL1 compared to the structure of *Drosophila melanganster* DELTA** *Not to scale*
DLK1 and DLK2 are single pass transmembrane proteins with short intracellular domains significantly shorter than those of their homologues DLL1 and DELTA. All proteins contain various numbers of epidermal growth factor repeats, with DLK1 and DLK2 each possessing 6 in mice. Both genes retain the complete suite of EGF repeats in all species studied thus far. DLK1 and DLK2 do not have Delta/Serrate/LAG-2 (DSL) domains. DLK1 makes isoforms possessing and lacking the extracellular cleavage domain in mice but nothing is known about DLK2 isoforms and whether they retain or excise the cleavage domain. All studied vertebrate species with DLK1 possess the cleavage domain in their amino acid sequence, except zebrafish. Zebrafish do however possess the cleavage domain sequence for DLK2.

isoform of DLK2 (S-DLK2) exists (PhD thesis, Dr. Ben Shaw, University of Cambridge (2017)).

Information on *Dlk1* transcripts is much more robust. Alternative splicing creates transcripts encoding at least six different DLK1 isoforms, producing membrane-bound (M-DLK1) and soluble forms of the protein [212, 211] in eutherian mammals. Isoforms A and B, encoding S-DLK1, contain the protein cleavage domain whereas spliceoforms C, C2, D and D2, encoding M-DLK1, lack the juxtamembrane domain, are not cleaved and remain tethered to the cell membrane [211]. Both isoforms have been reported to play distinct developmental roles in mice [78, 150]. The number of alternative *Dlk1* spliceoforms varies between species; expression of various *Dlk1* isoforms has been detected in pigs [57], cows [242], sheep [54], chickens [205], quails [205], turkeys [205], and even opossums [250]. Full-length *Dlk1* is believed to be the dominant isoform expressed in humans but this is difficult to verify experimentally as most publications appear to ignore isoforms when investigating DLK1 in humans.

1.2 Evolution of DLK1 and DLK2

Duplication events of the prototypical Notch ligand Delta ultimately resulted in the DLK genes (figure 1.2). Delta-like originally arose from the duplication of Delta at some point before the divergence of *Ciona intestinalis* from the rest of the chordate lineages. A subsequent duplication, early on in the vertebrate lineage, produced DLK1 and DLK2 (pers. comm. Dr. Carol Edwards). Although it is unclear when such duplication event occurred, it most likely happened during one of the vertebrate genome duplication events [56].

1.2.1 Imprinting of DLK1

Supporting the hypothesis that *Dlk1* is more evolutionarily dynamic than *Dlk2*, is the unique behaviour of *Dlk1* in eutherian mammals: genomic imprinting [119, 223]. Imprinted genes are expressed in a parental-origin specific manner, and many map in clusters [187]. Some imprinted genes may therefore be expressed exclusively from the paternally-inherited chromosome and others from the maternally inherited chromosome [77]. All work to date on *Dlk2* indicates that it is not imprinted in mice; for example, no study has identified it in any

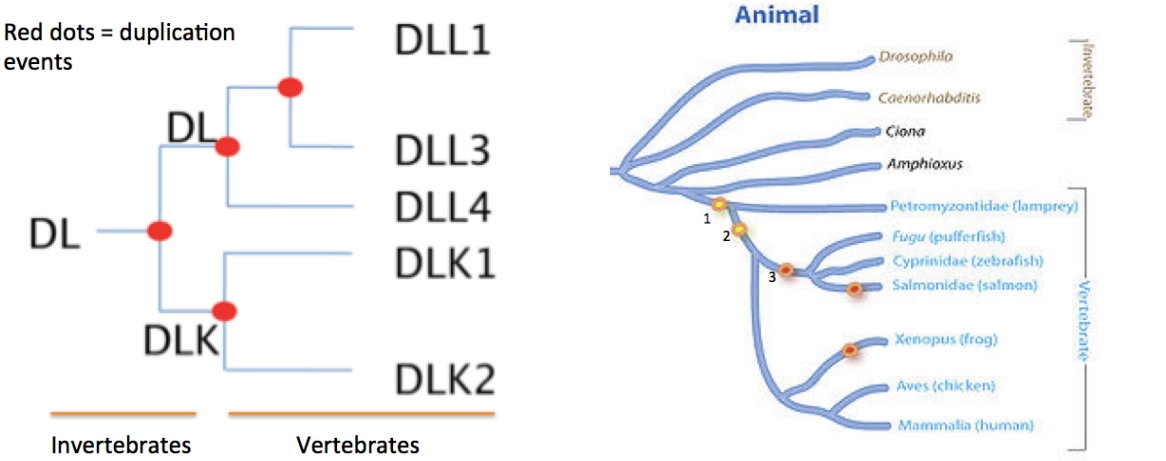

(a) Duplication of DLK1 and DLK2

(b) Vertebrate specific whole genome duplication events

Fig. 1.2 **Duplication of atypical Notch ligands DLK1 and DLK2 (Delta-like homologues 1 and 2) from canonical Notch ligand DL (Delta).**
Duplication likely occurred during one of the early vertebrate specific whole genome duplication events (coloured dots in b) although it is difficult to give an exact time. Figure a shows that vertebrate specific canonical notch ligands DLL1-3 (Delta like 1-3) also arose from duplication events of Delta. Both figures adapted from Carol Edwards.

screen for imprinted genes [21, 155, 174, 220].

Dlk1 resides within the imprinted delta-like homolog 1 and type III iodothyronine deiodinase (*Dlk1-Dio3*) cluster in mammals (figure 1.3), spanning 1.3Mb on mouse chromosome 12. *Dlk1* is not imprinted in avian species [205], fish and non-eutherian mammals [68] although expression of the gene has been observed in all vertebrates in which experimental analysis of *Dlk1* expression has been performed.

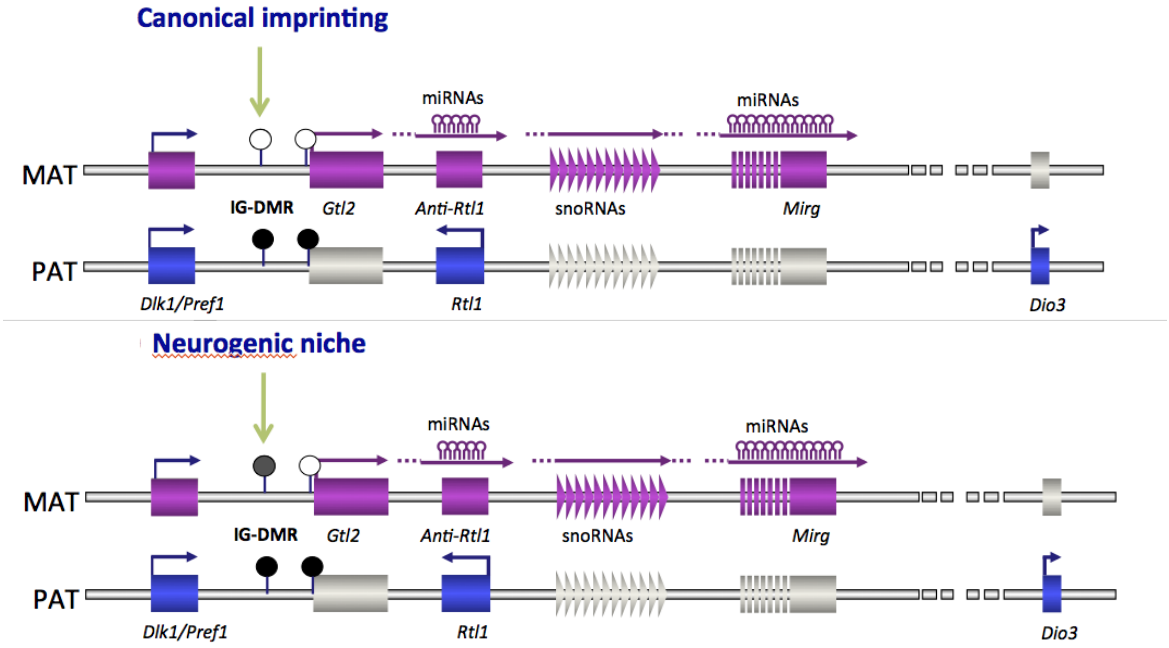

Fig. 1.3 **Schematic of the imprinted *Dlk1-Dio3* cluster on mouse chromosome 12** *Dlk1*, *Rtl1* and *Dio3* are protein coding genes that are expressed only from the paternally inherited chromosome (PAT). Multiple noncoding RNA (ncRNA) genes, including microRNAs (miRNAs) and small nucleolar RNAs (snoRNAs), are expressed exclusively from the maternally inherited chromosome (MAT). This imprinting is regulated by the intergenic DMR (IG-DMR), an intergenic element between *Dlk1* and *Gtl2* that causes the protein-coding genes to be repressed on the maternal chromosome and the ncRNAs to be active. The *Dlk1-Dio3* cluster is only methylated at the IG-DMR (intergenic differentially methylated region) on the paternal chromosome (PAT) under normal conditions. In the postnatal neurogenic niche, there is methylation of the IG-DMR on the maternal chromosome and maternal expression of *Dlk1*. Arrows indicate the direction of transcription. The cluster is syntenic to human chromosome 14. Figure adapted from Prof. Anne Ferguson-Smith.

In mammals, *Dlk1* is expressed predominantly from the paternally inherited allele. The intergenic differentially methylated region (IG-DMR) regulates gene expression within this

cluster. The IG-DMR is methylated on the paternal chromosome allowing expression of protein coding genes *Dlk1*, *Rtl1* and *Dio3* [67, 140]. Absence of methylation at the IG-DMR, on the maternal chromosome, leads to repression of these genes and expression of a plethora of non-coding RNAs [34, 199, 201].

Consistent with other clusters, the *Dlk1-Dio3* cluster acquires its imprint in the germ-line [187] and *Dlk1* is imprinted throughout embryogenesis at the gross level. After fertilisation, ZFP57, initially maternally derived, binds to the methylated IG-DMR [139, 220] in the zygote, protecting it from the global reprogramming of epigenetic marks that occurs very early in embryogenesis. KAP1/TRIM28 is also important for this process [13]. The importance of imprinting at this cluster in development is epitomised by the severe phenotypes associated with alterations of dosage of these genes [45, 187].

In addition to cluster level regulation of *Dlk1* expression, it is emerging that there is gene specific regulation of imprinting and expression, at least in mice. The postnatal neurogenic niche selectively loses imprinting solely of *Dlk1*shortly after birth, giving rise to bi-allelic gene expression [78] (figure 1.3). The consequential increase dosage of protein product is necessary for niche maintenance [78]. Selective loss of imprinting of one gene within a given cluster has been observed in additional clusters [79]. The mechanisms responsible for this remain poorly understood but are likely epigenetically regulated. Nevertheless increased dosage of a given gene, through selective absence of imprinting of it but not other genes gives further evidence into the importance of dosage regulation of imprinted genes.

1.3 Expression patterns of DLK genes

Dlk1: *In situ* hybridisations (ISHs) generally suggest that *Dlk1* is widely expressed in particular lineages throughout the developing embryo and may, amongst many other things, mark sites of branching morphogenesis [52, 69, 256]. With the exception of the postnatal neurogenic niche [78], quantitative isoform-specific, tissue-specific expression analysis has not been performed. In general, *Dlk1* RNA-seq data, which can be more sensitive but has lower resolution at the cellular level, is consistent with the expression patterns observed by ISHs. However, there is some variability within the public transcriptomes, consistent with their automated production and absence of validation. Overall, the protein localization for DLK1 is consistent with the mRNA expression studies [52, 256].

Dlk2: There is no reliable expression data, mRNA or protein, for DLK2, in part, due to the absence of a DLK2 antibody. For example, Eurexpress, a high-throughput ISH database, detected *Dlk2* in the brain and spinal-cord at embryonic-day 14.5 (e14.5) with high background staining [61]. However, the Allen Brain Atlas did not detect any *Dlk2* expression in the brain at any embryonic stage but did detect expression in the adult mouse brain [221]. Reverse-transcriptase polymerase-chain-reaction (rt-PCR) detected expression in a wide range of adult and foetal tissues, although the study did not state the age of the developing tissues [186]. *Dlk2* expression is extremely 'noisy' in RNA-seq databases, such as ENCODE [48] and FANTOM5 [142]. Collectively these datasets highlight the unreliability of high throughput databases for accurate expression information and the difficulty in determining where *Dlk2* is expressed without robust independent experimental analysis.

1.4 Functions of DLK1

It is challenging to elucidate the role of DLK1 for several reasons. Firstly, insights into DLK1 protein function come from a series of different cell lines and organisms. Evidence suggests that DLK1 is more evolutionarily dynamic than DLK2 (section 1.2); which means that DLK1 may have been co-opted to play different roles in different organisms. The imprinting of *Dlk1* in eutherian mammals is particularly supportive of this hypothesis as many imprinted genes have functions co-opted to help mammals transition to independent life, a significant challenge that is unique to mammalian organisms [36].

In addition, DLK1 can behave as a paracrine, endocrine and autocrine factor in most organisms. The potential interactions between these behaviours are perhaps the most challenging barrier to revealing the function of the gene. Consideration of DLK1 isoforms, and their potential signalling mechanisms, is especially important as work on neurospheres has demonstrated that S-DLK1 and M-DLK1 can interact with each other [78]. Furthermore, S-DLK1 can be detected in mouse serum and is likely produced by a variety of sources. How then can one be sure that circulating S-DLK1 is not acting on a tissue in which DLK1 has been selectively knocked out? There is evidence of this occurring when *Dlk1* is selectively removed in skeletal muscle in mice [243]. Additional weak phenotypes observed in a series of tissue specific DLK1 knock-out experiments [18, 243] may also have arisen because of S-DLK1 acting in an endocrine manner to mitigate a severe phenotype.

Elucidating the relationship between M-DLK1 and S-DLK1, receptor-ligand interactions, and the signalling pathways of different isoforms is thus essential to developing a robust understanding of DLK1 function. This will be difficult. Although a well-designed cell line experiment can take account of DLK1 isoforms, cell lines may not sufficiently model the *in vivo* context. However, deciphering the isoform specific functions *in vivo* in mouse models is difficult as it is challenging to modulate the different isoforms separately as they are expressed from the same gene locus.

Despite the described caveats, significant strides towards understanding the role of DLK1 have been made, particularly in mammals. The gene is implicated in many prenatal and postnatal processes, such as wound healing [64, 191, 188] and metabolism [35, 44]. It is also very clear that DLK1 plays a role as a stem cell regulator (discussed in section 1.4.1); it is likely that this is the ancestral function of the gene and is shared across all species. Mammalian (section 1.4.3) and avian (section 1.4.2) specific roles are also emerging. Although the precise contributions of the different isoforms remain mainly uncharacterised, our understanding of mammalian DLK1 function is the most comprehensive.

1.4.1 DLK1 as a stem cell regulator

A significant number of, predominantly mammalian, studies suggest that DLK1 functions as a stem cell regulator. Overall, DLK1 is believed to maintain progenitor cell pluripotency until it is appropriate for their differentiation. *In vivo* and *in vitro* studies found that DLK1 negatively regulates the switch from proliferating cells to a mature differentiated state in ameloblasts [178], DPCs [177], adult neural stem cells [78], immature chondrocytes [41, 248], osteoblasts [7, 6], hematopoietic-stem-cells [138, 152, 160, 168], hepatoblasts [153, 225], myoblasts [206], and preadipocytes [4, 18, 116, 158, 162, 213] in various mammals. A comprehensive analysis of all niches is beyond the scope of this thesis. However, some informative niches will be discussed below.

Where studied, the same stem cell regulatory behaviour has been observed in birds [204] and zebrafish [188]. In addition, where investigated *Dlk1* gains selective biallelic expression in adult mammalian stem cell pools [78, 217], suggesting that normal biallelic expression of DLK1 is necessary for the function of this gene as a stem cell regulator. *Dlk1* is not imprinted in birds [205] or fish [68]; in non-eutherian vertebrate species the gene will always show biallelic dosage when expressed. It is likely therefore that maintenance of progenitor pluripotency might be the ancestral function of DLK1, requiring biallelic gene dosage. The

breadth of mammalian tissues in which DLK1 functions as a stem cell regulator is further circumstantial evidence that supports this argument. However, investigation into the function of DLK1 in other non-eutherian vertebrates and imprinting patterns of *Dlk1* in other stem cell pools in mice will be necessary to probe this hypothesis.

Adipogenesis

No review of *Dlk1* is complete without discussing its role in adipogenesis. Its role in adipogenesis is perhaps the best characterised of any of its behaviours. Indeed, the gene is also known as preadipocyte factor 1 (*Pref*-1). Most research suggests that DLK1 inhibits adipogenesis of white [4, 18, 116, 158, 162, 213] and brown fat [19, 96, 37]. DLK1 expression is high in preadipocytes and abolished in adipocytes in both white [213] and brown adipose [209]. Furthermore overexpression of retinoic acid by preadipocytes inhibits adipogenesis in mice through upregulation of DLK1 [26]. In addition, endothelial stromal cells, located in adipose tissue, also have markedly high DLK1 levels [15], and there is some evidence that expression of DLK1 by stromal cells may also inhibit adipogenesis [8, 24, 248]. The accepted interpretation of this data is that DLK1 inhibits differentiation of pre-adipocytes. This is consistent with the behaviour of the gene in other progenitor cells (section 1.4.1) and fits the hypothesis that stem cell regulation is the ancestral function. However, this data could be interpreted another way.

Recent work suggests DLK1 may drive lipid metabolism, and that increased lipolysis is misinterpreted as inhibition of adipogenesis [35]. Given the number of tissues in which DLK1 seems to function as a stem cell regulator, this other hypothesis is sometimes ignored in support of the original conventional hypothesis of DLK1 function in adipogenesis. However, the two hypotheses are not mutually exclusive. DLK1 does probably function as a stem cell regulator in pre-adipocytes. Since stem cell regulation is likely the ancestral function of the gene, it is doubtful that this behaviour would have been lost in only one stem cell niche. Nevertheless, DLK1 displays autocrine, paracrine, and endocrine behaviours (section 1.6); with the latter most likely involved in the mammalian specific metabolic roles of *Dlk1* (section 1.4.3). Adipose tissue is tightly regulated and an integral part of whole body metabolism. It is unsurprising that additional mammalian specific endocrine gene functions might also be detected when studying this tissue, especially as it almost exclusively studied in mammalian models.

Neurogenesis

DLK1 also plays a role in adult neurogenesis but is dispensable for embryonic neurogenesis [78]. Interestingly *Dlk1* is not imprinted postnatally in adult murine neurogenic niches suggesting that DLK1 dosage is critical in this process [78]. This is the only study that investigates the function and imprinting status of this gene together. Other studies have detected biallelic expression of *Dlk1* in stem cell niches [217], or observed its role in stem cell regulation [7, 4, 6, 18, 41, 116, 138, 152, 153, 158, 160, 162, 168, 177, 206, 213, 225, 248].

This study also provides interesting insights into *Dlk1* signalling (section 1.6) S-DLK1 is secreted by niche astrocytes and M-DLK1 is present in neural stem-cells. Both the soluble and membrane-bound forms of DLK1 are necessary for neural stem-cell self-renewal: S-DLK1 induces renewal via membrane-bound DLK1 [78].

1.4.2 DLK1 avian neofunctionalism

Only a very small portion of the work on *Dlk1* has been performed on birds. Most of it focuses on sequencing different isoforms [205], confirming expression [205] and identifying the stem cell regulatory in behaviour in avian myoblasts [204] (discussed in section 1.4.1). None of which is specific to birds, nor particularly novel. Nevertheless, this research does contribute to our overarching understanding of *Dlk1* as it supports the hypothesis that the role *Dlk1* plays in stem cell regulation is an ancestral one. A recent study, however, has identified that *Dlk1* may play a role in the adaptive radiation of beak size in Darwin's finches [40].

During adaptive radiation organisms rapidly diversify from a single common ancestral species into a plethora of new forms [195]. Adaptive radiation often occurs when changes in the environment create new evolutionary challenges or make new resources available [195]. The speciation of Darwin's finches, of the genus Geospiza, is considered the prototypical example of adaptive radiation [195]. Currently 23 branches, consisting of 14 distinct species living in various Galapagos islands, are recognised for finch speciation [130].

The study looked three sympatric species of ground finches located on the same island as investigating on-going speciation will generate greater insights into adaptive radiation than studying well established lineages. They found that a single nucleotide polymorphism (SNP), located near *Dlk1*, was strongly associated with beak size and, to a lesser extent, body size [40]. Another studying investigating beak size across the entire clade also predicted *Dlk1* as

playing a role [130].

The observation that different *Dlk1* variants or alleles are predictive of different phenotypic outcomes in finches is exciting. The role of the gene in beak size may be an example of avian neofunctionalism – beaks are a trait specific to the avian clade. However, this may also simply be a reflection of the its role as a stem cell regulator. Different *Dlk1* variants have different activity levels that dictate its ability to modulate differentiation of stem cells, which, in turn, affects the gross phenotypic outcome of a given organ. The latter hypothesis may be the more likely as a mild association was also observed between *Dlk1* and body size [40]. Modulations to *Dlk1* dosage, in mice, also affect body size (section 1.4.3).

1.4.3 DLK1 neofunctionalism in eutherian mammals

Dlk1 evolved its imprinting in eutherian mammals [68], suggesting that dosage of this gene is highly important for its function. Although biallelic gene expression may be necessary for *Dlk1* to function as a stem cell regulator (section 1.4.1), alterations to *Dlk1* dosage at the gross level, in mice, result in severe phenotypes (section 1.4.3). This may suggest that phenotypes resulting from altering monoallelic gene dosage, may be due to functions that co-evolved with imprinting and are thus specific to eutherian mammals. Such functions are likely to be related to mammalian specific phenomena such as placentation (section 1.4.3) and puberty (section 1.4.3). Furthermore, metabolism is highly important in mammals: a key process in the transition of a mammalian organism to independent life is shift from lipolytic to lipogenic metabolism [**?**]. This shift allows the digestion of solid food and the storing of excess energy as fat [**?**].

Insights from *Dlk1* mutant mice

Given the wide expression of *Dlk1* throughout development (section 1.3) and its function as a stem cell regulator (section 1.4.1), it is worth noting that knocking out *Dlk1* causes a partially penetrant neonatal lethality on some genetic backgrounds but not on others. Deletion of exons 2-3 caused approximately 50% neonatal lethality on the C57BL/6J and genetic backgrounds [158]. The mutant generated by the Schmidt group lacks exons 5-6 and displays 25% lethality on a C57BL/6J background [18]. The Bauer group removed the promoter and exons one to three; their mice show minimal lethality in the C57BL/6J mouse strain [181]. *Dlk1* therefore, is clearly not an essential gene. Given the high sequence homology between *Dlk1* and *Dlk2* (section 1.1), *Dlk2* may be playing a compensatory role in the *Dlk1* mutants.

Only the study of mice carrying deletions of both genes would resolve this.

The surviving *Dlk1*-null mice have mild phenotypes. All mutants are growth retarded [18, 42, 158, 181]. Comparison of mutant and wild-type embryo weights, demonstrated that the *Dlk1*-null growth phenotype does not arise until late gestation at e18.5 [18, 42]. Overall, however, the gross morphological effects of losing *Dlk1* are not as dramatic as might be expected.

Overexpressing DLK1 seems to be more detrimental than deleting the gene. Tripling DLK1 dosage is lethal from e16 and despite an initial prenatal growth advantage [51]. These mice have oedema, and lung and skeletal defects [51]. Simply doubling DLK1 dosage causes developmental overgrowth and is lethal in the perinatal period in some but not all offspring [51].

The role of *Dlk1* in placentation

DLK1 likely plays a key role in placenta function. It is expressed in the endothelial cells of the foetal capillaries labyrinth zone and a subset of trophoblast cells [27, 256]. Labyrinth zone vasculature production of DLK1 is thought to regulate embryonic growth through paracrine signalling [18]. Loss of expression of *Dlk1* leads to a reduction in labyrinth zone size from late gestation [18, 158]. Placenta composition in *Dlk1* knock-out mice is also altered; the junctional zone has a decreased number of glycogen cells [18], which is surprising given that *Dlk1* expression has not been detected in junctional zone glycogen cells [52]. Abnormal glycogen cell migration occurs in uniparental disomies of chromosome 12 in mice [87]. Some researchers postulate that DLK1 is also responsible for glycogen cell migration [100] however this cannot be assessed without a placental *Dlk1* overexpression model.

The role of DLK1 in metabolism

The precise roles DLK1 plays in metabolism are unclear but are likely related to the endocrine function of the gene. Mice with alterations in DLK1 gene dosage display metabolic phenotypes [35, 158]. Since DLK1 is a tightly regulated imprinted gene and simply doubling the gene dosage to normal biallelic gene expression produces severe phenotypes [35], it is likely that the metabolic functions co-evolved with imprinting and are possibly mammalian specific.

Mice with increased gene dosage, fed a high fat diet, are leaner than wild type controls despite being hyperphagic [35]. Metabolic phenotypes are complex and difficult to resolve

but DLK1 may regulate whole body metabolism by modulating the IGF1 and growth hormone (GH) pathways. Additionally, recent work has shown that DLK1, secreted from the foetus, regulates maternal metabolic partitioning in mice [44].

Work in [explants from] mice over-expressing *Dlk1* shows that S- and M-DLK1 can inhibit insulin like growth factor 1 (IGF1) signalling in the pituitary gland [35]. In addition, over- or forced *Dlk1* expression in murine cell-lines reduces *Igf1* expression [260] but cell lines lacking insulin and IGF1 receptors show almost ablated *Dlk1* expression [28], suggesting a negative feedback loop between IGF1 and DLK1.

DLK1 is also likely involved in GH signalling. Interestingly, both mice overexpressing *Dlk1* display increased GH levels [35] and mice lacking *Dlk1* have reduced GH levels [42, 35], whereas mice with increased GH have reduced S-DLK1 levels [3]. The interaction between GH and DLK1 is clearly more complex but important as GH regulates whole body metabolism [156].

The role of DLK1 in puberty

Puberty is an essential mammalian process that marks the transition from childhood to adulthood, where individuals are capable of reproducing [10]. In humans, activation of the hypothalamic-pituitary-gonadal axis marks the onset of puberty [10]. The axis is characterised by increases in pulsatile gonadotropin-releasing hormone (GnRH) release, which, in turn, leads to secretion of luteinizing hormone (LH) and follicle stimulating hormone (FSH) from the pituitary gland [10]. Mutations in another imprinted gene, makorin RING-finger protein 3, cause central precocious puberty in humans [9], suggesting a role for imprinted genes in regulating the timing of human puberty. This is perhaps unsurprising given the over-representation of imprinted genes in processes necessary for the transition to independent life in mammals [36].

Work on humans demonstrates that DLK1 plays an important role in the age of puberty onset, although the exact nature of its role remains unclear. Genome wide association studies (GWAS) link low frequency variants of *Dlk1* with large effect sizes at age at menarche (first menstrual cycle) in females [53, 55, 70, 173], some delaying puberty by 6-9 months [55] and/or with an intriguing parent-of-origin bias [55, 173]. In addition, a male patient with an imprinting mutation in the IG-DMR, causing a predicted but experimentally unvalidated reduction in DLK1 expression, presented with precocious puberty among other clinical features [226]. Epimutations causing loss of methylation at the IG-DMR, effectively "maternalising

the paternal chromosome", and deletions of the full *Dlk1-Gtl2* imprinted gene cluster also result in early on set of puberty in humans [30]. Furthermore, maternal uniparental disomy of chromosome 14 (mUPD14) is thought to be caused by aberrant expression of genes, including DLK1, within the imprinted domain at 14q32 [109, 226]. Precocious puberty, a well documented phenotype in rare patients with mUPD14 [81, 99, 125, 224, 229], is conserved across the majority (>86% at the time of writing) of all studied cases of mUPD14 in humans [193, 105]. Perhaps the most compelling evidence for a role of DLK1 in puberty is the recent work by the Latronico group [53]. In this study they found that paternally inherited rare deletions covering the 5' UTS and first exon of *Dlk1* cause central precocious puberty [53]. The only other trait described in these patients was increased fat mass, suggesting that the other phenotypic traits observed in patients with mUPD or IG-DMR epimutations arise from aberrant expression of other genes. Together these data suggest that deletion of DLK1 is sufficient to cause early onset of puberty in humans.

Despite the compelling evidence suggesting that DLK1 helps determine puberty onset in humans, there is no mechanistic link between DLK1 function and pubertal development in any mammalian species. However, circumstantial evidence enables speculation that alternations in DLK1 levels may modulate the hypothalamic-pituitary-gonadal axis, which is essential for puberty [10]. *Dlk1* is expressed in the adult hypothalamus [53, 240]. qPCR detected *Dlk1* expression in the same hypothalamic substructure from which GnRH, an important player in puberty onset [10], is also expressed [53]. *Dlk1*-/- mice have fewer FSH-immunoreactive cells in the adult pituitary [176]. A subsequent radioimmunoassay of adult WT and *Dlk1*-/- pituitaries showed that *Dlk1*-/- pituitaries have reduced levels of all pituitary hormones, including FSH and LH [42]. Taken together, these data suggest that *Dlk1* may indirectly influence the hypothalamic-pituitary-gonadal axis and thus the age of puberty onset.

Although the supporting evidence for a mechanism by which DLK1 influences puberty onset comes from mice, no phenotypic reports of the *Dlk1* mouse models actually describe aberrant puberty onset. Perhaps a more targeted analysis of puberty is needed on the *Dlk1* mouse models to determine if DLK1 also influences the age of puberty onset in mice. Alternatively, should the link between DLK1 and the hypothalamic-pituitary-gonadal axis in mice prove unsubstantiated, it might be worth considering that the role that DLK1 plays in puberty may be human, or at least primate, specific. Puberty is a more dramatic event in the human/primate life spans compared to [66]: it lasts longer and may need to be more tightly regulated. Perhaps imprinted genes, such as DLK1, were co-opted to dynamically

regulate the process in primates, in the same way imprinted genes were co-opted to assist in the transition to independent life in mammals [68]. There is also some evidence to support this hypothesis; detailed MRIs on humans with central precocious puberty, caused by *Dlk1* deletions, show normal hypothalamic-pituitary regions [53]. DLK1 may be influencing puberty age onset in humans independently of the canonical hypothalamic-pituitary-gonadal axis.

The role of *Dlk1* in postnatal bone remodelling

Although *Dlk1* has been demonstrated to function in stem cell regulation (section 1.4.1) during embryonic chondrogenesis [41, 248], it may play a more interesting role in the postnatal skeleton. DLK1 may drive osteoclast differentiation. DLK1 activity in stromal cells activates NF-κB signaling [4, 233], ultimately increasing production of a number of pro-inflammatory osteoclast-activating cytokines [4, 170, 233, 251]. DLK1 activity has also been implicated in bone remodelling, a process that occurs throughout adulthood to maintain skeletal integrity [180]. Increasing serum DLK1 levels reduces bone mass in mice [4]. Similarly, reduction of bone-mineral density and body weight was observed in mice overexpressing *Dlk1* specifically in their osteoblasts [2]. In addition, soluble DLK1 levels and bone-mineral-density are negatively correlated in patients with anorexia nervosa [74, 75]. Furthermore, antibody based inhibition of circulating S-DLK1 prevented estrogen deficiency induced bone loss in mice [80]. Such results suggest that DLK1 enhances osteoclast activity, in an endocrine/autocrine manner, and thus drives bone reabsorption.

1.5 Functions of DLK2

Very little is known about the function and signaling of DLK2 despite high similarity to DLK1 (table 1.1). Electrical annotation by InterPro, suggests that it binds calcium ions [227], although this has yet be verified experimentally. Reliable investigation into *Dlk2* signalling pathways has yet to be performed. Some work suggests that *Dlk2* is a transcriptional target of KLF4 in preadipocytes [185], interacts with NOTCH [167, 192], and may modulate adipogenesis [166]. However such studies are conducted in cell lines and, as described in section 1.6.2, their physiological relevance is limited.

The most promising work into DLK2 gene function was carried out recently on ATDC5 cells which are typically used to investigate chondrogenesis [254]. The group found that *Dlk2* overexpression inhibited differentiation and promoted proliferation [254]. Silencing DLK2 produced the reverse phenotype [254]. Similar stem cell regulation has been observed for

Dlk1 across numerous cell types (section 1.4.1), and is thought to be the ancestral function of the gene. Given the high homology between both genes (section 1.1), it is plausible that *Dlk2* might also possess a similar function. Further *in vivo* and *in vitro* studies across many more lineages will be necessary to ascertain whether the behaviour of *Dlk2* is conserved across multiple niches or if it is an artefact of the ATDC5 cell line.

1.6 Known mechanisms of DLK1 and DLK2 function

How DLK1 and DLK2 function at the molecular level is perhaps the most poorly understood aspect of these genes. They are atypical NOTCH interactors, lacking the DSL domain present on canonical NOTCH ligands [65]. The absence of the crucial DSL domain has led to speculation that the DLK genes interact in an inhibitory manner with NOTCH (section 1.6.1), or function independently of NOTCH (section 1.6.2). However, some studies argue that DLK genes actually activate NOTCH (section 1.6.1). This quandary has been probed experimentally but, as discussed further in sections 1.6.1 and 1.6.2, the data can be confusing.

The majority of information is inferred indirectly, by looking at RNA and/or protein expression of *Dlk1* and *Dlk2*, and genes involved in key signalling pathways *in vivo* [2, 6, 18, 42, 133, 154, 181, 182, 198, 232, 262], and *in vitro* [3]. Another common strategy is to study the expression levels of genes responsive to the major signalling pathways, including NOTCH, in cell lines, following *Dlk1/2* knockdown [262], transfection of *Dlk1/2* constructs [3, 16, 41, 177, 198, 232, 260], external administration of S-DLK1 [3, 18, 41, 78, 92, 116, 182, 248], and pharmacological modulation [18, 41, 177, 182, 189, 248]. Another approach is to generate interactomes computationally; such as those generated in figure 1.4. However, these are subject to some of the same flaws present in most experimentally generated interactomes. Although the two proteins may interact *in vitro*, their interaction may not occur *in vivo*. The proteins may localise to distinct subcellular compartments or may not even be expressed in the same cells. They may also miss interactions that depend on specific post-translational modifications. Furthermore, most studies focus on DLK1 and the behaviour of DLK2 is subsequently extrapolated. Not all of the data is, therefore, reflective of the *in vivo* context. Nevertheless, it is highly likely that both NOTCH dependent and independent signalling mechanisms exist *in vivo*.

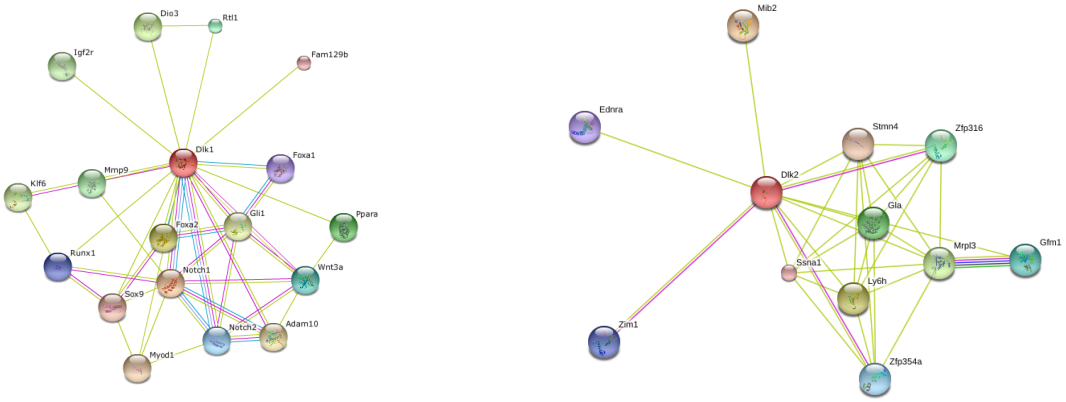

(a) DLK1

(b) DLK2

Fig. 1.4 **Putative interactomes of DLK1 and DLK2 in mice**
Putative murine DLK2 and DLK1 binding partners found using STRING (v10) [222]. All active prediction methods were considered. Only medium confidence interactors (>0.400) shown. Interactions found (from/by): experimentally – pink, databases – blue, text-mining – green, purple – homology.

1.6.1 Notch dependent DLK gene function

Given their homology with other Delta-like NOTCH ligands one might expect DLK1 or DLK2 to activate NOTCH signalling, in trans [84], but experimental evidence is conflicting. Direct binding of either DLK1 or DLK2 to a NOTCH protein, of which most vertebrates have four [148], has yet to be reported *in vivo*. Immunoprecipitation performed on COS-7 cells, transfected with both *Dlk1* and *Notch1*, found no binding between the two genes [249]. However, Mammalian [232] and yeast [23] two hybrid systems show binding of DLK1 to NOTCH1. Furthermore, unbiased screening approaches identified DLK1 as interacting *only* with IRAK1 [169, 171], fibronectin [249], or CFR [154], with only the latter two validated by immunoprecipitation [154, 249]. Such discrepancies highlight the limited physiological relevance of artificial systems when extrapolating to *in vivo* contexts.

The relationship between DLK1 and DLK2, and NOTCH must thus be inferred indirectly, and correlative [120, 123, 203, 232, 238] and antagonistic [23, 29, 89, 165, 198] relationships have been reported. The strongest support for NOTCH agonism, and indeed antagonism, comes from systems such as *Drosophila* where neither DLK gene is endogenously expressed, limiting the physiological relevance of these studies. Although both genes lack the canonical DSL domain that interacts with NOTCH in vertebrates [65], they retain the OSM-11 motif, which has been shown to activate NOTCH in *Caenorhabditis elegans*, a non vertebrate species

[120, 123]. There is also strong evidence that DLK1, at least, inhibits NOTCH signalling. NOTCH signalling is increased in *Dlk1-/-* mice [89], and DLK1 mediated cis-inhibition of NOTCH has been observed in murine cell-lines [23, 165] and when expressed in flies [29]. Alternatively, the DLK genes might simply block the interaction between NOTCH and a canonical ligand and thus, in a dominant negative fashion, prevent activation of NOTCH signalling. However, this phenomena has, thus far, only been demonstrated in non-NOTCH contexts [154].

A neat resolution to the controversy surrounding DLK signalling is that the different DLK isoforms interact differently with various NOTCH genes, especially in different cellular contexts. The work in the heterologous systems provides some preliminary evidence that this might occur. Only M-DLK1 possessed inhibitory behaviour when expressed in flies [29] and S-DLK1 was able to rescue the phenotype in C. elegans lacking osm-11, the agonist of NOTCH in worms [120]. Although promising, this hypothesis needs to be properly probed, *in vivo*, in a physiologically relevant setting. This will be challenging since it is likely that the DLK genes activate additional pathways to NOTCH (section 1.6.2), which may confound the results.

1.6.2 Notch independent DLK gene function

DLK1 and DLK2 likely interact with more proteins and signalling pathways than just NOTCH. Numerous studies have implicated non-NOTCH signalling in DLK gene function. DLK2 is associated with KLF4 signalling [185] whereas DLK1 is linked to AKT [35, 41], CFR [154], cytokine [3, 6], ERK1/2 [116, 177, 189, 248], FGF18 [154], fribronectin [41, 249], growth hormone [4, 14, 16, 18, 33, 35, 133, 181], miR-126-5p [198], NFκB [3, 6], oestrogen [2, 6], SOX9 [248], and WNT10b [262] signalling. Nearly all of the studies try to understand the molecular mechanism utilised by DLK1 to negatively regulate the switch from immature stem cells to mature differentiated cells, in various different lineages. Despite this broadly conserved function, multiple different systems have been implicated and not always consistently. *Dlk1* has been shown to upregulate GH levels [18, 35, 181] and repress it GH in GH3 cells (derived from rats) [16]. Both the ERK [116, 189, 248] and cytokine [3] signalling pathways were identified when studying the role DLK1 plays as a negative regulator of adipogenesis, in mouse and human models, respectively. Other work identified *Sox9* as being key in regulating chondrocytic differentiation [248], but a later study, using a different cell line, found no evidence of *Sox9* expression modulation by DLK1 during chondrogenesis despite specifically testing for it [41]. Such contradictions highlight the limitations of using

cell lines to model *in vivo* phenomena.

It is plausible that DLK1 interacts with different signalling pathways at the cellular level to achieve the same gross output (e.g. negative regulation of cell fate in stem cell niches). Since an ancestral role in stem cell regulation is inferred, it might therefore be evolutionarily expensive and unlikely for DLK1 to behave, on a molecular level, differently between niches and across species, especially as core stemness genes are so broadly conserved. It is much more probable that there is a core, conserved, signalling mechanism that DLK1 implements when regulating stem cells. However, currently the collective data is insufficient to determine which of these signalling pathways are physiologically relevant, and which may be cell culture artefacts. Further *in vivo* studies will be necessary to resolve this issue.

DLK1 can act in autocrine, endocrine and paracrine manner, and it is possible these different signalling modes interact. Such interactions could obfuscate the data, making it challenging to work out what the gene is doing in each specific situation. Indeed, this is potentially one of the causes of the contradictions the literature, and especially in the cell line work, as most studies seem to ignore the different DLK1 isoforms. Most, but not [18, 78, 182] all, studies only look at the full-length gene and/or add S-DLK1 (often in the form of *Dlk1*-Fc) to culture media. Such strategies essentially ignore M-DLK1. Given the preliminary data on DLK1 and NOTCH (section 1.6.1) that there is some evidence that different isoforms may behave in opposing manners, this is perhaps short sighted. Arguably only one study properly accounted for the different isoforms, performing co-cultures between the target cell and cells expressing M-DLK1 or S-DLK1 [78]. Supported by *in vivo* work, these experiments showed that the different DLK1 isoforms actually interact with one another to negatively regulate neurogenesis in the murine adult neurogenic niche [78].

Interestingly, at the time of writing, no reports of NOTCH independent signalling have been identified for the canonical NOTCH ligands. This suggests that the NOTCH independent signalling of the DLK genes may be a vertebrate specific phenomenon.

1.7 DLK1 and disease

DLK1 has been implicated in numerous diseases perhaps due to its far-reaching role as a stem cell regulator. Indeed, its roles in cancer (section 1.7.2), autoimmune and liver diseases (sections 1.7.1 and 1.7.4, respectively), and diabetes (section 1.7.3) may all be attributable to malignant adaptation of *Dlk1* stem cell function. Well-studied diseases will

be discussed in detail below. It is less clear what *Dlk1* might be doing in other disorders. It is downregulated in Parkinson's disease [137] and decreased in the placenta of mothers with prenatal depression and/or anxiety/obsessive compulsive disorder/panic [141]. It is also implicated in atherosclerosis [198] and imprinting disorders: Kagami-Ogata [100], Silver Russell [86], and Temple [88], syndromes. The involvement of DLK1 in such a wide variety of diseases makes it an excellent therapeutic target. Although, at the time of writing, no clinical or pre-clinical studies modulating DLK1 as a treatment have been announced, patents for *Dlk1* modulators have been filed [47].

1.7.1 Autoimmune diseases and DLK1

Multiple sclerosis (MS) is an autoimmune disease that ultimate demyelinates and damages the central nervous system [164]. Although the cause of MS is unknown [163], it is a somewhat heritable disease [253]. Interestingly experimental autoimmune encephalomyelitis, the murine model of MS, demonstrated that lower *Dlk1* expression enhances disease progression and severity and modulates adaptive immune reactions [219]. As with liver diseases (section 1.7.4), the role of the gene in disease progression may simply be reflective of its core function as a stem cell regulator (section 1.4.1). Reductions in DLK1 activity will enhance cellular differentiation at a given niche. Should this niche be responsible for the production of rogue immune cells that self recognize, then it is logical that individuals with more active DLK1 levels would be better protected against the condition. This work is exciting as it may explain the partial heritability of the condition and set the stage for potential therapies. Patients with paternal *Dlk1* variants with lower activity may have more severe disease progression, though this still needs to be clinically investigated.

1.7.2 DLK1 and cancer

Dlk1 has long been implicated in cancer; indeed it was originally cloned as a tumour protein [129]. With few exceptions [72, 93, 144], *Dlk1* expression has since been found to be increased in various cancer types including acute myeloid leukemia [190], alveolar rhabdomyosarcomas [197], erthroleukemia [190], ganglioneuroma [101], glioma [257], hepatoblastoma [32, 59, 73, 143, 145], hepatocellular carcinoma [255], megakaryocytic leukemia [190], myelodysplastic syndromes [190], nephroblastoma [83], neuroblastoma [101, 104, 236, 255], neurofibromatosis [93], pancreatic tumours [231], pituitary adenoma [14, 43], pheochromocytoma [14], small cell lung cancer [93], and testicular adrenal rest tumours [144].

Identifying whether a gene implicated in cancer is the driver or a consequence of the disease is challenging. Increased *Dlk1* levels may be a response to the disease phenotype. *Dlk1* is a stem cell regulator, preventing progenitor cells from differentiating and promoting self-renewal (section 1.4.1). Promotion of self-renewal and differentiation inhibition is, in general, a cancer hallmark; perhaps *Dlk1* is activated early during cancer evolution to promote stem cell like behaviour. Increased expression of DLK1 resulted in increase in clonogenic growth in cell lines modelling cancer [117], while knockdown of DLK1 limited *in vivo* tumour generation from mice injected with carcinogenic cells [202].

However, our understanding of *Dlk1* is incomplete and it is possible that *Dlk1* plays another role. Morpholino mediated knockdown of *Dlk1*, promoted tumour induced angiogenesis in xenograph assays in zebrafish [188] . This phenotype of was reversed when the morpholino was co-injected with human *Dlk1* mRNA [188]. This experiment suggests that *Dlk1* may prevent angiogenesis during tumourgenesis. Vascularisation is a limiting factor on tumour size and is considered a therapeutic target in cancer treatment (reviewed in [12]). In contrast work on cultured endothelial cells suggests that DLK1 promotes angiogenesis [104]. However, this work was performed with recombinant protein of only the extracellular portion of DLK1 [104] and the gene may behave differently in normal endothelial cells as opposed to endothelial cells within a tumour. If *Dlk1* does limit angiogenesis perhaps the organism increases *Dlk1* expression to limit tumour growth. DLK1 has an endocrine signalling isoform and it is plausible for the whole organism to produce S-DLK1 from an alternate source to regulate tumourgenesis. Indeed some of the early characterisations of DLK1 were performed on S-DLK1 identified in the serum of cancer patients [93].

This hypothesis does not explain the increased gene expression observed within actual tumours. However, DLK1 may be playing opposing roles in the different contexts. *Dlk1* might be activated during tumourgenesis to enhance stem cell self-renewal whereas whole organisms could drive S-DLK1 expression to prevent angiogenesis and limit tumour size. Interestingly, hypoxia is sufficient to increase *Dlk1* expression in cancer cells *in vitro* [117]. Perhaps tumour survival or destruction results from conflict between these two processes. Functional experiments, investigating the role of DLK1 within a tumour and within a diseased animal, would be needed to test this hypothesis and probe the role of the gene.

1.7.3 DLK1 and diabetes

Given that *Dlk1* is highly expressed in pancreatic-β-cells [5, 33, 110], including those of embryonic [230, 231] and adult [63], humans, it is fairly unsurprising that it is implicated in

diabetes mellitus. A recent GWAS found a paternally inherited risk of type 1 diabetes of a variant in a region known to alter expression of DLK1 [245]. Furthermore, *Dlk1* seems to be repressed in islets of patients with type-2-diabetes [110] and a recent nested population based case-control study, looking at the incidence of diabetes over a four year period, found that the disease occurred threefold more frequently in women with low DLK1 levels [135]. A positive correlation between S-DLK1 levels and serum insulin levels was also observed in 231 Spanish children [95]. In addition, selective overexpression of *Dlk1* in pancreatic-β-cells, in mice, leads to increased insulin production, pancreatic-islet hypertrophy and hyperinsulinemia in fasting and fed conditions, and *Dlk1*-/- mice have smaller islets [246]. These results suggest DLK1 might be a positive regulator of insulin release and high DLK1 levels may protect against diabetes. However there might be an alternative explanation for the correlation between *Dlk1* and diabetes.

Rather than protecting against diabetes, *Dlk1* might be involved in the response of an organism to the disease. *Dlk1* is a stem cell regulator and maintains pluripotency of progenitor cells. Perhaps *Dlk1* expression is increased as a result diabetes and is part of a response that dedifferentiates ductal or alpha cells into a progenitor like state, whereby they are subsequently differentiated into beta cells. Exogenous administration of S-DLK1 to PANC1 cells, a human pancreatic ductal cell line, ultimately resulted in differentiation into insulin secreting cells [183]. In addition, high levels of DLK1 were seen in the acinar cells surrounding pancreatic islets, a tissue not previously shown to express DLK1, in wild type mice [18]. Furthermore, pancreatectomised rats treated with DLK1 show improved pancreas regeneration compared to rats not receiving treatment [183].

1.7.4 Liver diseases

Non-alcoholic fatty and alcoholic liver disease refer to a broad spectrum of liver diseases with hepatosteatosis in the absence [228] and presence [234] of 20g/day alcohol consumption, respectively. Remarkably, *Dlk1*-overexpressing adult mice, with an obesogenic genetic background, had reduced hepatosteatosis [35]. This is thought to be due to a reduction in circulating growth-hormone [35]; as the hormone, in conjunction to others, regulates liver fatty acid metabolism [156]. This may also be a consequence of the its function as a stem cell regulator. DLK1 limits differentiation in stem cell niches; thus higher DLK1 levels may limit differentiation into adipocytes in the liver and, in turn, reduce hepatosteatosis. In addition, DLK1 also seems to reprogram hepatic lipid metabolism in alcoholic liver disease [234]. Such findings may have implications for disease susceptibility in humans; for example individuals with low activity *Dlk1* variants may be more likely to develop hepatosteatosis

and individuals that produce more DLK1 may be protected against the conditions. Although such a hypothesis will need to be verified with clinical population studies, investigations into the clinical potential of this have already begun. Exogenous administration of S-DLK1 wad found to ameliorate hepatic steatosis in mice [136].

1.7.5 The role of DLK1 in obesity

Given that *Dlk1* is a stem cell regulator of preadipocytes (section 1.4.1) and plays a role in whole body metabolism in mammals (section 1.4.3), including driving lipolysis [35], it is unsurprising that *Dlk1* has been implicated in obesity in mice [35, 134, 158, 241] and humans [252]. Placental *Dlk1* levels mildly correlate with birth weight in humans [159] and serum S-DLK1 levels are significantly lower in pregnant women who go on to deliver offspring that are small for their gestational age [44]. Mice lacking *Dlk1* are obese [158]; whereas those overexpressing the gene are leaner [35, 134, 241] even if the strain is fed on a high fat diet [241] or possesses an obesogenic genetic background [35]. Interestingly, *Dlk1* levels are increased in the adipose of rats whose mothers were fed high fat diets 21 days before mating, throughout pregnancy and during lactation [200]. Such rats have abnormal metabolic programmes and were heavier than the offspring of mothers fed normal diets [200]. Perhaps *Dlk1* expression is increased in response to the disease to restrain adipogenesis. Further studies will be needed to probe this hypothesis. However, attempts to modulate DLK1 levels for clinical treatment of obesity will likely need to increase expression of both isoforms as exogenous administration of S-DLK1 to mice had no effect on adipose deposits compared to vehicle treated controls [136].

1.8 DLK2 and disease

Given the paucity of information regarding *Dlk2*, it is unsurprising that almost nothing is known about the gene in the context of disease. Only one study has specifically investigated the involvement of *Dlk2* in any disease: when looking at the role of NOTCH ligands in suicide, Monsalve and colleges found no difference in DLK2 expression in studied brain regions between normal individuals and victims of suicide [157]. To the author's knowledge, no genome wide association studies or other such screens have identified significant misregulation of *Dlk2* in any disease context.

The absence of any data concerning *Dlk2* and disease might be informative. The importance of *Dlk1* in some diseases (section 1.7) such as diabetes (section 1.7.3) and obesity

(section 1.7.5) was initially identified through unbiased and agnostic GWASs and expression analyses, such as RNAseq or microarray, between healthy and diseased tissues. Importantly the involvement of *Dlk1* in many of its associated diseases is likely related to its function as a stem cell regulator (section 1.7). Given that *Dlk2* may also, tentatively, function as a stem cell regulator under certain contexts, such as chondrogenesis (section 1.5), it is surprising that no disease is associated with the gene. Perhaps *Dlk2* contributes weakly to stem cell regulation and so the effect size is too small to be detected in current projects. Alternatively, *Dlk2* might be an essential gene and alterations to its activity could be lethal. Finally, it is possible the *Dlk1* can act redundantly with *Dlk2* in particular contexts and rescue any phenotypic anomalies associated with *Dlk2* mutation. Until a detailed understanding of the basic function of the gene is achieved, it is difficult to favour either hypothesis.

1.9 Project aims

This research project aimed to characterise DLK2, and compare it to DLK1. Although the evolutionary relationship between the two genes was assessed across various vertebrates, their expression and function was studied in mice. Classical expression studies were performed on both genes and a DLK2 mutant was generated to investigate the function of the gene.

2 Investigating the evolutionary relationship between DLK1 and DLK2

DLK1 and DLK2 are vertebrate specific NOTCH ligands. Preliminary evolutionary analysis of both genes has only covered a subset of vertebrate species (section 1.2). Investigating the evolution of both genes across a selection of species covering the entire vertebrate phylum would yield greater insights into their relationship.

2.1 DLK2 is ancestral to DLK1

Protein and DNA sequences (appendix A.1) for DLK1 and DLK2 were identified in representative species of all vertebrate clades (table 2.1). Mammalian clades were over-represented because *Dlk1* is an imprinted gene and evolved to imprint during the eutherian lineage [68]. Sequences for DLK1 and DLK2 were found for all investigated species except representatives of petromyzontiformes, leptocardii, and ascidiacea: lamprey, amphioxus and *C. intestinalis*, respectively. *Dlk1* is not found in any of these species but a truncated version of *Dlk2* is present in the lamprey genome (data not shown). The *Dlk* orthologue found in *C. intestinalis* is most similar to *Dlk2* (see section 2.3) and for subsequent analysis (sections 2.3, 2.4, and 2.5) *Dlk2* is considered to be the version present in *C. intestinalis*.

Phy. class	**Phy. order/clade**	**Representative species**	**Common name**	**Genes present**
Mammalia	Euarchontoglires	*Homo sapiens*	Human	Both
Mammalia	Euarchontoglires	*Mus musculus*	Mouse	Both
Mammalia	Laurasiatheria	*Bos taurus*	Cow	Both
Mammalia	Laurasiatheria	*Canis lupus familiaris*	Dog	Both

Table 2.1 (continued)

Phy. class	**Phy. order/clade**	**Representative species**	**Common name**	**Genes present**
Mammalia	Afrotheria	*Loxodonta africana*	Elephant	Both*
Mammalia	Afrotheria	*Elephantulus edwadii*	Elephant shrew	Both^{+}
Mammalia	Xenarthra	*Dasypus novemcinctus*	Nine banded armadillo	Both^{+}
Mammalia	American marsupialia	*Monodelphis domestica*	Opossum	Both
Mammalia	Australian marsupialia	*Macropus eugenii*	Tammar wallaby	Both^{+}
Mammalia	Australian marsupialia	*Sarcophilus harrisii*	Tasmanian devil	Both
Mammalia	Monotremes	*Ornithorhynchus anatinus*	Platypus	Both^{+}
Aves		*Gallus gallus*	Chicken	Both
Reptilia	Lepidosauria	*Anolis carolinesis*	Anole lizard	Both
Reptilia	Pantestudines	*Pelodiscus sinensis*	Chinese soft shell turtle	Both
Amphibia		*Xenopus tropicalis*	Western clawed frog	Both^{+}

Table 2.1 (continued)

Phy. class	**Phy. order/clade**	**Representative species**	**Common name**	**Genes present**
Sarcoptery-gii		*Latimeria chalumnae*	Ceolacanth	Both
Actinoptery-gii		*Danio rerio*	Zebrafish	Both
Actinoptery-gii		*Oryzias latipes*	Medaka	Both
Chon-drichthyes		*Callorhinchus milii*	Australian ghost shark	Both
Hyperoartia[&]		*Petromyzon marinus*	Lamprey	Truncated DLK2
Leptocardii[&]		*Branchiostoma floridae*	Lancelet/am-phioxus	Neither
Ascidiacea		*Ciona intestinalis*	Ciona	DLK2

Table 2.1 **Identification of DLK1 and DLK2 gene sequences in representative species of major vertebrate clades**

DLK1 and DLK2 were studied in phylogenetic classes and order/clades of vertebrates with at least one species investigated per clade. Neither DLK1 nor DLK2 were found in leptocardii, and only truncated DLK2 was found in the chondrichthyes. Some clades had more than one species investigated if a gene protein or DNA sequence was of insufficient quality to use in subsequent analyses. [+] *and * denote species that possessed only sequences of sufficient quality for DLK1 and DLK2, respectively.* [&] *Convention holds that of the three chordate groups, cephalochordates, which includes leptocardii and thus lancelets, are closer to vertebrates than ascidiacea or tunicates. This convention is still utilised by many databases, such as UCSC genomes [113]. However, recent phylogenomic data suggests that*

tunicates, including ascidiacea, may be more closely related to vertebrates [58]. This will have implications on interpreting these results. Acronyms used: Phy. — phylogenetic.

Dlk2 is present in two representative species of the three earliest clades (*petromyzontiformes*, *leptocardii*, and *ascidiacea*), including what is conventionally considered the most ancestral clade: ascidiacea. Although unlikely *Dlk2*, could have been lost in the amphioxus genome but the poor quality annotation and high number of gaps in that reference genome means that it is much more likely that *Dlk2* is present ascidiacea but is not represented in the available sequence.

The poor quality of the genomes also raises the possibility that *Dlk1* is present but undetectable in lamprey, amphioxus and *C. intestinalis*. However, early vertebrate whole genome duplications occurred between the divergence of amphioxus and lamprey, and lamprey and the early tetrapod (fish) lineages [56]. It is most likely that duplication of a *Dlk* precursor gene to generate *Dlk1* and *Dlk2* occurred during a whole genome duplication event and thus the orthologue present in ascidiacea (of *Dlk2*) is the ancestral version of the gene. Overall, this suggests that *Dlk2* is ancestral and that *Dlk1* arose from a subsequent genome duplication event.

The absence of a *Dlk1* sequence from the petromyzontiformes clade (lamprey) could be due to a poor-quality reference genome. However, it may also be reflective of actual biology. If this is the case, then duplication of *Dlk1* from *Dlk2* likely occurred during the whole genome duplication event occurring between the petromyzontiformes and tetrapod clades [56].

There is an alternative interpretation. Historically, the overall scientific consensus has been that the ascidiacea is phylogenitically older than the leptocardii clade. This conclusion was drawn primarily because of morphological similarities (and differences) at the adult stage of representative organisms from the ascidiacea and leptocardii clades, and early true vertebrates, such as lamprey. Many organisations and databases, such as UCSC genomes [113], still adhere to this. However, a recent phylogenomic study of 28 species, including four types of tunicate (and including *C. intestinalis*), eight vertebrates, and one species of lancelet, has concluded that lancelets are older than ascidiacea. If this were the case, it provide a far stronger argument that *Dlk2* is the more ancient gene. No *Dlk2* sequence is present in the lancelet genome however *Dlk2* sequences are present in the genomes of *C. intestinalis* and lamphrey. In this scenario, *Dlk2* would have arisen between a duplication

event occurring between the leptocardii and ascidiea lineages. *Dlk1* would still have likely arisen during the whole genome duplication event occurring between the petromyzontiformes and tetrapod clades [56]. Nevertheless, whether leptocardii or ascidicea is the most ancient clade, it is clear that *Dlk2* is the most ancient gene.

It is also worth noting that single copies of *Dlk1* and *Dlk2* are present in coelacanths and all ray-finned fish studied (including zebrafish, medaka, stickleback, and the tatraodon and fugu genuses of pufferfish — data not shown). A further fish-specific round of genome duplication occurred after they diverged from the common ancestor shared with coelacanths [56]. This means both *Dlk1* and *Dlk2* were duplicated again in fish but the second copies were rapidly lost. This suggests that dosage of both genes is highly important to their functions.

2.2 DLK1 and DLK2 are highly conserved genes

Percentage similarity (figure 2.2) and identity (figure 2.1) were calculated across all species for both DLK1 and DLK2 (section 8.6.3). The closer two species are in evolution, the higher the percentage identity and similarity between their protein sequences; and percentage similarity is always higher then percentage identity.

In general, the percentage similarity or identity between two species is higher for DLK2 than DLK1. This provides further support that DLK2 is the ancestral form of the gene and suggests that DLK1 may be undergoing further evolution. This would not be surprising given the number of functions for the gene that are hypothesised to be mammalian specific (section 1.4.3). Notably, DLK1 in zebrafish (figure 2.1) shares a particularly low percentage identity with other species; indeed it never rises above 33%. Zebrafish DLK1 lacks the juxtamembrane cleavage domain (section 2.3) suggesting that it may be more evolutionary dynamic. The poor conservation between species could be reflective of this.

The percentage similarities and identities of the *C. intestinalis* DLK orthologue were determined against all species for DLK1 and DLK2. The percentage similarities are higher between DLK2 and the *C. intestinalis* DLK orthologue across all species. This is consistent with what one might expect, given the identity of the DLK genes present in ancient vertebrates relative to known whole genome duplication events (section 2.1). The higher conservation of the *C. intestinalis* DLK orthologue to DLK2 lends support to the hypothesis that DLK2 is the ancestral gene variant. It also suggests that it is appropriate to call the

Fig. 2.1 **Percentage identities of DLK1 and DLK2 shared between various vertebrate species**

Protein sequences, obtained as described in section 8.6.5, were aligned using ClustalO (V1.2.4) [132] (section 8.6.1). Percentage identity of the sequences between species were obtained using 'Ident & Sim' tool in the sequence manipulation suite [218] using default settings. *Hs – human, Mm – mouse, Bt – cow, Cf – dog, Ee – elephant shrew, La — elephant, Dn – nine banded armadillo, Md – opossum, Me – tammar wallaby, Sh – Tasmanian devil, Oa – platypus, Gg – chicken, Ac – anole lizard, Ps – Chinese soft shell turtle, Xt – western clawed frog, Lc – coelacanth, Dr – zebrafish, Ol – medaka, Cm – Australian ghost shark, and Ci — C. intestinalis.*

Fig. 2.2 **Percentage similarities of DLK1 and DLK2 shared between various vertebrate species**

Protein sequences, obtained as described in section 8.6.5, were aligned using ClustalO (V1.2.4) [132] (section 8.6.1). Percentage similarity of the sequences between species were obtained using 'Ident & Sim' tool in the sequence manipulation suite [218] using default settings. *Hs – human, Mm – mouse, Bt – cow, Cf – dog, Ee – elephant shrew, La — elephant, Dn – nine banded armadillo, Md – opossum, Me – tammar wallaby, Sh – Tasmanian devil, Oa – platypus, Gg – chicken, Ac – anole lizard, Ps – Chinese soft shell turtle, Xt – western clawed frog, Lc – coelacanth, Dr – zebrafish, Ol – medaka, Cm – Australian ghost shark, and Ci — C. intestinalis.*

orthologue present in *C. intestinalis* DLK2.

2.3 Key functional domains are conserved in most vertebrates for DLK1 and DLK2

Although assessing the conservation of a given protein across various species is useful at the gross whole protein level, it yields little insight into the conservation of the functional domains of the protein. Investigating the conservation of specific protein regions is useful as it can create awareness about which domains are essential or dispensable for gene function.

Good quality protein sequences for DLK1 (figure 2.3) and DLK2 (figure 2.4), found in the species studied in section 2.1, were aligned (section 8.6.1). Key protein domains were annotated using Interpro (section 8.6.1). Each protein sequence was independently annotated; no region was found using homology. This approach ensures that the striking domain conservation was determined in an unbiased fashion.

The annotated alignments suggest that DLK1 and DLK2 are highly conserved across vertebrates. DLK2 domains are generally much better conserved than DLK1 domains, but this is expected given that it is more strongly conserved (section 2.2), and is likely to be the ancestral version of the gene (section 2.1). However, this strong consensus makes it challenging to infer if any of the 6 EGF repeats are vital for DLK2 function. One interpretation is that all of them are extremely important for DLK2 function. DLK1 EGFs are less well conserved.

The majority of species possess 6 EGF repeats in DLK1, except zebrafish and platypus which both lack EGF 6. This suggests that EGF 6 is not essential for gene function. It is much more likely that EGFs 2 or 3 that are functionally relevant in gene signalling as they are perfectly conserved across all vertebrates. This is inconsistent with a recent study that concluded that EGFs 5 and 6, of DLK1, interact with NOTCH [232]; however this work was conducted using a mammalian yeast-2-hyrid system and so may not be reflective of the *in vivo* context.

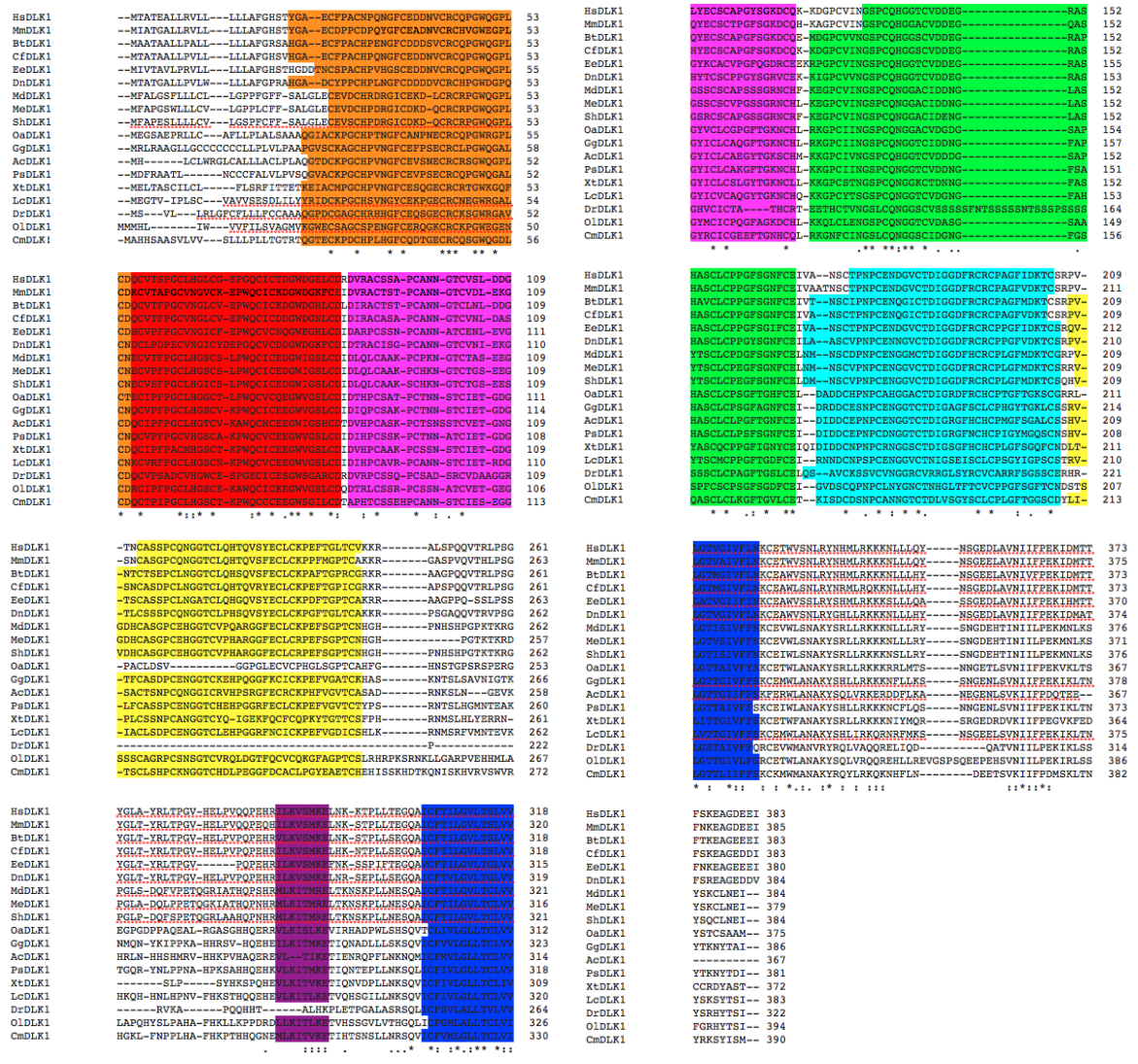

Fig. 2.3 **Alignments of DLK1 protein sequences across various vertebrates** Orange — EGF1, Red — EGF2, Pink — EGF3, Green — EGF4, Turquoise — EGF5, Yellow — EGF6, Aubergine — juxtamembrane domain, and Blue — transmembrane domain. Sequences obtained as described in section 8.6.5 were aligned using ClustalO (V1.2.4) [132] and annotated as described in section 8.6.1. Identified regions were then manually highlighted in the alignment at correct coordinates. *Hs – human, Mm – mouse, Bt – cow, Cf – dog, Ee – elephant shrew, Dn – nine banded armadillo, Md – opossum, Me – tammar wallaby, Sh – Tasmanian devil, Oa – platypus, Gg – chicken, Ac – anole lizard, Ps – Chinese soft shell turtle, Xt – western clawed frog, Lc – coelacanth, Dr – zebrafish, Ol – medaka, and Cm – Australian ghost shark.* Larger views of the same annotations are located in the appendix A.1.5.

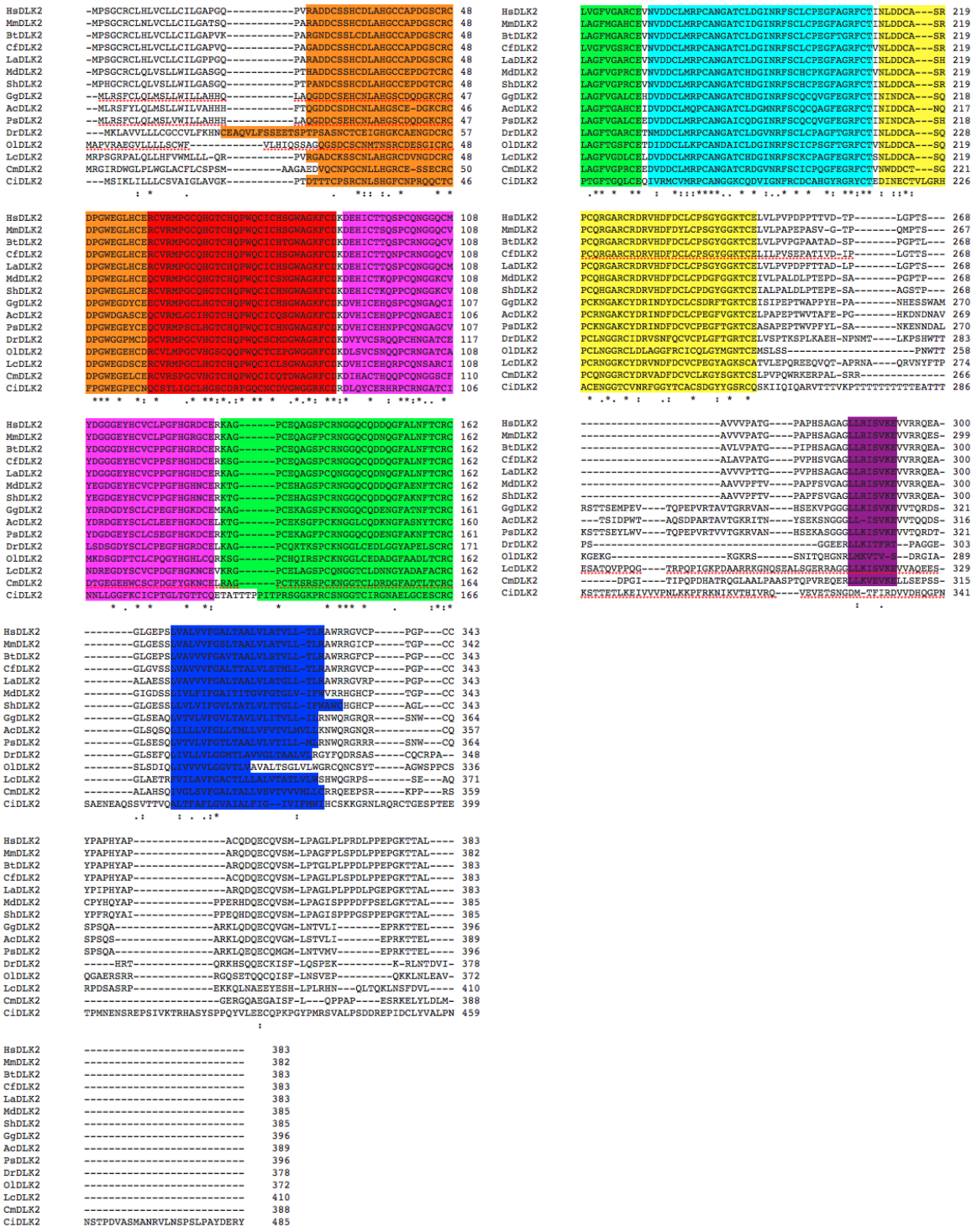

Fig. 2.4 **Alignments of DLK2 protein sequences across various vertebrates** Orange — EGF1, Red — EGF2, Pink — EGF3, Green — EGF4, Turquoise — EGF5, Yellow — EGF6, Aubergine — juxtamembrane domain, and Blue — transmembrane domain. Sequences obtained as described in section 8.6.5 were aligned using ClustalO (V1.2.4) [132] and annotated as described in section 8.6.1. *Hs — human, Mm — mouse, Bt – cow, Cf – dog, La – elephant, Md – opossum, Sh – Tasmanian devil, Gg – chicken, Ac – anole lizard, Ps – Chinese soft shell turtle, Dr – zebrafish, Ol – Medaka, Lc – coelacanth, Cm – Australian ghost shark, and Ci – ciona.* Larger views of the same annotations are located in the appendix A.1.6.

2.3.1 The juxtamembrane domain may be less evolutionarily dynamic than expected

The assessment of domains across various vertebrates for DLK1 and DLK2, may confirm earlier findings that zebrafish lack the juxtamembrane cleavage domain in DLK1 (pers. comm. Dr. Carol Edwards). No true vertebrate that has been investigated has been found to lack the cleavage domain in DLK2, perhaps reflective of the its stronger conservation. The conventional interpretation of the lack of an obvious cleavage domain in only zebrafish DLK1 is that this particular gene is highly divergent; this hypothesis is generally supported with various measures of its gene conservation (sections 2.2, 2.4, 2.5) where zebrafish DLK1 is generally the most poorly conserved gene. However, there may be another interpretation. Nonetheless, because of the absence of the juxtamembrane cleavage domain, zebrafish is a good model to investigate isoform specific gene function.

Motif recognition of the TACE enzyme, which cleaves at the juxtamembrane site, is poorly understood and sites are generally identified experimentally rather than through sequence identification based approaches [31]. Perhaps the sequence coding for the juxtamembrane domain has altered sufficiently to possess amino acids that are difficult to align bioinformatically but are still recognised by the TACE enzyme. There may be some circumstantial evidence to support this hypothesis. *Delta*, from which the DLK gene ultimately evolved, does possess an extracellular cleavage domain targeted by the same TACE enzyme [258]; but *C. intestinalis* does not possess a convincing cleavage domain sequence. However the canonical NOTCH ligand *Delta like 1* (*Dll1*), which also arose from duplication of *Delta* (figure 1.2), possesses a juxtamembrane domain that is cleaved by ADAM10, a protein in the same family as the TACE enzyme [210]. These data might suggest that the juxtamembrane domain region may have been subject to some dynamic evolution during the genome duplications and was lost during the duplication of *Delta* to the *C. intestinalis Dlk2*. It may have then subsequently been regained in later vertebrates and the domain then again lost in *Dlk1* throughout the speciation of zebrafish. Alternatively, primitive *C. intestinalis* may have retained the cleavage domain but then lost it after the separation of other evolutionary clades, with the domain also being lost in zebrafish *Dlk1*. A final explanation is that both *C. intestinalis Dlk2* and zebrafish *Dlk1* possess experimentally unvalidated cleavage domains that are recognisable by the TACE enzyme or ADAM10 but that are sufficiently different to be missed in bioinformatics analysis.

2.3.2 The intracellular portions of DLK1 and DLK2 are well conserved

Another interesting observation in the annotated alignments is the high conservation of the intracellular portions of both proteins. DLK1, in particular, possesses residues that are identical across all species. There is also very high conservation in this region within DLK2, however the expanded intracellular domain in *C. intestinalis* somewhat obscures this in the alignments. Conservation in this region could be vestigial, or it may reflect hitherto unconsidered residues that are important for DLK gene function. The conserved residues and/or regions may be important for intracellular protein-protein interactions. Proteins are known to associate with the internal domain of *Delta* and are thought to play functionally important roles [131]. The intracellular domains have been largely ignored because they are so short (pers. comm. Dr. Ben Shaw), but perhaps it would be worth considering them in future investigations into gene signalling.

2.4 DLK1 is more evolutionarily dynamic than DLK2

A maximum likelihood tree (figure 2.5) assessed the phylogenetic relationship between both DLK1 and DLK2 across the same vertebrate species. The branch lengths of the tree represent evolutionary distance – the longer the branches the further the two sequences have diverged. The natural grouping of DLK1 and DLK2 sequences is expected.

The phylogenetic tree provides insights that further support the hypothesis that DLK2 is ancestral to DLK1. The branch lengths of DLK2 between the different species are dramatically shorter than the DLK1 branch lengths. This suggests that DLK2 is more tightly conserved between species. The branching pattern is broadly consistent with the evolutionary history of the species. Notably, species from afrotheria and laurasiatheria cluster together on the same node. This is perhaps further evidence of just how highly conserved DLK2 is.

The phylogenetic analysis also provides evidence that DLK1 is more evolutionarily dynamic than DLK2. The branch lengths are much longer, especially within the mammalian clade. It is somewhat surprising that DLK1 has longer branch lengths within the mammalian clade given that DLK1 evolved imprinting within eutherian mammals [68]. Representative species of monotremes and marsupialia cluster together separately from the eutherian mammals. Within the eutherian node, xenarthra, afrotheria, laurasiatheria, and euarchotoglires form distinct subnodes. The branch lengths between these nodes are perhaps unexpectedly

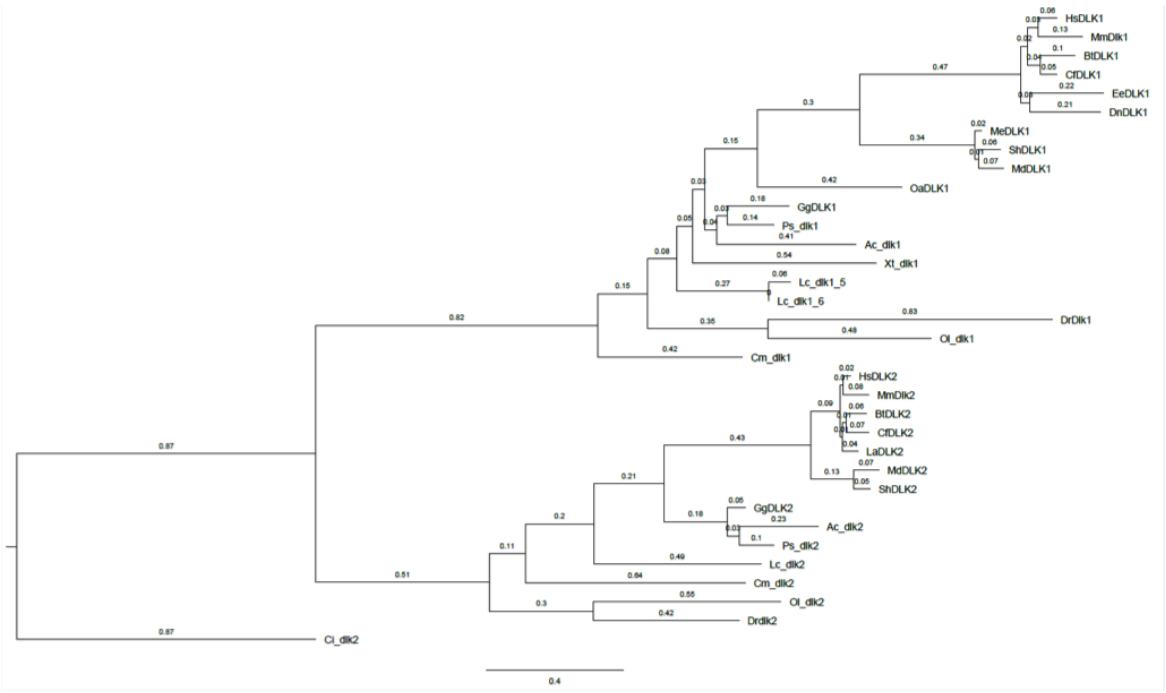

Fig. 2.5 **Evolutionary tree of DLK1 and DLK2 across various vertebrates** Maximum likelihood tree drawn from ClustalO (V1.2.4) alignments (section 8.6.1) of DLK1 and DLK2 by Dr. Carol Edwards. The tree was drawn using PhyML [90] as described in section 8.6.4. *Hs – human, Mm – mouse, Bt – cow, Cf – dog, La – elephant, Ee – elephant shrew, Dn – nine banded armadillo, Md – opossum, Me – tammar wallaby, Sh – Tasmanian devil, Oa – platypus, Gg – chicken, Ac – anole lizard, Ps – Chinese soft shell turtle, Xt – western clawed frog, Lc – coelacanth, Dr – zebrafish, Ol – medaka, Cm – Australian ghost shark, and Ci – C. intestinalis.*

long given how short they are for DLK2. This could be reflective solely of the evolution of imprinting. However, it might also reflect the novel functions that are evolving perhaps as a consequence of dosage control by genomic imprinting (as discussed in section 1.4).

Although the evolution of imprinting is the strongest candidate to explain the dynamic phylogenetic behaviour of DLK1, it cannot be the only one. Zebrafish DLK1 is a clear phylogenetic out-group. This is perhaps unsurprising given that it probably lacks a cleavage domain (section 2.3) and shares low percentage identities and similarities with other species (figures 2.1 and 2.2). DLK1 is not imprinted in zebrafish and so the pressures driving its diversification must be imprinting independent. Furthermore, branch lengths between other vertebrate clades are much longer for DLK1 than DLK2, suggesting that DLK1 is generally more evolutionarily dynamic across all species than DLK2.

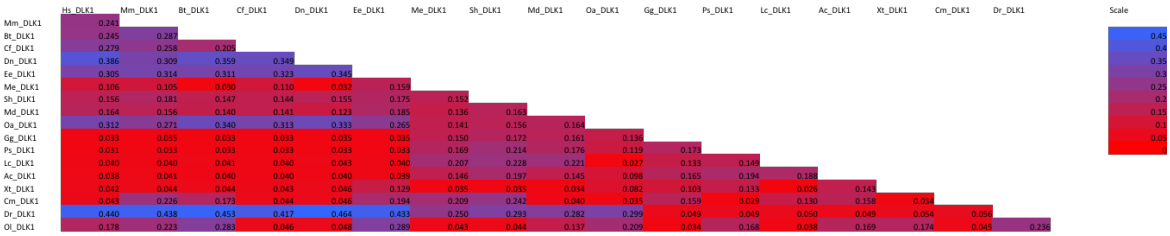

Fig. 2.6 **Ka/Ks values for DLK1 across various vertebrates**
The Ka/Ks values of DLK1 were calculated, by Dr. Carol Edwards, as described in section 8.6.2. The redder the Ka/Ks value the greater the purifying evolutionary selection. Colour scale is the same as in figure 2.7. *Hs – human, Mm – mouse, Bt – cow, Cf – dog, Ee – elephant shrew, Dn – nine banded armadillo, Md – opossum, Me – tammar wallaby, Sh – Tasmanian devil, Oa – platypus, Gg – chicken, Ac – anole lizard, Ps – Chinese soft shell turtle, Xt – western clawed frog, Lc – coelacanth, Dr – zebrafish, Ol – medaka, and Cm – Australian ghost shark.*

2.5 Both DLK1 and DLK2 are under purifying evolutionary selection

Calculating the Ka/Ks values of a given gene between various species is another effective way to determine its evolutionary status [244]. Ka/Ks values less than one, between two given species, indicate that a gene is under purifying evolutionary selection: more non-synonymous mutations were eliminated compared to silent mutations, indicating that some amino-acid changes had deleterious effects [244]. Genes with Ka/Ks values greater than one have change selected for and are considered to be under positive evolutionary selection [244].

Ka/Ks values were calculated (section 8.6.2) for DLK1 and DLK2 across the suitable vertebrate species identified in section 2.1. The Ka/Ks values are less than one for DLK1 (figure 2.6) and DLK2 (figure 2.7) between all studied species, suggesting that both genes are under purifying evolutionary selection. This is consistent with genome-wide studies investigating the evolution of duplicated genes and shows that duplicated genes are generally under purifying evolutionary selection [121, 147, 235].

The Ka/Ks values support the findings of all the other evolutionary analyses (sections 2.1, 2.3, and 2.4). The Ka/Ks values are more consistent for DLK2 than DLK1, supporting the phylogenetic analysis that indicates that DLK2 is better conserved between species and probably the ancestral form of the gene. DLK1 is likely under more dynamic evolution, reflective of becoming imprinted (section 1.2.1) and developing some neofunctionalism (sec-

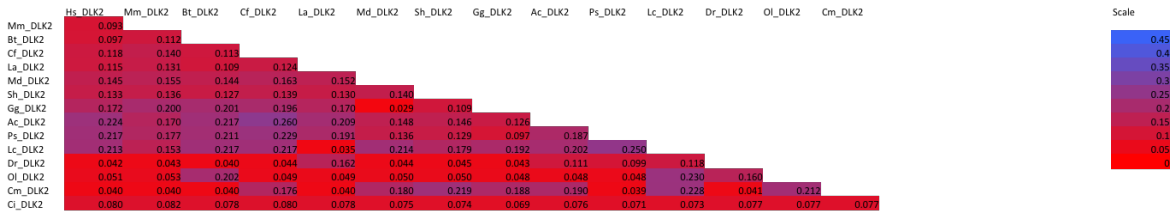

Fig. 2.7 **Ka/Ks values for DLK2 across various vertebrates**
The Ka/Ks values of DLK2 were calculated, by Dr. Carol Edwards, as described in section 8.6.2. The redder the Ka/Ks value the greater the purifying evolutionary selection. Colour scale is the same as in figure 2.6. *Hs – human, Mm – mouse, Bt – cow, Cf – dog, La – elephant, Md – opossum, Sh – Tasmanian devil, Gg – chicken, Ac – anole lizard, Ps – Chinese soft shell turtle, Dr – zebrafish, Ol – Medaka, Lc – coelacanth, Cm – Australian ghost shark, and Ci – ciona.*

tion 1.4). Zebrafish DLK1 perhaps epitomises this evolutionary dynamism. It is interesting that this on-going evolution for DLK1, for which there seems to be substantial evidence, is constrained within the parameters of purifying evolutionary selection. This is likely due to the its function as a stem cell regulator (section 1.4.1), which may indicate just how important the role DLK1 plays in stem cell regulation is.

3 Qualitative analysis of *Dlk1* and *Dlk2* embryonic expression

The comparative analysis of the expression of *Dlk1* and *Dlk2* not only provides an opportunity to consider their relative roles in development but also could provide insight into possible functional redundancy between the two proteins. Expression of *Dlk1* and *Dlk2* was compared by *in situ* hybridisation (ISH). Relative expression patterns for the two genes could already be inferred by examining RNA-seq databases, such as ENCODE [48] and FANTOM5 [142]. However, as discussed in section 1.3, these databases are fairly noisy for *Dlk1* and *Dlk2* expression and as such provided little insight into the true sites of expression for each gene. Furthermore, they lack cellular resolution. ISHs can thus be a better way of investigating gene expression. High through put ISH databases, such as Eurexpress [61] and the Allen Brain Atlas [221], do exist but their findings are inconsistent, particularly for *Dlk2*. The unreliability of the high throughput approaches for determining *Dlk2* expression, suggests a need for robust independent experimental analysis of *Dlk2* expression both temporally and spatially.

ISH expression data for *Dlk1* is much more reliable, predominantly because independent gene-focused experimental analysis has been performed by more than one group, including ours [256, 52]. However, these datasets do not cover the entirety of embryogenesis. Furthermore, when comparing the expression of two genes, it is best to perform ISHs on adjacent sections of the same biological samples. Thus ISH of both *Dlk1* and *Dlk2* were performed.

The original experimental plan was to investigate gene expression throughout embryogenesis in two day intervals — e.g. embryonic day 18.5 (e18.5), e16.5, e14.5, e12.5, and so on. However, I was unable to dissect embryos with sufficient integrity for histological analysis below e12.5. Thus only e12.5, e14.5, e16.5, and e18.5 time-points were investigated. This covers a large part of embryogenesis and includes the development of many organs. The *Dlk1* riboprobe plasmid described by da Rocha et al. [52] had already been generated in the lab, whereas a *Dlk2* riboprobe (section 3.1) was generated by myself.

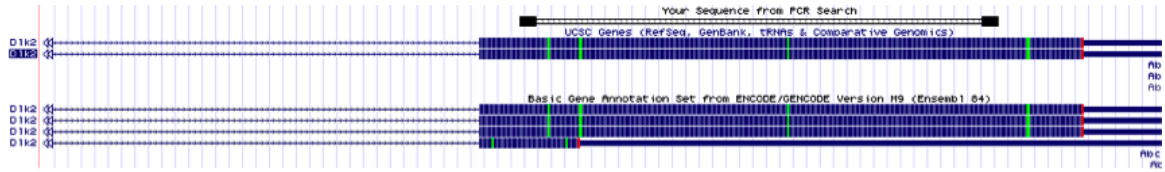

Fig. 3.1 **Genomic location of *in situ* hybridisation probe designed for *Dlk2*** Screen-shot from UCSC [113].

3.1 Generation of *Dlk2 in situ* hybridisation probe

The ISH probe for *Dlk2* was designed to span the final exon of *Dlk2* (figure 3.1). Primer3 [124] was used to find good quality primers (section 8.2.3) within exon 6; this was chosen because a full length transcript is the most likely candidate for functional protein generation.

Importantly, the *Dlk2* probe spans the region including the cleavage domain. It is unlikely that any isoforms splicing out the cleavage domain (as yet unverified) would be detected with this probe. The *Dlk1* probe used covers the full length mRNA [52], and has the same problem in that shorter isoforms lacking the cleavage domain are unlikely to be detected. However, a study using ISH probes designed to distinguish between the different *Dlk1* isoforms found that all isoforms are co-expressed at e8.5 and e10.5 [151]. Without experimental validation, this trend cannot be assumed to occur throughout the entirety of embryogenesis for *Dlk1*, and certainly not for *Dlk2*. However, the limitation regarding isoform detection is consistent between both probes.

3.2 *In situ* hybridisations of *Dlk1* and *Dlk2* during embryogenesis

ISH of *Dlk1* and *Dlk2* were performed (section 8.5.2) using previously described [52] and novel (section 3.1) riboprobes. The experiments were conducted on paraffin wax sections of whole embryos and placentae (figure 3.2) harvested at embryonic days 12.5, 14.5, 16.5, and 18.5 (e12.5, e14.5, e16.5, and e18.5, respectively). Sense controls are shown in the Appendix A.2.

Overall, the sagittal sections used provide good representation of the majority of the growing organ primordia and established tissues present at the given developmental stage. However, some tissues are missing from some sections, such as the adrenal gland and pan-

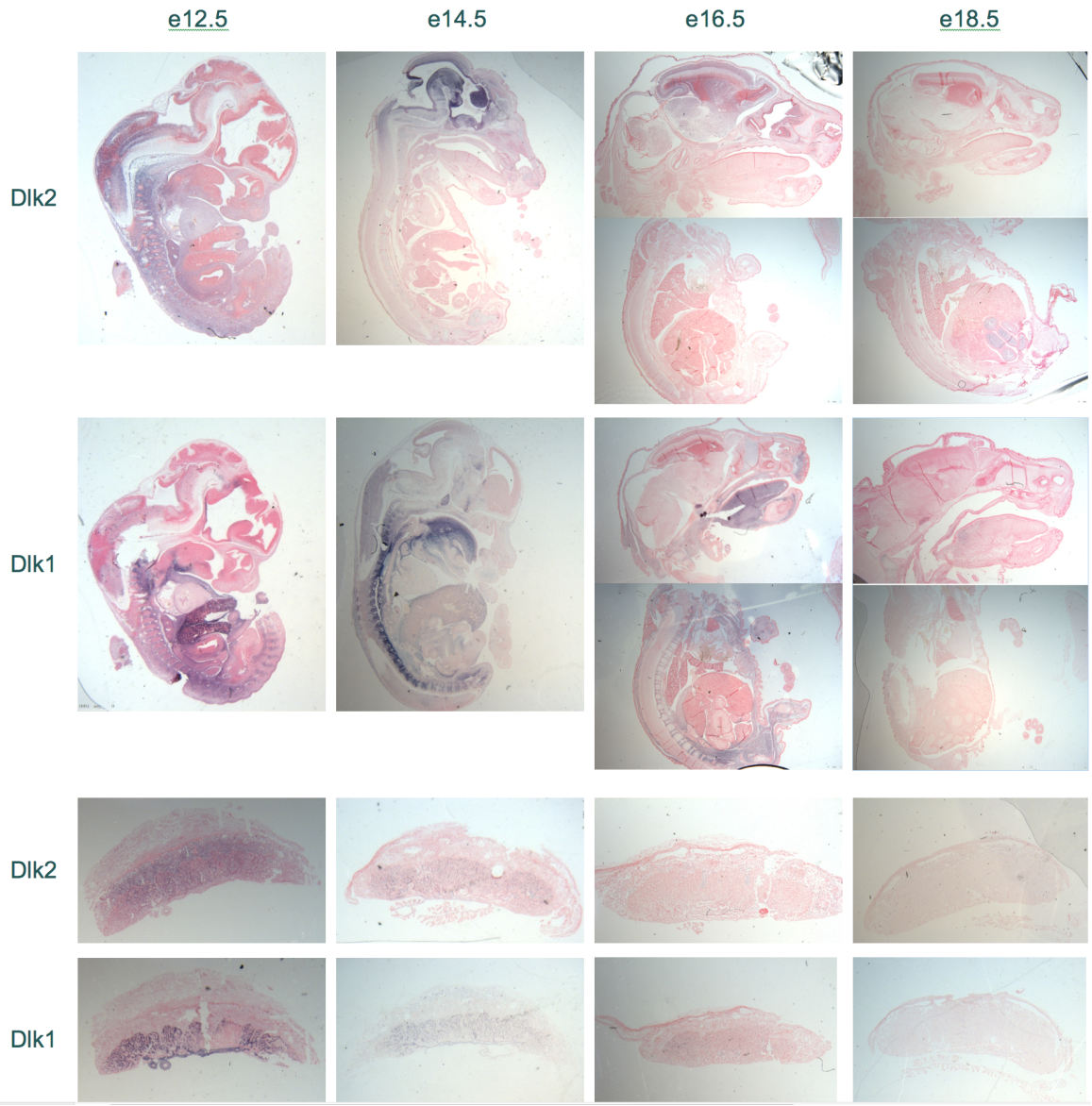

Fig. 3.2 ***In situ* hybridizations of *Dlk1* and *Dlk2* in developing murine wild-type embryos and placentae**
Staining performed at embryonic day 18.5 (e18.5), e16.5, e14.5 and e12.5. Sense controls shown in the Appendix A.2. N = 2, 3, 1, 2 for *Dlk1 in situ* hybridizations at e12.5, e14.5, e16.5 and e18.5, respectively, for embryos and placentae. N=3, 4, 1, 3 for *Dlk2 in situ* hybridizations at e12.5, e14.5, e16.5 and e18.5, respectively, for embryos. The same number of biological replicates was used for *Dlk2 in situ* hybridizations on placentae except at e14.5 where only 2 biological replicates had successful sense and antisense staining.

Tissue/organ		E12.5	E14.5	E16.5	E18.5
Adrenal gland	*Dlk1*	N.V	Strong exp.	Strong	None
	Dlk2	N.VC	None	None	None
Brain	*Dlk1*	MR	MR	MR	None
	Dlk2	MR	MR	MR	None
Cartilage	*Dlk1*	Intramembranous and endochondral	Intramembranous and endochondral	Intramembranous and endochondral	None
	Dlk2	Intramembranous and endochondral	None	None	None
Heart	*Dlk1*	Exp. throughout whole heart	Wall of right ventricle	None	None
	Dlk2	Exp. throughout whole heart	None	None	None
Intestine	*Dlk1*	Inner and outer epithelia	Outer epithelium	None	None
	Dlk2	Epithelia	None	None	None
Liver	*Dlk1*	Hepatoblasts	Hepatoblasts	None	None
	Dlk2	None	None	None	None
Lung	*Dlk1*	Endothelial cells	Endothelial cells of bronchioles	Endothelial cells at sites of branching & mesothelium	None
	Dlk2	Endothelial cells	None	None	None
Pancreas	*Dlk1*	PN/V	Acini	Weak	None
	Dlk2	N/V	None	None	None
Placenta	*Dlk1*	Endothelial cells in labyrinth zone	Endothelial cells in labyrinth zone	Weak exp. in labyrinth zone	None
	Dlk2	Labyrinthine trophoblast & giant cells	Labyrinthine trophoblast	Weak exp. in Labyrinthine trophoblast	None
Nasal cavity	*Dlk1*	None	None	None	None
	Dlk2	Epithelium	Epithelium	Epithelium	None
Somites	*Dlk1*	Dermomyotome, myotome, sclerotome	Dermomyotome, myotome, sclerotome	N/A	None
	Dlk2	Dermomyotome, myotome, sclerotome	None	N/A	None
Stomach	*Dlk1*	Mucous membrane lining	Mucous membrane lining	None	None
	Dlk2	Mucous membrane lining	None	None	None
Skeletal muscle: tongue, diaphragm & intercostal muscles	*Dlk1*	MF	MF	MF	Tg. MF
	Dlk2	None	None	None	None
Thymus	*Dlk1*	N/V	Surrounding epithelium	Weak	None
	Dlk2	N/V	None	None	None

Fig. 3.3 **Summary of *Dlk1* and *Dlk2* expression in embryonic development**
Expression patterns were observed in the *in situ* hybridisations conducted on wild-type embryos at various embryonic stages (figure 3.2). Cell types were identified using the Kaufman Mouse Atlas [111]. N/A – tissue/organ is not yet present or has been lost. N/V – structure not visible in all sections at embryonic stage. Acronyms used: ant. – anterior, exp. – expression, MF. – myofibers, MR. – multiple regions, PLVB. – primordium of lumbar vertebral body, post. – posterior, R. – right, tg. – tongue.

creas at e12.5. Staining was only performed in the regions displayed in figure 3.2. Although investigating expression of both genes throughout entire embryos would be ideal, the ventral sagittal sections used are sufficient to investigate the relationship between *Dlk1* and *Dlk2*.

3.3 *Dlk1* and *Dlk2* have distinct but overlapping expression during embryogenesis

The ISHs show that *Dlk1* and *Dlk2* are expressed in all germ layers and have distinct expression patterns with some overlap in developing murine embryos and placentae (figure 3.3). As *Dlk2* expression is increasingly restricted to the brain throughout embryogenesis (figure 3.2), a more detailed analysis of *Dlk2* and *Dlk1* expression throughout development was conducted on the brain alone (figure 3.4).

Brain region		E12.5	E14.5	E16.5	E18.5
Cerebellar primordium	*Dlk1*	N/A	None	None	None
	Dlk2	N/A	Intraventricular portion	Strong	None
Choroid plexus	*Dlk1*	**Weak exp.**	**Weak exp.**	N/V	None
	Dlk2	**Stronger exp.**	**Strong exp.**	N/V	None
Corpus striatum	*Dlk1*	None	None	None	None
	Dlk2	None	Moderate	Strong	None
Diencephalon	*Dlk1*	**Hypothalamus & dorsal thalamus**	**Hypothalamus & optic recess**	None	None
	Dlk2	**Dorsal thalamus**	**Thalamus & hypothalamus**	Thalamus	None
Forth ventricle	*Dlk1*	None	None	None	None
	Dlk2	Roof	Roof	Posterior horn	None
Medulla oblongata	*Dlk1*	**Stochastic exp.**	None	N/V	None
	Dlk2	**Constitutive exp.**	Dorsal part	N/V	None
Midbrain	*Dlk1*	**Roof, pons midbrain jxn**	None	None	None
	Dlk2	**Roof, pons midbrain jxn, wall**	Ventral part & roof	Right lateral wall	None
Neopallial cortex	*Dlk1*	None	None	Weak	None
	Dlk2	Roof (weak)	Roof	Strong	None
Pituitary	*Dlk1*	**Vascular diff. – dev. into R. pch.**	**Ant. & post.**	Lateral extremity	None
	Dlk2	**Vascular diff. – dev. into R. pch. & infundibulum**	**Ant. & post.**	None	None

Fig. 3.4 **Summary of *Dlk1* and *Dlk2* expression in embryonic murine brains**
Expression patterns were observed in the *in situ* hybridisations conducted on wild-type embryos at various embryonic stages (figure 3.2). Rathke's pouch develops into the anterior pituitary. The infundibulum develops into the *pars nervosa*. Brain regions were identified using the Kaufman Mouse Atlas [111]. N/A – structure has not formed yet. N/V – structure not visible in all sections at embryonic stage. Acronyms used: ant. – anterior, dev. – develops, diff. – differentiation, exp. – expression, jxn. – junction, post. – posterior, R. pch. – Rathke's pouch.

Dlk1 and *Dlk2* are co-expressed in the choroid plexus, diencephalon, medulla oblongata, mid-brain, neopallial cortex, and pituitary (figure 3.4) at e12.5. As the embryo ages *Dlk1* expression is increasingly reduced in the brain, and expression of both genes is lost between e16.5 and e18.5. As *Dlk2* is likely the ancestral gene (section 2.1), it is most likely that the functions *Dlk1* carries out in the areas of co-expression are its more ancient ones. *Dlk1* and *Dlk2* are also co-expressed at e12.5, in liver hepatoblasts, lung endothelial cells, intestinal epithelia, and the somites and the heart.

Their roles in areas of overlapping expression are likely to be ancient. Given the evidence that stem cell regulation is the ancestral function of *Dlk1* (section 1.4.1), it is likely that they are regulating cellular differentiation in these regions. Furthermore, unpublished work in zebrafish suggests that *Dlk2* limits differentiation of stem cells in a manner similar to *Dlk1* during embryonic neurogenesis (pers. comm. Dr. Ben Shaw). Thus it is a fair hypothesis that both genes are regulating stem cells in these tissues at given time points. However, more interesting questions arise from this conclusion: for example, why does expression of these genes overlap in the first place, and why is their co-expression lost?

The evolution of imprinting may answer these questions. Dosage is thought to be highly important for the functions of these genes. Not only do experimental alterations of dosage in mice have extreme phenotypic consequences [45, 51], but all fish studied have only one copy of each gene despite whole genome duplication events (section 2.1); the extra copies appear to have been actively lost. *Dlk2* is biallelically expressed and, although its dosage cannot be altered in the same way as *Dlk1* can be since it is not imprinted [78], its expression is perhaps more robust. In scenarios where regulation of stem cell differentiation is potentially more important, such as in brain development, *Dlk2* expression would perhaps have been more likely selected for. The early *Dlk1* expression could be reflective of redundancy. This hypothesis could only really be tested with ISH of *Dlk1* on *Dlk2-/-* mice at the same stages in the brain.

The restriction of *Dlk1* to the other developing tissues could be consistent with this hypothesis. Biallelic, but not monoallelic, expression of *Dlk1* was sufficient to regulate postnatal neurogenesis [78], and so it is possible that biallelic *Dlk1* dosage is necessary for stem cell regulation in other tissues – if that is indeed its function in the described developing tissues. However, *Dlk1* is imprinted and although there is some preliminary evidence that suggests that *Dlk1* imprinting is lost in some progenitor cells in the later stages of developing intestines [217], this observation has not been replicated across other developing tissues. Most studies look at the imprinting status of bulk tissues [21, 155, 174, 220], of which progenitor cells form a tiny portion, and so subtle cellular specific loss of imprinting may have been missed. If *Dlk1* does gain biallelic expression in stem cell niches during development, then it is reasonable for *Dlk2* expression to have been lost from the sites of co-expression.

Nuanced study of *Dlk1* imprinting status at the cellular level in developing, and indeed postnatal, tissues would help resolve this hypothesis. The findings of this work would also give further crucial insight into whether stem cell regulation is truly the ancestral function of *Dlk1*. If *Dlk1* is biallelicly expressed in most non-neural stem cells it is likely that stem cell regulation is the ancestral function. However, if *Dlk1* is not then this suggests that there is a more recently evolved stem cell role for the imprinted *Dlk1* in mammals.

The default state for *Dlk1*, if expressed, is to be imprinted; this state was established in the germ-line [187]. It could take developmental time for *Dlk1* to gain biallelic expression. *Dlk2* might retain early expression patterns in these tissues to ensure that correct DLK dosage is present. It would provide mirror image redundancy to the hypothesis outlined above for the roles of *Dlk1* and *Dlk2* in the brain. As before, *Dlk2* expression is lost at later stages

of development in wild-type embryos. The redundancy hypothesis can only be properly explored with expression analysis of *Dlk2* in *Dlk1-/-* embryos.

Dlk1 is also exclusively expressed in some tissues: the adrenal glands, the pancreas, and the thymus (figure 3.3). These are also endocrine tissues. Metabolic functions are hypothesised as being eutherian specific (section 1.4.3). Imprinting is known to be eutherian specific [68]. Perhaps expression in these tissues co-evolved with imprinting? There is no ideal functional experiment to test this hypothesis, but its validity could be inferred by looking at *Dlk1* (and *Dlk2*) expression patterns in other vertebrates.

In conclusion, the distinct, but overlapping, expression patterns of *Dlk1* and *Dlk2* throughout murine development are likely reflective of functions of the genes. The roles the genes play in tissues with overlapping expression are more likely to be ancient ones. *Dlk2* seems to be more dominantly expressed in the developing brain. Its biallelic expression may provide a more robust initiator of DLK gene signalling. Whereas imprinted expression of *Dlk1* in this tissue arises for redundancy and, perhaps, to fine tune the DLK gene activity levels. However, it is also possible that the *Dlk1* expression observed in the developing brain is biallelic in the stem cell niches, which would alter the interpretation of this data. Further analysis of *Dlk1* imprinting at the single cell level in these developing tissues will be necessary to probe these hypotheses.

Analysis of *Dlk1* and *Dlk2* expression patterns in other vertebrates would give insights into all the hypotheses that this ISH data generates. If expression of *Dlk1* in endocrine organs is restricted to eutherian mammalians, then its most likely that this expression co-evolved with imprinting. If *Dlk1* is expressed throughout vertebrates in these tissues perhaps the function is more ancestral and related to the regulation of stem cells. Seeing where *Dlk1* and *Dlk2* expression overlaps, and (or, if it) is lost during development of non-mammalian species, would also be interesting. This would give insights into whether the proposed redundancy is related to imprinting. Should the pattern of expression observed in mice be consistent throughout vertebrates, then perhaps *Dlk1* and *Dlk2*, sharing an ancient stem cell regulatory function, have specialised into different tissues.

4 Quantitative analysis of *Dlk1* and *Dlk2* expression

ISH of *Dlk1* and *Dlk2* is useful as it allows assessment of expression patterns with cellular resolution. However, this approach is not quantitative and so gives little insight into which gene is expressed predominantly in a given region of co-expression. Quantitative real-time PCR (qPCR) is perhaps the gold standard test of gene expression. Assessing *Dlk1* and *Dlk2* expression using qPCR would thus generate useful insights into their relative expression levels.

Dr. Lisa Hulsman and Billy Watkinson generated a large tissue panel for qPCR analysis for a different project in our group. They kindly gifted me aliquots of excess samples to test for DLK gene expression. These samples were derived from wild-type hybrid reciprocal hybrid mice allowing quantification of imprinting and assessment of strain effects. However my study focused on the relative quantification of the two genes. For each sample, three biological replicates were taken from C57BL/6J X CAST/EiJ crosses, and three from the reciprocal crosses. For the purposes for my analysis, I assumed that there was no strain effect on either *Dlk1* or *Dlk2* expression and the samples were treated equally, regardless of cross origin. Reassuringly, Billy Watkinson observed no strain effect for *Dlk1* when he performed pyrosequencing based analysis (of *Dlk1*) on the same panel. He did not perform pyrosequencing on *Dlk2*.

The dataset consists of various tissues at three different developmental time points: e16.5, postnatal day 7 (p7), and p60. There was an overrepresentation of different brain regions in the postnatal stages. This is highly advantageous given that *Dlk2* is highly expressed in the embryonic brain. Although *Dlk1* expression is lost at e18.5, mRNA expression returns in the early postnatal period [78]. It would not be surprising therefore, to detect *Dlk2* expression in postnatal tissues. Another advantage of the panel is that there is overlap between the selected e16.5 tissues and the ISH panel. This should allow for validation of the e16.5 embryonic ISH data.

Primers were designed to target late exons in *Dlk2* and *Dlk1*. Although these regions possess single nucleotide polymorphisms (SNPs) between the C57BL/6J and CAST/EiJ genomes, they were largely ignored for the qPCR experiment, as the primers were desired to target regions of homology between the two genomes. However, the PCR products were chosen so that they included at least one SNP. This would enable the same samples to be assessed by pyrosequencing after qPCR. Pyrosequencing is used to assess the imprinting status of a gene. Although no imprinted gene screen has ever detected *Dlk2* [21, 155, 174, 220], many of the screens do not sufficiently validate and independent validation attempts suggest a high false positive rate. Confirmation of the imprinting status of *Dlk2* by a targeted experimental approach would thus be valuable. Although such an experiment was attempted during this project, it failed due to technical reasons.

4.1 TBP was selected as the control

To ensure that differences in expression between two genes or tissues are genuine, qPCR data are normally normalised to a housekeeping gene [118]. Theoretically housekeeping genes are vital for cell function and are thus expressed at constant levels between tissues [118]. By normalising target genes to housekeeper genes technical variability between samples, introduced for example through unequal efficiencies in RNA extraction or cDNA synthesis,is theoretically accounted for [118]. Housekeeper gene expression profiles have been published in response to this [126].

Some consider housekeeping gene normalisation to be an over-simplification of the underlying biology: there may be tissue specific variances in housekeeping gene expression and with housekeeping gene normalisation noise is unintentionally introduced [237]. New approaches normalising to the geometric mean of several housekeeper genes have thus been proposed [237]. However, members of our group have observed that geometric mean normalisation also introduces noise and may obscure subtle differences in relative gene expression.

It is therefore best to test the expression of several candidate housekeeping genes for each experiment. TATA binding protein (*Tbp*), 18s ribosomal RNA (*18s*), and *Actin* were chosen as candidate housekeeping genes based on colleague advice. In the group, *Tbp* displayed the most consistent expression between the tissues of all three genes (figure 4.1). Furthermore, it had the lowest expression. Normalising against highly expressed genes can sometimes obscure differences in relative expression of lowly expressed genes, and *Dlk1* and *Dlk2* are

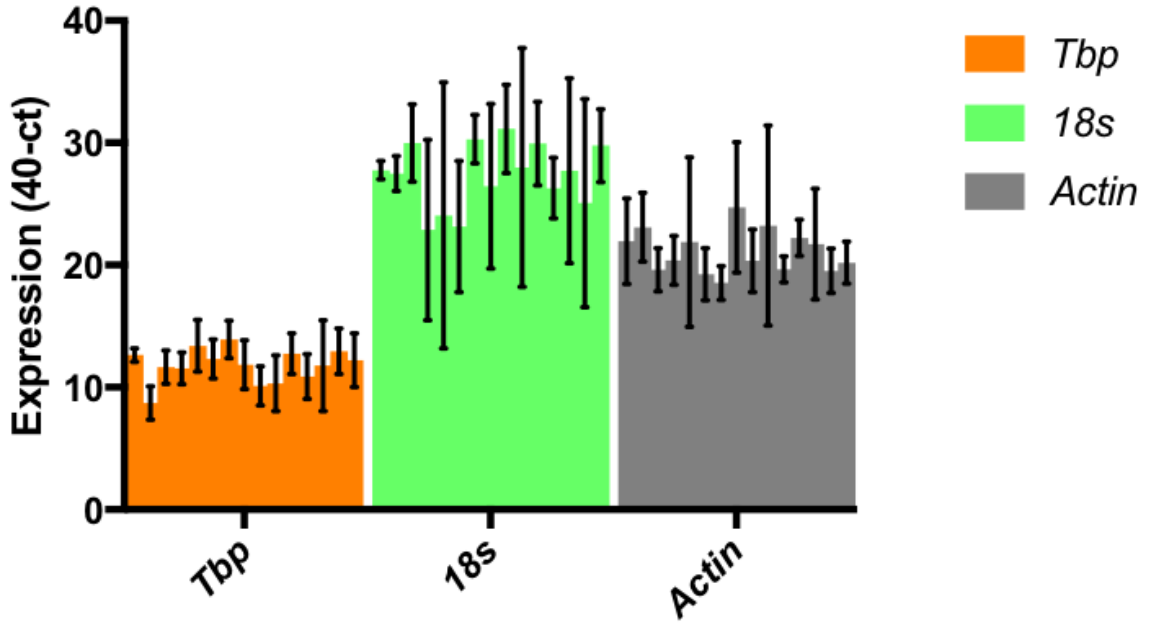

Fig. 4.1 **Expression levels of candidate housekeeper control genes in tissues investigated in sections 4.2, 4.3, and 4.4**
Expression (40-ct) of Tata binding protein (*Tbp*), 18s ribosomal RNA (*18s*), and *Actin*. ct values are the raw read out of relative gene expression from the qPCR machine and were processed as described in section 8.3.13. Expression tested on e16.5 brain, liver, and placenta; p7 and p60 brainstem, cerrebellum, cortex, hippocampus, and hypothalamus; and p7 liver, and muscle.

expected to be expressed in the low to intermediate range. *Tbp* was thus selected as the housekeeper gene for qPCR normalisation.

4.2 *Dlk2* is expressed more than *Dlk1* in e16.5 brain

qPCR investigated *Dlk1* and *Dlk2* gene expression in e16.5 brain, liver and placenta. Expression of both genes was detected in all tissues (figure 4.2). Expression of both genes was also detected in the brain and placenta of e16.5 embryos using ISH (section 3.3). This suggests that the ISHs are accurate. However, no expression of either gene was observed in e16.5 livers by ISH.

There are several explanations for this discrepancy: there was a false detection in the qPCR, or, more likely the qPCR is more sensitive than the ISH. This emphasises the value of taking both approaches when conducting expression analyses. Other hypotheses explaining

the lack of consistency between the ISHs and qPCR in e16.5 livers are biological in nature.

The ISH were performed on C57BL/6J embryos whereas the qPCR was performed on samples derived from C57BL/6J X CAST/EiJ hybrids. Perhaps gene expression in the liver is influenced by genetic background. However, this is unlikely given that the range of *Dlk1* and *Dlk2* expression in the e16.5 livers is broadly consistent between C57BL/6J X CAST/EiJ and CAST/EiJ X C57BL/6J derived samples. This similarity of *Dlk1* and *Dlk2* expression ranges between the reciprocal crosses is also consistent across all tissues. Nevertheless, exploring the data from the genetic background perspective reduces the sample size for each condition and more subtle trends could emerge were this number of animals studied increased.

The unlikelihood that genetic background accounts for the presence of *Dlk1* and *Dlk2* is detected in e16.5 livers by qPCR but not ISH, means that something else may be occuring. Notably both *Dlk1* and *Dlk2* display high ranges of expression in the e16.5 livers (assessed by qPCR). Perhaps expression of these genes is being dynamically lost during the e16.5 period, which would be unsurprising given thedynamic downregulation that is occurring during the e16.5-e18.5 time-window (section 3.2). No dissections are carried out at identical periods of embryogenesis due to precise differences in the times of fertilisation. Embryos from different litters are thus be slightly older or younger than each other, even if they are considered to be in the e16.5 range. If *Dlk* gene expression is being dynamically lost in the e16.5 period, variance in embryo age might result in populations with retained or lost *Dlk* gene expression.This hypothesis is supported by the fact that samples that express high levels of *Dlk1* also express high *Dlk2*. The same pattern of *Dlk1* and *Dlk2* expression levels may also suggest coordinate regulation of these genes; indeed this may be responsible for the widespread loss of *Dlk1* and *Dlk2* expression between e16.5 and e18.5. The absence of any detected expression by ISH in the liver at e16.5 may be an artefact of only testing one biological replicate. Although ISH was performed on other biological replicates at e16.5 it was not successful. However, if the ISHs were repeated they may reveal inter-individual variation in absence or presence of *Dlk1* and *Dlk2* gene expression in the e16.5 liver.

The qPCR suggests that *Dlk2* is expressed at a higher level in 16.5 brains than *Dlk1* (figure 4.2). This is not surprising given that ISHs suggest *Dlk2* is more widely expressed than *Dlk1* at this stage (section 3.3). At e16.5, *Dlk1* is only expressed in the lateral extremity of the pituitary and in the neopallial cortex. Whereas *Dlk2* is expressed in the cerebellar primordium, the corpus striatum, the thalamus, the posterior horn of the forth ventricle, the right lateral wall of the midbrain, and the neopallial cortex. Given the widespread expression

of *Dlk2* (section 3.3) it is surprising how small its difference in level is compared to *Dlk1* expression. This might suggest that *Dlk2* is expressed at lower levels in more tissues, whereas *Dlk1* is highly expressed from just the lateral extremity of the pituitary and in the neopallial cortex. It is also possible that a brain region not covered by the ISHs sections (section 3.2) is responsible for relatively high *Dlk1* expression at e16.5.

In an opposing expression pattern, *Dlk1* is expressed much more strongly than *Dlk2* in the e16.5 placenta (figure 4.2). ISHs suggest that, at e16.5, *Dlk1* is expressed in the labyrinth zone, and *Dlk2* in the Labyrinthine trophoblast . Interestingly, the labyrinth zone is the largest placental zone at e16.5 [46]. The qPCR is performed at the level of the whole tissue and hence may reflect this greater tissue representation at this stage. These findings suggest that Dlk1 and Dlk2 are acting in different functional zones within the placenta and that they may function independently of each other in that tissue. However, it is noteworthy that given that the ISHs show dramatically stronger staining in their respective zones e12.5 and e14.5 placentas is likely a better initial use of resources. Given that the ISHs show dramatically stronger staining at e12.5 and e14.5 compared to e16.5 it is most likely that both genes carry out their main functions during these periods.

It is interesting to speculate on the function of both genes during placental development. No other tissue has *Dlk1* and *Dlk2* expressed so clearly in adjacent cell types. Given that *Dlk2* is thought to be ancestral to *Dlk1* (section 2.1) and that the oldest *Dlk1* gene function is probably stem cell regulation, it is reasonable to hypothesise that *Dlk2* may also play a regulatory role in stem cells. Perhaps both genes are carrying out this function in the placenta but instead of different *Dlk1* isoforms working together in adjacent (as in postnatal neurogenesis [78]), the gene paralogs are signalling with each other to carry out their placental function. However, there are fewer 'stem cells in the labyrinthine zone than in the spongiotrophoblast zone [46]. This might suggest that *Dlk2* evolved an unknown additional function, independent to stem cell regulation, for the spongiotrophoblast. In this scenario, *Dlk1* would likely still act as a stem cell regulator via traditional signalling methods, thought to be independent of *Dlk2*. Further experiments will be necessary to probe these hypotheses.

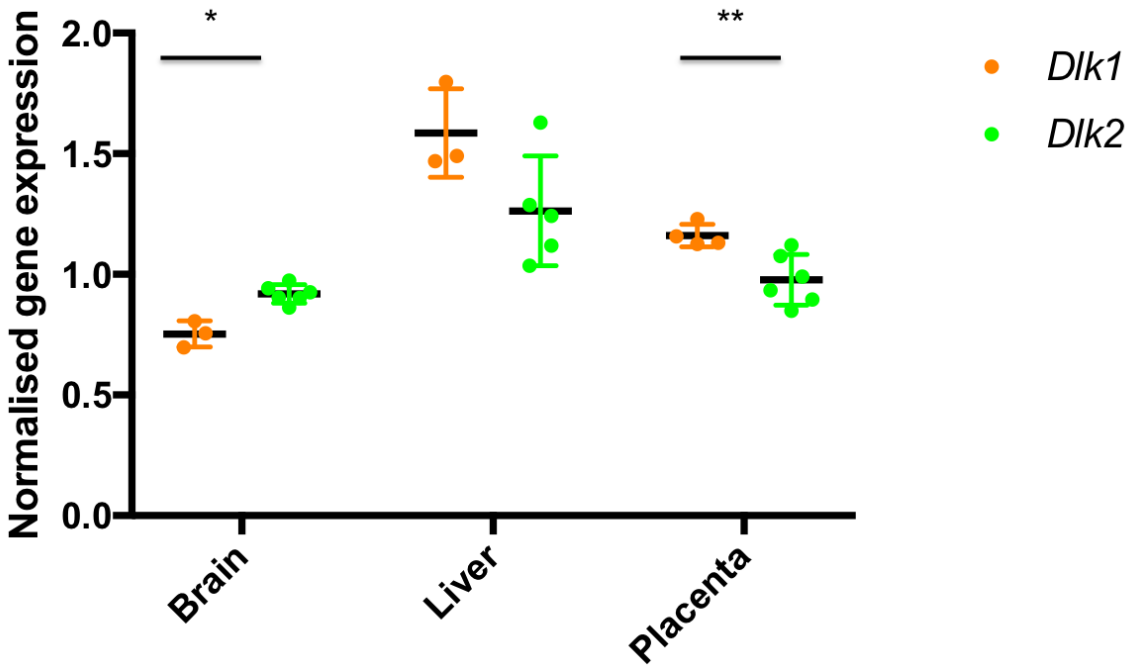

Fig. 4.2 **Normalised expression of *Dlk1* and *Dlk2* in e16.5 brain, liver, and placenta** Expression was was calculated as: 40 - ct to ensure a positive integer. Each individual expression value (40 - ct) of either *Dlk1* and *Dlk2* reflects the technical replicate mean for the expression data of either *Dlk1* or *Dlk2* in a given tissue normalised against the corresponding technical replicate mean of *Tpb* expression in the same tissue. ct values are the raw read out of relative gene expression from the qPCR machine and were processed as described in section 8.3.13. 6 biological replicates were examined for each tissue. Biological replicates were discarded from the analysis if technical replicates were of insufficient quality in either the target gene or *Tbp*: ct value differences less than 0.4 between technical replicates were considered to be of sufficient quality to use the biological replicate in the analysis. A minimum of 3 biological replicates were retained per tissue. Unpaired non-parametric Mann-Whitney tests were performed (GraphPad Prism V7) for expression levels of *Dlk1* and *Dlk2* in the brain (p=0.0238), liver (p=0.1429), and placenta (p=0.0095).

4.3 *Dlk2* is dominantly expressed in all tested P7 brain regions

Dlk1 and *Dlk2* mRNA expression were investigated in P7 brainstem, cerebellum, cortex, hippocampus, hypothalamus, liver, and muscle. Expression of both genes was detected in all tissues (figure 4.3), suggesting that *Dlk1* and *Dlk2* mRNA expression returns in the early postnatal period despite being almost completely lost at e18.5 (section 3.3). This is consistent with previous observations for *Dlk1* [78]. Interestingly, *Dlk2* expression levels are broadly consistent between the e16.5 brain and the various brain regions tested at P7. *Dlk1* expression, however, seems lower in the postnatal ages.

qPCR data is semi-quantitative and does not necessarily reflect the expression of the same gene at the protein level. The half-life of the mRNA is not taken into account here and the protein may or may not be translated in cell types analysed. The mRNA may have shorter or longer half lives than expected, and so may be absent or more abundant than expected, respectively. As proteins are generally responsible for gene function, qPCR data alone is not sufficient to infer the quantitative function of a given gene. Further functional experiments, of *Dlk2* in particular, will thus be necessary.

Dlk2 is predominantly expressed in all studied brain regions, whereas the two genes are expressed equally in the liver and muscle (figure 4.3). *Dlk2* is probably ancestral to *Dlk1* (section 2.1), and the most ancient function of *Dlk1* is likely stem cell regulation (section 1.4.1). Therefore perhaps both genes are regulating stem cell niches in all tissues with *Dlk2* playing a predominant role in the p7 brain. Unpublished characterisation of *Dlk2*-/- zebrafish by Dr. Ben Shaw, suggest that *Dlk2* does negatively regulate neurogenesis in fish (section 7.3), in a manner analogous to *Dlk1* regulation of various stem cell niches in mice [78].

However, in the absence of expression data for a comprehensive range of additional postnatal murine tissues, such as muscle, kidney, spleen, lung, and more, it is an assumption to conclude, as above, that *Dlk2* displays widespread expression throughout postnatal stem cell niches. Perhaps *Dlk2* is exclusively expressed in the brain, postnatally. In this scenario, it would be likely that *Dlk1* and *Dlk2* both play key roles in neural stem cells (and that this is the ancestral function of the genes). Throughout vertebrate, and in particular mammalian, evolution, additional functions emerged and diverged, with *Dlk1* still performing stem cell regulation in a range of tissues (even as an imprinted gene) and *Dlk2* gaining new and yet unknown functions. Further experiments are necessary to identify where *Dlk2* is expressed

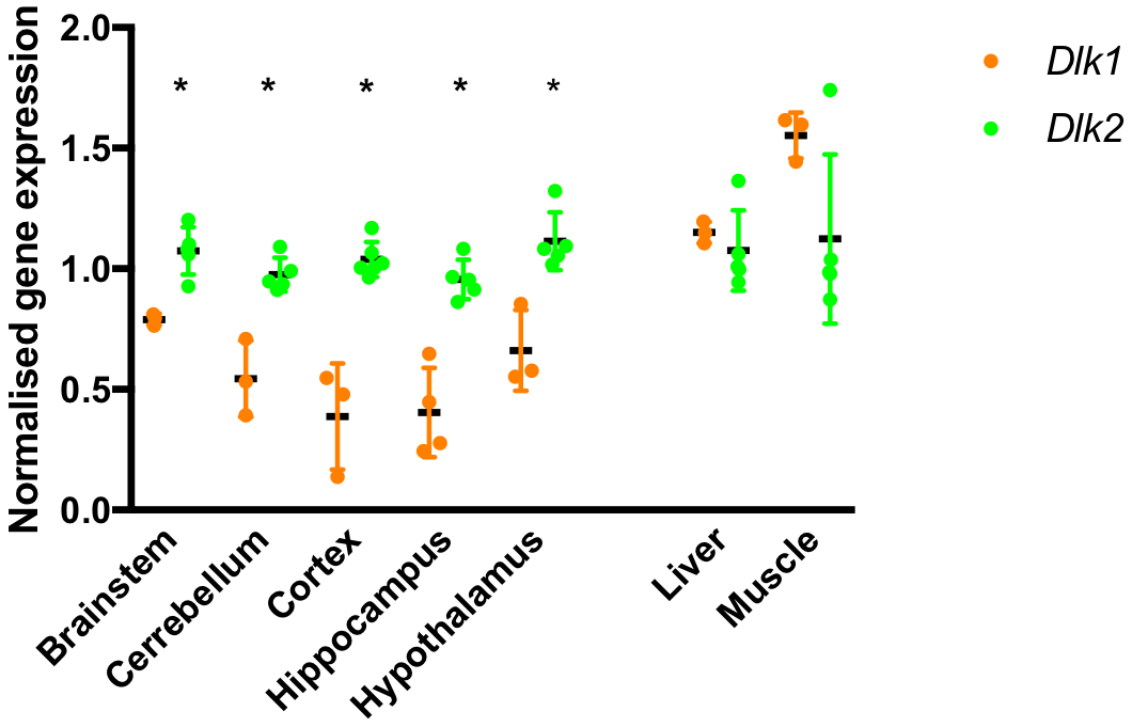

Fig. 4.3 **Normalised expression of *Dlk1* and *Dlk2* in p7 brainstem, cerebellum, cortex, hippocampus, hypothalamus, liver, and muscle**
Expression was was calculated as: 40 - ct to ensure a positive integer. Each individual expression value (40 - ct) of either *Dlk1* and *Dlk2* reflects the technical replicate mean for the expression data of either *Dlk1* or *Dlk2* in a given tissue normalised against the corresponding technical replicate mean of *Tpb* expression in the same tissue. ct values are the raw read out of relative gene expression from the qPCR machine and were processed as described in section 8.3.13. 6 biological replicates were examined for each tissue. Biological replicates were discarded from the analysis if technical replicates were of insufficient quality in either the target gene or *Tbp*: ct value differences less than 0.4 between technical replicates were considered to be of sufficient quality to use the biological replicate in the analysis. A minimum of 3 biological replicates were retained per tissue. Unpaired non-parametric Mann-Whitney tests were performed (GraphPad Prism V7) for expression levels of *Dlk1* and *Dlk2* in the brainstem (p=0.0357), cerebellum (p=0.0357), cortex (p=0.0238), hippocampus (p=0.0159), hypothalamus (p=0.0357), liver (p=0.2500), and muscle (p=0.2500).

postnatally and what its functions are.

If *Dlk2* is found to regulate neurogenesis in mice, then this expression data still may not be sufficient to fully interpret the interplay between *Dlk1* and *Dlk2*. *Dlk1* unequivocally regulates postnatal neurogenesis in mice [78], however *Dlk2* is predominantly expressed, even in the brain regions containing the postnatal neurogenic niches (figure 4.3). Ferron et al. showed that *Dlk1* regulates postnatal neurogenesis via the interaction of two different DLK1 isoforms [78]. They also demonstrated that the signalling takes place independently of NOTCH, but were unable to fully determine the gene's interacting partners [78]. Could DLK2 be playing such a role? If so, are the observed expression patterns (figure 4.3) of both genes at P7 reflective of tissues in which they cooperate to regulate differentiation of stem cells, with each gene playing a cell type specific role within the niche? Alternatively, the expression patterns may reflect redundancies. Perhaps *Dlk2* functions predominantly in the brain with weak *Dlk1* expression as a 'back-up'; the situation being reversed in other co-expressing somatic tissues such as muscle, where there is a slight statistically non-significant bias towards*Dlk1* expression.

4.4 *Dlk1* and *Dlk2* show similar expression levels in most brain regions at P60

Despite significant preferential expression of *Dlk2* throughout the P7 brain, expression levels between *Dlk1* and *Dlk2* are more similar at P60. There is arguably a trend that *Dlk2* is still predominantly expressed in all tested brain regions but this is only statistically significant in the cerebellum and the cortex (figure 4.4).

Interestingly the decrease in the difference of expression between the two genes seems to come mostly from an increase in *Dlk1* levels in the brainstem, hypothalamus, and hippocampus. In addition, *Dlk2* seems to be moderately less expressed within a given tissue at p60 (figure 4.4) compared to p7 (figure 4.3).

Testing gene expression at given time points only indicates how a given gene is behaving at a particular moment in time; far more time points will need to be investigated to get an accurate understanding dynamic relationship between the expression of the two genes. Thus, the expression dynamics of *Dlk1* and *Dlk2* at e16.5 (figure 4.2), P7 (figure 4.3), and P60 (figure 4.4) may tentatively suggest dynamic gene behaviour meriting further investigation with

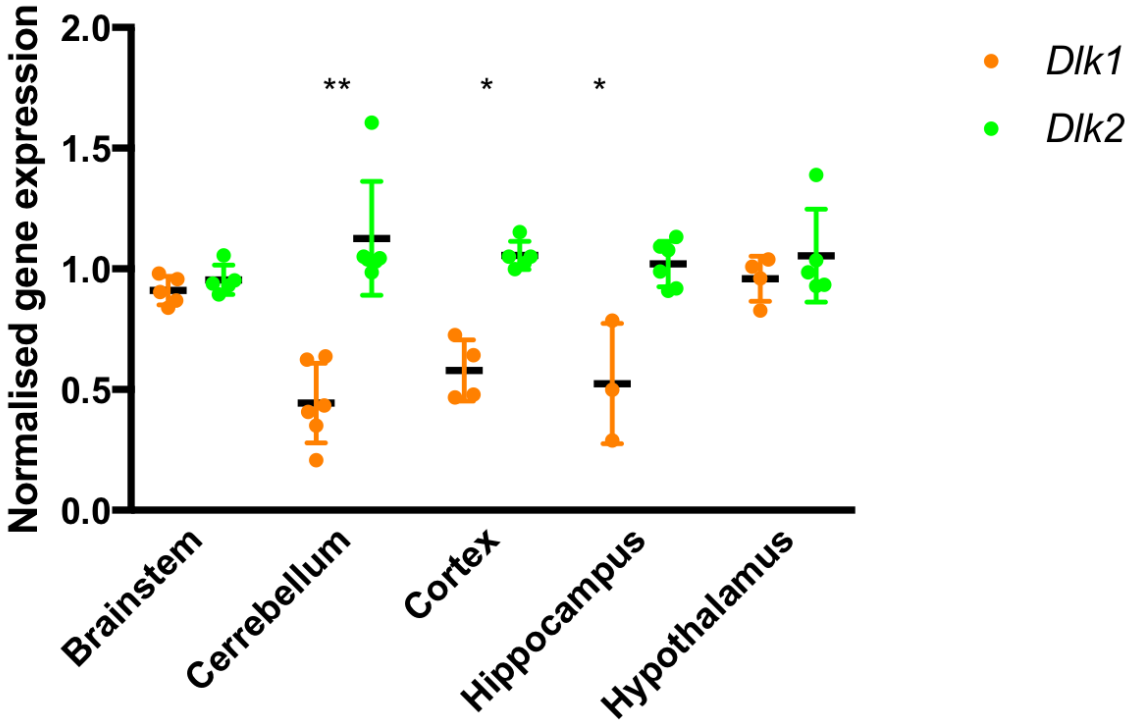

Fig. 4.4 **Normalised expression of *Dlk1* and *Dlk2* in p60 brainstem, cerebellum, cortex, hippocampus, and hypothalamus**
Expression was was calculated as: 40 - ct to ensure a positive integer. Each individual expression value (40 - ct) of either *Dlk1* and *Dlk2* reflects the technical replicate mean for the expression data of either *Dlk1* or *Dlk2* in a given tissue normalised against the corresponding technical replicate mean of *Tpb* expression in the same tissue. ct values are the raw read out of relative gene expression from the qPCR machine and were processed as described in section 8.3.13. 6 biological replicates were examined for each tissue. Biological replicates were discarded from the analysis if technical replicates were of insufficient quality in either the target gene or *Tbp*: ct value differences less than 0.4 between technical replicates were considered to be of sufficient quality to use the biological replicate in the analysis. A minimum of 3 biological replicates were retained per tissue. Unpaired non-parametric Mann-Whitney tests were performed (GraphPad Prism V7) for expression levels of *Dlk1* and *Dlk2* in the brainstem (p=0.5476), cerebellum (p=0.0022), cortex (p=0.0159), hippocampus (p=0.0238), and hypothalamus (p=0.9048).

similar expression analysis at more time points, and, perhaps more importantly, functional studies in *Dlk2* mutant mice.

Dlk2 and *Dlk1* may both regulate embryonic/early and adult neurogenesis, respectively. *Dlk2* expression is high in the embryonic brain and at P7 during periods of rapid brain expansion. However at P60 its expression is generally decreasing, as *Dlk1* expression generally increases. Testing the expression of both genes at later adult stages, such as P90, P240, and P365, would give insight into whether this trend continues and if the expression profile switches, so that *Dlk1* is the predominantly expressed gene. *Dlk1* is known to regulate adult neurogenesis. More primary neurospheres were derived from *Dlk1*-/- mice than wild type at p7 [78]. However by P60 wild-type mice yielded far greater numbers of primary neurospheres — this trend increased as the mice aged because the early expansion of the neurogenic niche experienced by the *Dlk1*-/- ultimately depleted their neural stem cell pool [78]. It would be interesting to perform similar experiments in *Dlk2*-/- mice. If *Dlk2* regulates embryonic neurogenesis then it would be likely that knocking out *Dlk2* would deplete the neurogenic niche very early in a murine life-cycle. In this scenario, mutant mice would produce far more embryonically derived neurospheres compared to wild-type controls, a phenotype expected to be reversed for neurospheres derived from stem cells harvested in the early postnatal period.

5 Generation of a *Dlk2-/-* mouse using CRISPR

A common approach to understanding the *in vivo* function of a gene is to knock it out, and study the phenotypic consequences. *Dlk2* was knocked-out in mice using the Clustered Regular Interspaced Short Palindromic Repeats/Cas9 (CRISPR) system with microinjection of guide RNAs and Cas9 protein into newly fertilised mouse zygotes. This was attempted twice for *Dlk2* with successful mutants being generated on the second attempt. The injections were performed by the Cambridge Stem Cell Institute.

Exon	**mRNA/ Prot.**	**No. zyg. trans.**	**No. mice born**	**No. muts.**	**Efficacy (%)**	**Mut. sum.**
2	Prot.	74	40	1	2.5	1*3bp del. (in-frame)
5	mRNA	28	12	0	0	N/A

Table 5.1 **Summary of the first CRISPR-Cas9 genome editing strategy**

The gRNAs are described in section 8.7. Acronyms used: Del. — deletion, Muts. — mutants, No. — number, N/A. — not applicable, Prot. — protein, Sum. — summary, Trans. — transferred, Zyg. — zygotes

The first attempt at CRISPR mediated genome editing of *Dlk2* was perhaps too ambitious. Exons 2 and 5 were targets (section 8.7). Experimental design was based around information presented at a genome editing course I attended run by CamBioScience with two guideRNAs (gRNAs) injected per F1 x F1 (CBA x C57BL6/J) hybrid zygote per site to increase the likelihood of large deletions. In addition, we attempted to test the difference between injecting Cas9 mRNA and Cas9 protein into the zygotes. Since the editing was unsuccessful in this

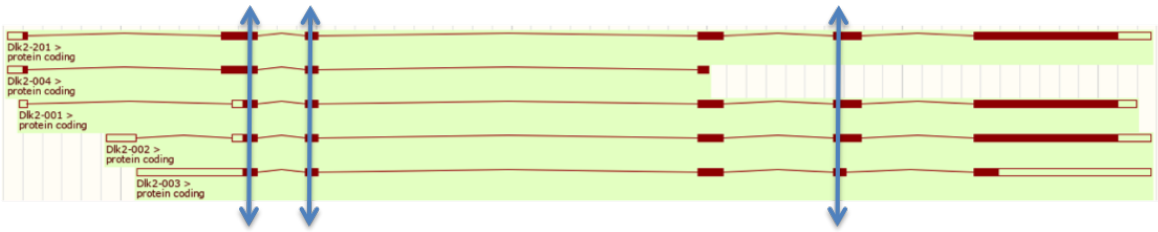

Fig. 5.1 **Locations of gRNA targets within *Dlk2* for CRISPR-mediated genome editing attempt 2**
The gRNAs targeted exon 2, 3, and 5 (blue arrows), which are present in all *Dlk2* isoforms. Exons 2 and 5 were also targeted in attempt one, although different gRNAs were used.

round (table 5.1) this additional assessment could not be made. However, in parallel Dr Celia Delahaye in the lab determined that the Cas9 protein gave higher frequency targeting than injected Cas9 mRNA. This was consistent with other studies (reviewed in [208]), hence Cas9 protein was used in the subsequent CRISPR attempts. Only one mutant animal was generated in the first attempt (table 5.1). The mutation was in-frame and so not followed up further. It is recognised that the nature of the genetic sequence surrounding the on-target cleavage site can promote undesirable in-frame mutations via microhomology-mediated end-joining [22, 179], however accurately predicting how prone a given genomic region is to this process is limited.

The second attempt at CRISPR was more successful. New gRNAs were designed to target exons 2, 3, and 5 (figure 5.1). The Stem Cell Institute performed pronuclear microinjection of the gRNAs and spCas9 protein into (CBA x C57BL6/J) F1 x F1 hybrid zygotes (section 8.7). The strategy was successful and multiple mutant animals were generated from each gRNA (table 5.2), with high efficiency.

Ex.	No. zyg. trans.	No. mice born	No. muts.	Effi-cacy (%)	Summary of mutations
2	66	12	10	15.15	5 compound heterozygotes
					3 with same 1bp substitution (possible strain specific SNP)
					1 in-frame homozygous deletion
					1 out-of-fram homozygous deletion
3	42	8	7	16.67	5 compound heterozygotes
					1 in-frame homozygous deletion
					1 out-of-frame homozygous deletion
5	54	7	6	11.11	1 in-frame homozygous deletion
					5 compound heterozygotes

Table 5.2 **Summary of the second CRISPR-Cas9 genome editing attempt**

The gRNAs are described in section 8.7. Acronyms used: Ex. — exon, No. — number, Trans. — transferred, w/. Zyg. — zygotes

5.1 Genetic characterisation of mutant mice

The majority of founder animals generated were compound heterozygotes (table 5.2) and were difficult to genotype accurately because of the poor signal-to-noise ratios in the DNA sequence traces. However, this ambiguity made such mice excellent founders as they are able to transmit both mutations to offspring. Thus the two most promising compound heterozygote females were selected per exon for breeding. 11 distinct mutations (figure 5.2) were identified in their offspring (table 5.3).

All but one of the mutations characterised in the F1 animals were out-of-frame. Many also were nonsense mutations introducing premature stop codons. Non-sense mediated decay generally targets and degrades transcripts that are prematurely translated [94, 114, 146], a system regularly taken advantage of in CRISPR mediated genome editing (reviewed in [175]). However, without experimental validation of tissues derived from homozygous animals the consequences of these mutations can only be speculated upon. All F1 animals were heterozygous and, depending on the number and genders of animals with each mutation, would require 1-2 further generations of breeding to generate homozygous animals. Breeding for further generations for 11 different mouse lines is highly time consuming and expensive. Thus a subset of animals was selected for further characterisation.

Exon	**Total no. animals inv.**	**Mutation**	**No. mice**
5	24	13bp del	4
		2bp del	3
		INDEL	1
		73bp del	7
		12bp del	5
		84bp del	3
		WT	1

Table 5.3 (continued)

Exon	Total no. animals inv.	Mutation	No. mice
3	14	16bp del	1
		2G INS	1
		1G INS	4
		1C INS	5
		WT	3
2	5	INDEL	1
		70bp del	3
		WT	1

Table 5.3 **The number of animals identified for each mutation in the genotyped F1 animals**

All animals were heterozygous for their given mutation. Acronyms used: del — deletion, INDEL — insertion and deletion, INS — insertion, inv. — investigated, WT — wild-type

5 mutations (figure 5.3) were chosen to validate whether DLK2 protein expression was ablated. Should all 5 lines successfully validate, only 2 will be taken forward for comprehensive phenotypic validation. 2 lines will be analysed to compare consistency of phenotype and as an additional control against off-target effects (section 5.2).

Initial selection of the 5 lines for validation was straightforward. Lines with in-frame mutations were discarded. One exon 2 mutant caused intron retention and produced a premature stop codon (figure 5.2). However, there was concern that exon 2 could simply be skipped with transcription initiation beginning on exon 3, especially as all the major protein domains are located from exon 3 onwards. This mutation was thus discarded.

From the remaining mutations, the 73bp deletion (DK73) in exon 5 was a very clear choice. Three animals with this mutation had eye defects in the F1 generation. In addition, one F1 animal, heterozygous for the DK73 mutation, was born large for its litter but failed to thrive in the early postnatal period, and displayed an abnormally shaped skull. It was sacrificed on postnatal day 14 (p14) in compliance with the Home Office regulations. To control

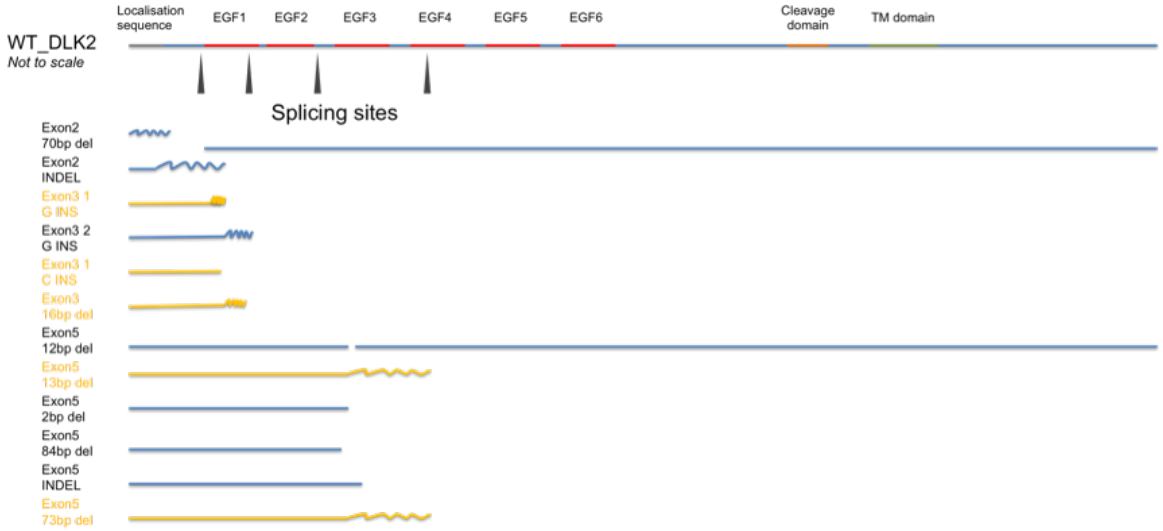

Fig. 5.2 **Summary of mutations identified in offspring of 6 founder *Dlk2* CRISPR mutants**
Predicted gross effects of 11 CRISPR generated mutations in *Dlk2* compared to the wild-type protein. Wiggly lines indicate that the mutant sequence diverges from the wild-type. The 70bp deletion in exon 2 may result in exon skippage that might produce a functional protein from exon 3 onwards. Exon 1 is not translated and so is not represented in this figure. Yellow mutations were pursued for phenotypic characterisation. *EGF – epidermal growth factor like repeat, INDEL – insertion and deletion, TM – transmembrane.*

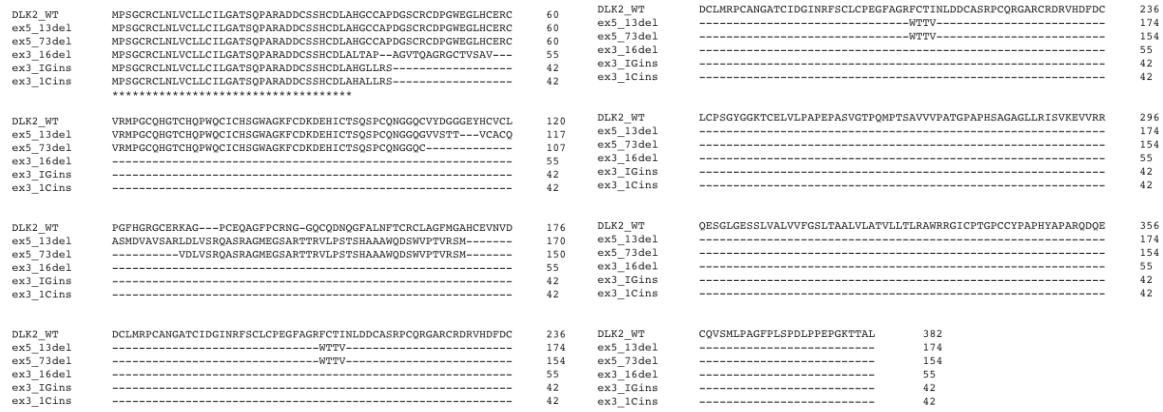

Fig. 5.3 **Alignment of the predicted amino acid sequences of the DLK2 mutants kept for phenotypic analysis against the wild-type protein**
Protein sequences were obtained by *in silico* translating the DNA sequences of the mutant animals with Transeq [184]. The amino acid sequences selected for this analysis stopped at the first premature stop codon as predicted by Transeq. Sequences were aligned using ClustalO (V1.2.4) [132].

for off-target effects, mutants without this defect were selected for colony establishment. A 13bp deletion in exon 5 (DK13) produced a truncated sequence of similar length (table 5.4) and divergence from wild-type to DK73 (figure 5.2) but its F1 animals did not display any abnormalities. This line was also selected.

The three remaining lines were selected from exon 3: DK1G, DK1C, and DK16. They all introduced premature stop codons that, if translated, would produce short peptides (table 5.4). The lines chosen produced the shortest predicted peptides from mutations in exon 2 or 3.

Line name	Exon	Mutation	Predicted protein length (aa)
DK13	5	13bp deletion	176
DK73	5	73bp deletion	154
DK16	3	16bp INDEL	55
DK1G	3	1G insertion	42
DK1C	3	1C insertion	42

Table 5.4 **Summary of the 5 lines with CRISPR mediated mutations in *Dlk2* kept for experimental validation**

Acronyms used: aa — amino acids, INDEL — insertion and deletion

5.2 *In-silico* analysis of predicted off-target effects

Arguably over-estimated [214, 239], off-target binding of gRNAs is a concern [82]; theoretically gRNAs may bind to other non-target regions of the genome, resulting in cleavage at off-target sites. This is especially alarming since single or double mismatches are tolerated [102], and off-target binding and cleavage has been observed experimentally in more sites than predicted computationally for given gRNAs [128]. However three or more interspaced mismatches eliminated detectable *Sp*Cas9 cleavage in the majority of loci studied in cell lines [103]and a comprehensive analysis in cell lines indicates that off-target cleavage is much

less efficient than on-target cleavage [128].

gRNA target	Off-target binding location	1 MM	2 MM	3 MM	4 MM
Exon 3	Exonic	0	0	1	16
	Intronic	0	0	3	43
	Intergenic	0	0	3	43
Exon 5	Exonic	0	0	0	4
	Intronic	0	0	3	42
	Intergenic	0	0	4	39

Table 5.5 **Summary of off-target binding, relative to number of sequence mismatches, for gRNAs targeting exon 3 and 5 of *Dlk2***

Off-target binding locations were found using the Wellcome Trust Sanger Institute Genome Editing database [97]. Acronyms used: MM — mismatches

During gRNA selection period, the Wellcome Trust Sanger Institute Genome Editing database [97] was used to identify off-target binding sites for the gRNAs that targeted exon 3 and exon 5 of *Dlk2*. 109 and 92 binding sites were predicted for exon 3 and exon 5, respectively (table 5.5); the majority of sites possessed 3 or more mismatches suggesting that *Sp*Cas9 off-target cleavage would be minimal [103]. Selected off-target sites in other mice mutated by CRISPR by the group, using the same protocol, show no off-target mutations (pers. comm. Dr. Celia Delahaye). However, there is still a risk that off-target binding would occur in this model. The backcrossing protocol (section 5.3) was designed to overcome this: off-target cleavage on other chromosomes can be segregated out via breeding.

Gene targeted	Chromosome	No. MM	Phenotypes
FBXO44	4	3	Creatinine levels increased in females, decreased in males.
SLC17A7	7	4	CNS defects.
LNX2	5	4	N/A
LRRC24	15	4	N/A
ADMTS3	10	4	N/A
SCAMP4	10	4	N/A
POGLUT1	6	4	Completely penetrant lethality: severely abnormal heart development, absent somites, embryo growth retardation, abnormal neural plate.
2900026A02-RIK	5	4	Increased startle reflex, decreased body length.
MAR-CKSL1	4	4	Abnormal neural tube, fertility & retina; severe neural and brain defects; pre-weaning lethality with incomplete penetrance.
FBXO6	4	4	N/A
CYR61	4	4	Abnormal heart morphology, abnormal placenta morphology, incomplete embryonic lethality during embryogenesis.
NARFL	17	4	HETs prenatal lethality with incomplete penetrance, HOMs embryonic lethality during organogenesis complete penetrance.
SYNE2	12	4	Abnormal retinal cell morphology (various) but normal vision, thick epidermis, decreased fibroblast cell migration.
ILDR2	1	4	Decreased circulating insulin & beta cell mass.
SENP6	9	4	Completely penetrant prenatal lethality.

Table 5.6 (continued)

Gene targeted	**Chromosome**	**No. MM**	**Phenotypes**
KDM4D	9	4	Decreased body weight, enlarged testis, abnormal spermatid morphology, abnormal male germ cell apoptosis, enlarged seminiferous tubules.
GM128	3	4	Decreased fertilization frequency.

Table 5.6 **The locations of predicted exonic off-target binding sites of the gRNA targeting *Dlk2* exon 3, and associated phenotypes**

Off-target binding locations were found using the Wellcome Trust Sanger Institute Genome Editing database [97]. Where possible, the phenotypes associated with mutations in the genes with predicted exonic off-target binding were obtained from the Mouse Genome Database [215] and the International Mouse Phenotyping Consortium [60]. Acronyms used: MM — mismatches, No. — number, N/A — not applicable because there was no phenotypic information available.

Another approach to assess for off-target effects was taken: the off-target binding in exonic regions was investigated in detail. Only exonic off-target cleavage was studied since it is likely to be more severe than intronic cleavage. The exonic off-target cleavage sites were explored for the gRNAs targeting *Dlk2* exon 3 (table 5.6) and exon 5 (table 5.7). Only one off-target binding site is located on chromosome 17 for both exon 3 and 5, suggesting that the majority of potential off-target alterations will be easily removed during the breeding plan (section 5.3). Furthermore, the phenotypes associated with mutations in the genes with the predicted off-target binding (obtained from the Mouse Genome Database [215] and the International Mouse Phenotyping Consortium [60] where possible) are fairly severe, even lethal in cases, and should be easily identified if present.

Gene targeted	**Chromosome**	**No. MM**	**Phenotypes**
SYNM	7	4	Abnormal behaviour and alterations in muscle.
TCT23	7	4	N/A
CAVIN2	1	4	Cardiovascular, adipose, and respiratory problems.
NFASC	1	4	Abnormal aging, behaviour, and growth.

Table 5.7 **The locations of predicted exonic off-target binding sites of the gRNA targeting *Dlk2* exon 5, and associated phenotypes**

Off-target binding locations were found using the Wellcome Trust Sanger Institute Genome Editing database [97]. Where possible, the phenotypes associated with mutations in the genes with predicted exonic off-target binding were obtained from the Mouse Genome Database [215] and the International Mouse Phenotyping Consortium [60]. Acronyms used: MM — mismatches, No. — number, N/A — not applicable because there was no phenotypic information available.

5.3 Breeding strategy

As discussed in section 5.1, five *Dlk2* mutant lines were chosen for validation and preliminary phenotypic analysis. Since maintaining five mutant mouse lines is very expensive, after validation by Western blotting (not conducted in this thesis) two lines will be selected for

comprehensive analysis. Since the mutations were generated in C57BL/6JXCBA hybrid animals the animals will need to be backcrossed onto a pure C57BL6/J genome for the final analysis. Nine generations of backcrossing (table 5.8) should be sufficient to transfer the mutation onto a pure C57BL6/J genome. This approach also has the advantage that any undesirable off-target effects, located on other chromosomes, should be segregated out at the end of the breeding plan.

Backcrossed generation	**Percentage C57BL/6J (%)**
N0	50
N1	75
N2	87.5
N3	93.75
N4	96.875
N5	98.4375
N6	99.21875
N7	99.609375
N8	99.8046875
N9	99.9023438

Table 5.8 **Percentage of genome as C57BL/6J for each generation of backcrossed mutant mice**

Homozygous biological material will be needed for validation by Western blotting. Thus the initial stages of the breeding plan (figure 5.2) will run concurrently for all 5 lines but the complete breeding plan will only be conducted on two.

The breeding plan has two parts. Backcrossing of a line until generation 9 (N9) will be maintained using heterozygous mutants. In addition, at generations 1 or 2 (N1 or N2, respectively) heterozygous animals will be mated together to generate homozygous offspring as material for molecular studies including Western blotting. These additional colonies can also be used for preliminary phenotypic analyses such as breeding ratios and pre- and post-natal weights. Together, these early generation analyses they will provide data that should influence which two lines are retained for comprehensive analysis.

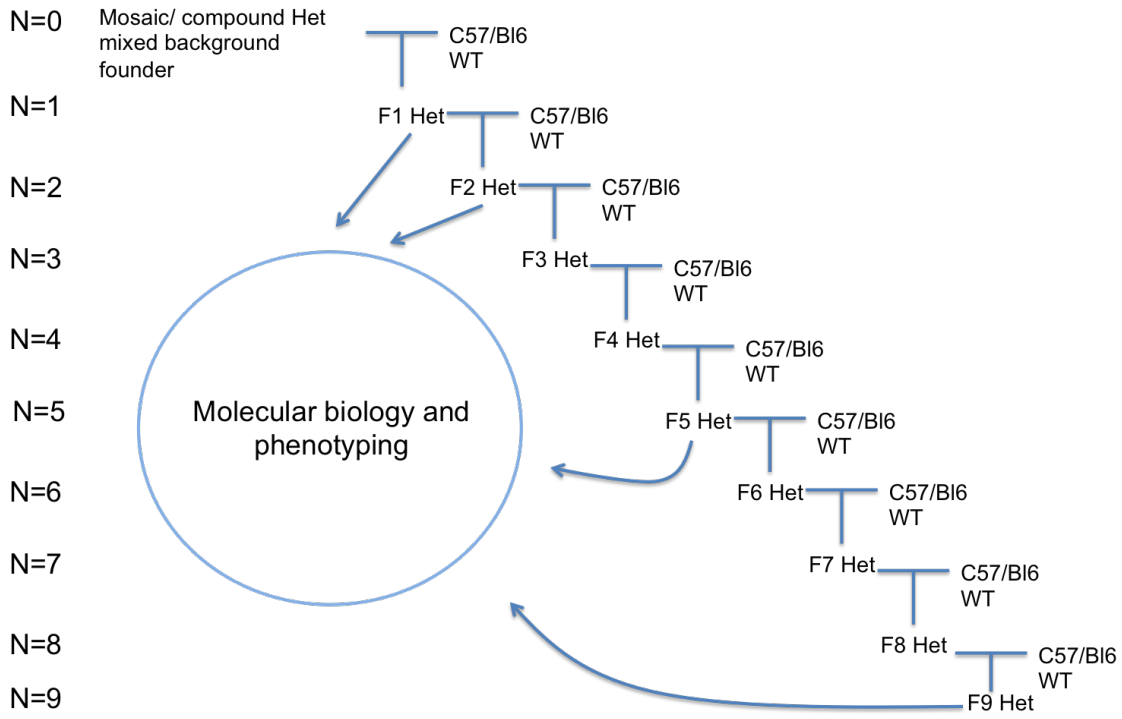

Fig. 5.4 **Breeding strategy for *Dlk2* CRISPR mutants**
Founder animals (backcross generation N0) are crossed with wild-type C57BL/6J mice. Offspring from these crosses (N1/F1) are genotyped and 5 different mutations were selected for colony generation (section 5.1). These heterozygotes will be backcrossed for 9 generations until N9/F9 by crossing each generation with a pure C57BL/6J wild-type mice. Heterozygotes from backcross generations N1, N2, N5, N9 will be breed together to generate N1, N2, N5, N9 specific colonies respectively for each mutation. Mice from these separate colonies will be used for molecular biology and phenotypic analysis. *Acronyms used: Het — heterozygote*.

Similar heterozygous intercross sub-colonies will be generated at backcross generations 5 and 9 (N5 and N9, respectively). More detailed phenotypic analysis will be conducted on the N5 colony, and comprehensive analysis on the N9 colony. Comprehensive analysis must be conducted on the purest C57BL/6J genome as it the same reference genome on which the *Dlk1* line is maintained [181]. However, having preliminary phenotypic data from colonies derived from other generations, such as N5, N2, or N1, is advantageous. It allows comparison of phenotypes between generations, enabling assessment of genetic background effects. Genetic background can dramatically influence phenotype and phenotypic interpretation; for example the C57BL/6N strain possesses a *Crb1* allele that causes retinal degeneration and may confound other ocular phenotypes [149]. In addition, exploratory investigations can be conducted on colonies derived from these earlier generations allowing the final experiments to be hypothesis driven.

6 Preliminary phenotypic analysis of *Dlk2*-/- mice

The five selected *Dlk2* mutant lines will not be validated by Western blotting in this thesis as initial attempts at Western Blotting, using DLK2 antibodies custom generated by Abcam were unsuccessful in my hands. However, the biological materials necessary for such validation were generated. As discussed in section 5.3, preliminary phenotypic observations can be drawn secondary to the backcrossing and validation breeding protocols. Such observations include litter sizes, pre- and post-natal body weights, and genotype ratios. Where possible this information will be compared to similar data for the *Dlk1* mutant line, maintained on a pure C57BL/6J background. Given that genetic background effects are expected, it is not ideal to compare the *Dlk1* mutants (equivalent to N9) to N1 and N2 *Dlk2* CRISPR mutants. For similar reasons, pure C57BL/6J mice are imperfect wild-type control models. Nonetheless, considerable insight into the value of the mutants can be generated from the preliminary data I have generated on the early backcross generations.

6.1 There is no obvious difference in litter size between the *Dlk2* CRISPR lines

The litters from N2 heterozygous intercrosses have no significant size difference between the five *Dlk2* mutant lines, as assessed by a one-way ANOVA (figure 6.1). A similar trend is seen for the offspring of crosses between N2 heterozygotes and pure C57BL/6J wild-type animals (figure 6.1). This suggests that there is no off-target, on-target, or indeed any effect that modulates litter size disproportionately for any mutation. However, the gross similarities in litter size may belie significant alterations in genotype and sex ratios (assessed in sections 6.2 and 6.3, respectively).

In general, there is a trend for litters born from heterozygotes intercrosses to be of a smaller size than the litters generated when mice with the same mutation are crossed with pure C57BL/6J mice (table 6.1). This was observed when all the offspring are of an equiva-

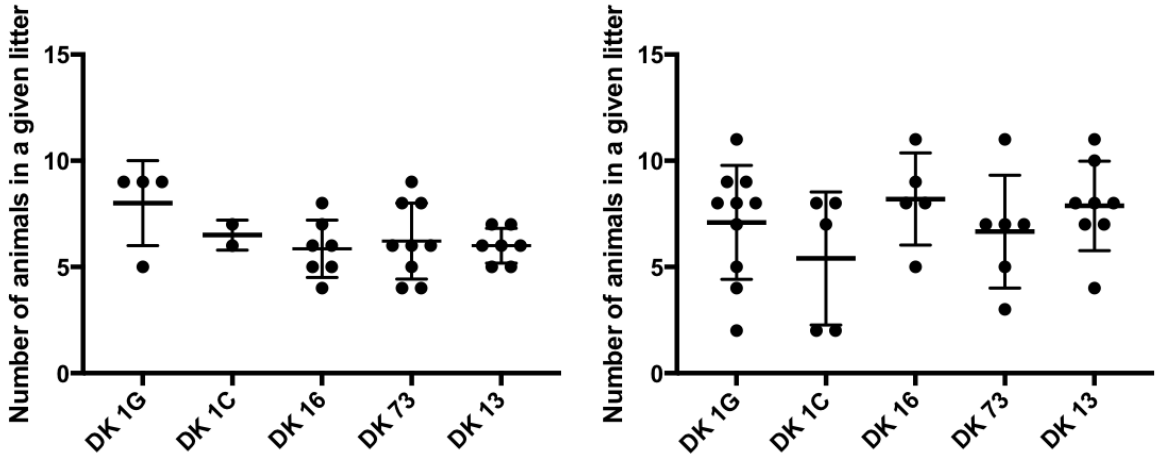

(a) Litter sizes from heterzygous intercrosses of N2 mutants

(b) Litter sizes from N1 heterozygous mutants crossed with C57BL/6J WT animals

Fig. 6.1 **Litter sizes (mean, standard deviation) of various *Dlk2* mutant crosses generating N2 off-spring**
There is no significant difference in the number of animals in each litter for (a) N2 mutants crossed heterozygously, or (b) N1 heterzygotes crossed to wild-type animals (generatating N2 offspring). p=0.3978 and 0.3939, respectively (Non-parametric Kruskal-Wallis test, GraphPad Prism V7.0). *Acronyms used: WT — wildtype.*

lent backcrossed generation (N2). However, the standard deviations of the mean litter sizes overlap dramatically between each cross, making it difficult to ascertain whether the trend is an artefact or due to underlying biology. The *Dlk1*-/- mutants show reduced numbers of homozygotes (PhD Thesis Mary Cleaton, University of Cambridge (2015)); given the homology between *Dlk1* and *Dlk2* it would not be unexpected for litters from *Dlk2* heterozygous intercrosses to be smaller due to homozygous loss. This will be assessed with genotyping (section 6.2).

Line	Mean (SD) litter size hetXwt cross	Mean (SD) litter size hetXhet cross
DK1G	7.10 (2.69)	8.00 (2.00)
DK1C	5.40 (3.13)	6.50(0.71)
DK16	8.20 (2.17)	5.86 (1.35)
DK73	6.67 (2.66)	6.22 (1.79)
DK13	7.89 (2.10)	6.00 (0.82)

Table 6.1 **Mean (SD) litter sizes of N2 litters born from N2 heterozygous intercrosses and from crosses between N1 heterozygotes and C57Bl/6J wils type mice**

Acronyms used: het — heterozygote, SD — standard deviatio, wt — wild-type

The number of litters assessed for each cross is fairly low (table 6.2) and is not consistent between experimental groups. This, coupled with the high variability of litter size per cross (figure 6.1), may suggest a trend that is not genuine. Furthermore, the mean litter size, from 21 litters, of the wild type C57BL/6J colony is 6.00 (+/- 2.28), which is also highly similar to the values of the *Dlk2* intercross litter sizes. The mean size of wild-type litters also possesses a similarly high standard deviation, emphasising the inherent variability of animal work, at least in the Combined animal facility where these mice are housed, and the need for large sample sizes. It is worth noting however, that the *Dlk2* mutants analysed are at the N2 stage in backcrossing and possess only 87.5% of the C57BL/6J genome (table 5.8). Wild-type C57BL/6JXCBA hybrid animals may display higher birth rates than pure C57BL/6J animals.

Line	No. litters hetXwt cross	No. litters hetXhet cross
DK1G	10	4
DK1C	5	2
DK16	5	7
DK73	6	9
DK13	8	7

Table 6.2 **Number of litters analysed in table 6.1 and figure 6.1 for heterozygous intercrosses and heterzygote - wild-type crosses**

Acronyms used: het — heterozygote, wt — wild-type

Elucidating whether different litter sizes are artefactual or not can only be completed by comparing litter sizes across all backcrossed generations. This analysis will thus be completed at the end of the backcrossing protocol at generation N9. However, some lines were backcrossed to generation N3 (figure 6.2) and some mutants were bred together at N1 (figure 6.2). These preliminary data suggest that litter sizes are generally decreasing across backcrossed generations. Further litters and generations will need to be assessed to ascertain whether the trend is genuine.

Observing a reduction in litter size gives little insight into why mice may have smaller litters. Only by analysing the sex and genotypic ratios will it become possible to answer that question.

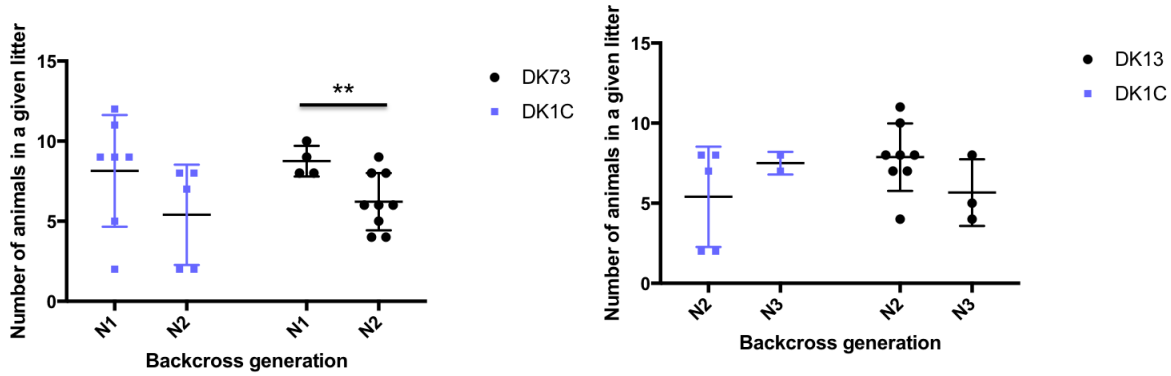

(a) Litter sizes from N1 and N2 heterzygous intercrosses of DK73 and DK1C *Dlk2* mutants

(b) Litter sizes from N1 and N2 heterozygous DK1C and DK13 mutants crossed with C57/Bl6 WT animals

Fig. 6.2 **Comparison of litter sizes (mean, standard deviation) of various *Dlk2* mutant crosses across N1, N2, and N3 generations**
Litter sizes of heterozygous intercrosses were compared for DK73 and DK1C at backcross generations N1 and N2 (a). There was no significant difference in litter size between generations for DK1C (p=0.2485, unpaired non-parametric Mann-Whitney test; GraphPad Prism V7). However, litters born at the N2 generation had significantly fewer offspring compared to N1 litters of DK73 heterozygous intercrosses (p=0.0448, non-parametric Mann-Whitney test; GraphPad Prism V7). Litter sizes were also assessed between backcross generations N2 and N3 for DK1C and DK13 heterozygotes crossed with C57BL/6J wild-type animals. There was no significant difference in litter size between generations for DK13 (p=0.2485, on-parametric Mann-Whitney test; GraphPad Prism V7). No statistical analysis was performed on the DK1C line as the N3 generation possessed only 2 litters which was too few for accurate statistical analysis.

6.2 *Dlk2* mutant mice are generated at non-Mendelian frequencies

Cross	Percentage homs	Percentage hets	Percentage WTs
WTXHet	0	50	50
HetXHet	25	50	25

Table 6.3 **Expected Mendelian ratios**

Acronyms used: het — heterozygote, hom — homozygote, wt — wild type

The genotypes of offspring derived from heterozygous intercrosses and heterozygous by wild type crosses were analysed. The lines behave differently from each other — especially when observing the genotypes of offspring from heterozygous intercrosses. However, litter numbers are low and quite variable between lines, hence within line and between line comparisons should be conducted with caution. Some of the differences may be due to underlying biology: phenotypes are expected to alter and stabilise during the backcrossing protocol (section 5.3), and some phenotypes may arise postnatally but not embryonically. Characterisation of further litters will be needed to carry out to comprehensively determine whether the offspring are being generated at Mendelian frequencies.

Wild type X N1 heterozygote crosses produce litters with a reduced number of wild-type off-spring (table 6.4). However, the sample sizes are quite low for each litter and so the slight biases observed may be artefacts of small sample sizes. On the other hand, if the data from all lines is aggregated together to increase the sample size then there is still a slight bias towards heterozygous births: specifically there are 85 heterozygous animals (57%) and 63 wild types (43%). However, due to potential variability between the five lines it would be unwise to draw conclusions from aggregated data. Thus, the number of offspring born to wild type X N1 heterozygote crosses will need to be increased, for all lines, to investigate whether there is a heterozygous bias.

Line	Total no. litters	Total no. pups	No. het. pups (%)	No. wt pups (%)
DK1G	2	15	8 (53.33%)	7 (46.67%)
DK1C	5	13	7 (53.86%)	6 (46.15%)
DK16	5	31	17 (54.84%)	14 (45.16%)
DK73	5	37	25 (67.57%)	12 (32.43%)
DK13	7	51	28 (54.90%)	24 (47.10%)

Table 6.4 **Number of heterozygous and wild type N2 offspring resulting from N1 heterozygote x wild type crosses**

Acronyms used: het — heterozygote, no. — number, wt — wild-type

If such further experiments did indicate a heterozygous bias, this might suggest that mice lacking the paternal copy of *Dlk2* have a survival advantage; perhaps due to unequal resource allocation during embryogenesis.

Line	Backcross gen.	Total no. pups	No. hom. pups (%)	No. het. pups (%)	No. wt pups (%)
DK1G	N2	7	3 (42.86%)	4 (57.14%)	0
DK1C	N1	23	1 (4.34%)	18 (78.26%)	4 (17.39%)
DK16					
DK73	N1	35	9 (25.71%)	17 (48.58%)	9 (25.71%)
DK73	N2	22	10 (45.45%)	5 (22.73%)	7 (31.82%)
DK13	N2	6	0	4 (66.67%)	2 (33.33%)

Table 6.5 **Number of homozygous, heterozygous and wild type offspring resulting from heterozygous intercrosses**

Acronyms used: gen. — generation, het — heterozygote, hom. — homozygous, no. — number, wt — wild-type

Small sample sizes also plague the heterozygous inter-crosses, making it challenging to draw conclusions. Heterozygous inter-crosses for DK1G, DK13, and DK1C (generations N2, N2, and N1, respectively) all show expansion in the proportion of heterozygous animals

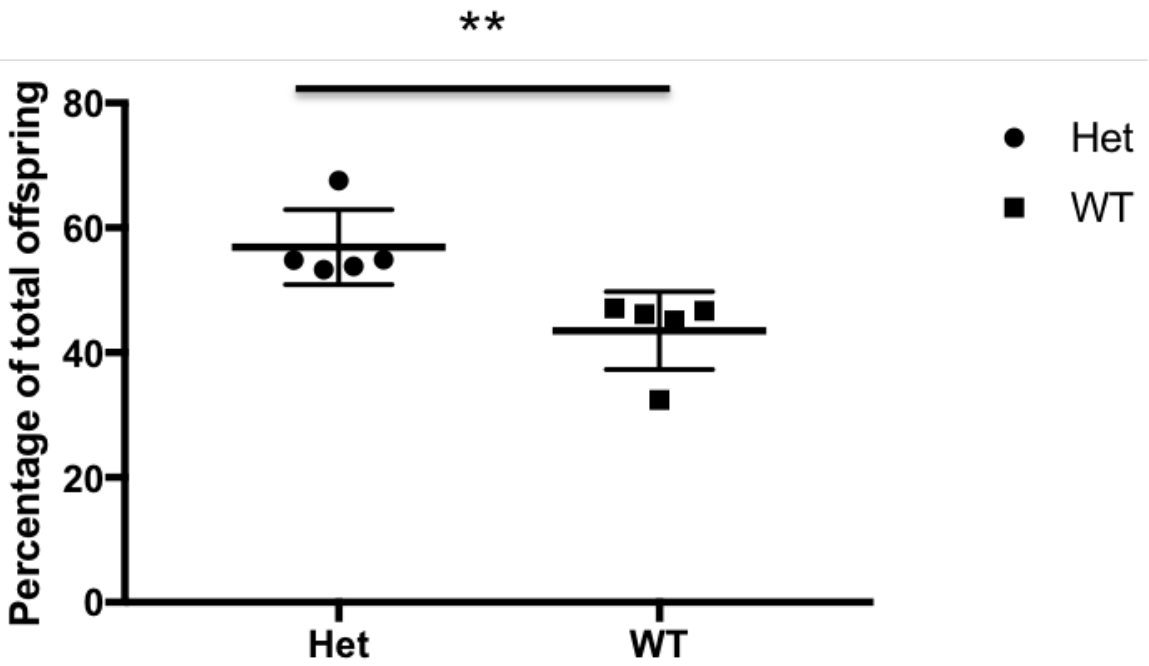

Fig. 6.3 **Percentage of heterozygous and wild type N2 offspring born from N1 heterozygote X C57Bl/6J wild type crosses for all *Dlk2* mutant lines**
Percentage of heterozygotes and wild-type N2 offspring born from crosses between C57Bl/6J wild type animals and m N1 heterozygous mice from DK1C, DK1G, DK16, DK73, and DK13 lines. Total number of animals per genotype for each line are located in table 6.4. Unpaired parametric t-test with Welch's correction performed between both experimental groups (p=0.0076) using GraphPad Prism V7. *Acronyms used: Het — heterozygotes, WT — wild type*.

(table 6.5) compared to the expected Mendelian ratios (table 6.3). This trend is also seen in N2 embryos harvested from heterozygous intercrosses of DK16 (e14.5), DK73 (e16.5), and DK13 (e14.5) (table 6.6). However, if the data from table 6.5 is aggregated then the Mendelian ratios are normal: 48 heterozygotes, 22 wild types, and 23 homozygotes. This suggests that the expansion of heterozygous animals observed for some litters postnatally (table 6.5) and embryonically (table 6.6) may be artefacts of small sample sizes. However, it is worth noting that it may be inappropriate to aggregate this data, especially as the intercrosses were performed on different backcross generations for different lines. In short, these experiments must be repeated with far higher sample sizes to enable reliable interpretation.

Line	Back. gen.	Em. stage	Total no.	No. homs. (%)	No. hets. (%)	No. WTs (%)
DK1G						
DK1C						
DK16	N2	e14.5	14	1 (7.14%)	10 (71.43%)	3 (21.43%)
DK73	N1	e14.5	6	0	2 (33.33%)	4 (66.67%)
DK73	N2	e14.5	6	1 (16.67%)	3 (50.00%)	2 (33.33%)
DK73	N2	e16.5	9	2 (22.22%)	5 (55.56%)	2 (22.22%)
DK13	N2	e14.5	8	1(12.50%)	6 (75.00%)	1 (12.50%)

Table 6.6 **Number of homozygous, heterozygous, and wild type embryos resulting from heterozygous intercrosses**

Acronyms used: Back. — backcross, Em. — embryonic, gen. — generation, het — heterozygote, hom. — homozygous, no. — number, wt — wild-type

6.3 *Dlk2* mutant may mice display abnormal sex ratios

Line	Back. gen. pups	Total no. pups	No. fem. (%)	No. male (%)
DK1G	N2	11	7 (63.64%)	4 (36.36%)
DK1C	N2	11	7 (63.64%)	4 (36.36%)
DK16	N2	28	16 (57.14%)	12 (42.86%)
DK73	N2	34	20 (58.82%)	14 (41.18%)
DK13	N2	49	21 (42.86%)	28 (57.14%)

Table 6.7 **Number of female and male N2 offspring born to C57BL/6J wild type X N1 heterozygote crosses for all *Dlk2* mutant lines**

Acronyms used: Back. — backcross, fem. — female, gen. — generation, no. — number

Offspring of *Dlk2* mutant mice may display abnormal sex ratios type (table 6.7). As with the genotype data (section 6.2), the trend is more clear within the N1 heterozygote X

C57BL/6J crosses (figure 6.4) where there may be a potential bias towards female offspring. This trend is observed in all lines except DK13 for this cross type (table 6.7). However, the DK13 line has the largest overall sample size so this data may be more reliable. Sex bias is extremely difficult to assess without large sample sizes. For instance, the C57BL/6J and *Dlk1*-/- colonies housed in the same facility (table 6.8) are known not to have sex biases. Yet, their relatively small sizes produce sex biases comparable to those in table 6.7. It is therefore likely that the observed sex bias in the heterozygote X C57BL/6J crosses may simply be an artefact of insufficient numbers. Further experiments will be necessary to confirm this.

Line	**Total no. pups**	**No. fem. (%)**	**No. male (%)**
WT	131	69 (52.67%)	62 (47.33%)
Dlk1-/-	67	36 (53.73%)	31 (46.29%)

Table 6.8 **Number of female and male offspring born to intercrosses of C57BL/6J wild-type and *Dlk1*-/- mice, housed in the same facility, in 2017**

Acronyms used: fem. — female, no. — number, WT — wild type

Insufficient numbers of animals are also problematic when investigating the sex ratios of offspring of heterozygous intercrosses (table 6.9). Collectively these crosses show dramatic ranges of percentages female and male offspring per cross (figure 6.4). Nevertheless, DK1G, DK1C, and DK13 lines show similar sex bias trends in the offspring from heterozygous intercrosses (table 6.9) and heterozygote X C57BL6/J crosses (table 6.7). Although promising, the impact of the poor sample sizes on interpreting this data cannot be discounted. Sex biases may occur when animals of a certain sex *and* genotype are depleted. However, as the overall sample sizes are generally very low, often insufficient numbers of animals of a given phenotype and sex are born to draw any conclusions (table 6.10). For example, no homozygous females and heterozygous males were born to the DK1C line.

Line	**Back. gen. pups**	**Total no. pups**	**No. fem. (%)**	**No. male (%)**
DK1G	N2	7	4 (57.14%)	3 (42.86%)
DK1C	N1	11	9 (81.82%)	2 (18.18%)
DK16				

Table 6.9 (continued)

Line	**Back. gen. pups**	**Total no. pups**	**No. fem. (%)**	**No. male (%)**
DK73	N1	35	15 (42.86%)	20 (57.14%)
DK73	N2	14	5 (35.71%)	9 (64.29%)
DK13	N2	6	1 (16.67%)	5 (83.33%)

Table 6.9 **Number of female and male offspring born to heterozygous intercrosses for all *Dlk2* mutant lines**

Acronyms used: Back. — backcross, fem. — female, gen. — generation, no. — number

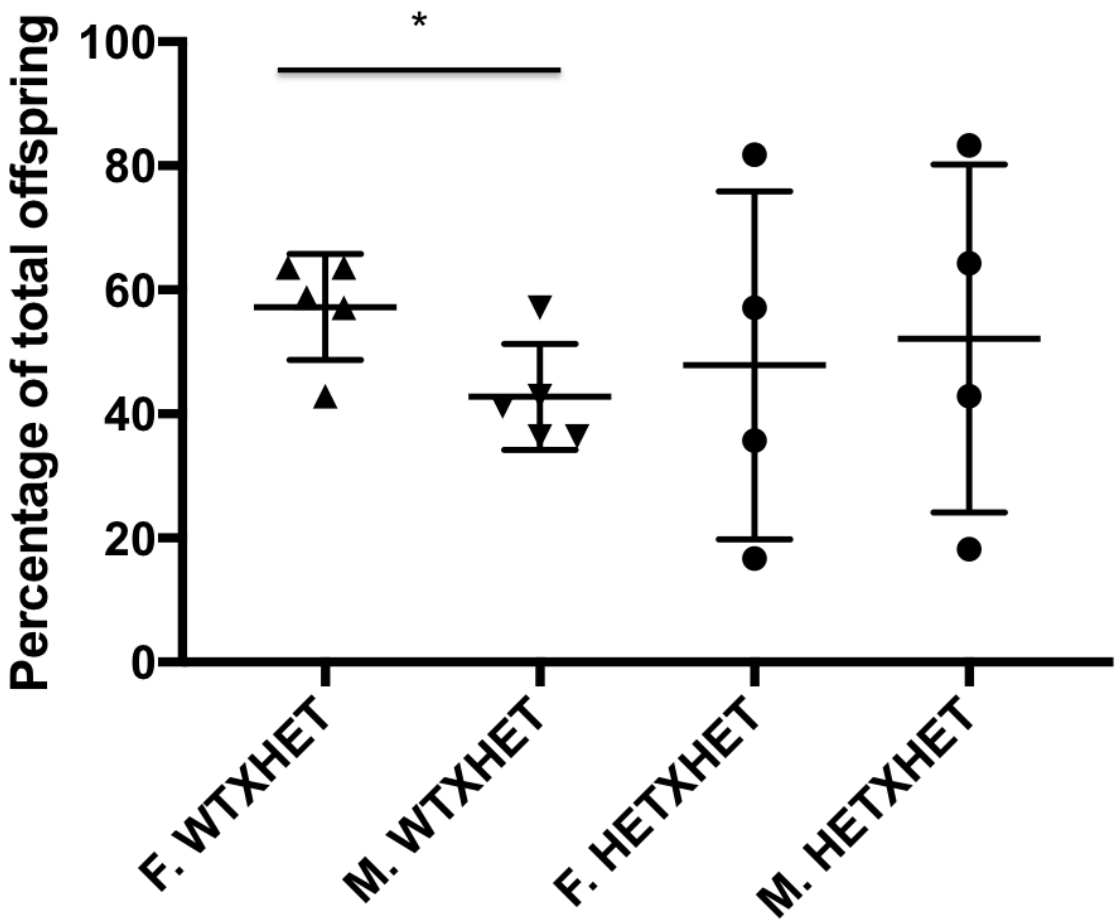

Fig. 6.4 **Percentage of female and male N2 offspring born from N2 heterozygous intercrosses and N1 heterozygote X C57Bl/6J wild type crosses for all *Dlk2* mutant lines**
Percentage of female and male N2 offspring born from crosses between C57Bl/6J wild type animals and N1 heterozygous mice from DK1C, DK1G, DK16, DK73, and DK13 lines; and from N2 heterozygous intercrosses from the same lines. Total number of animals per genotype for each line are located in tables 6.7 and 6.9 for the heterozygote X WT and heterozygote X heterozygote crosses, respectively. Unpaired non-parametric Mann-Whitney tests were performed between both experimental groups for the wild type x heterozygote crosses (p=0.0397) and the heterozgous intercrosses (p=0.6857), using GraphPad Prism V7. *Acronyms used: Het — heterozygotes, WT — wild type.*

Line	Back. gen. pups	Total no. pups	No. hom. fem. (%)	No. hom. male (%)	No. het. fem. (%)	No. het. male (%)	No. WT fem. (%)	No. WT male (%)
DK1G	N2	7	2 (28.57%)	1 (14.29%)	2 (28.57%)	2 (28.57%)	0 (0.00%)	(0.00%)
DK1C	N1	11	0 (0.00%)	1 (9.09%)	6 (54.55%)	0 (0.00%)	3 (27.27%)	1 (9.09%)
DK16								
DK73	N1	35	4 (11.43%)	5 (14.49%)	9 (25.71%)	8 (22.86%)	2 (5.71%)	7 (20.00%)
DK73	N2	14	1 (7.14%)	4 (28.57%)	1 (7.14%)	4 (28.57%)	3 (21.43%)	1 (7.14%)
DK13	N2	6	0 (0.00%)	0 (0.00%)	1 (16.67%)	3 (50.00%)	0 (0.00%)	2 (33.33%)

Table 6.10 **Number of female and male homozygous, heterozygous, and wild type offspring born to heterozygous intercrosses for all *Dlk2* mutant lines**

Acronyms used: Back. — backcross, fem. — female, gen. — generation, het. — heterozygotes, hom. — homozygotes, no. — number, WT — wild type

6.4 There is no striking difference in postnatal weights between *Dlk2* mutant and wild type mice

Postnatal weights can reflect several processes. These include developmental effects, the influence of maternal care and, at post-weaning stages, metabolic phenotypes. Mice born to N1 heterozygote x C57BL/6J wild type crosses (figure 6.5) and N2 heterozygote intercrosses (figure 6.6) were weighed until they reached breeding age. Overall, there is no convincing evidence of differences in postnatal weight between any of the genotypes for each line. However, the sample sizes are generally too low (tables A.1 and A.2) to draw conclusions. Increasing the sample sizes may reveal a subtle phenotype or confirm a current trend.

The mice were weighed for approximately 6 weeks for females, and 8 weeks for males. However, since some postnatal weight phenotypes do not emerge until much later stages it is typical to weigh each mouse for one year. Proper investigation of postnatal weights should thus be conducted on a subset of mice from the two lines selected for extensive phenotypic analysis.

DK73 *Dlk2*-/- females may have reduced mass compared to wild type littermate controls (figure 6.6); although the sample size will need to be increased to verify this. This trend is seen in offspring from both N1 and N2 heterozygous intercrosses (figure 6.7). If validated, this would be an interesting phenotype since Dlk1-/- mice are heavier due to increased adiposity [158]. Further analysis, such as DEXA assessments, would be necessary to determine why the Dlk2 mice have less mass.

6.5 There is no obvious difference in weight between wild-types and *Dlk2*-/- mice for DK16, DK73, and DK13 lines at e14.5

E14.5 embryos, were generated from heterozygous intercrosses from DK16, DK73, and DK13 lines When performing detailed phenotypic analysis of the embryogenesis of mutant animals it is typical to obtain the wet and dry weights of entire embryos and the placentae, the latter to account for any oedema related phenotype.

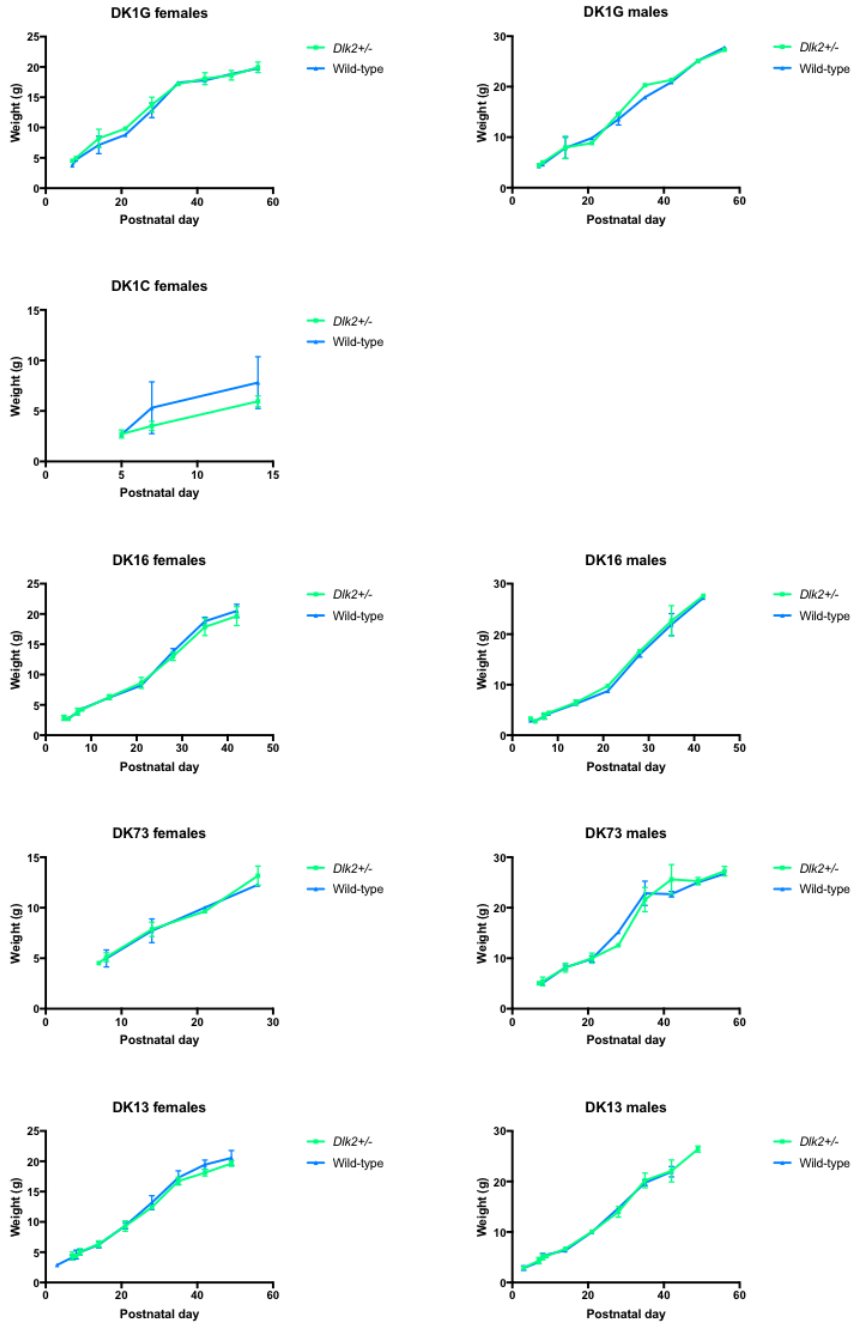

Fig. 6.5 **Postnatal weights of offspring of N1 heterozygote X C57Bl/6J wild type crosses for all *Dlk2* mutant lines**
Sample sizes for each time point per line in table A.1.

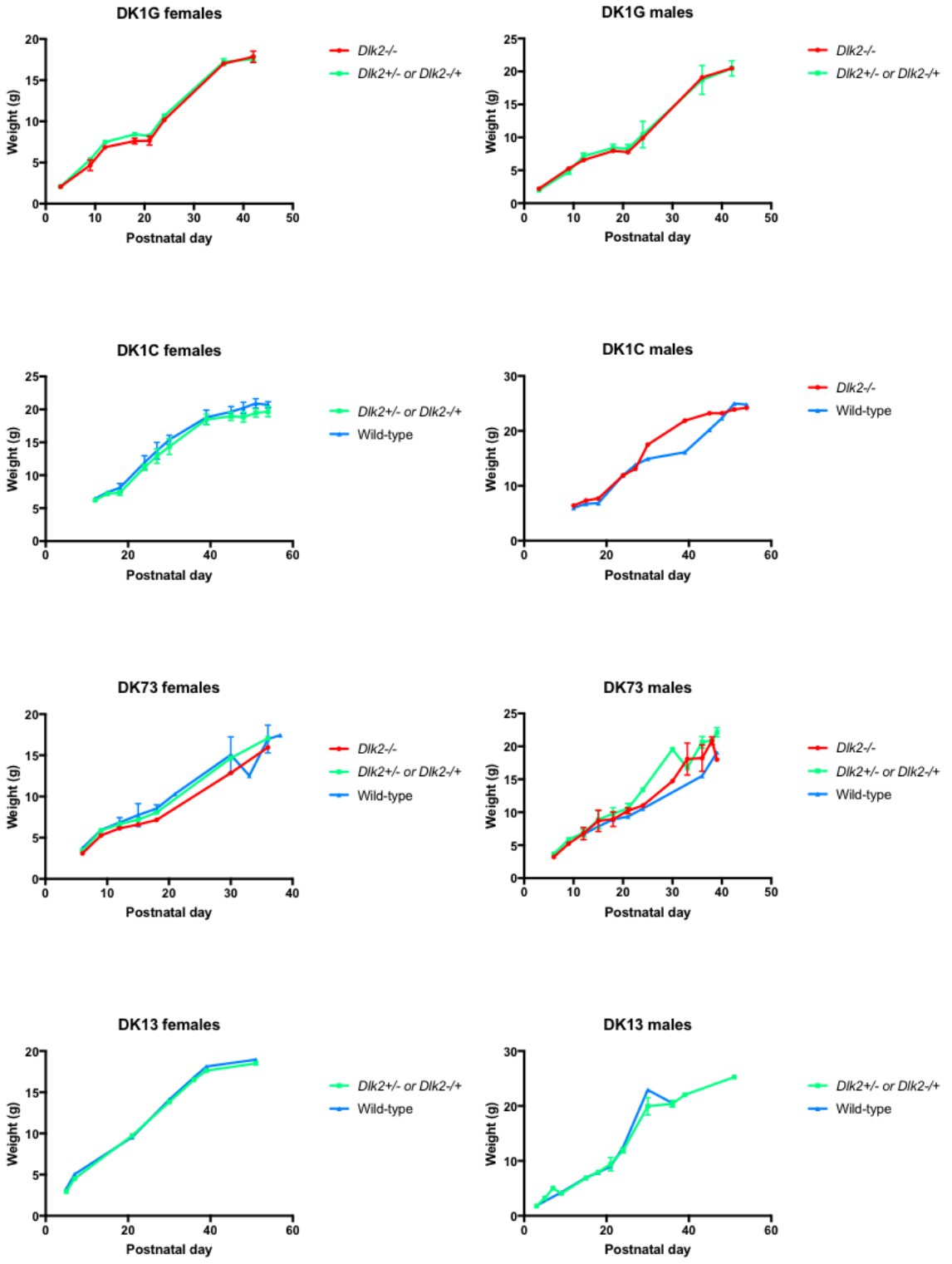

Fig. 6.6 **Postnatal weights of offspring from N2 heterozygous intercrosses of DK1G, DK73, and DK13, and DK1C N1 heterozygous intercrosses**
Sample sizes for each time point per line in table A.2.

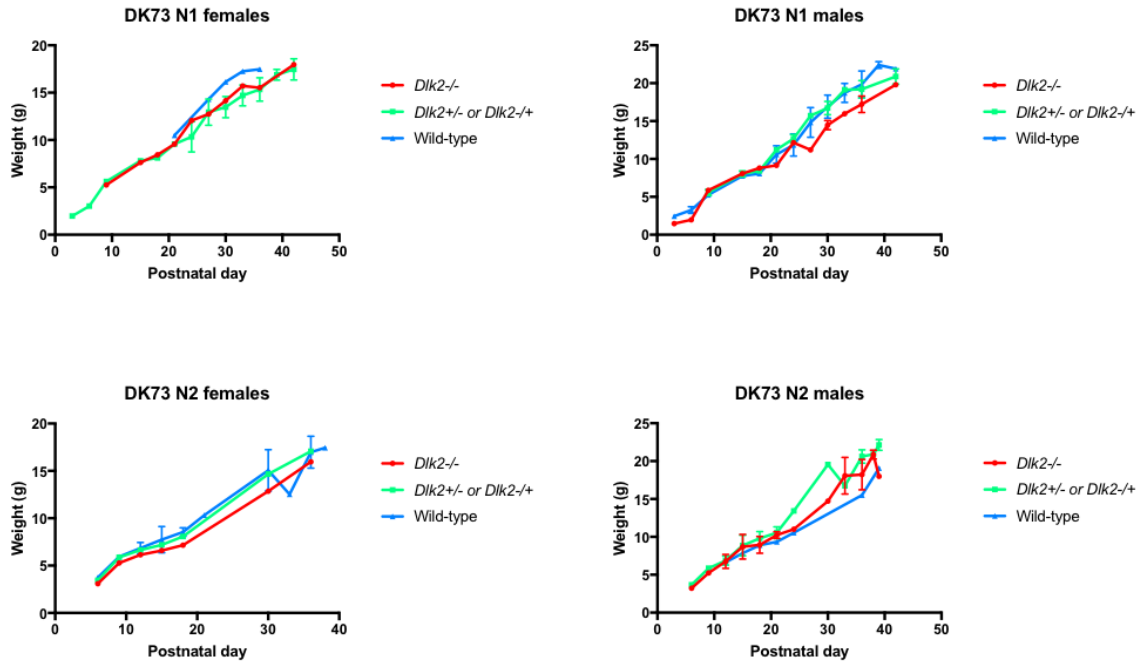

Fig. 6.7 **Postnatal weights of offspring from N2 heterozygous intercrosses of DK1G, DK73, and DK13, and DK1C N1 heterozygous intercrosses**
Sample sizes for each time point per line in table A.3.

The low sample sizes and high variability make interpreting the embryonic wet weight and length data challenging. DK16 heterozygotes and homozygotes embryos may be lighter than littermate wild type controls (figure 6.8). However, DK73 embryos show the opposite trend with heavier homozygote and heterozygote animals, whereas there is no clear relationship between genotype and embryonic weight for the DK13 line. It is unlikely that each line possesses unique embryonic weight phenotypes. It is much more likely that these trends are simply artefacts of sample size. Increasing the number of dissected litters will be necessary to ascertain whether any of the trends hold true.

Similar limitations plague the wet placental weights (figure 6.9). Reassuringly the same trends are maintained for the DK16 and DK73 placentae weights. This could be reflective of genuine population wide phenotypes or may simply be due to uniquely heavy or light homozygotes. Interestingly, the DK13 homozygote placenta is strikingly lighter than the wild-type littermate control. However, no conclusions can be drawn and the sample size must be increased.

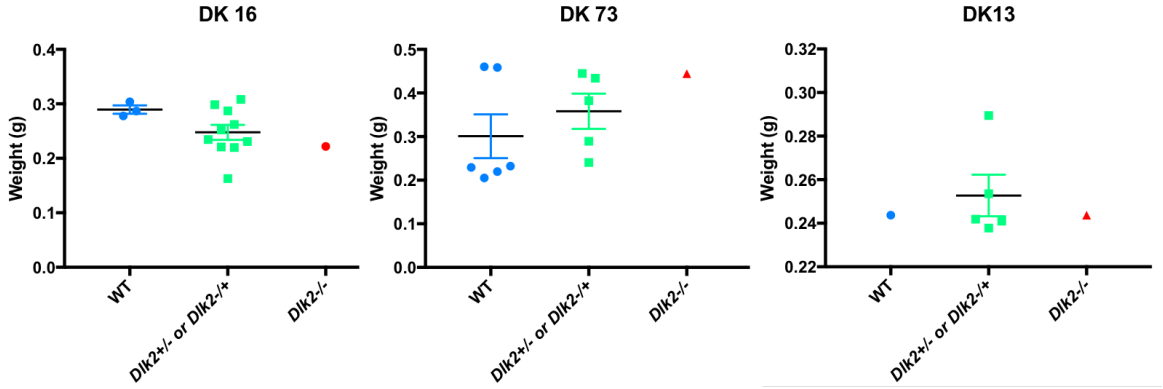

Fig. 6.8 **Wet weights of heterozygous intercross N2 offspring 14.5 embryos for DK16, DK73, and DK13 lines**
Dlk2-/-, *Dlk12+/-* or *Dlk2-/+*, and wild type embryos were weighed at e14.5 for DK16, DK73, and DK13 lines. Samples sizes for DK16: N (*Dlk2-/-*) = 1, N (*Dlk2+/-* or *Dlk2-/+*) = 10, N (wild type) = 3. Unpaired non-parametic Mann-Whitney tests were performed using GraphPad Prism V7 between wild type and heterozygous (p=0.2128) mutants. Samples sizes for DK73: N (*Dlk2-/-*) = 1, N (*Dlk2+/-* or *Dlk2-/+*) = 5, N (wild type) = 6. Unpaired non-parametic Mann-Whitney tests were performed using GraphPad Prism V7 between wild type and heterozygous (p=0.4286) mutants. Samples sizes for DK13: N (*Dlk2-/-*) = 1, N (*Dlk2+/-* or *Dlk2-/+*) = 5, N (wild type) = 1. Statistical analysis was not performed between groups where one had a sample size less than 3.

Crown-rump lengths of the same embryos (figure 6.8) show the same general trends as the embryonic wet weights (figure 6.10). Homozygotes may be smaller for the DK16 line, but larger in the DK73 line, and there is no real difference between the DK13 homozygote and the wild type littermate control. It is not unexpected that the trend is maintained between embryonic wet weight (figure 6.8) and crown rump length (figure 6.10); it is likely that heavier animals are also longer. Without larger sample sizes no conclusions can be drawn

Nevertheless, the trends observed are interesting. The postnatal weights, which also have sample sizes insufficient for strong conclusions, suggest that the homozygotes, especially of the DK73 line, may be lighter postnatally. That a similar trend may be seen in DK16 embryos and placentae, and DK13 placentae is thus reassuring. However, the DK73 homozygotes may be larger embryonically — a trend maintained at the e16.5 stage (figure 6.11). It is unexpected for larger embryos to show postnatal growth restriction. However, mice with restricted embryonic growth often catch up and then overtake their wild type littermates postnatally. Indeed maternal undernutrition, forcing embryonic growth restriction, is often used as an experimental model of this process [107].

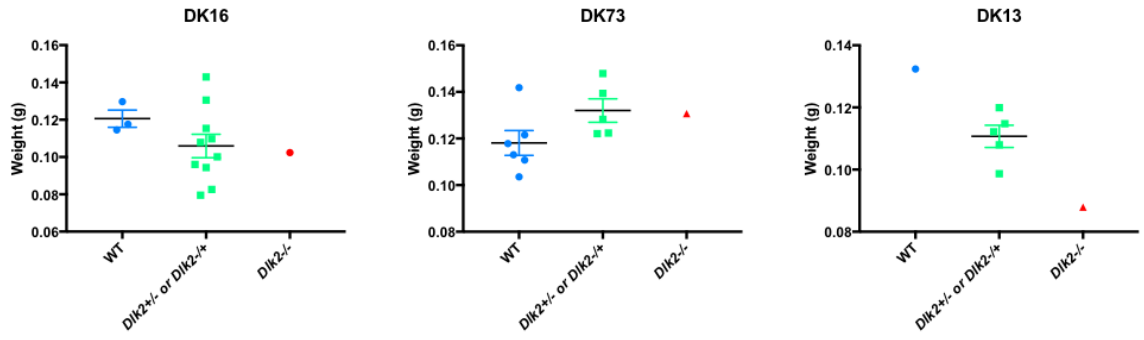

Fig. 6.9 **Wet weights of heterozygous intercross N2 offspring 14.5 placentae for DK16, DK73, and DK13 lines**
Dlk2-/-, *Dlk12+/-* or *Dlk2-/+*, and wild type placentae were weighed at e14.5 for DK16, DK73, and DK13 lines. Samples sizes for DK16: N (*Dlk2-/-*) = 1, N (*Dlk2+/-* or *Dlk2-/+*) = 10, N (wild type) = 3. Unpaired non-parametic Mann-Whitney tests were performed using GraphPad Prism V7 between wild type and heterozygous (p=0.2168) mutants. Samples sizes for DK73: N (*Dlk2-/-*) = 1, N (*Dlk2+/-* or *Dlk2-/+*) = 5, N (wild type) = 6.Unpaired non-parametic Mann-Whitney tests were performed using GraphPad Prism V7 between wild type and heterozygous (p=0.0519) mutants. Samples sizes for DK13: N (*Dlk2-/-*) = 1, N (*Dlk2+/-* or *Dlk2-/+*) = 5, N (wild type) = 1. Statistical analysis was not performed between groups where one had a sample size less than 3.

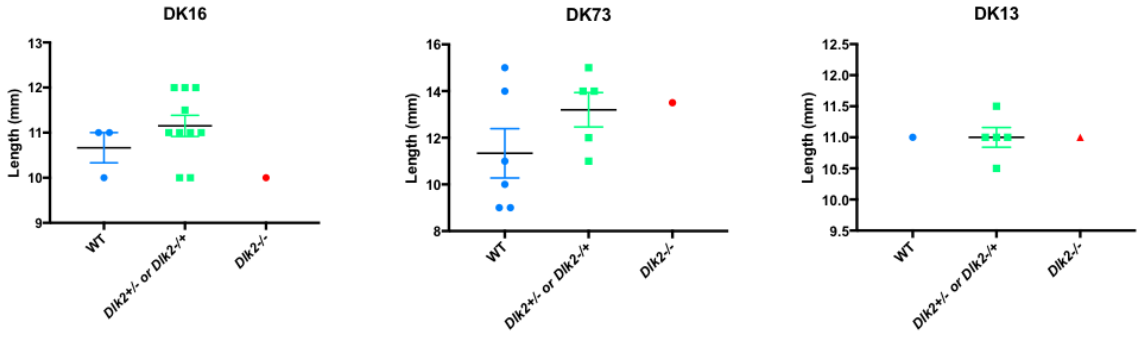

Fig. 6.10 **Crown-rump lengths of heterozygous intercross N2 offspring 14.5 embryos for DK16, DK73, and DK13 lines**
Dlk2-/-, *Dlk12+/-* or *Dlk2-/+*, and wild type crown-rump lengths were measured at e14.5 for DK16, DK73, and DK13 lines. Samples sizes for DK16: N (*Dlk2-/-*) = 1, N (*Dlk2+/-* or *Dlk2-/+*) = 10, N (wild type) = 3. Unpaired non-parametic Mann-Whitney tests were performed using GraphPad Prism V7 between wild type and heterozygous (p=0.3741) mutants. Samples sizes for DK73: N (*Dlk2-/-*) = 1, N (*Dlk2+/-* or *Dlk2-/+*) = 5, N (wild type) = 6. Unpaired non-parametic Mann-Whitney tests were performed using GraphPad Prism V7 between wild type and heterozygous (p=0.2251) mutants. Samples sizes for DK13: N (*Dlk2-/-*) = 1, N (*Dlk2+/-* or *Dlk2-/+*) = 5, N (wild type) = 1. Statistical analysis was not performed between groups where one had a sample size less than 3.

Dlk1-/- mice are thought to display embryonic growth restriction and postnatal growth expansion [158]. Wet embryonic (figure 6.12) and placental (figure 6.13) weights were collected for offspring of *Dlk1* heterozygous intercrosses High variability and low sample size also limit the Dlk1 embryonic and placental weight data. *Dlk1*-/- embryos tend have reduced mass compared to their wild type littermates at e12.5, e14.5, e16.5, and e18.5 (PhD Thesis Isabel Gutteridge, University of Cambridge (2010)) (figure 6.12), with the weight deficit increasing with developmental age. No such trend is seen in the placental weights (figure

The similar relationship between genotype and embryonic wet weights at e14.5 in the offspring of DK16 (figure 6.8) and *Dlk1* (figure 6.12) heterozygous intercrosses is exciting. Homozygotes tend to be lighter. Should the trends validate after increasing the sample sizes, it would be interesting to speculate on the phenotypic similarities. Would this mean that the embryonic growth retardation is related to the function of *Dlk1* and, putatively, *Dlk2* as stem cell regulators? Which tissues would show growth restrictions, and would this help determine where *Dlk2* plays a dominant role, and vice versa. Comparisons to *Dlk2*-/-; *Dlk1*-/- double mutants would also be beneficial. Increasing the quality of the postnatal weight data for the *Dlk2* mutants is also imperative. If both *Dlk2*-/- and *Dlk1*-/- embryos are lighter than wild type littermates, but only *Dlk2*-/- animals maintain the trend postnatally and *Dlk1*-/-

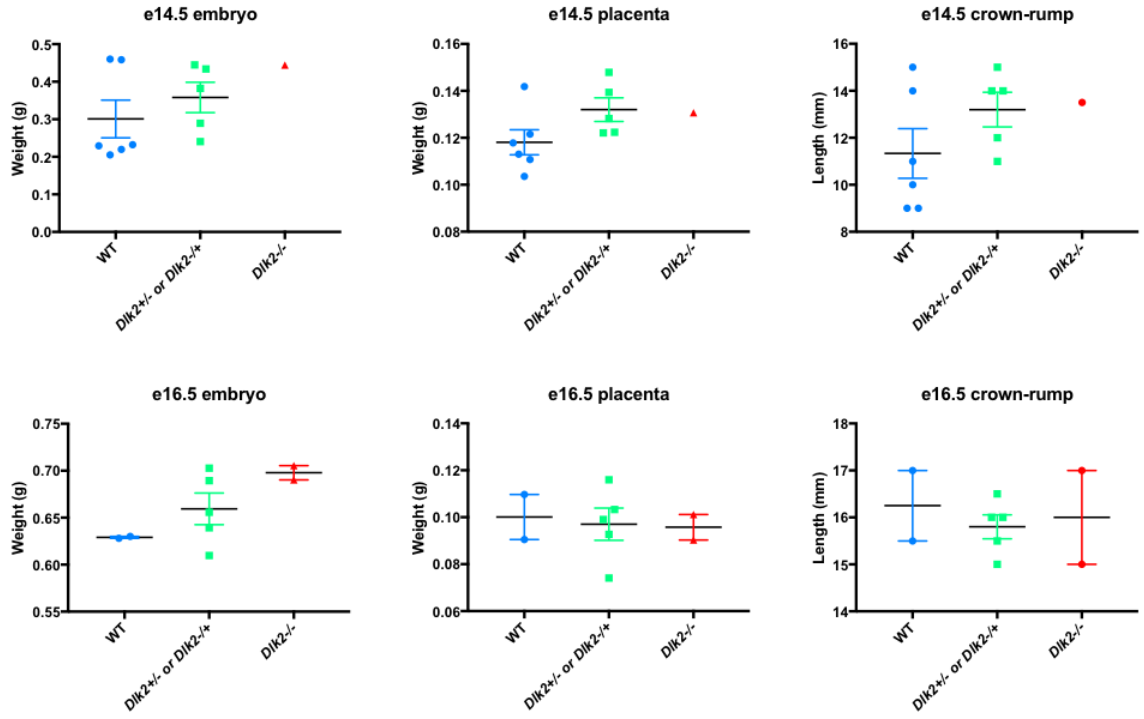

Fig. 6.11 **Crown-rump lengths and embryonic and placental weights of DK73 heterozygous intercross N2 offspring at 14.5, and e16.5**
Dlk2-/-, *Dlk12+/-* or *Dlk2-/+*, and wild type embryos and placentae were weighed, and their crown-rump lengths measured, at e14.5 and e16.5 for the DK73 line. Samples sizes for e16.5 animals: N (*Dlk2-/-*) = 2, N (*Dlk2+/-* or *Dlk2-/+*) = 5, N (wild type) = 2. Samples sizes for e14.5 animals: N (*Dlk2-/-*) = 1, N (*Dlk2+/-* or *Dlk2-/+*) = 5, N (wild type) = 6. Unpaired non-parametic Mann-Whitney tests were performed using GraphPad Prism V7 between wild type and heterozygous mutants for e14.5 embryos (p=0.4286), placentae (p=0.0519), and crown rump lengths (p=0.2251). Statistical analysis was not performed between groups where one had a sample size less than 3.

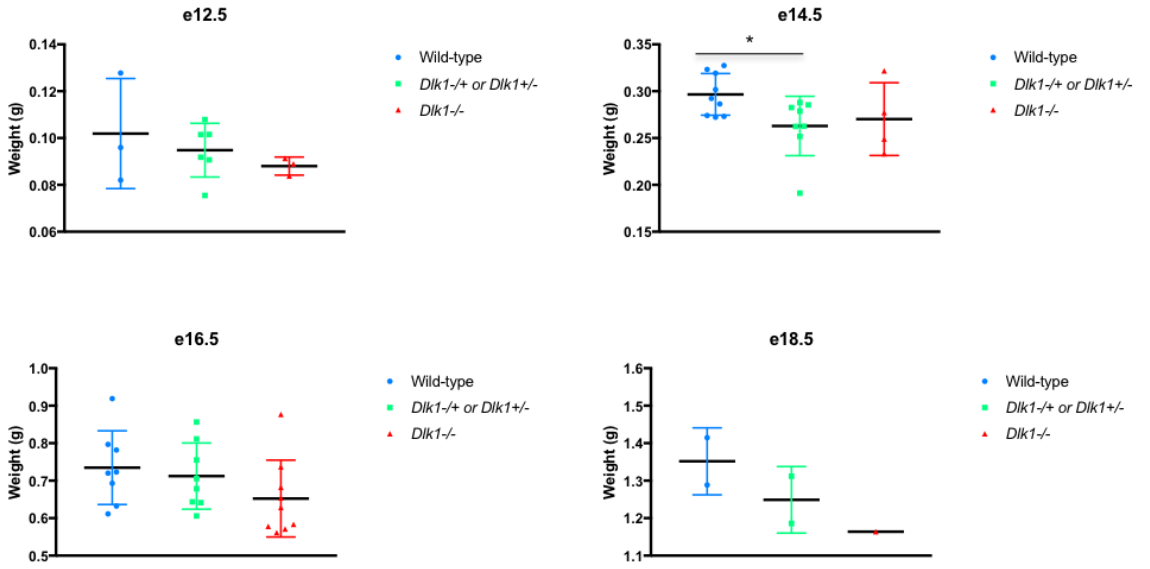

Fig. 6.12 **Wet weights of *Dlk1* mutant heterozygous intercross offspring embryos at e12.5, e14.5, e16.5, and e18.5**

Dlk1-/-, *Dlk1*+/- or *Dlk1*-/+, and wild type embryos were weighed at e12.5: N (*Dlk1*-/-) = 3, N (*Dlk1*+/- or *Dlk1*-/+) = 6, N (wild type)=3. Unpaired non-parametic Mann-Whitney tests were performed using GraphPad Prism V7 between wild type and homozygous (p=0.7000) and heterozygous (p=0.9048) mutants. Sample sizes of embryos weighed at e14.5 were 4, 8, and 9 for *Dlk1*-/-, *Dlk1*+/- or *Dlk1*-/+, and wild type, respectively. Unpaired non-parametic Mann-Whitney tests were performed using GraphPad Prism V7 between wild type and homozygous (p=0.2601) and heterozygous (p=0.0274) mutants. Sample sizes of embryos weighed at e16.5 were 9, 8, and 9 for *Dlk1*-/-, *Dlk1*+/- or *Dlk1*-/+, and wild type, respectively. Unpaired non-parametic Mann-Whitney tests were performed using GraphPad Prism V7 between wild type and homozygous (p=0.0745) and heterozygous (p=0.7021) mutants. Sample sizes of embryos weighed at e18.5 were 1, 2, and 2 for *Dlk1*-/-, *Dlk1*+/- or *Dlk1*-/+, and wild type, respectively. Statistical analysis was not performed on e18.5 weights due to insufficient sample sizes.

animals show postnatal growth expansion, the then genes may be playing opposing roles. Furthermore, homozygous placentae may only be lighter for *Dlk2*-/- mice (DK16 and DK13 lines) compared to wild type littermates (figure 6.9), whereas *Dlk1*-/- placentae are generally comparable (figure 6.13).

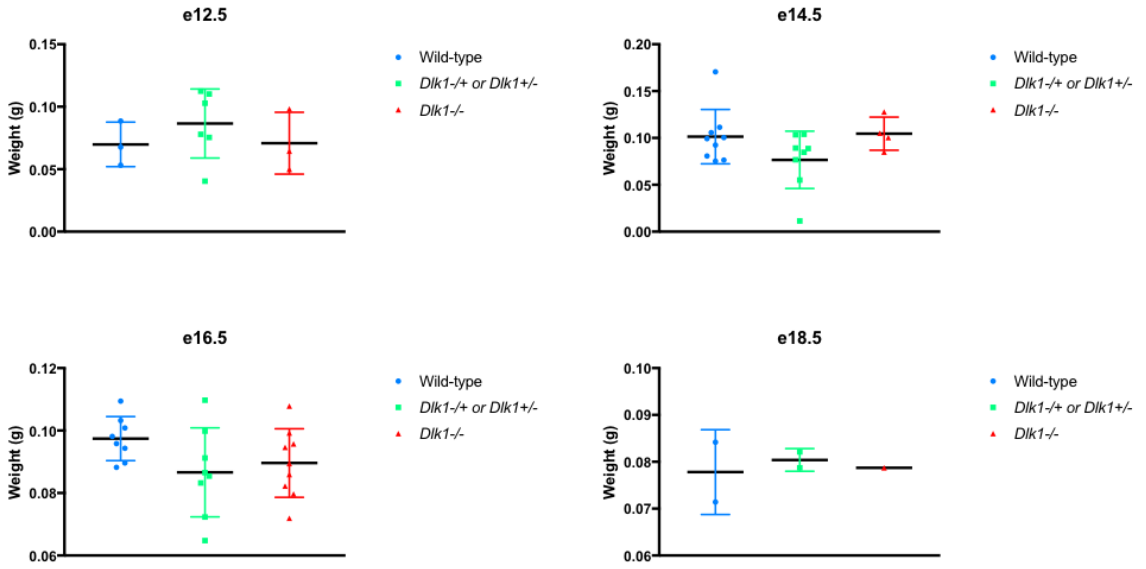

Fig. 6.13 **Wet weights of *Dlk1* mutant heterozygous intercross offspring placentae at e12.5, e14.5, e16.5, and e18.5**

Dlk1-/-, *Dlk1+/-* or *Dlk1-/+*, and wild type placentae were weighed at e12.5: N (*Dlk1-/-*) = 3, N (*Dlk1+/-* or *Dlk1-/+*) = 6, N (wild type)=3. Unpaired non-parametic Mann-Whitney tests were performed using GraphPad Prism V7 between wild type and homozygous (p=0.9999) and heterozygous (p=0.3810) mutants. Sample sizes of placentae weighed at e14.5 were 4, 8, and 9 for *Dlk1-/-*, *Dlk1+/-* or *Dlk1-/+*, and wild type, respectively. Unpaired non-parametic Mann-Whitney tests were performed using GraphPad Prism V7 between wild type and homozygous (p=0.5287) and heterozygous (p=0.2359) mutants. Sample sizes of placentae weighed at e16.5 were 9, 8, and 9 for *Dlk1-/-*, *Dlk1+/-* or *Dlk1-/+*, and wild type, respectively. Unpaired non-parametic Mann-Whitney tests were performed using GraphPad Prism V7 between wild type and homozygous (p=0.1139) and heterozygous (p=0.0830) mutants. Sample sizes of placentae weighed at e18.5 were 1, 2, and 2 for *Dlk1-/-*, *Dlk1+/-* or *Dlk1-/+*, and wild type, respectively. Statistical analysis was not performed on e18.5 weights due to insufficient sample sizes.

7 General discussion

The purpose of this project was to contribute to our understanding of the role of *Dlk2* in mammalian development using classical expression studies and by generating a *Dlk2*-/- mouse line. This work could then be compared to established knowledge regarding *Dlk1* in mice (section 1.4.3), and unpublished data concerning both genes in zebrafish (PhD thesis, Dr. Ben Shaw). The multi-gene and multi-species analysis, combined with *in silico* evolutionary analysis (section 2), will generate insights into the relationship between both genes and ultimately address questions such as:

1. What role does *Dlk2* play in mammalian development, and how well is it evolutionarily conserved?
    (a) Do more ancient and conserved gene functions rely more on NOTCH signalling than more recently evolved functions?
2. What is the (functional) relationship between *Dlk1* and *Dlk2*?
    (a) Does *Dlk2* share regions of expression overlap with *Dlk1*?
    (b) Do *Dlk1* and *Dlk2* interact with each other in a similar manner to S- and M-DLK1 in the postnatal neurogenic niche [78]?
    (c) If *Dlk1* and *Dlk2* interact with each other or share functional redundancy, does this overlap imprinting related functions?
3. What is the evolutionary relationship between *Dlk1* and *Dlk2*?
    (a) Are the expression and functions of *Dlk2* better conserved than *Dlk1* across vertebrates?
    (b) Why did *Dlk1* but not *Dlk2* evolve to imprint?
    (c) Are recently evolved imprinting related functions NOTCH independent?

This project was not completed due to time constraints, but will be continued by other group members. Nevertheless despite the limited phenotypic analysis of the *Dlk2* mutant mice, preliminary insights can be drawn that address some of proposed questions.

In summary, the results presented in this thesis demonstrate that although both *Dlk2* and *Dlk1* are highly conserved across vertebrates, *Dlk2* is the ancestral version of the gene. *Dlk1* is much more evolutionarily dynamic than *Dlk2*, which may reflect the putative vertebrate clade specific functions identified in section 1.4, especially those related to the emergence of genomic imprinting (section 1.2.1). *Dlk1* and *Dlk2* show unique expression patterns, with some overlap, throughout mouse development. *Dlk2*, in particular, is expressed widely throughout the murine embryonic brain. Postnatally, both *Dlk1* and *Dlk2* are expressed in various brain regions, with *Dlk2* generally displaying predominant expression. Preliminary analysis of the *Dlk2*-/- mice suggest that they do not display any significant gross phenotypic abnormalities. Additional breeding is required to determine whether normal Mendelian ratios are evident in offspring.

7.1 *Dlk2* expression patterns are better conserved between mice and zebrafish compared to those of *Dlk1*

A key conclusion from this project is that *Dlk2* is most likely the ancestral of the two DLK genes. Only DLK2 is found in three earliest vertebrate clades: hyperoartia, leptocardii, and ascideiacea (section 2.1) and is better conserved across vertebrates than DLK1 (sections 2.2 and 2.3). The expression patterns of *Dlk2* are more broadly conserved than those of *Dlk1* between mice and zebrafish (data from Dr. Ben Shaw). It would be incorrect to assume that the conservation of *Dlk2* expression patterns relative to *Dlk1* further suggests that *Dlk2* is the ancestral gene. After gene duplication, the parent gene is equally likely to show neofunctionalisation and unique expression patterns as the child gene [20]. Overall then, the conserved expression patterns (section 7.1) and evolutionary analysis (section 2.1) suggest that not only is *Dlk2* ancestral to *Dlk1* but also its function has been retained across vertebrates.

It is challenging to compare heterologous systems, such as mice and zebrafish, especially as they have such different life histories. For example, zebrafish possess a larval stage not seen in mice. Nevertheless, comparisons of the overall expression patterns can be made. In general, both *Dlk1* and *Dlk2* are broadly expressed early in murine development with *Dlk2* expression becoming increasingly restricted to the mouse brain, and subsequently cortex, until expression is lost at the end of development (section 3.2). Whereas *Dlk1* remains more widely expressed for longer in mouse development, although again expression is ultimately lost. In zebrafish, *Dlk1* is ubiquitously expressed during segmentation but is then constrained to neuronal regions after hatching (48-72 h.p.f); and *Dlk2* expression is restricted to the anterior portion during segmentation and is also only expressed in neuronal lineages after

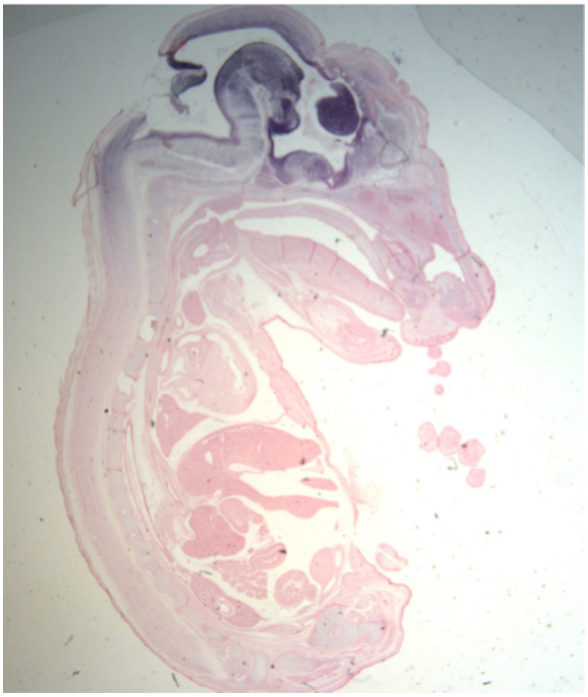

(a) Mouse

(b) Zebrafish

Fig. 7.1 **ISHs of *Dlk2* on e14.5 wild-type mouse embryos and 5dpf zebrafish larvae** The ISHs on zebrafish were performed by Dr. Ben Shaw during his PhD. Sense controls not shown.

hatching (PhD Thesis Dr. Ben Shaw, University of Cambridge (2017)). To the author's knowledge, *Dlk1* and *Dlk2* expression have never been examined during the segmentation phase in mice making comparisons between this developmental stage challenging. Investigating this in mice might be useful to fully interpret the evolutionary relationship of both genes. Nevertheless, overall it seems that the overarching expression patterns of *Dlk2* (figure 7.1) are better conserved than those of *Dlk1* (figure 7.2) between zebrafish and mice.

Both *Dlk1* and *Dlk2* are more broadly expressed in the brain in zebrafish compared to mice. The reduction in *Dlk1* expression in murine brains, coupled with expanded expression throughout the body, may reflect that as *Dlk1* gained additional mammalian specific

(a) Mouse (b) Zebrafish

Fig. 7.2 **ISHs of *Dlk1* on e14.5 wild-type mouse embryos and 5dpf zebrafish larvae** The ISHs on zebrafish were performed by Dr. Ben Shaw during his PhD. Sense controls not shown.

functions (section 1.4.3), it lost a more ancient brain specific function. This could be related to the emergence of imprinting since many of the tissues with murine specific expression are associated with putative mammalian neofunctionalism (section 1.4.3). *Dlk1* is expressed in lineages associated with multiple different parts of whole body metabolism including the adrenal glands, placenta, pancreas, and stomach (section 3.2). Endocrine signalling by S-DLK1 may be vital for the gene's roles in metabolism (section 1.7.5), which are postulated to be mammalian specific and to have co-evolved with imprinting (section 1.7.5). Biallelic *Dlk1* expression, outside the postnatal neurogenic niche, results in gross phenotypes [52] (discussed further in section 1.4.3), highlighting the evolutionary pressures of its dosage.

If the neuronal function of *Dlk1* and *Dlk2* is ancestral, conserved, and redundant, it is not unexpected that *Dlk1* expression is substantially reduced in embryonic murine brains compared to *Dlk2*. As mammalian imprinting related neofunctionalism evolved, *dlk2* may have been evolutionarily selected to retain the ancient neuronal function in the developing mammalian brain. The evidence of more stringent purifying evolutionary selection on *Dlk2* (section 2.5) and reduced evolutionary dynamism (section 2.4) supports this hypothesis. Furthermore, *Dlk1* expression is biallelic in sites of postnatal neurogenesis in mice [78]. The broader expression of *Dlk2* expression in zebrafish compared to mice (figure 7.1) does not compromise this hypothesis. Embryonic neurogenesis is not identical between both species. There are far more sites of neurogenesis in the developing zebrafish (reviewed in [196]) compared to the developing mouse (reviewed in [261]).

There are some limitations with the proposed hypothesis to explain the expression patterns of *Dlk1* and *Dlk2* in mice and zebrafish. Some murine ISHs were conducted on insufficient numbers of biological replicates at certain developmental time points, in particular e16.5, to be certain of their accuracy. However, the consistency of the *Dlk1* ISHs to published datasets (section 1.3) enables confidence in the *Dlk1* data, at least. Furthermore, extensive validation of the ISHs by qPCR or rtPCR was not performed. Brain, liver, heart, lung, tongue, kidney, and placenta were harvested from litter mates of the dissected wild type embryos at all developmental time points. However, attempts at qPCR and rtPCR, conducted over a 9 month period, on these tissues were extremely unsuccessful. In addition, the differences in *Dlk1* expression patterns between zebrafish and mice may be due to the absence of an S-DLK1 isoform in zebrafish. Zebrafish *Dlk1* lacks the juxtamembrane cleavage domain (figure 2.3) and has evolved the most of any of the DLK1 genes (section 2.4). Until *Dlk1* expression is assessed in another vertebrate species, ideally of the actinopterygii clade, it is difficult to be sure that the absence of widespread *Dlk1* in the zebrafish body at later stages of development is not due to the absence of S-DLK1.

7.2 *Dlk2* as a stem cell regulator

Given that *Dlk2* is the ancestral paralogue and that the ancient function of *Dlk1* is stem cell regulation (section 1.4.1), it is a reasonable hypothesis that *Dlk2* is a stem cell regulator as well. Detailed phenotypic analysis of *Dlk2*-/- zebrafish suggest that *Dlk2* is s regulator of neurogenesis. There is an expansion in the number of neurons born early in neurogenesis and a reduction in later stage neuron number (PhD thesis, Dr. Ben Shaw). This suggests that there is a depletion of the progenitor pool and that *Dlk2* might be behaving in a similar

manner to *Dlk1* in the postnatal murine neurogenic niche [78]: *Dlk2* may limit differentiation and promote the self-renewal of progenitor cells.

Although the evidence of *Dlk2* mediated stem cell regulation is robust in zebrafish (pers. comm. Dr. Ben Shaw), it is only circumstantial in mice. *Dlk2* is expressed in intramembranous and endochondral cartiladge at e12.5 (section 3.3) and work in cell lines suggests that *Dlk2* negatively regulates chondrogenesis [254]. *Dlk2* is expressed in the same lineages embryonically (section 3.2) and postnatally (sections 4.2, 4.3, and 4.4) in mice as it is in zebrafish (pers. comm. Dr. Ben Shaw). However, the consequences of removing *Dlk2* in murine neurogenesis has not been investigated making it challenging to ascertain whether the role *Dlk2* plays in murine neurogenesis is the same as in zebrafish. The preliminary analyses of the gross phenotypic consequences of removing *Dlk2* in mice (section 6) suggest that there are none. However, there were also no gross phenotypic abnormalities in *Dlk2*-/- zebrafish (pers. comm. Dr. Ben Shaw). The absence of a clear preliminary phenotype in the *Dlk2*-/- mice is thus not discouraging.

7.3 The *Dlk* genes and NOTCH signalling

After resolving whether *Dlk2* is indeed a stem cell regulator, a natural follow-up project is to investigate the mechanisms underlying its function (section 7.4). Determining if the mechanisms are shared with *Dlk1* is imperative to working out the evolutionary relationship between the genes. Did *Dlk2* regulate stem cells across multiple tissues but then specialised in brain specific regulation as *Dlk1* took over stem cell regulation in non-brain lineages, and was co-opted for additional clade specific functions (section 1.4.2 and 1.4.3)? If stem cell regulation is the more ancient shared role between both genes, it is likely that *Dlk2* and *Dlk1* utilise the same signalling methods to carry out this function. Furthermore, it is also likely to be related to NOTCH signalling since the DLK gene family evolved from duplication events from the canonical NOTCH ligands: the DLL genes (section 1.2).

The Taylor group recently demonstrated that *Notch2* is necessary for maintenance of neural stem cell quiescence in the postnatal neurogenic niche in mice [71]. Knocking out *Notch2* leads to aberrant differentiation of neural stem cells and ultimately exhaustion of the neurogenic niche [71], similar to the phenotypes seen in *Dlk1*-/- mice [78]. Although the common phenotypes suggest that *Dlk1* and *Notch2* might regulate postnatal neurogenesis in mice, Ferron and colleges were unable to detect any alterations of NOTCH activity via the secreted isoform, measured as *Hes5* expression, in the neurospheres derived from *Dlk1*-/-

mice [78]. The study did not rule out the possibility that membrane-bound *Dlk1* in neural stem cells interact with NOTCH. Nevertheless, this characterisation of *Notch* signalling was performed in *ex vivo* neurospheres [78] and the absence of *Notch* activity may not reflect *in vivo* functions. Furthermore, *in vivo* reduction of *Hes5* expression was used to validate the *Notch2* mutant [71]. The plethora of other signalling pathways implicated in *Dlk1* stem cell regulation (section 1.6.2) may reflect *in vitro* work; such studies were conducted almost exhaustively on immortalised cell lines (section 1.6.2).

The phenotypes of *Dlk2-/-* zebrafish (unpublished characterisation by Dr. Ben Shaw) and various Notch mutant zebrafish (table 7.1) are broadly consistent. However, the *Dlk2-/-* fish show an increase in GFAP positive cells at 48hpf when the other mutants show a reduction, however, by 72hpf the reduced/absence of radial glial are found in all phenotypes of all members of the pathway, including *Dlk2*.

The subtle differences between the phenotypes of *Dlk2-/-* zebrafish and the other *Notch* mutants is likely due to *Dlk2* and *Delta* regulating NOTCH signalling in temporally specific manners. *Delta* likely regulates neurogenesis in the earlier stages of zebrafish development and is responsible for stem cell formation and/or early stem cell proliferation. This is why knocking out various *Delta* ligands results in an expansion of the earliest neurons, a subsequent depletion of the neurogenic cells and a reduction in later neural cell types. *Dlk2*, however, probably regulates Notch signalling later in development. It is likely responsible for maintaining cells in the neurogenic niche in a quiescent state, preventing premature differentiation into neural cell types, in a manner similar to the role *Dlk1* plays in the murine postnatal neurogenic niche [78]. Knocking out *Dlk2* has no affect on the earlier neural populations. However, the absence of *Dlk2* results in a premature expansion of a transient amplifying cell population midway during neurogenesis. This expansion in turn depletes the neurogenic stem cell pool within the niche and reduces the number of later born neurons. Since there are no abnormalities in the earlier neurons, the overall neurogenesis defect is less severe in *Dlk2* mutants compared to *Notch* mutants; this is why the *Dlk2* mutants are homozygous viable.

Cell type	**Vis. from (hpf)**	**Glo. *Nt.* inhib.**	**O.e. *Nt.***	***Nt.1a-/-***	***Nt.3a-/-***	***DelA-/-***	***DelD-/-***	***Mnb-/-***	***Sly-/-***	***Dlk2***	**Refs.**
1’ M.N.	10.33-11.66			UP			UP				[17, 50, 98, 216]
R. Brd.	10.33-11.66					UP			UP		[17, 50, 216]
Mau.N.	19-22	UP		UP		UP		UP			[17, 50, 85, 216]
RoL2 cells	Unkwn.			UP							[17, 50, 216]
2’ M.N.	22-24					DOWN		DOWN	Pat. def.		[17, 50, 216]
Rad.G.	24-30	DOWN			DOWN	DOWN		DOWN	DOWN		[17, 50, 85, 216, 259]
GFAP+ve-48	48			UP		DOWN		DOWN	DOWN	UP	[17, 50, 85, 172, 194, 216]
GFAP+ve-72	72					DOWN		DOWN	DOWN	DOWN	[17, 50, 85, 216, 259]

Table 7.1 (continued)

Cell type	**Vis. from (hpf)**	**Glo. *Nt.* inhib.**	**O.e. *Nt.***	***Nt.1a-/-***	***Nt.3a-/-***	***DelA-/-***	***DelD-/-***	***Mnb-/-***	***Sly-/-***	***Dlk2***	**Refs.**
Olig. Pre.	90dpf		UP	DOWN				DOWN			[216, 172, 194, 259]
Rad. G.-ad. tel.		*	*	*	*	*	*	*	*	NONE	[17, 50, 85, 216, 259]

Table 7.1 **Comparison of effects of mutations in *Dlk2* and other *Notch* genes on neural cell numbers in Zebrafish**

*Alterations are homozygous lethal and fish do not survive to adulthood. Postnatal radial glia cell number has not been investigated in heterozygous animals. *Dlk2-/-* zebrafish were obtained, from the zebrafish mutation project [115], and characterised by Dr. Ben Shaw. All *Dlk2-/-* phenotypes are unpublished. Black cells, no information available. *Slytherin* is a GDP-mannose 4, 6 dehydratase and plays a rate-limiting role in the fucoslyation of many different proteins, probably including *Notch* [216]. Mindbomb is an E3 ligase. It is thought to associate with the internal domain of *Delta*. In the absence of mindbomb, *Delta* fails to internalise [131]. Acronyms used: *Ad. tel. — adult telencephalon, Del. — delta, dpf. — days post fertilisation, GFAP+ve-48 — GFAP positive cells visible at 48 hpf, GFAP+ve-72 — GFAP positive cells visible at 72 hpf, Glo. — global, hpf. — hours post-fertilisation, Inhib. — inhibition, Mau.N. — Mauthner neuron, Mnb. — mindbomb, M.N. — motor neurons, NT. — Notch, O.e. — overexpress, Olig. pre. — oligodendrocyte precursors, Pat. def. — pattern defect, Rad.G. — radial glia, R. Brd. - Rohon beard cells, Refs. — references, Sly. — slytherin, Unkwn. — unknown, Vis. — visible,*

Despite the discussed caveats, these data collectively suggest that *Dlk2* and *Dlk1* both behave as NOTCH agonists, at least with regards to functioning as stem cell regulators. This is very interesting given the data suggesting that *Dlk1* might function as a NOTCH antagonist (section 1.6.1). Most of the evidence for DLK1 mediated NOTCH inhibition comes from work in cell lines [232] or heterologous systems [29]. It is therefore unsurprising that the most ancient gene functions likely arise through NOTCH agonism. The proposed NOTCH interacting sites on DLK1 (EGFs 5 and 6) [232] are not fully conserved across the 18 vertebrate species in which the protein sequence was studied (section 2.3). On the other hand, the DLK genes retain the OSM-11 motif, which has been shown to activate NOTCH in *C. elegans* [123, 120], which is not a vertebrate. It might make sense for a likely ancient and conserved gene function to have utilised a vestigial signalling method after its genome duplication and early evolution.

7.4 Further experiments

Although the preliminary data is presented in this thesis is informative, a substantial body of further work is needed to truly characterise the role of *Dlk2* in mice and address its (evolutionary) relationship with *Dlk1*.

7.4.1 Completion of our understanding of *Dlk2* expression in wild type mice

In order to fully interpret future experiments characterising *Dlk2* function in mice (section 7.4.2), it is necessary to generate a robust understanding of the *Dlk2* expression in wild-type animals. The ISHs performed on wild type embryos (section 3.2) should be repeated such that *Dlk2* expression is investigated on a minimum of 3 biological replicates per time point. These results should also be validated using an independent experimental method, such as rtPCR or qPCR. Brain, liver, heart, lung, tongue, kidney, and placenta were harvested from wild-type embryos from the same developmental stages investigated by ISH (section 3.2). However, repeated attempts at qPCR and rtPCR were unsuccessful. With a *Dlk2* qPCR protocol now established (section 4.2), it might be appropriate to revisit validating the ISH data using the collected samples.

It will also be necessary to characterise postnatal expression of *Dlk2*. The semi-quantitative assessment of *Dlk2* expression, relative to *Dlk1*, in postnatal wild-type brains does not yield cellular resolution. Performing ISHs on coronal, saggital, and transverse postnatal brain

sections would thus be useful. The sections have already been generated for brains harvested from p7 C57BL/6J wild-type animals but similar sections from p60 mice will need to be created. However, *Dlk2* may also be expressed in non-neuronal tissues in the adult mouse. It might be better to identify such tissues using methods with a higher throughput, such as rtPCR or qPCR, before assessing the cellular resolution of the expression with ISH.

mRNA and protein expressions do not always correlate. Therefore, immunohistochemistry of DLK2 should be repeated on embryonic and postnatal wild-type sections *Dlk2* ISH was performed on. The retention or exclusion of the juxtamembrane domain has yet to be experimentally observed for *Dlk2* in any species. Experiments to resolve this are probably essential for interpreting the relationship between *Dlk1* and *Dlk2*. cDNA derived from RNA extracted from a variety of murine tissues at a number of different time points could be used to clone various *Dlk2* variants in *Escherichia coli*. Gel electrophoresis of the mixture of cloned proteins could determine if there are any size variants, which would likely represent distinct DLK2 isoforms. These could then be sequenced.

7.4.2 Characterisation of *Dlk2*-/- mice

The generation of a *Dlk2*-/- mouse is perhaps the biggest contribution of this project to the study of DLK gene function. Before the *Dlk2* mutants can be used for characterisation of *Dlk2* gene function, validation is required. Western Blotting, using custom DLK2 antibodies developed by Abcam, on homozygous animals at developmental time points, such as e12.5 or e14.5, with known high *Dlk2* expression will be necessary to validate that DLK2 protein expression is ablated. qPCR of *Dlk2* on similar tissues and time points from wild-type and mutant could also determine whether non-sense mediated decay occurs [94, 114, 146]. In addition, assessment of off-target effects will also be necessary before any phenotypic conclusions can be drawn. Sequencing the exonic predicted off-target sites (described in tables 5.6 and 5.7) from the founder animals would be useful. However, since off-target mutagenesis can occur at non-computationally predicted sites [128]; it may be worth performing systematic genome wide off-target analysis, perhaps using the recently described VIVO system [11]. It is probably best that such a approach is used on the animals backcrossed to generation 9 will have segregated out all but closely linked off-target effects and none are predicted (section 5.3).

After validating the mutant and selecting 2 of the five *Dlk2* mutant lines to characterise, detailed phenotypic analysis can begin. As discussed in section 5.3, it is ideal to generate heterozygous intercross colonies from mice backcrossed to an early (N=2), an intermediate

(N=5), and a late (N=9) generation to look for phenotypic stabilisation. Some, but not all, proposed experiments should be performed on all the colonies. Indeed, only the most comprehensive analysis should be performed on the final generation to limit costs.

Initial phenotypic characterisation of the *Dlk2* mutants should be very similar to the approach used in section 6, but with significantly larger sample sizes. The sex and genotype ratios of offspring born to heterozygous intercrosses should be assessed. These animals should also be weighed postnatally. Should any gross weight phenotype arise, DEXA assessments could be performed on a subset of the heterozygous intercrosses offspring at an appropriate time point. DEXA assessments would identify an bone density and lean:fat mass and so could identify the underlying cause of a weight phenotype. In addition, the wet and dry embryo and placental weights should be assessed for the offspring of heterozygous intercrosses throughout various stages of development. Furthermore, the sex and genotype ratios of such offspring should also determine to ascertain when homozygous loss occurs, if relevant.

It is challenging to predict what further phenotypic analyses would be useful to perform on the *Dlk2* mutant lines as the preliminary phenotypic data is so inconclusive (section 6). As the mutations are moved onto pure C57BL/6J backgrounds gross phenotypes may emerge that might inform the experimental design. However, given the widespread expression of *Dlk2* in the embryonic (sections 3.2 and 4.2) and postnatal (sections 4.3 and 4.4) wild-type mouse brains, investigating the behaviour, though classic experiments such as the Morris Water Maze, of *Dlk2*-/- mice versus wild-type litter-mate controls would probably be informative. Given the hypothesis that *Dlk2* is a stem cell regulator, it would be useful to derive neurospheres from *Dlk2*-/- mice and perform similar experiments to those used to characterise the role of *Dlk1* in postnatal neurogenesis [78]. This experiment is on-going in the Ferguson-Smith laboratory.

7.4.3 Investigating the relationship between *Dlk1* and *Dlk2*

In order to understand the evolutionary relationship of *Dlk1* and *Dlk2* across various vertebrates, it may be worth studying them in additional model organisms. In addition, it will be essential to investigate the expression of both genes during segmentation in mice. *Dlk1* and *Dlk2* have distinctive expression patterns during segmentation in zebrafish (PhD Thesis Ben Shaw, University of Cambridge (2017)) but the expression patterns, during segmentation, not been reported in mice. This makes it challenging to compare the overall expression dynamics between the two species and limits the potential interpretation of *Dlk1* function

and expression relative to the evolution of imprinting (section 7.1). ISH of both genes should thus be conducted during the segmentation period in mice.

Experiments investigating the expression of *Dlk2*, mRNA and protein, at various embryonic and postnatal stages in *Dlk1*-/- mice will help elucidate the relationship between *Dlk1* and *Dlk2*. *Dlk1*-/- murine wax sections were harvested at the standard developmental time points used in this study for *Dlk2* ISHs that were not completed. Similarly brain, liver, heart, lung, tongue, kidney, and placenta were extracted from *Dlk1*-/- mouse embryos but qPCR was attempted, due to the lack of success of *Dlk2* qPCR on wild-type tissues. A reciprocal set of experiments for *Dlk1* expression should be performed on the *Dlk2*-/- mice, after the appropriate backcross generation has been reached.

Evaluating the functional relationship between DLK1 and DLK2 will be more challenging, as they likely share some functional redundancy. After the appropriate backcross has been reached, the *Dlk2*-/- mice can be crossed with *Dlk1-/-* mutants. Offspring of these crosses (*Dlk1*+/-; *Dlk2*+/-, *Dlk1*+/-; *Dlk2*-/+, *Dlk1*-/+; *Dlk2*+/-, and *Dlk1*-/+; *Dlk2*-/+) can be crossed together to generate litters potentially including double knockouts which could be compared to wild-type litter-mate controls. If the double mutant is viable then the comprehensive phenotypic analysis, including neurosphere assessment, described in section 7.4.2 should be repeated. If the double knockout mice display more severe phenotypes than the individual knockout mice then there is likely some functional redundancy. The double knockout could prove to be lethal. In such a scenario, it might be worth crossing the *Dlk2-/-* mice with conditional *Dlk1* mutants [18].

Although a zebrafish *Dlk2* mutant has been generated, attempts to edit *Dlk1* in zebrafish to create mutations have been unsuccessful to date, however these experiments remain in progress. Generating *Dlk1*-/- zebrafish and performing a similar suite of phenotypic experiments would help inform the evolutionary relationship between *Dlk1* and *Dlk2*. Generating and phenotyping *Dlk1*-/-; *Dlk2*-/- zebrafish, if viable, would be ideal for this purpose.

8 Materials and methods

All procedures were performed in accordance with the Home Office Guidance on the Operation of the Animals (Scientific Procedures) Act 1986, published by Her Majesty's Stationery Office.

8.1 Mice

Mouse lines were maintained in the Combined Animal Facility, University of Cambridge. Routine maintenance was performed by animal technicians, in particular Wendy Cassidy. All mouse work was carried out in accordance with UK Government Home Office licensing regulations under project licence PC9886123.

8.1.1 Routine mouse maintenance

All mice were housed in a temperature- and humidity-controlled room (21^{o}C, 55% humidity) with 15-20 air changes per hour and a 12 hour/12 hour light-darkness cycle (light 07:00-19:00, dark 19:00-07:00). All mice were fed standard RM3 (E) diet (Special Diets Services) *ad libitum*. They were given fresh tap water daily and re-housed in clean cages weekly. Mice were weaned at 21 days postnatally, or a few days later if particularly small. Thereafter, except when breeding, they were housed in single-sex groups (5 per cage maximum). If the litter was small, mice would be single-sex housed in a maximum of 6 individuals for no more than a week to enable genotyping. Mice were also occasionally singly housed.

The presence of pathogens was monitored using sentinel animals. Routine monitoring detected the presence of murine norovirus, murine hepatitis virus, pinworm and *Helicobacter* species. Early in 2017 the unit discovered a widespread mite infestation in the facility. This was treated with 6 treatments of selamectin followed by 5 weeks of invermectin treated diet.

8.1.2 Timed matings

Timed matings were used to harvest embryonic materials at the correct developmental stage. Matings between receptive females and relevant males were set up towards the end of the

working day. The following morning, staff at the Combined Animal Facility checked if the female had a waxy vaginal plug — indicating a successful mating. If there was no visible plug the process was repeated the following morning. When a female had an observable plug, she was removed to a new cage and the 'plug' date recorded. From around e10.5, the pregnant female was weighed daily to ensure that her weight increased as expected during pregnancy. Pregnant females were sacrificed by a schedule 1 method at the correct developmental time point and the embryos harvested. Non-pregnant females were returned to the male to repeat the timed mating process.

8.1.3 Mouse lines used and their routine breeding

The *Dlk1*-/- mice were maintained on a C57BL/6J background, having previously been backcrossed into this background for 10 generations. The various *Dlk2* mutant lines were generated using CRISPR/Cas9 in CBA x C57BL/6J hybrids. Backcrossing these mutants onto a pure C57BL/6J background is on-going.

C57BL/6J

C57BL/6J mice were initially purchased from Harlan Laboratories, Charles River Laboratories, or the Jackson Laboratories and thereafter maintained in-house by mating C57BL/6J females with C57BL/6J males.

CAST/EiJ

CAST/EiJ mice were initially purchased from the Jackson Laboratories and thereafter maintained in-house by mating CAST/EiJ females with CAST/EiJ males.

C57BL/6J X CAST/EiJ hybrids

C57BL/6J X CAST/EiJ hybrids were generated by crossing C57BL/6J females (section 8.1.3) with CAST/EiJ males (section 8.1.3). CAST/EiJ X C57BL/6J hybrids were generated by crossing CAST/EiJ females (section 8.1.3) with C57BL/6J males (section 8.1.3).

The *Dlk1* knockout line

The *Dlk1* knock-out line was created by homologous recombination in SvJ129 embryonic stem cells that resulted in the replacement of 3.8 kb of the endogenous *Dlk1* allele with a neomycin resistance cassette in the opposite orientation to the gene [181]. This recombination removed the *Dlk1* promoter and its first three exons [181]. The *Dlk1* knock-out line

was routinely maintained by homozygous crosses (*Dlk1*-/- x *Dlk1*-/-) by Jennifer Cornish or myself.

To compare embryonic weights of *Dlk1*-/- mice and wild type mice (section 6.5), internal wild type littermate controls were needed. To achieve this C57BL/6J wild type animals were crossed with *Dlk1*-/- mice to generate heterozygous offspring. These offspring were then mated together in a timed mating (section 8.1.2) and the females sacrificed by a schedule 1 method at the relevant embryonic stage.

The *Dlk2* mutant lines

The DK1C, DK1G, DK16, DK73, and DK13 lines were generated using CRISPR (section 8.7). Founder animals were initially housed in the MRC Cambridge Stem Cell Institute, University of Cambridge, Animal Facility where routine mouse maintenance (section 8.1.1) was performed by Clare Cunstance. She also collected ear biopsies (section 8.1.4) for the founder mice. When the founder animals reached breeding age they were transferred to the Combined Animal Facility, at the University of Cambridge, where they were mated to C57BL/6J and their offspring genotyped.

The described lines were characterised and selected at the F1 stage. F1 mice of each kept *Dlk2* mutant line were then crossed again with C57BL/6J mice. This backcrossing process was continued: F2 heterozygous offspring were crossed with C57BL/6J mice, then F3 heterozygous offspring were crossed with C57BL/6J, and so on.

Heterozygous intercrosses of each line were achieved by crossing heterozygous F1 or F2 mutants with each other. These colonies were then maintained by mating heterozygous offspring of each cross together.

8.1.4 Collection of tissues for genotyping

All mouse lines were routinely genotyped from an ear biopsy taken, from p6 onwards, using 'The Punch' (National Band). Ear biopsies were also taken between p3 and p6 for *Dlk2* mutant lines using scissors by William Watkinson. Ear biopsies were stored at -20^{o}C prior to use.

8.1.5 Genotyping

Dlk1 knock-out mice

Mice from the *Dlk1* knock-out line were genotyped by PCR (section 8.3.10) using low-quality DNA extracted (section 8.3.2) from ear biopsies (section 8.1.4). This identified the presence or absence of the neomycin resistance cassette or the BAC.

Dlk2 mutant lines

All *Dlk2* mutant mice were genotyped by PCR (section 8.3.10) targeting exon 2, 3, or 5, as required, using low-quality DNA extracted (section 8.3.2) from ear biopsies (section 8.1.4). The PCR results were visualized using gel electrophoresis (section 8.3.4). With the exception of the DK73 line, the DNA producted was extracted from the agarose gel (section 8.3.5). Sanger sequencing by Genewiz or Source BioScience was performed on the extracted DNA. The sequence traces were analysed by manual annotation to determine the genotype of each animal.

8.1.6 Dissection of mice

Dissections of embryos and placentae were performed on pregnant females sacrificed by a schedule 1 method, often with technical assistance of Jennifer Corish, Billy Watkinson, and Frances Dearden. Embryos, contained inside their yolk sac, were removed from perinatal cavity and placed into 1XPBS on ice until needed. During dissection of the embryos and placentae, they were carefully removed from the yolk sac and amnion. After allowing as much amniotic fluid to be removed as possible, the embryos and placentae were separately weighed, and the embryo measured using a transparent ruler. From e16,5 onwards, embryos were then decapitated. Tails were taken for genotyping (section 8.3.10). Afterwards the embryos and placentae were then added to 4% PFA for histology (section 8.3.6) or further tissues, such as brain and liver, were then dissected and snap frozen using liquid nitrogen (section 8.3.14).

C57BL/6J X CAST/EiJ hybrids, and their reciprocal hybrids, were sacrificed using a schedule 1 method by Dr. Lisa Hulsmann, and then dissected. She performed such dissections on hybrids at p7 and p60 and isolated the brainstem, cerrebellum, cortex, hippocampus, hypothalamus, liver (p7 only), and muscle (p7 only). She also dissected 16.5 hybrid embryos as described above, isolating brain, liver and placenta. All tissues were snap frozen using liquid nitrogen for RNA extraction (section 8.3.14).

8.1.7 Weighing postnatal mice

Ear biopsies, taken as early as p3 (section 8.1.4), also functioned as IDs for individual mice. From the biopsy onwards relevant litters were weighed postnatally, at regular intervals, in the Combined Animal Facility, occasionally by William Watkinson or Frances Dearden. The animals were placed into a large transparent container and weighed using the same scales.

8.2 General materials and equipment used

8.2.1 Common materials used

Where relevant the kits used will be described in the method text, however common materials used are outlined below:

1. 0.2ml 8-Strip Non-Flex PCR Tubes: STARLAB I1402-3700-C
2. 10μl, 20μl, 300μl, and 1000μl filter sterile pipette tips: STARLAB S1120-3710-C, S1123-1710-C, S1120-9710, and S1122-1800-C, respectively
3. 10μl, 200μl, 1000μl pipette tips: STARLAB, S1111-3700-C, S1113-1700-C, and S1112-1720, respectively
4. 15ml centrifuge tube: Corning 430791 or ThermoFischer Scientific 11849650
5. 50ml centrifuge tube: Greiner Bio-One 227261 or ThermoFischer Scientific 430046
6. 96 well PCR plate: Axygen AXP401
7. 384 transparent qPCR plate: Roche 5102430001
8. 1kb ladder: Newmarket Scientific DM010X5
9. 100bp ladder: Newmarket Scientific DM001X5
10. Absolute ethanol: Sigma-Aldrich 32221
11. Ethylenediaminetetraacetic acid (EDTA): Sigma E5134
12. Formamide: Sigma-Aldrich 613339
13. Microcentrifuge tube; 1.5ml and 2ml: STARLAB e1415-1500 and LabCon 211-0034, respetively

14. Nuclease free water: Roche R0581, Sigma W4502, or DEPC treated water (section 8.2.2)
15. Plate sealers (PCR): STARLAB E2796-0793
16. Plate sealers (qPCR): Roche 4729757001
17. Protinase K: ThermoFischer Scientific 10103533
18. RNase A: Sigma-Aldrich A2760
19. Sodium Citrate: ThermoFischer Scientific S3320
20. Sodium Hydroxide (NaOH): ThermoFischer Scientific S4880
21. Sodium Chloride (NaCl): Honeywell Fluka 31343 or ThermoFischer Scientific S3120/60

8.2.2 Solutions generated

1X Maleic Acid Buffer

0.58g Maleic acid (ThermoFischer Scientific 63186), 0.44g NaCl, and 0.36g NaOH were dissolved in a total of 50mL distilled water, which was subsequently filter sterilised.

1X Phosphate Buffered Saline (PBS)

Phosphate Buffered Saline (Dulbecco A) tablets (Oxoid) in nuclease free or distilled water, as per the manufacturer's instructions.

4% Paraformaldehyde (PFA)

5 PFA tablets (Oxoid BR0014G) were dissolved into 500ml distilled water on ice. 50ml aliquots of the solution were stored at -20^{o}C until use. The frozen PFA was used exclusively for ISHs (section 8.5.2). All other PFA was generated by dilution of 40% PFA solution (Sigma-Aldrich 441244).

20X SSC

175.3g NaCl and 88.2g sodium citrate were dissolved in 1L distilled water and the pH adjusted to 7.0 using 10M NaOH.

100X Denharts

20g ficoll (Sigma-Aldrich F5415), 20g polyvinylpyrrolidone (Bio Basic Canada 9003-39), and 20g BSA (Fraction V, Sigma) were dissolved in 1L of distilled water and then filter sterilised.

Blocking solution

1% blocking reagent (Roche 11096176001) was dissolved at 37^{o}C in maleic acid buffer.

Chamber buffer

50ml chamber buffer was created with 20ml formamide, 12.5ml 20x SSC, and 17.5ml nuclease free water.

Cresol-Red loading buffer

28% w/v Sucrose (ThermoFischer Scientific S-9378) and 0.008% w/v Cresol-red were added to 50mL of distilled water. Communal lab stock originally generated by Frances Dearden.

DEPC treated water

0.1% DEPC (Sigma D5758) was added to distilled water and left over night. The mixture was autoclaved the following morning to degrade the DEPC.

LB agar

10g tryptone, 5g yeast extract, and 10g NaCl were added to 1L distilled water before the pH was adjust to 7.0 using 5M NaOH. The mixture was then autoclaved.

LB agar plates

10g tryptone, 5g NaCl, 5g yeast extract, and 15g agar were added to 1L distilled water. The mixture was autoclaved. Before pouring the plates the autoclaved solution was melted in the microwave and 0.5mL ampicillin (100ng/ml) was added.

NTMT solution

20ml 5M NaCl, 50ml 1M MgCl2, 100ml 1M TrisHCL pH9.5, and 5ml 20% Triton (Sigma-Aldrich X100) were added to sufficient distilled water to create a solution with a total volume of 1L.

RNase free 0.5M sodium hydroxide

20g of NaOH was dissolved in RNase free water (section 8.2.1).

SOC media

20 mg/ml Tryptone, 5 mg/ml Yeast Extract, 85.6 mM NaCl, 2.5 mM KCl , 0.01 mM MgCl2, 0.02 mM Glucose were dissolved in distilled water. The pH was adjusted to 7.0, and the solution was sterilised by autoclaving.

Tris-Glycine buffer

18.77g Tris-Base (Sigma-Aldrich T1503) and 30.29g glycine (Sigma-Aldrich G8898) were dissolved in 500mL of distilled water.

8.2.3 Primers used

Name	Use	Forward	Reverse
18s rRNA	qPCR	CGGCTACCACATCCAAG-GAA	GCTGGAATTACCGCG-GCT
Actin	qPCR	CCGGGACCTGACAGAC-TACCT	GCCATCTCCTGCTC-GAAGTCTA
DLK1	qPCR	GCTTCGCAAGAAGAA-GAACC	CTCATCACCAGCCTC-CTTGT
DLK1 (WT)	GT *Dlk1* line	CCAAATTGTC-TATAGTCTCCC	CTGTATGAAGAGGAC-CAAGG
DLK1 (KO)	GT *Dlk1* line	CATCTGCACGAGAC-TAGTG	CTGTATGAAGAGGAC-CAAGG
DLK2	qPCR	CCACTGGACCCTGCTGC-TAC	TGCTAACCTGGCACTC-CTGATC
DLK2 ex. 2	GT CRISPR mut.	CAGACCTGGC-TAGTGGGTTC	GTTGGCGAGGCAAG-GTATC
DLK2 ex. 3	GT CRISPR mut.	TGACCTCTGCTGGCTA-GAGA	GAGAGTTCCCGAA-GACAGGG
DLK2 ex. 5	GT CRISPR mut.	ACTACCAGAGCTGAGAC-CGG	AGAAAAGGGCGTTTAC-CACA

Table 8.1 (continued)

Name	**Use**	**Forward**	**Reverse**
DLK2 ex2. gRNA-1	CRISPR gRNA — 1st apt.	TAATACGACTCAC-TATAGCCAGACGTGTAGA-CACCTGT	TTCTAGCTCTAAAACCC-CACAGGTGTCTA-CACGTC
DLK2 ex2. gRNA-2	CRISPR gRNA — 1st apt.	TAATACGACTCAC-TATAGCCCACAGGTGTC-TACACGTC	TTCTAGCTCTAAAACCC-CACAGGTGTCTA-CACGTC
DLK2 ex2. gRNA	CRISPR gRNA — 2nd apt.	TAATACGACTCACTATAG-GCACACGAGATTTAGGCA	TTCTAGCTCTAAAACCT-GCCTAAATCTCGTGTGC
DLK2 ex3. gRNA	CRISPR gRNA — 2nd apt.	TAATACGACTCACTATAG-GTCAGGAGCGCAGCAG	TTCTAGCTCTAAAA-CACGGCTGCTGCGCTC-CTGA
DLK2 ex5. gRNA	CRISPR gRNA — 1st apt.	TAATACGACTCACTATAGT-GCAACCGCTCCGTTC-CATA	TTCTAGCTCTAAAA-CACGGCTGCTGCGCTC-CTGA
DLK2 ex5. gRNA	CRISPR gRNA — 1st apt.	TAATACGACTCACTATAGT-GCAACCGCTCCGTTC-CATA	TTCTAGCTCTAAAA-CACGGCTGCTGCGCTC-CTGA
DLK2 ex5. gRNA	CRISPR gRNA — 2nd apt.	TAATACGACTCACTATA-GATTCTGGCAGGGT-GATTGTG	TTCTAGCTCTAAAACC-CGTCATACACA-CACTGGC
TBP	qPCR	AGAGCAACAAA-GACAGCAGC	CTGTGTGGGTTGCTGA-GATG

Table 8.1 **Primer pairs used throughout the project**

Acronyms used: apt. — attempt, ex. — exon, GT — genotyping, KO — knockout allele, mut. — mutants, WT — wild type allele.

8.3 Common techniques used

8.3.1 Cloning

Prior to cloning, the plasmid was dephosphorylated to prevent self-ligation of and promote plasmid phosphorylated insert ligation. Approximately 4mg of pBluescript II (gift from Dr. Mitsu Ito) was added to 40μl NEBuffer 3 (New England Biolabs B7003S), 4μl 100X fortified BSA (New England Biolabs B9000S), 4μl of EcoRV (Roche 000000011040197001) and sufficient distilled water to make a total reaction volume of 400μl. After vortexing and brief centrifugation, the reaction was incubated overnight at 37^{o}C. 4μl of the reaction was added to 4μl of Cresol Red (section 8.2.2) and run on a 1% agarose gel (section 8.3.4) to check that the digestion was successful.

Following successful digestion, 4μl of Calf Intestinal Alkaline Phosphatase (New England Biolabs M0290S) was added to the reaction and incubated at 37^{o}C for 1 hour. Phenol Chloroform extraction (section 8.3.7) was then performed followed by ethanol precipitation (section 8.3.3) where the final product was resuspended in 20μl of nuclease free water. The concentration was then assessed using the BioDrop uLite.

4μl of the ethanol precipitated linearised plasmid was added to a sufficient volume of the phosphorylated (section 8.3.8) target insert for a vector:insert ratio of 1:3. This mixture was added to 1μl of T4 DNA ligase (New England Biolabs (M0202S) and incubated at 16^{o}C for 30 minutes and then 65^{o}C for 10 minutes. 1μl EcoRV (Roche 000000011040197001) was then added to the reaction, which was the incubated at 37^{o}C for another 30 minutes, to break down any vector that self ligated. Finally, ethanol precipitation (section 8.3.3) was performed and the product was resuspended into a final volume of 5μl of distilled water.

8.3.2 DNA extraction

DNA extraction of mouse ear clips was performed using the Rapid Extract PCR Kit (PCR-BIO PB10.24-08), according to manufacturer instructions, or using the Extract-N-Amp kit (Sigma-Aldrich XNAT2-1KT). Extractions using the sigma kit were prepared on ice: 20μl lysis solution and 2L protienase K (10ng/μl) were added to cover each ear-notch. The samples were then briefly centrifuged before being incubated at 55^{o}C for 10 – 15 minutes and subsequently 94^{o}C for no more than 5 minutes. 20μl of neutralising solution was then immediately added to each sample. Extracted DNA from both kits was stored at -20^{o}C until

used.

The DNA of transformed cells was extracted differently. After a colony of a desired target (plasmid) had been expanded (section 8.4.1), the cells were centrifuged at 4^{o}C for 10 minutes at 3000rpm. The broth and tooth pick were then removed and discarded appropriately (addition of 2% Virkon (Appleton Woods 330013) for over an hour before disposal), before the DNA of the pellet was extracted using the GenElute Plasmid Miniprep kit (Sigma PLN10). DNA concentration was obtained using the BioDrop uLite.

8.3.3 Ethanol precipitation

Ethanol precipitation was performed using 20μl of the required RNA or DNA product. This was added to 80μl of nuclease free water, 1μl of glycogen(ThermoFischer Scientific R0561), 35μl of 10M ammonium acetate and 250μl of 100% ethanol (at a temperature of -20^{o}C). Ethanol precipitation was performed at -20^{o}C for at least 2 hours or overnight. The reaction was then centrifuged for 20 minutes at 13,500rpm, and the supernatant removed. 500l of 70% ethanol (made with nuclease free water) was added to the pellet. The mixture was then vortexed and subsequently centrifuged at 13,500rpm for 20 minutes. The supernatant was again removed and the pellet was resuspended in the appropriate volume of nuclease free water.

8.3.4 Gel electrophoresis

Ordinary agarose gels were generated by dissolving agarose (Melford Laboratories A20090-500) into 0.5X TBE (Invitrogen 15581044) buffer using a microwave in a glass bottle. Typical gel percentages were 1%, 1.5%, and 2%. After melting the agarose, the gel was gently cooled by holding the bottle under a cold tap and shaking, carefully ensuring that no water entered the gel. This step was taken as excessively hot gels can denature the SafeView (NBS Biologicals NBS-SV1) used to visualise the DNA (pers. comm. Dionne Gray) and damage the mould/cassette (pers. comm. Jennifer Cornish). After the cooling step, SafeView was added to the gel at 5μl per 100ml gel. The SafeView was then dissolved in by gently shaking the bottle and the gel poured into the prepared cassette, containing appropriately sized combs. The gel was allowed to solidify for at least 20 minutes before being placed into the tank.

If necessary 0.5X TBE buffer was added to the tank until the gel was completely covered. The combs were removed and the samples, and appropriate ladders (section 8.2.1), were

loaded into the wells. Unless stated all gels were then run at 120mV for 40-50 minutes using voltmeter (Elektrophorese PP389). Gels were then visualised using a transilluminator (Sygene Ugenius 3).

RNase free gels were also generated. Agarose gels were generated as described above using 0.5X TBE buffer (diluted in nuclease free water). The bottle used to melt the agarose was also autoclaved and soaked in 0.5M RNase free NaOH (section 8.2.2) for at least 15 minutes prior to use. The tank, combs and mould were also soaked in 0.5M RNase free NaOH for at least 15 minutes before use.

8.3.5 Gel extraction

Gel extraction was performed using the MinElute Gel Extraction Kit (Qiagen 28604). The manufacturer recommended protocol was modified for reagent conservation. The gels were melted in buffer QG at 30^{o}C using a heat block and were continuously shaken. Jennifer Cornish had observed that the columns could only contain 650μl of solution and so this was the maximum volume loaded at a given step. Furthermore, only 650μl of buffer PE and 300μl of the second use of buffer QG were used. Finally the distilled water, in which the DNA was finally dissolved, was pre-warmed to 55^{o}C.

8.3.6 Histology

Samples, dissected as described in section dissections, were fixed in 4% (w/v) paraformaldehyde pH 7.4 (Sigma-Aldrich 441244) in 1X PBS at room temperature or at 4^{o}C for an appropriate time period. Samples greater than 1cm wide or long were fixed for at least overnight. Samples greater than 2cm wide or long were fixed for 48 hours. E16.5 and e18.5 embryos were decapitated to aid the fixation process.

Fixed samples were transferred to 70% ethanol for short-term storage. Samples with bone were transferred to PBS as ethanol reacts with EDTA used in the decalcification process. Samples were stored in PBS for no more than a week before transfer to the Helen Skelton in the Histology Unit at the Pathology Department, University of Cambridge. Samples stored in 70% ethanol, and some still undergoing the fixation process, were also delivered to her.

She performed all subsequent steps, including decalcification of bone, necessary for embedding the samples in paraffin wax. She also sectioned the samples using a microtome to

produce 10μm thick sections – this was the same thickness Dr. Mary Cleaton found optimal for histological analysis during her PhD.

8.3.7 Phenol Chloroform extraction

An equal volume of phenol-chloroform was added to the target DNA and vortexed. The mixture was then centrifuged at maximum speed for 15 minutes. The upper aqueous phase was transferred to a new tube where an equal volume of phenol-chloroform was again added. The mixture was again vortxed and centrifuged at maximum speed for 15 minutes and the upper aqueous phase transferred to a new tube.

8.3.8 Phosphorylation of PCR products

1.5μl NEBuffer 3 (New England Biolabs B7003S), 1μl T4 Polynucleotide Kinase (New England Biolabs M0201S), 2μl 10M ATP, and 0.5μl distilled water were added to 10ul of ethanol precipitated (section 8.3.3) poly A tailed (section 8.3.9) PCR product (section 8.3.10). This reaction was incubated at 37^{o}C for 30 minutes followed by a 20 minute incubation at 60^{o}C.

8.3.9 Poly A tailing

3μl of substrate DNA was added to 1μl dATP, 1μl Taq polymerase (Bioline BIO-21040), 1μl Taq polymerase buffer (Bioline BIO-21040), and 3μl of distilled water. The reaction was incubated for 15 minutes at 70^{o}C before being stored on ice until use.

8.3.10 Polymerase chain reaction (PCR)

All PCRs were performed in 8 piece strips or plates (section 8.2.1) and contained negative water controls, using the primers outlined in section 8.2.3.

Genotyping of *Dlk1* mutant mice

7.5μl of Red Taq (Sigma-Aldrich R2523), 0.5μl 10mM forward primer (table 8.1), 0.5μl 10mM reverse primer (table 8.1), and 5.5μl of distilled water were added to 1$\mu$of DNA of sample (extracted as in section 8.3.2). Presence of the WT and KO allelles were tested separately. PCR conditions testing for the WT allele: 95^{o}C for 5 minutes; 40 cycles of 95^{o}C for 30s, 50^{o}C for 30s, and 72^{o}C for 30s; 72^{o}C for 5 minutes; 10^{o}C until needed. PCR conditions testing for the KI allele: 95^{o}C for 5 minutes; 35 cycles of 95^{o}C for 30s, 60^{o}C for 30s, and 72^{o}C for 30s; 72^{o}C for 5 minutes; 10^{o}C until needed.

Genotyping of *Dlk2* mutant mice

This PCR was performed on 1:10 dilutions of extracted DNA (section 8.3.2) of samples. Although different primers were used (table 8.1), the following protocol was the same for genotyping alterations in all three targeted exons. 10μl Red Taq (Sigma-Aldrich R2523), 1μl 10mM forward primer (table 8.1), 1μl 10mM reverse primer (table 8.1), and 7μdistilled water were added to 1μl of the sample DNA. PCR conditions: 95^{o}C for 30s; 40 cycles of 95^{o}C for 30s, 60^{o}C for 30s, and 72^{o}C for 1 minute; 72^{o}C for 5 minutes; 10^{o}C until needed.

ISH probe generation

This reaction was performed on C57BL/6J postnatal brain cDNA (section 8.3.11), using high-fidelity DNA polymerase kit (Phusion M0530), to generate the substrate from which a *Dlk2* riboprobe could be generated (section 8.5.1). For 1 20μl reaction: 4μl 5X GC buffer, 0.4μl 10mM dNTPs, 1μl 10mM forward primer (table 8.1), 1μl 10mM reverse primer (table 8.1), 0.2μl DNA polymerase, 20-75ng of template cDNA (variable volume), and sufficient nuclease free water to create a total reaction volume of 20μl. PCR conditions: 98^{o}C for 30s; 35 cycles of 98^{o}C for 30s, 67^{o}C for 15s, and 72^{o}C for 30s; 72^{o}C for 10 minutes; 10^{o}C until needed.

8.3.11 Production of cDNA

cDNA synthesis was conducted in a RNase and DNase free area and RNase free filter tips. The area, pipettes and pipette boxes were cleaned using the antibacterial spray followed by 70% ethanol. cDNA was synthesised using the RevertAid H minus first strand cDNA synthesis kit (ThermoFischer Scientific K1631) and, unless stated, took place on ice. 1μg of template RNA, extracted as described in section 8.3.14, per sample was added to sterile, nuclease free PCR tubes labelled as the *rt* (reverse transcriptase negative) controls. 1μl of the kits random hexamers were then added to the same tubes. Nuclease free water was added to create a total volume of 12μl in each *rt* tube. The overall reaction mastermix was then assembled: a total volume of 7μl per sample included 4μl of 5X reaction buffer, 1L RiboLock RNase inhibitor (20U/μl) and 2μl 10mM mixed dNTP (Qiagen 201913). All reagents were vortexed and briefly centrifuged before assembly. The mastermix was then briefly centrifuged before 7μl was added to each of the *rt* tubes. 1μl of RevertAid H minus M-MuLV Reverse transcriptase (200U/μl) was then added to a fresh set of PCR tubes labelled at the +*rt* (reverse transcriptase positive) samples. 16μl of the vortexed and briefly centrifuged samples from each the *rt* controls was then added to the corresponding +*rt* tubes. *rt* and +*rt* reactions were then incubated at 25^{o}C for 5 minutes and then 45^{o}C for 60 minutes. Samples were

then immediately stored on ice to aliquot and, if appropriate, dilute. All cDNA was stored at -80^{o}C.

8.3.12 qPCR

qPCR was performed, with technical assistance from Billy Watkinson, on extracted RNA (section 8.3.14) that had been converted to cDNA (section 8.3.11). A single reaction consisted of 0.5μl of the 10mM forward primer (section 8.2.3), 0.5μl of the 10mM reverse primer (section 8.2.3), 5μl of Sybr II Brilliant master mix (Aligent 600828), 3μl of nuclease free water, and 1μl of cDNA samples. The primers used are available in section 8.2.3. The reaction mixture (total volume 9μl) without the cDNA sample was generated and then added to the 384 qPCR plates, before 1μl of cDNA (diluted 1/20 from the cDNA synthesis product, generated as described in section 8.3.11) was added to the relevant well as quickly as possible to limit cDNA degradation. The negative control of every sample was included in every qPCR experiment. Negative controls were the result of a portion of the same RNA sample that underwent the same cDNA synthesis reaction without the reverse transcriptase enzyme. Theoretically these samples should have no cDNA present and thus they test for contamination. After successfully loading the plate, it was sealed with a Thermo Scientific AB-0580 Thermal adhesive seal. The qPCR was centrifuged for 10-20 seconds prior to qPCR.

The qPCR was run on a LightCycler 480 (Roche) machine using LightCycler 480 SW1.5 software. Reaction conditions were 95^{o}C for 10 minutes, followed by 45 cycles of 95^{o}C for 15 seconds and 60^{o}C for 15 seconds. The reaction ended with a melt curve assessment step.

Several quality control measures were taken. Technical duplicates or triplicates of the same sample were loaded on every qPCR plate. The duplicates with the closest absolute ct values were used in the analysis. Samples, with technical duplicates with differences greater than 0.4 between ct values, were excluded from the analysis. In addition, samples with single in the negative control reactions were also discarded. The melt curve of every sample was also assessed to ensure that there was only one correctly sized peak (representing a pure cDNA product). Samples with poor melt curves were also excluded.

8.3.13 qPCR data processing

Since the entirety of the cDNA samples used for qPCR had been diluted 1/20 before being gifted to me, it was not possible to create standard curves of pooled samples. Standard curves

are essential for the Delta-Delta CT method of analysing qPCR data. Consequentially an alternative approach was used.

After the initial quality control steps described in section 8.3.12 to control for technical variability, the raw ct values were added the value of 40 (arbitrarily chosen). This was because the raw ct values are negative and adding them to a positive number made all the ct values positive. In other words, the negative ct value was made positive and then subtracted from the value of 40. This step insured that graphically all the data was positive, which puts the expression data on the conventional axis, and the relationships between each sample are maintained.

After this cosmetic processing, normal data analysis steps were performed. The technical replicates of a given sample were averaged. The *Dlk1* and *Dlk2* expression averages of each sample were then normalised against the corresponding average expression of *Tbp* in the sample sample.

8.3.14 RNA extraction

All RNA was extracted from tissues. Prior to dissection, 0.2-0.3mL of lysing matrix P bulk beads (MP Biomedicals 116540434) were added to labelled 2ml graduated skirted tubes (STARLAB e1420-2340), ensuring that the beads never touched anything but the inside of the sterile RNase and DNase free tubes. During the dissection, the tissues were added to the relevant prepared tube and snap frozen in liquid nitrogen. The snap frozen tissues were stored at -80^{o}C before RNA extraction.

Sterile, RNase free, and DNase free filter pipette tips were used during all stages of RNA extraction. TRI reagent (Sigma-Aldrich T9424) was first added to the samples (1 ml per 50100 mg of tissue), which were then homogenised for 40 seconds with a MagNA Lyser (Roche). The homogenate was then centrifuged at 12,000g for 10 minutes at 4^{o}C. The clear supernatant was subsequently carefully transferred to freshly labelled tubes. With samples possessing high fat contents, there was a layer of fatty material on the surface of the aqueous phase that was removed.

The transferred samples were then allowed to stand at room temperature for 5 minutes to allow dissociation of the nucleoprotein complexes. 0.1mL of 1-bromo-3-chloropropane (Sigma-Aldrich B9673) per 1ml of TRI reagent used was the added to the samples. Samples were vortexed for 15 seconds before standing at room temperature for 2-15 minutes. Centrifugation followed at 10,000g for 10 minutes at 4^{o}C. The upper aqueous phase was

then transferred to fresh tubes. 0.5ml of 2-propanol (Sigma-Aldrich 278475) per 1ml of TRI reagent used were added to the samples. The samples were again allowed to stand at room temperature, for 5-10 minutes, and were again centrifuged: 12,000g for 10 minutes at 4^{o}C. All subsequent steps of RNA extraction took place in an RNase free environment: the entire workstation, pipettes, and pipette boxes were cleaned with the antibacterial spray and 70% ethanol.

In the RNase free environment, the supernatant was carefully removed and 1mL of 70% ethanol (diluted in nuclease free water) was added per 1ml of TRI reagent used. The samples were then vortexed and centrifuged at 7,500g for 5 minutes at 4^{o}C; if the pellets floated upon addition of ethanol they were centrifuged at 12,000g. The supernatant was removed and the pellet air-dried for 5-10 minutes at room temperature. An experimentally relevant volume of nuclease free water was then added before the samples. The sample concentration and quality were ascertained using the BioDrop. Samples with A_{260}/A_{280} ratios less than 1.7 were not used.

8.3.15 Sequencing

Sanger sequencing was performed by Genewiz and Source Bioscience. Samples and, where relevant, corresponding primers were prepared according to company instructions. Sequencing was performed on samples directly after gel extraction (section 8.3.5) or on an undigested plasmid. Results were analysed using SnapGene Viewer (V4.2.1).

8.4 Microbiology

8.4.1 Colony expansion

Colonies to expand were taken from glycerol stocks (stored at -80oC) or from LB/Amp plates (stored at 4^{o}C). Sterile toothpicks were used to obtain cells from the glycerol stocks, by scraping off a tiny piece of frozen cells, or from a single colony on an LB/Amp plate. The toothpicks were added to 5mL LB/Amp media (1μl Ampicillin per 1 mL LB) and incubated overnight at 37^{o}C in a shaking incubator. The expanded colonies were then used immediately or stored at 4^{o}C.

8.4.2 Glycerol stock generation

Sterile 100% glycerol (sigma G551G) was microwaved for 20 seconds before 500μl was added to a cryovial (STARLAB E1420-2340). 500μl of an expanded colony (section 8.4.1) was subsequently added. The glycerol stocks were then stored at -80^{o}C.

8.4.3 Transformation

2μl of target plasmid was added to 1.5ml tubes on ice, where competent cells were being defrosted. After the competent cells had thawed, 30μl were added to the plasmid and mixed gently by flicking the tube. The cell-plasmid mix was left on ice for 30 minutes before being heat shocked at 42^{o}C for 42 seconds. The cells were returned to the ice for 2 minutes. Afterwards, 100μl room temperature SOC media was added. The cells were the incubated, shaking, at 37^{o}C for 1 hour. 10-100μl of transformed cells was spread onto LB/Amp plates (pre-warmed to 37^{o}C). The plates were then wrapped in Clingfilm and incubated overnight at 37^{o}C. The following morning, the plates were removed from the incubator and stored at 4^{o}C.

8.4.4 Testing transformation success of a given colony

Successful transformation was tested using restriction digestion or by PCR. To test via restriction digestion, restriction endonucleases were chosen that would confirm the presence of the plasmid (and its insert). For each digestion, 10μl of colony DNA (previously extracted as described in section 8.3.2) was added to 15μl of distilled water, 3μl of the appropriate buffer, 1μl of restriction endonuclease 1 and 1μl of restriction endonuclease 2. The reaction was incubated at 37^{o}C for 2 hours or overnight. Transformation of the *Dlk1* riboprobe was confirmed using restriction enzymes BamHI (NEB R0136L) and EcoRI (NEB R0101S) with a NEB 2.1 buffer (NEB B7202S).

15μl of Cresol red (section 8.2.1) was added to the each reaction before all 15μl of the dyed reaction was run on a 1% agarose gel section 8.3.4 against a 1kb ladder. The results were then visualised using the transilluminator to check the band size and assess whether successful transformation occurred. Sequencing was used to validate colonies with transformations confirmed by restriction digest. Undigested DNA (extracted as described in section 8.3.2) was Sanger sequenced (section 8.3.15). The resulting sequence was then analysed to ensure correct transformation occurred.

8.5 *In situ* hybridisation

8.5.1 Generating *in situ* hybridisation probes

The ISH probe for *Dlk2* was designed to span the final exon of *Dlk2*. Primer3 [124] was used to find good quality primers (section 8.1) within exon six. BLAT [112] then confirmed that the *in silico* PCR product was specific to the targeted region. The target region was amplified from C57BL/6J genomic DNA by PCR (section 8.3.10). The product was run on a 1-2% agarose gel (section 8.3.4) and then purified (section 8.3.5). This product was then phosphorylated (section 8.3.8) before being cloned into the pBlueScriptII vector (section 8.3.1). The *Dlk1* riboprobe described by Da Rocha et. al [51] was originally cloned into pBlueScript and was provided as a gift by Dr. Marika Charalambous. The plasmids containing *Dlk1* and *Dlk2* riboprobes were then transformed into competent cells (section 8.4.3), whose colonies were then expanded (section 8.4.1) before glycerol stocks were generated (section 8.4.2). After the transformation of the colonies was tested (section 8.4.4), and colonies with the optimal clone were chosen to generate riboprobes from.

DNA previously extracted (section 8.3.2) from the chosen colonies was used for riboprobe generation. The circular DNA was linearized using an appropriate endonuclease: antisense *Dlk1* probes were linearized with EcoRI (NEB R0101S) and *Dlk1* sense probes with BamHI (NEB R0136L). 10μl DNA was added to 16μl distilled water, 3μl of an appropriate buffer and 1μl of an appropriate endonuclease per reaction. The reaction was incubated at 37^{o}C for 2 hours. The success of the digestion was confirmed by running 5μl of the reaction (added to 5μl of Cresol red loading buffer) on a 1% agarose gel (section 8.3.4). The concentration of DNA was ascertained using the BioDrop. The MinElute PCR Purification kit (Qiagen 28004) was used to purify the DNA according to manufacturer instructions.

In vitro transcription produced sense and antisense RNA probes from the forward and reverse linearized plasmids. A single reaction was generated by adding 2μl of DTT (Stratagene 600098-S3)to 0.5μl RNase inhibitor, 2μl of a mix of DIG-labelled nucleotides (Roche 11277065910), 2μl RNA polymerase (MEGAscript T7 and MEGAscript T3 enzymes for antisense and sense probes, respectively (ThermoFischer Scientific AM1334 and AM1338, respetively)), and 1μg of the linearized DNA. Sufficient volume of nuclease free water was added to create a total reaction volume of 20μl. The reaction was incubated overnight at 37^{o}C.

Prior to continuing the protocol the following day, the workstation was prepared so that it was RNase free. The area, pipettes and pipette boxes were cleaned using the antibacterial spray followed by 70% ethanol. 100% ethanol was also placed in the -20°C freezer. 2μl of DNase I (ThermoFischer Scientific EN0521) was added to each sample and incubated for 1 hour at 37°C before 2μl of DNase I stop solution was added followed by a 10-minute incubation at 65°C.

Ethanol precipitation (section 8.3.3) was then performed using 20μl of the existing reaction. The product was ultimately resuspended in 100μl of nuclease free water. The transcribed RNA was stored at -80°C until needed.

The quality of the transcribed RNA was tested in two ways. The concentration of the transcribed RNA was tested using the BioDrop. In addition, 1l of the transcribed RNA was added to 9μl of an RNase free loading buffer (gift from Dione Gray) and run on a 1% RNase free agarose gel (section 8.3.4) against a 100bp RNA ladder.

8.5.2 *In situ* hybridisation

ISH initially took place in an RNase free environment. The area, pipettes and pipette boxes were cleaned using the antibacterial spray followed by 70% ethanol. In addition, all solutions were generated with nuclease free water. 50mL copffin jars, their lids, and tweezers were sterilised by heating them at 65°C for 40 minutes.

ISH was performed on paraffin wax sections of whole embryos and placentae prepared as described in section 8.3.6. Prior to ISH the selected sections would be labelled, using pencil, for the probe being used. Sense and antisense probes were used for each gene in every experiment.

The slides were placed into the sterilised and cooled copffin jars using the tweezers. The relevant solution would be poured into the jar and the lid added for each was. Changing solutions was achieved by pouring away the previous solution (either saving for reuse or for disposal), and immediately pouring in the next solution. This step was performed as quickly as possible to minimise dehydration of the wax samples. Certain washes had to be performed in the fume hood; during these steps slides were transferred between copffin jars using tweezers. This ensured that one sterile copffin jar (and lid) was suitable work outside the fume hood as it wouldnt have been exposed to the chemicals requiring the same degree

of projection.

ISH was initiated by rehydrating the sections. Slides were washed in histoclear (National Diagnostics HS202) for 10 minutes. This step was then repeated. The histoclear washes were followed by 2 5-minute washes in 100% ethanol. This was followed by a rehydration series consisting of 1-minute washes of 95% ethanol, 90% ethanol, 80% ethanol, 70% ethanol, 50% ethanol, and ending with 30% ethanol. A 5-minute wash in PBS then followed. The slides were then refixed in 4% PFA in PBS for 30 minutes. This step was followed by 2 5-minute PBS washes.

Proteolysis achieved antigen retrieval. The slides were incubated in proteinase K solution (0.025mg/mL proteinase K in PBS) for up to 2 minutes before 2 5-minute PBS washes, and a 15 minute refixation step in 4% PFA in PBS. 2 5-minute washes in PBS then followed. This was succeeded by 2 5-minute washes in 2X SSC and incubation in tris-glycine buffer for at least 30 minutes.

Hybridisation then followed. The hybridisation buffer was generated by adding 400l of 40% formamide to 10μl of 100x denharts, 250μl of 20x SSC, 9.2μl of 10g/l tRNA (Sigma R5636), and 8.8μl of 100g/l herring sperm (Sigma D7290). 25ng/μl of sense or antisense *Dlk1* probe was added to the total whereas 15ng/μl were added for the *Dlk2* probes. After the probes were added to the hybridisation buffers, they were heated at 95^{o}C for 5 minutes and immediately removed to ice.

60μl of the hybridisation buffer was added per slide, which was then covered using a custom generated parafilm coverslip (paraffin cut to just cover the sample). The prepared slides were then placed on the exposed pipettes in a damp chamber; two 20ml pipettes per slide kept the slides flat. The damp chamber consisted of a plastic box that had pipettes cut to exactly fill it lying above tissues soaked in chamber buffer. The chamber was sealed to prevent evaporation by several rounds of wrapping with parafilm. The chamber was incubated at 65oC in a hybridisation oven over the weekend.

All solutions used in steps after hybridisation were made with distilled, but not nuclease free, water. After hybridisation, the damp chamber was opened and the parafilm coverslips were carefully removed from the slides submerged under pre-warmed 5xSSC. After the coverslips were removed the slides were placed in another copffin jar for the subsequent steps. Unless stated, all steps were performed with rocking. The first washes were 3 15-

minute washes in 5xSSC at room temperature. Slides were then incubated for 40 minutes at 60^{o}C in Posthyb buffer (20% formamide/0.5xSSC). This was followed by a 15-minute room temperature wash in 2xSSC. The slides were then incubated in RNase A solution (1.25mg RNase A/100ml 2xSSC) at 37^{o}C for 15 minutes, and was followed by another 15-minute wash in 2xSSC at room temperature. A 20-minute wash in Posthyb buffer at 60^{o}C followed. This process was ended by 2 25-minute room temperature washes in 2xSSC.

During the final washing steps, the antibody was prepared. Anti-DIG AP fab fragments (Roche 11093274910) were diluted 1:1000 in blocking solution. After the final washing steps, 200μl of the diluted antibody solution was added per slide and covered with parafilm coverslips as described above. The prepared slides were again added to a damp chamber, filled with 2xSSC, and incubated at 4^{o}C overnight.

The following day the slides were submerged in PBS to remove the coverslips. Afterwards, they were washed, with rocking, in PBS for at least 4 hours. Typical timings of the washes were 3 10-minute washes, 3 30-minute washes, and then 2 1-hour washes. After the PBS washes, the slides were washed 3 further times in NTMT solution with each wash lasting 10 minutes. During the final wash the staining solution was generated: 1 NBT/BCIP tablet (Roche 11697471001) was added to 10ml distilled water and kept in the dark.

0.5ml of staining solution was added per slide and covered with a parafilm coverslip as described above. The staining reaction was incubated in the dark until a signal was visible, typically overnight. Incubating the slides in 1mM EDTA/PBS in copffin jars stopped the staining reaction. The slides were then counterstained with Fast Red (G-Biosciences 786-1053).

After counterstaining, the slides were washed several times in PBS until no red colour was visible in the liquid and glass of the copffin jar. Afterwards, the sections were dehydrated via an ascending ethanol series. This consisted of 1 minute washes of 30% ethanol, 50% ethanol, 70% ethanol, 80% ethanol, 90% ethanol, and 95% ethanol. This was followed by 2 5-minute washes in 100% ethanol, and 2 10-minute washes in Histoclear. The slides were then mounted.

Prior to mounting the slides were removed from the copffin jar and the excess liquid surrounding the section was carefully removed using tissue paper. Afterwards, DPX (Sigma-Aldrich 44581) was dropped onto the slide above the sections and the coverslips were then

placed on top of the slides. Coverslip placement was done extremely carefully to avoid the introduction of bubbles. After the DPX dried the slides could be studied and imaged.

8.6 Evolutionary analysis

8.6.1 Alignments

DNA and protein sequences were aligned using ClustalO (V1.2.4) [132] with default settings aligned against the input order. The protein domains were identified for each species using InterPro (V29.0) or through comparison the the amino acid sequence for the juxtamembrane domain previously characterised in the lab by Dr. Carol. Edwards for a variety of species (unpublished data). Identified regions were then manually highlighted in the alignment at correct coordinates.

8.6.2 Calculation of Ka/Ks values

Ka/Ks values were calculated for DLK1 and DLK2 with Dr. Carol Edwards. Coding sequences (appendix A.1) for each orthologue of each gene were in silico translated and aligned with ClustalW using TranslatorX [1], under default conditions. The Ka/Ks values were then calculated using SeqinR (V1.0) [39].

8.6.3 Calculation of percentage identity and percentage similarity

Protein sequences, obtained as described in section 8.6.5, were aligned using ClustalO (V1.2.4) [132] (section 8.6.1). Percentage similarity of the sequences between species were obtained using 'Ident & Sim' tool in the sequence manipulation suite [218] using default settings.

8.6.4 Evolutionary distances analysis

Dr. Carol Edwards generated a maximum likelihood tree for DLK1 and DLK2 from sequences, aligned by ClustalO (V1.2.4) [132], using PhyML [90]. Unless stated default settings were used. The akaike information criterion was used in the default model selection setting. No starting tree was used and the algorithm was bootstrapped 500 times.

8.6.5 Sequences used

Protein sequences for DLK1 and DLK2 were obtained by Dr. Carol Edwards or myself from Ensembl, UCSC [113] and NCBI. The sequences were assessed for their quality; poor sequences were discarded. For instance a significantly truncated DLK2 protein sequence was observed in the Sep2010 WUGSC 7.0/petMar2 Lamprey genome on the UCSC browser. This sequence was not used in the analysis. Additional quality control measures included removing additional start sequences. The relevant cDNA sequences were then obtained from the same source. A list of the cDNA and protein sequences used in this analysis in located within Appendix A.1.

8.7 CRISPR/Cas9 mediated genome editing

Genetically altering *Dlk2* with CRISPR/Cas9 was attempted twice (tables 5.1 and 5.2).

8.7.1 gRNA design and synthesis

gRNAs for the first CRISPR/Cas9 genome editing attempt were designed using the Wellcome Trust Sanger Institute Genome Editing database [97]. 2 gRNAs targeted exon 2 and 2 gRNAs targeted exon 5 (table 8.2). Dr. Celia Delahaye designed the gRNAs for the second CRISPR/Cas9 genome editing attempt targeting exons 2, 3, and 5 (table 8.2). All gRNAs were selected so that there would be a guanine adjacent to the PAM domain, as it has been demonstrated that this strongly promotes cleavage *Sp*Cas9 in cell lines [38, 62] and zebrafish embryos [161].

CRISPR attempt	Exon targeted	gRNA
1	2	CCAGACGTGTAGACACCTGTGGG
1	2	CCCACAGGTGTCTACACGTCTGG
1	5	TGCAACCGCTCCGTTCCATAGGG
1	5	ATTCTGGCAGGGTGATTGTGAGG
2	2	GGCACACGAGATTTAGGCAG
2	3	GTCAGGAGCGCAGCAGCCGT
2	5	GGCCAGTGTGTGTATGACGG

Table 8.2 **gRNAs used in CRISPR/Cas9 mediated genome editing**

The gRNAs were synthesised using the GeneArt Precision gRNA Synthesis Kit (ThermoFischer A29377) according to manufacturer instructions using the primers described in section 8.2.3. The concentration of the gRNAs was ascertained using a Qubit 3.0 according to manufacturer instructions.

8.7.2 Pronuclear microinjections

gRNAs (section 8.2) and Cas9 mRNA (ThermoFischer A29378) or protein (ThermoFischer B25640) were injected into F1 x F1 (CBA x C57BL6/J) hybrid zygotes by William Mansfield at the MRC Cambridge Stem Cell Institute, University of Cambridge.

During the CRISPR mediated genome editing attempt 1, 74 zygotes were injected with Cas9 protein (42ng/μl) and gRNAs targeting exon 2 (table 8.2) at 50ng/μl (25ng/μl of each gRNA) and transferred into psuedopregnant females. 28 zygotes were also injected with Cas9 mRNA (100ng/μl) and gRNAs targeting exon 5 (table 8.2) at 50ng/μl (25ng/μl of each gRNA) and transferred into psuedopregnant females.

During CRISPR mediated genome editing attempt 2, only Cas9 protein (42ng/μl) was injected into the hybrid zygotes, along with a single gRNA (50ng/μl) targeting exons 2, 3, or 5 (table 8.2). 66 injected zygotes were transferred into pseudopregnant females for exon 2, 42 for exon 3, and 54 for exon 5.

References

[1] Abascal, F., Zardoya, R., and Telford, M. J. (2010). TranslatorX: multiple alignment of nucleotide sequences guided by amino acid translations. *Nucleic Acids Research*, 38(Web Server issue):W7–13.

[2] Abdallah, B. M., Bay-Jensen, A.-C., Srinivasan, B., Tabassi, N. C., Garnero, P., Delaisse, J.-M., Khosla, S., and Kassem, M. (2011a). Estrogen inhibits Dlk1/FA1 production: a potential mechanism for estrogen effects on bone turnover. *Journal of Bone and Mineral Research*, 26(10):2548–2551.

[3] Abdallah, B. M., Boissy, P., Tan, Q., Dahlgaard, J., Traustadottir, G. A., Kupisiewicz, K., Laborda, J., Delaisse, J.-M., and Kassem, M. (2007a). dlk1/FA1 regulates the function of human bone marrow mesenchymal stem cells by modulating gene expression of pro-inflammatory cytokines and immune response-related factors. *Journal of Biological Chemistry*, 282(10):7339–7351.

[4] Abdallah, B. M., Ding, M., Jensen, C. H., Ditzel, N., Flyvbjerg, A., Jensen, T. G., Dagnæs-Hansen, F., Gasser, J. A., and Kassem, M. (2007b). Dlk1/FA1 is a novel endocrine regulator of bone and fat mass and its serum level is modulated by growth hormone. *Endocrinology*, 148(7):3111–3121.

[5] Abdallah, B. M., Ditzel, N., Laborda, J., Karsenty, G., and Kassem, M. (2015). DLK1 regulates whole body glucose metabolism: A negative feedback regulation of the osteocalcin-insulin loop. *Diabetes*, page db141642.

[6] Abdallah, B. M., Ditzel, N., Mahmood, A., Isa, A., Traustadottir, G. A., Schilling, A. F., Ruiz-Hidalgo, M. J., Laborda, J., Amling, M., and Kassem, M. (2011b). DLK1 is a novel regulator of bone mass that mediates estrogen deficiency-induced bone loss in mice. *Journal of Bone and Mineral Research*, 26(7):1457–1471.

[7] Abdallah, B. M., Jensen, C. H., Gutierrez, G., Leslie, R. G. Q., Jensen, T. G., and Kassem, M. (2004a). Regulation of human skeletal stem cells differentiation by Dlk1/Pref-1. *Journal of Bone and Mineral Research*, 19(5):841–852.

[8] Abdallah, B. M., Jensen, C. H., Gutierrez, G., Leslie, R. G. Q., Jensen, T. G., and Kassem, M. (2004b). Regulation of human skeletal stem cells differentiation by Dlk1/Pref-1. *Journal of Bone and Mineral Research*, 19(5):841–852.

[9] Abreu, A. P., Dauber, A., Macedo, D. B., Noel, S. D., Brito, V. N., Gill, J. C., Cukier, P., Thompson, I. R., Navarro, V. M., Gagliardi, P. C., Rodrigues, T., Kochi, C., Longui, C. A., Beckers, D., de Zegher, F., Montenegro, L. R., Mendonca, B. B., Carroll, R. S., Hirschhorn, J. N., Latronico, A. C., and Kaiser, U. B. (2013). Central precocious puberty caused by mutations in the imprinted gene MKRN3. *New England Journal of Medicine*, 368(26):2467–2475.

[10] Abreu, A. P. and Kaiser, U. B. (2016). Pubertal development and regulation. *The lancet. Diabetes & endocrinology*, 4(3):254–264.

[11] Akcakaya, P., Bobbin, M. L., Guo, J. A., Malagon-Lopez, J., Clement, K., Garcia, S. P., Fellows, M. D., Porritt, M. J., Firth, M. A., Carreras, A., Baccega, T., Seeliger, F., Bjursell, M., Tsai, S. Q., Nguyen, N. T., Nitsch, R., Mayr, L. M., Pinello, L., Bohlooly-Y, M., Aryee, M. J., Maresca, M., and Joung, J. K. (2018). In vivo CRISPR editing with no detectable genome-wide off-target mutations. *Nature*, 2:1.

[12] Albini, A., Tosetti, F., Li, V. W., Noonan, D. M., and Li, W. W. (2012). Cancer prevention by targeting angiogenesis. *Nature reviews. Clinical oncology*, 9(9):498–509.

[13] Alexander, K. A., Wang, X., Shibata, M., Clark, A. G., and García-García, M. J. (2015). TRIM28 Controls Genomic Imprinting through Distinct Mechanisms during and after Early Genome-wide Reprogramming. *CellReports*.

[14] Altenberger, T., Bilban, M., Auer, M., Knosp, E., Wolfsberger, S., Gartner, W., Mineva, I., Zielinski, C., Wagner, L., and Luger, A. (2006). Identification of DLK1 variants in pituitary- and neuroendocrine tumors. *Biochemical and Biophysical Research Communications*, 340(3):995–1005.

[15] Andersen, D. C., Petersson, S. J., Jørgensen, L. H., Bollen, P., Jensen, P. B., Teisner, B., Schroeder, H. D., and Jensen, C. H. (2009). Characterization of DLK1+ cells emerging during skeletal muscle remodeling in response to myositis, myopathies, and acute injury. *Stem cells (Dayton, Ohio)*, 27(4):898–908.

[16] Ansell, P. J., Zhou, Y., Schjeide, B.-M., Kerner, A., Zhao, J., Zhang, X., and Klibanski, A. (2007). Regulation of growth hormone expression by Delta-like protein 1 (Dlk1). *Molecular and Cellular Endocrinology*, 271(1-2):55–63.

[17] Appel, B., Givan, L. A., and Eisen, J. S. (2001). Delta-Notch signaling and lateral inhibition in zebrafish spinal cord development. *BMC Developmental Biology*, 1(1):13.

[18] Appelbe, O. K., Yevtodiyenko, A., Muniz-Talavera, H., and Schmidt, J. V. (2013). Conditional deletions refine the embryonic requirement for Dlk1. *Mechanisms of Development*, 130(2-3):143–159.

[19] Armengol, J., Villena, J. A., Hondares, E., Carmona, M. C., Sul, H. S., Iglesias, R., Giralt, M., and Villarroya, F. (2012). Pref-1 in brown adipose tissue: specific involvement in brown adipocyte differentiation and regulatory role of C/EBPδ. *Biochemical Journal*, 443(3):799–810.

[20] Assis, R. and Bachtrog, D. (2015). Rapid divergence and diversification of mammalian duplicate gene functions. *BMC evolutionary biology*, 15(1):138.

[21] Babak, T., DeVeale, B., Tsang, E. K., Zhou, Y., Li, X., Smith, K. S., Kukurba, K. R., Zhang, R., Li, J. B., van der Kooy, D., Montgomery, S. B., and Fraser, H. B. (2015). Genetic conflict reflected in tissue-specific maps of genomic imprinting in human and mouse. *Nature Publishing Group*, 47(5):544–549.

[22] Bae, S., Kweon, J., Kim, H. S., and Kim, J.-S. (2014). Microhomology-based choice of Cas9 nuclease target sites. *Nature methods*, 11(7):705–706.

[23] Baladrón, V., Ruiz-Hidalgo, M. J., Nueda, M. L., Díaz-Guerra, M. J. M., García-Ramírez, J. J., Bonvini, E., Gubina, E., and Laborda, J. (2005). dlk acts as a negative regulator of Notch1 activation through interactions with specific EGF-like repeats. *Experimental Cell Research*, 303(2):343–359.

[24] Bauer, S. R., Ruiz-Hidalgo, M. J., Rudikoff, E. K., Goldstein, J., and Laborda, J. (1998). Modulated expression of the epidermal growth factor-like homeotic protein dlk influences stromal-cell-pre-B-cell interactions, stromal cell adipogenesis, and pre-B-cell interleukin-7 requirements. *Molecular and Cellular Biology*, 18(9):5247–5255.

[25] Berman, H. M., Westbrook, J., Feng, Z., Gilliland, G., Bhat, T. N., Weissig, H., Shindyalov, I. N., and Bourne, P. E. (2000). The Protein Data Bank. *Nucleic Acids Research*, 28(1):235–242.

[26] Berry, D. C., DeSantis, D., Soltanian, H., Croniger, C. M., and Noy, N. (2012). Retinoic acid upregulates preadipocyte genes to block adipogenesis and suppress diet-induced obesity. *Diabetes*, 61(5):1112–1121.

[27] Bondjers, C., He, L., Takemoto, M., Norlin, J., Asker, N., Hellström, M., Lindahl, P., and Betsholtz, C. (2006). Microarray analysis of blood microvessels from PDGF-B and PDGF-Rbeta mutant mice identifies novel markers for brain pericytes. *FASEB journal : official publication of the Federation of American Societies for Experimental Biology*, 20(10):1703–1705.

[28] Boucher, J., Charalambous, M., Zarse, K., Mori, M. A., Kleinridders, A., Ristow, M., Ferguson-Smith, A. C., and Kahn, C. R. (2014). Insulin and insulin-like growth factor 1 receptors are required for normal expression of imprinted genes. *Proceedings of the National Academy of Sciences of the United States of America*, 111(40):14512–14517.

[29] Bray, S. J., Takada, S., Harrison, E., Shen, S.-C., and Ferguson-Smith, A. C. (2008). The atypical mammalian ligand Delta-like homologue 1 (Dlk1) can regulate Notch signalling in Drosophila. *BMC Developmental Biology*, 8(1):11.

[30] Buiting, K., Kanber, D., Martín-Subero, J. I., Lieb, W., Terhal, P., Albrecht, B., Purmann, S., Gross, S., Lich, C., Siebert, R., Horsthemke, B., and Gillessen-Kaesbach, G. (2008). Clinical features of maternal uniparental disomy 14 in patients with an epimutation and a deletion of the imprinted DLK1/GTL2 gene cluster. *Human mutation*, 29(9):1141–1146.

[31] Caescu, C. I., Jeschke, G. R., and Turk, B. E. (2009). Active-site determinants of substrate recognition by the metalloproteinases TACE and ADAM10. *Biochemical Journal*, 424(1):79–88.

[32] Cairo, S., Armengol, C., De Reyniès, A., Wei, Y., Thomas, E., Renard, C.-A., Goga, A., Balakrishnan, A., Semeraro, M., Gresh, L., Pontoglio, M., Strick-Marchand, H., Levillayer, F., Nouet, Y., Rickman, D., Gauthier, F., Branchereau, S., Brugières, L., Laithier, V., Bouvier, R., Boman, F., Basso, G., Michiels, J.-F., Hofman, P., Arbez-Gindre, F., Jouan, H., Rousselet-Chapeau, M.-C., Berrebi, D., Marcellin, L., Plenat, F., Zachar, D., Joubert, M., Selves, J., Pasquier, D., Bioulac-Sage, P., Grotzer, M., Childs, M., Fabre, M., and Buendia, M.-A. (2008). Hepatic stem-like phenotype and interplay of Wnt/beta-catenin and Myc signaling in aggressive childhood liver cancer. *Cancer Cell*, 14(6):471–484.

[33] Carlsson, C., Tornehave, D., Lindberg, K., Galante, P., Billestrup, N., Michelsen, B., Larsson, L. I., and Nielsen, J. H. (1997). Growth hormone and prolactin stimulate the expression of rat preadipocyte factor-1/delta-like protein in pancreatic islets: molecular cloning and expression pattern during development and growth of the endocrine pancreas. *Endocrinology*, 138(9):3940–3948.

[34] Cavaille, J., Seitz, H., Paulsen, M., Ferguson-Smith, A. C., and Bachellerie, J.-P. (2002). Identification of tandemly-repeated C/D snoRNA genes at the imprinted human 14q32 domain reminiscent of those at the Prader-Willi/Angelman syndrome region. *Human Molecular Genetics*, 11(13):1527–1538.

[35] Charalambous, M., Da Rocha, S. T., Radford, E. J., Medina-Gomez, G., Curran, S., Pinnock, S. B., Ferrón, S. R., Vidal-Puig, A., and Ferguson-Smith, A. C. (2014). DLK1/PREF1 regulates nutrient metabolism and protects from steatosis. *Proceedings of the National Academy of Sciences*, 111(45):16088–16093.

[36] Charalambous, M., Ferron, S. R., da Rocha, S. T., Murray, A. J., Rowland, T., Ito, M., Schuster-Gossler, K., Hernandez, A., and Ferguson-Smith, A. C. (2012a). Imprinted Gene Dosage Is Critical for the Transition to Independent Life. *Cell Metabolism*, 15(2):209–221.

[37] Charalambous, M., Ferron, S. R., da Rocha, S. T., Murray, A. J., Rowland, T., Ito, M., Schuster-Gossler, K., Hernandez, A., and Ferguson-Smith, A. C. (2012b). Imprinted Gene Dosage Is Critical for the Transition to Independent Life. *Cell Metabolism*, 15(2):209–221.

[38] Chari, R., Mali, P., Moosburner, M., and Church, G. M. (2015). Unraveling CRISPR-Cas9 genome engineering parameters via a library-on-library approach. *Nature methods*, 12(9):823–826.

[39] Charif, D. and Lobry, J. R. (2007). SeqinR 1.0-2: A Contributed Package to the R Project for Statistical Computing Devoted to Biological Sequences Retrieval and Analysis. In *Structural Approaches to Sequence Evolution*, pages 207–232. Springer, Berlin, Heidelberg, Berlin, Heidelberg.

[40] Chaves, J. A., Cooper, E. A., Hendry, A. P., Podos, J., De León, L. F., Raeymaekers, J. A. M., MacMillan, W. O., and Uy, J. A. C. (2016). Genomic variation at the tips of the adaptive radiation of Darwin's finches. *Molecular ecology*, 25(21):5282–5295.

[41] Chen, L., Qanie, D., Jafari, A., Taipaleenmaki, H., Jensen, C. H., Säämänen, A.-M., Sanz, M. L. N., Laborda, J., Abdallah, B. M., and Kassem, M. (2011). Delta-like 1/fetal antigen-1 (Dlk1/FA1) is a novel regulator of chondrogenic cell differentiation via inhibition of the Akt kinase-dependent pathway. *The Journal of biological chemistry*, 286(37):32140–32149.

[42] Cheung, L. Y. M., Rizzoti, K., Lovell-Badge, R., and Le Tissier, P. R. (2013). Pituitary Phenotypes of Mice Lacking the Notch Signalling Ligand Delta-Like 1 Homologue. *Journal of Neuroendocrinology*, 25(4):391–401.

[43] Cheunsuchon, P., Zhou, Y., Zhang, X., Lee, H., Chen, W., Nakayama, Y., Rice, K. A., Tessa Hedley-Whyte, E., Swearingen, B., and Klibanski, A. (2011). Silencing of the imprinted DLK1-MEG3 locus in human clinically nonfunctioning pituitary adenomas. *The American journal of pathology*, 179(4):2120–2130.

[44] Cleaton, M. A. M., Dent, C. L., Howard, M., Corish, J. A., Gutteridge, I., Sovio, U., Gaccioli, F., Takahashi, N., Bauer, S. R., Charnock-Jones, D. S., Powell, T. L., Smith, G. C. S., Ferguson-Smith, A. C., and Charalambous, M. (2016). Fetus-derived DLK1 is required for maternal metabolic adaptations to pregnancy and is associated with fetal growth restriction. *Nature Genetics*, 48(12):1473–1480.

[45] Cleaton, M. A. M., Edwards, C. A., and Ferguson-Smith, A. C. (2014). Phenotypic Outcomes of Imprinted Gene Models in Mice: Elucidation of Pre- and Postnatal Functions of Imprinted Genes. *Annual Review of Genomics and Human Genetics*, 15(1):93–126.

[46] Coan, P. M., Ferguson-Smith, A. C., and Burton, G. J. (2004). Developmental dynamics of the definitive mouse placenta assessed by stereology. *Biology of reproduction*, 70(6):1806–1813.

[47] Collard, J., Sherman, O. K., Coito, C., and Inc, C. (2018). Treatment of delta-like 1 homolog (dlk1) related diseases by inhibition of natural antisense transcript to dlk1.

[48] Consortium, T. E. P., Consortium, T. E. P., data analysis coordination, O. c., data production, D. p. l., data analysis, L. a., group, W., scientific management, N. p. m., steering committee, P. i., Boise State University and University of North Carolina at Chapel Hill Proteomics groups (data production and analysis), Broad Institute Group (data production and analysis), Cold Spring Harbor, University of Geneva, Center for Genomic Regulation, Barcelona, RIKEN, Sanger Institute, University of Lausanne, Genome Institute of Singapore group (data production and analysis), Data coordination center at UC Santa Cruz (production data coordination), Duke University, EBI, University of Texas, Austin, University of North Carolina-Chapel Hill group (data production and analysis), Genome Institute of Singapore group (data production and analysis), HudsonAlpha Institute, Caltech, UC Irvine, Stanford group (data production and analysis), targeted experimental validation, L. B. N. L. g., data production, analysis, N. g., Sanger Institute, Washington University, Yale University, Center for Genomic Regulation, Barcelona, UCSC, MIT, University of Lausanne, CNIO group (data production and analysis), Stanford-Yale, Harvard, University of Massachusetts Medical School, University of Southern California/UC Davis group (data production and analysis), University of Albany SUNY group (data production and analysis), University of Chicago, Stanford group (data production and analysis), University of Heidelberg group (targeted experimental validation), University of Massachusetts Medical School Bioinformatics group (data production and analysis), University of Massachusetts Medical School Genome Folding group (data production and analysis), University of Washington, University of Massachusetts Medical Center group (data production and analysis), and Data Analysis Center (data analysis) (2013). An integrated encyclopedia of DNA elements in the human genome. *Nature*, 488(7414):57–74.

[49] Consortium, T. U. (2015). UniProt: a hub for protein information. *Nucleic Acids Research*, 43(D1):D204–D212.

[50] Cornell, R. A. and Eisen, J. S. (2000). Delta signaling mediates segregation of neural crest and spinal sensory neurons from zebrafish lateral neural plate. *Development*, 127(13):2873–2882.

[51] Da Rocha, S. T., Charalambous, M., Lin, S.-P., Gutteridge, I., Ito, Y., Gray, D., Dean, W., and Ferguson-Smith, A. C. (2009). Gene dosage effects of the imprinted delta-like

homologue 1 (dlk1/pref1) in development: implications for the evolution of imprinting. *PLoS Genetics*, 5(2):e1000392.

[52] da Rocha, S. T., Tevendale, M., Knowles, E., Takada, S., Watkins, M., and Ferguson-Smith, A. C. (2007). Restricted co-expression of Dlk1 and the reciprocally imprinted non-coding RNA, Gtl2: implications for cis-acting control. *Developmental Biology*, 306(2):810–823.

[53] Dauber, A., Cunha-Silva, M., Macedo, D. B., Brito, V. N., Abreu, A. P., Roberts, S. A., Montenegro, L. R., Andrew, M., Kirby, A., Weirauch, M. T., Labilloy, G., Bessa, D. S., Carroll, R. S., Jacobs, D. C., Chappell, P. E., Mendonca, B. B., Haig, D., Kaiser, U. B., and Latronico, A. C. (2017). Paternally Inherited DLK1 Deletion Associated With Familial Central Precocious Puberty. *The Journal of Clinical Endocrinology & Metabolism*, 102(5):1557–1567.

[54] Davis, E., Jensen, C. H., Schroder, H. D., Farnir, F., Shay-Hadfield, T., Kliem, A., Cockett, N., Georges, M., and Charlier, C. (2004). Ectopic expression of DLK1 protein in skeletal muscle of padumnal heterozygotes causes the callipyge phenotype. *Current Biology*, 14(20):1858–1862.

[55] Day, F. R., Thompson, D. J., Helgason, H., Chasman, D. I., Finucane, H., Sulem, P., Ruth, K. S., Whalen, S., Sarkar, A. K., Albrecht, E., Altmaier, E., Amini, M., Barbieri, C. M., Boutin, T., Campbell, A., Demerath, E., Giri, A., He, C., Hottenga, J. J., Karlsson, R., Kolcic, I., Loh, P.-R., Lunetta, K. L., Mangino, M., Marco, B., McMahon, G., Medland, S. E., Nolte, I. M., Noordam, R., Nutile, T., Paternoster, L., Perjakova, N., Porcu, E., Rose, L. M., Schraut, K. E., Segrè, A. V., Smith, A. V., Stolk, L., Teumer, A., Andrulis, I. L., Bandinelli, S., Beckmann, M. W., Benitez, J., Bergmann, S., Bochud, M., Boerwinkle, E., Bojesen, S. E., Bolla, M. K., Brand, J. S., Brauch, H., Brenner, H., Broer, L., Bruning, T., Buring, J. E., Campbell, H., Catamo, E., Chanock, S., Chenevix-Trench, G., Corre, T., Couch, F. J., Cousminer, D. L., Cox, A., Crisponi, L., Czene, K., Davey Smith, G., de Geus, E. J. C. N., de Mutsert, R., De Vivo, I., Dennis, J., Devilee, P., dos Santos-Silva, I., Dunning, A. M., Eriksson, J. G., Fasching, P. A., Fernandez-Rhodes, L., Ferrucci, L., Flesch-Janys, D., Franke, L., Gabrielson, M., Gandin, I., Giles, G. G., Grallert, H., Gudbjartsson, D. F., Guénel, P., Hall, P., Hallberg, E., Hamann, U., Harris, T. B., Hartman, C. A., Heiss, G., Hooning, M. J., Hopper, J. L., Hu, F., Hunter, D. J., Ikram, M. A., Im, H. K., Jarvelin, M.-R., Joshi, P. K., Karasik, D., Kellis, M., Kutalik, Z., LaChance, G., Lambrechts, D., Langenberg, C., Launer, L. J., Laven, J. S. E., Lenarduzzi, S., Li, J., Lind, P. A., Lindstrom, S., Liu, Y., Luan, J., Mägi, R., Mannermaa, A., Mbarek, H., Mccarthy, M. I., Meisinger, C., Meitinger, T., Menni, C., Metspalu, A., Michailidou, K., Milani, L., Milne, R. L., Montgomery, G. W., Mulligan, A. M., Nalls, M. A., Navarro, P., Nevanlinna, H., Nyholt, D. R., Oldehinkel, A. J., O'Mara, T. A., Padmanabhan, S., Palotie, A., Pedersen, N., Peters, A., Peto, J., Pharoah, P. D. P., Pouta, A., Radice, P., Rahman, I., Ring, S. M., Robino, A., Rosendaal, F. R., Rudan, I., Rueedi, R., Ruggiero, D., Sala, C. F., Schmidt, M. K., Scott, R. A., Shah, M., Sorice, R., Southey, M. C., Sovio, U., Stampfer, M., Steri, M., Strauch, K., Tanaka, T., Tikkanen, E., Timpson, N. J., Traglia, M., Truong, T., Tyrer, J. P., Uitterlinden, A. G., Edwards, D. R. V., Vitart, V., Volker, U., Vollenweider, P., Wang, Q., Widen, E., van Dijk, K. W., Willemsen, G., Winqvist, R., Wolffenbuttel, B. H. R., Zhao, J. H., Zoledziewska, M., Zygmunt, M., Alizadeh, B. Z., Boomsma, D. I., Ciullo, M., Cucca, F., Esko, T., Franceschini, N., Gieger, C., Gudnason, V., Hayward, C.,

Kraft, P., Lawlor, D. A., Magnusson, P. K. E., Martin, N. G., Mook-Kanamori, D. O., Nohr, E. A., Polasek, O., Porteous, D., Price, A. L., Ridker, P. M., Snieder, H., Spector, T. D., Stöckl, D., Toniolo, D., Ulivi, S., Visser, J. A., Völzke, H., Wareham, N. J., Wilson, J. F., LifeLines Cohort Study, InterAct Consortium, kConFab/AOCS Investigators, Endometrial Cancer Association Consortium, Ovarian Cancer Association Consortium, PRACTICAL consortium, Spurdle, A. B., Thorsteindottir, U., Pollard, K. S., Easton, D. F., Tung, J. Y., Chang-claude, J., Hinds, D., Murray, A., Murabito, J. M., Stefansson, K., Ong, K. K., and Perry, J. R. B. (2017). Genomic analyses identify hundreds of variants associated with age at menarche and support a role for puberty timing in cancer risk. *Nature Genetics*.

[56] Dehal, P. and Boore, J. L. (2005). Two rounds of whole genome duplication in the ancestral vertebrate. *PLoS Biology*, 3(10):e314.

[57] Deiuliis, J. A., Li, B., Lyvers-Peffer, P. A., Moeller, S. J., and Lee, K. (2006). Alternative splicing of delta-like 1 homolog (DLK1) in the pig and human. *Comparative biochemistry and physiology. Part B, Biochemistry & molecular biology*, 145(1):50–59.

[58] Delsuc, F., Brinkmann, H., Chourrout, D., and Philippe, H. (2006). Tunicates and not cephalochordates are the closest living relatives of vertebrates. *Nature*, 439(7079):965–968.

[59] Dezso, K., Halász, J., Bisgaard, H. C., Paku, S., Turányi, E., Schaff, Z., and Nagy, P. (2008). Delta-like protein (DLK) is a novel immunohistochemical marker for human hepatoblastomas. *Virchows Archiv : an international journal of pathology*, 452(4):443–448.

[60] Dickinson, M. E., Flenniken, A. M., Ji, X., Teboul, L., Wong, M. D., White, J. K., Meehan, T. F., Weninger, W. J., Westerberg, H., Adissu, H., Baker, C. N., Bower, L., Brown, J. M., Caddle, L. B., Chiani, F., Clary, D., Cleak, J., Daly, M. J., Denegre, J. M., Doe, B., Dolan, M. E., Edie, S. M., Fuchs, H., Gailus-Durner, V., Galli, A., Gambadoro, A., Gallegos, J., Guo, S., Horner, N. R., Hsu, C.-W., Johnson, S. J., Kalaga, S., Keith, L. C., Lanoue, L., Lawson, T. N., Lek, M., Mark, M., Marschall, S., Mason, J., McElwee, M. L., Newbigging, S., Nutter, L. M. J., Peterson, K. A., Ramirez-Solis, R., Rowland, D. J., Ryder, E., Samocha, K. E., Seavitt, J. R., Selloum, M., Szoke-Kovacs, Z., Tamura, M., Trainor, A. G., Tudose, I., Wakana, S., Warren, J., Wendling, O., West, D. B., Wong, L., Yoshiki, A., International Mouse Phenotyping Consortium, Jackson Laboratory, Infrastructure Nationale PHENOMIN, Institut Clinique de la Souris (ICS), Charles River Laboratories, MRC Harwell, Toronto Centre for Phenogenomics, Wellcome Trust Sanger Institute, RIKEN BioResource Center, Macarthur, D. G., Tocchini-Valentini, G. P., Gao, X., Flicek, P., Bradley, A., Skarnes, W. C., Justice, M. J., Parkinson, H. E., Moore, M., Wells, S., Braun, R. E., Svenson, K. L., de Angelis, M. H., Herault, Y., Mohun, T., Mallon, A.-M., Henkelman, R. M., Brown, S. D. M., Adams, D. J., Lloyd, K. C. K., McKerlie, C., Beaudet, A. L., Bucan, M., and Murray, S. A. (2016). High-throughput discovery of novel developmental phenotypes. *Nature*, 537(7621):508–514.

[61] Diez-Roux, G., Banfi, S., Sultan, M., Geffers, L., Anand, S., Rozado, D., Magen, A., Canidio, E., Pagani, M., Peluso, I., Lin-Marq, N., Koch, M., Bilio, M., Cantiello, I., Verde, R., De Masi, C., Bianchi, S. A., Cicchini, J., Perroud, E., Mehmeti, S., Dagand, E., Schrinner, S., Nürnberger, A., Schmidt, K., Metz, K., Zwingmann, C., Brieske, N., Springer, C., Hernandez, A. M., Herzog, S., Grabbe, F., Sieverding, C., Fischer, B., Schrader, K., Brockmeyer, M., Dettmer, S., Helbig, C., Alunni, V., Battaini, M.-A., Mura,

C., Henrichsen, C. N., Garcia-Lopez, R., Echevarria, D., Puelles, E., Garcia-Calero, E., Kruse, S., Uhr, M., Kauck, C., Feng, G., Milyaev, N., Ong, C. K., Kumar, L., Lam, M., Semple, C. A., Gyenesei, A., Mundlos, S., Radelof, U., Lehrach, H., Sarmientos, P., Reymond, A., Davidson, D. R., Dollé, P., Antonarakis, S. E., Yaspo, M.-l., Martinez, S., Baldock, R. A., Eichele, G., and Ballabio, A. (2011). A High-Resolution Anatomical Atlas of the Transcriptome in the Mouse Embryo. *PLoS Biology*, 9(1):e1000582.

[62] Doench, J. G., Hartenian, E., Graham, D. B., Tothova, Z., Hegde, M., Smith, I., Sullender, M., Ebert, B. L., Xavier, R. J., and Root, D. E. (2014). Rational design of highly active sgRNAs for CRISPR-Cas9-mediated gene inactivation. *Nature biotechnology*, 32(12):1262–1267.

[63] Dorrell, C., Schug, J., Lin, C. F., Canaday, P. S., Fox, A. J., Smirnova, O., Bonnah, R., Streeter, P. R., Stoeckert, C. J., Kaestner, K. H., and Grompe, M. (2011). Transcriptomes of the major human pancreatic cell types. *Diabetologia*, 54(11):2832–2844.

[64] Driskell, R. R., Lichtenberger, B. M., Hoste, E., Kretzschmar, K., Simons, B. D., Charalambous, M., Ferrón, S. R., Herault, Y., Pavlovic, G., Ferguson-Smith, A. C., and Watt, F. M. (2015). Distinct fibroblast lineages determine dermal architecture in skin development and repair. *Nature*, 504(7479):277–281.

[65] D'Souza, B., Miyamoto, A., and Weinmaster, G. (2008). The many facets of Notch ligands. *Oncogene*, 27(38):5148–5167.

[66] Dutta, S. and Sengupta, P. (2018). Rabbits and men: relating their ages. *Journal of Basic and Clinical Physiology and Pharmacology*, 29(5):427–435.

[67] Edwards, C. A. and Ferguson-Smith, A. C. (2007). Mechanisms regulating imprinted genes in clusters. *Current Opinion in Cell Biology*, 19(3):281–289.

[68] Edwards, C. A., Mungall, A. J., Matthews, L., Ryder, E., Gray, D. J., Pask, A. J., Shaw, G., Graves, J. A. M., Rogers, J., the SAVOIR consortium, Dunham, I., Renfree, M. B., and Ferguson-Smith, A. C. (2008). The Evolution of the DLK1-DIO3 Imprinted Domain in Mammals. *PLoS Biology*, 6(6):e135.

[69] El Faitwri, T. and Huber, K. (2018). Expression pattern of delta-like 1 homolog in developing sympathetic neurons and chromaffin cells. *Gene expression patterns : GEP*.

[70] Elks, C. E., Perry, J. R. B., Sulem, P., Chasman, D. I., Franceschini, N., He, C., Lunetta, K. L., Visser, J. A., Byrne, E. M., Cousminer, D. L., Gudbjartsson, D. F., Esko, T., Feenstra, B., Hottenga, J.-J., Koller, D. L., Kutalik, Z., Lin, P., Mangino, M., Marongiu, M., McArdle, P. F., Smith, A. V., Stolk, L., van Wingerden, S. H., Zhao, J. H., Albrecht, E., Corre, T., Ingelsson, E., Hayward, C., Magnusson, P. K. E., Smith, E. N., Ulivi, S., Warrington, N. M., Zgaga, L., Alavere, H., Amin, N., Aspelund, T., Bandinelli, S., Barroso, I., Berenson, G. S., Bergmann, S., Blackburn, H., Boerwinkle, E., Buring, J. E., Busonero, F., Campbell, H., Chanock, S. J., Chen, W., Cornelis, M. C., Couper, D., Coviello, A. D., d'Adamo, P., de Faire, U., de Geus, E. J. C., Deloukas, P., Doring, A., Smith, G. D., Easton, D. F., Eiriksdottir, G., Emilsson, V., Eriksson, J., Ferrucci, L., Folsom, A. R., Foroud, T., Garcia, M., Gasparini, P., Geller, F., Gieger, C., GIANT Consortium, Gudnason, V., Hall, P., Hankinson, S. E., Ferreli, L., Heath, A. C., Hernandez, D. G., Hofman, A., Hu, F. B., Illig, T., Jarvelin, M.-R., Johnson, A. D., Karasik, D., Khaw, K.-T., Kiel, D. P., Kilpelainen,

T. O., Kolcic, I., Kraft, P., Launer, L. J., Laven, J. S. E., Li, S., Liu, J., Levy, D., Martin, N. G., McArdle, W. L., Melbye, M., Mooser, V., Murray, J. C., Murray, S. S., Nalls, M. A., Navarro, P., Nelis, M., Ness, A. R., Northstone, K., Oostra, B. A., Peacock, M., Palmer, L. J., Palotie, A., Pare, G., Parker, A. N., Pedersen, N. L., Peltonen, L., Pennell, C. E., Pharoah, P., Polasek, O., Plump, A. S., Pouta, A., Porcu, E., Rafnar, T., Rice, J. P., Ring, S. M., Rivadeneira, F., Rudan, I., Sala, C., Salomaa, V., Sanna, S., Schlessinger, D., Schork, N. J., Scuteri, A., Segrè, A. V., Shuldiner, A. R., Soranzo, N., Sovio, U., Srinivasan, S. R., Strachan, D. P., Tammesoo, M.-L., Tikkanen, E., Toniolo, D., Tsui, K., Tryggvadottir, L., Tyrer, J., Uda, M., van Dam, R. M., van Meurs, J. B. J., Vollenweider, P., Waeber, G., Wareham, N. J., Waterworth, D. M., Weedon, M. N., Wichmann, H. E., Willemsen, G., Wilson, J. F., Wright, A. F., Young, L., Zhai, G., Zhuang, W. V., Bierut, L. J., Boomsma, D. I., Boyd, H. A., Crisponi, L., Demerath, E. W., van Duijn, C. M., Econs, M. J., Harris, T. B., Hunter, D. J., Loos, R. J. F., Metspalu, A., Montgomery, G. W., Ridker, P. M., Spector, T. D., Streeten, E. A., Stefansson, K., Thorsteinsdottir, U., Uitterlinden, A. G., Widen, E., Murabito, J. M., Ong, K. K., and Murray, A. (2010). Thirty new loci for age at menarche identified by a meta-analysis of genome-wide association studies. *Nature Genetics*, 42(12):1077–1085.

[71] Engler, A., Rolando, C., Giachino, C., Saotome, I., Erni, A., Brien, C., Zhang, R., Zimber-Strobl, U., Radtke, F., Artavanis-Tsakonas, S., Louvi, A., and Taylor, V. (2018). Notch2 Signaling Maintains NSC Quiescence in the Murine Ventricular-Subventricular Zone. *Cell Reports*, 22(4):992–1002.

[72] Evans, C.-O., Moreno, C. S., Zhan, X., McCabe, M. T., Vertino, P. M., Desiderio, D. M., and Oyesiku, N. M. (2008). Molecular pathogenesis of human prolactinomas identified by gene expression profiling, RT-qPCR, and proteomic analyses. *Pituitary*, 11(3):231–245.

[73] Falix, F. A., Aronson, D. C., Lamers, W. H., Hiralall, J. K., and Seppen, J. (2012). DLK1, a serum marker for hepatoblastoma in young infants. *Pediatric blood & cancer*, 59(4):743–745.

[74] Fazeli, P. K., Bredella, M. A., Freedman, L., Thomas, B. J., Breggia, A., Meenaghan, E., Rosen, C. J., and Klibanski, A. (2012). Marrow fat and preadipocyte factor-1 levels decrease with recovery in women with anorexia nervosa. *Journal of Bone and Mineral Research*, 27(9):1864–1871.

[75] Fazeli, P. K., Bredella, M. A., Misra, M., Meenaghan, E., Rosen, C. J., Clemmons, D. R., Breggia, A., Miller, K. K., and Klibanski, A. (2010). Preadipocyte factor-1 is associated with marrow adiposity and bone mineral density in women with anorexia nervosa. *The Journal of Clinical Endocrinology & Metabolism*, 95(1):407–413.

[76] Ferguson-Smith, A. C. (2011a). Genomic imprinting: the emergence of an epigenetic paradigm. *Nature Reviews Genetics*, 12(8):565–575.

[77] Ferguson-Smith, A. C. (2011b). Genomic imprinting: the emergence of an epigenetic paradigm. *Nature Reviews Genetics*, 12(8):565–575.

[78] Ferrón, S. R., Charalambous, M., Radford, E., McEwen, K., Wildner, H., Hind, E., Morante-Redolat, J. M., Laborda, J., Guillemot, F., Bauer, S. R., Fariñas, I., and Ferguson-Smith, A. C. (2012). Postnatal loss of Dlk1 imprinting in stem cells and niche astrocytes regulates neurogenesis. *Nature*, 475(7356):381–385.

[79] Ferron, S. R., Radford, E. J., Domingo-Muelas, A., Kleine, I., Ramme, A., Gray, D., Sandovici, I., Constância, M., Ward, A., Menheniott, T. R., and Ferguson-Smith, A. C. (2015). Differential genomic imprinting regulates paracrine and autocrine roles of IGF2 in mouse adult neurogenesis. *Nature Communications*, 6:8265.

[80] Figeac, F., Andersen, D. C., Nipper Nielsen, C. A., Ditzel, N., Sheikh, S. P., Skjødt, K., Kassem, M., Jensen, C. H., and Abdallah, B. M. (2018). Antibody-based inhibition of circulating DLK1 protects from estrogen deficiency-induced bone loss in mice. *Bone*, 110:312–320.

[81] Fokstuen, S., Ginsburg, C., Zachmann, M., and Schinzel, A. (1999). Maternal uniparental disomy 14 as a cause of intrauterine growth retardation and early onset of puberty. *The Journal of pediatrics*, 134(6):689–695.

[82] Fu, Y., Foden, J. A., Khayter, C., Maeder, M. L., Reyon, D., Joung, J. K., and Sander, J. D. (2013). High-frequency off-target mutagenesis induced by CRISPR-Cas nucleases in human cells. *Nature biotechnology*, 31(9):822–826.

[83] Fukuzawa, R., Heathcott, R. W., Morison, I. M., and Reeve, A. E. (2005). Imprinting, expression, and localisation of DLK1 in Wilms tumours. *Journal of Clinical Pathology*, 58(2):145–150.

[84] Geffers, I., Serth, K., Chapman, G., Jaekel, R., Schuster-Gossler, K., Cordes, R., Sparrow, D. B., Kremmer, E., Dunwoodie, S. L., Klein, T., and Gossler, A. (2007). Divergent functions and distinct localization of the Notch ligands DLL1 and DLL3 in vivo. *The Journal of Cell Biology*, 178(3):465–476.

[85] Geling, A., Steiner, H., Willem, M., Bally Cuif, L., and Haass, C. (2002). A gamma-secretase inhibitor blocks Notch signaling in vivo and causes a severe neurogenic phenotype in zebrafish. *EMBO reports*, 3(7):688–694.

[86] Geoffron, S., Abi Habib, W., Chantot-Bastaraud, S., Dubern, B., Steunou, V., Azzi, S., Afenjar, A., Busa, T., Pinheiro Canton, A., Chalouhi, C., Dufourg, M.-N., Esteva, B., Fradin, M., Genevieve, D., Heide, S., Isidor, B., Linglart, A., Morice Picard, F., Naud-Saudreau, C., Oliver Petit, I., Philip, N., Pienkowski, C., Rio, M., Rossignol, S., Tauber, M., Thevenon, J., Vu-Hong, T.-A., Harbison, M. D., Salem, J., Brioude, F., Netchine, I., and Giabicani, E. (2018). Chromosome 14q32.2 Imprinted Region Disruption as an Alternative Molecular Diagnosis of Silver-Russell Syndrome. *The Journal of Clinical Endocrinology & Metabolism*, 103(7):2436–2446.

[87] Georgiades, P., Watkins, M., Surani, M. A., and Ferguson-Smith, A. C. (2000). Parental origin-specific developmental defects in mice with uniparental disomy for chromosome 12. *Development*, 127(21):4719–4728.

[88] Gillessen-Kaesbach, G., Albrecht, B., Eggermann, T., Elbracht, M., Mitter, D., Morlot, S., van Ravenswaaij-Arts, C. M. A., Schulz, S., Strobl-Wildemann, G., Buiting, K., and Beygo, J. (2018). Molecular and clinical studies in 8 patients with Temple syndrome. *Clinical Genetics*, 93(6):1179–1188.

[89] González, M. J., Ruiz-García, A., Monsalve, E. M., Sánchez-Prieto, R., Laborda, J., Díaz-Guerra, M. J. M., and Ruiz-Hidalgo, M. J. (2015). DLK1 is a novel inflammatory inhibitor which interferes with NOTCH1 signaling in TLR-activated murine macrophages. *European journal of immunology*, pages n/a–n/a.

[90] Guindon, S., Dufayard, J.-F., Lefort, V., Anisimova, M., Hordijk, W., and Gascuel, O. (2010). New algorithms and methods to estimate maximum-likelihood phylogenies: assessing the performance of PhyML 3.0. *Systematic biology*, 59(3):307–321.

[91] Haas, J., Roth, S., Arnold, K., Kiefer, F., Schmidt, T., Bordoli, L., and Schwede, T. (2013). The Protein Model Portal—a comprehensive resource for protein structure and model information. *Database*, 2013.

[92] Hansen, L. H., Madsen, B., Teisner, B., Nielsen, J. H., and Billestrup, N. (1998). Characterization of the inhibitory effect of growth hormone on primary preadipocyte differentiation. *Molecular endocrinology (Baltimore, Md.)*, 12(8):1140–1149.

[93] Harken Jensen, C., Drivsholm, L., Laursen, I., and Teisner, B. (1999). Elevated serum levels of fetal antigen 1,a member of the epidermal growth factor superfamily, in patients with small cell lung cancer. *Tumor Biology*, 20(5):256–262.

[94] He, F. and Jacobson, A. (2015). Nonsense-Mediated mRNA Decay: Degradation of Defective Transcripts Is Only Part of the Story. *Annual Review of Genetics*, 49(1):339–366.

[95] Hermida, C., Garcés, C., De Oya, M., Cano, B., Martínez-Costa, O. H., Rivero, S., García-Ramírez, J. J., Laborda, J., and Aragón, J. J. (2008). The serum levels of the EGF-like homeotic protein dlk1 correlate with different metabolic parameters in two hormonally different children populations in Spain. *Clinical endocrinology*, 69(2):216–224.

[96] Hernandez, A., Garcia, B., and Obregon, M.-J. (2007). Gene expression from the imprinted Dio3 locus is associated with cell proliferation of cultured brown adipocytes. *Endocrinology*, 148(8):3968–3976.

[97] Hodgkins, A., Farne, A., Perera, S., Grego, T., Parry-Smith, D. J., Skarnes, W. C., and Iyer, V. (2015). WGE: a CRISPR database for genome engineering. *Bioinformatics*, 31(18):3078–3080.

[98] Holley, S. A., Geisler, R., and Nüsslein-Volhard, C. (2000). Control of her1 expression during zebrafish somitogenesis by a delta-dependent oscillator and an independent wave-front activity. *Genes & Development*, 14(13):1678–1690.

[99] Hordijk, R., Wierenga, H., Scheffer, H., Leegte, B., Hofstra, R. M. W., and Stolte-Dijkstra, I. (1999). Maternal uniparental disomy for chromosome 14 in a boy with a normal karyotype. *Journal of medical genetics*, 36(10):782–785.

[100] Howard, M. and Charalambous, M. (2015). Molecular basis of imprinting disorders affecting chromosome 14: lessons from murine models. *Reproduction (Cambridge, England)*, 149(5):R237–49.

[101] Hsiao, C.-C., Huang, C.-C., Sheen, J.-M., Tai, M.-H., Chen, C.-M., Huang, L. L. H., and Chuang, J.-H. (2005). Differential expression of delta-like gene and protein in neuroblastoma, ganglioneuroblastoma and ganglioneuroma. *Modern pathology : an official journal of the United States and Canadian Academy of Pathology, Inc*, 18(5):656–662.

[102] Hsu, P. D., Lander, E. S., and Zhang, F. (2014). Development and applications of CRISPR-Cas9 for genome engineering. *CELL*, 157(6):1262–1278.

[103] Hsu, P. D., Scott, D. A., Weinstein, J. A., Ran, F. A., Konermann, S., Agarwala, V., Li, Y., Fine, E. J., Wu, X., Shalem, O., Cradick, T. J., Marraffini, L. A., Bao, G., and Zhang, F. (2013). DNA targeting specificity of RNA-guided Cas9 nucleases. *Nature biotechnology*, 31(9):827–832.

[104] Huang, C.-C., Kuo, H.-M., Wu, P.-C., Cheng, S.-H., Chang, T.-T., Chang, Y.-C., Kung, M.-L., Wu, D.-C., Chuang, J.-H., and Tai, M.-H. (2018). Soluble delta-like 1 homolog (DLK1) stimulates angiogenesis through Notch1/Akt/eNOS signaling in endothelial cells. *Angiogenesis*, 21(2):299–312.

[105] Ioannides, Y., Lokulo-Sodipe, K., Mackay, D. J. G., Davies, J. H., and Temple, I. K. (2014). Temple syndrome: improving the recognition of an underdiagnosed chromosome 14 imprinting disorder: an analysis of 51 published cases. *Journal of medical genetics*, 51(8):495–501.

[106] Jensen, C. H., Teisner, B., Højrup, P., Rasmussen, H. B., Madsen, O. D., Nielsen, B., and Skjødt, K. (1993). Studies on the isolation, structural analysis and tissue localization of fetal antigen 1 and its relation to a human adrenal-specific cDNA, pG2. *Human Reproduction*, 8(4):635–641.

[107] Jimenez-Chillaron, J. C., Isganaitis, E., Charalambous, M., Gesta, S., Pentinat-Pelegrin, T., Faucette, R. R., Otis, J. P., Chow, A., Diaz, R., Ferguson-Smith, A., and Patti, M.-E. (2009). Intergenerational transmission of glucose intolerance and obesity by in utero undernutrition in mice. *Diabetes*, 58(2):460–468.

[108] K, F., N, T., and M, K. (1998). Endothelial cell specific protein S-1. Technical report.

[109] Kagami, M., Sekita, Y., Nishimura, G., Irie, M., Kato, F., Okada, M., Yamamori, S., Kishimoto, H., Nakayama, M., Tanaka, Y., Matsuoka, K., Takahashi, T., Noguchi, M., Tanaka, Y., Masumoto, K., Utsunomiya, T., Kouzan, H., Komatsu, Y., Ohashi, H., Kurosawa, K., Kosaki, K., Ferguson-Smith, A. C., Ishino, F., and Ogata, T. (2008). Deletions and epimutations affecting the human 14q32.2 imprinted region in individuals with paternal and maternal upd(14)-like phenotypes. *Nature Genetics*, 40(2):237–242.

[110] Kameswaran, V., Bramswig, N. C., McKenna, L. B., Penn, M., Schug, J., Hand, N. J., Chen, Y., Choi, Inchan, Vourekas, A., Won, K.-J., Liu, C., Vivek, K., Naji, A., Friedman, J. R., and Kaestner, K. H. (2014). Epigenetic Regulation of the DLK1-MEG3 MicroRNA Cluster in Human Type 2 Diabetic Islets. *Cell Metabolism*, 19(1):135–145.

[111] Kaufman, M. H. (1992). *The atlas of mouse development*, volume 428. Academic press London.

[112] Kent, W. J. (2002). BLAT–the BLAST-like alignment tool. *Genome Research*, 12(4):656–664.

[113] Kent, W. J., Sugnet, C. W., Furey, T. S., Roskin, K. M., Pringle, T. H., Zahler, A. M., and Haussler, D. (2002). The human genome browser at UCSC. *Genome Research*, 12(6):996–1006.

[114] Kervestin, S. and Jacobson, A. (2012). NMD: a multifaceted response to premature translational termination. *Nature Reviews Molecular Cell Biology*, 13(11):700–712.

[115] Kettleborough, R. N. W., Busch-Nentwich, E. M., Harvey, S. A., Dooley, C. M., de Bruijn, E., van Eeden, F., Sealy, I., White, R. J., Herd, C., Nijman, I. J., Fényes, F., Mehroke, S., Scahill, C., Gibbons, R., Wali, N., Carruthers, S., Hall, A., Yen, J., Cuppen, E., and Stemple, D. L. (2013). A systematic genome-wide analysis of zebrafish protein-coding gene function. *Nature*, 496(7446):494–497.

[116] Kim, K.-A., Kim, J.-H., Wang, Y., and Sul, H. S. (2007). Pref-1 (preadipocyte factor 1) activates the MEK/extracellular signal-regulated kinase pathway to inhibit adipocyte differentiation. *Molecular and Cellular Biology*, 27(6):2294–2308.

[117] Kim, Y., Lin, Q., Zelterman, D., and Yun, Z. (2009). Hypoxia-regulated delta-like 1 homologue enhances cancer cell stemness and tumorigenicity. *Cancer research*, 69(24):9271–9280.

[118] Klein, D. (2002). Quantification using real-time PCR technology: applications and limitations. *Trends in Molecular Medicine*, 8(6):257–260.

[119] Kobayashi, S., Wagatsuma, H., Ono, R., Ichikawa, H., Yamazaki, M., Tashiro, H., Aisaka, K., Miyoshi, N., Kohda, T., Ogura, A., Ohki, M., Kaneko-Ishino, T., and Ishino, F. (2000). Mouse Peg9/Dlk1 and human PEG9/DLK1 are paternally expressed imprinted genes closely located to the maternally expressed imprinted genes: mouse Meg3/Gtl2 and human MEG3. *Genes to Cells*, 5(12):1029–1037.

[120] Komatsu, H., Chao, M. Y., Larkins-Ford, J., Corkins, M. E., Somers, G. A., Tucey, T., Dionne, H. M., White, J. Q., Wani, K., Boxem, M., and Hart, A. C. (2008). OSM-11 facilitates LIN-12 Notch signaling during Caenorhabditis elegans vulval development. *PLoS Biology*, 6(8):e196.

[121] Kondrashov, F. A., Rogozin, I. B., Wolf, Y. I., and Koonin, E. V. (2002). Selection in the evolution of gene duplications. *Genome Biology*, 3(2):1.

[122] Kopan, R. and Ilagan, M. X. G. (2009a). The canonical Notch signaling pathway: unfolding the activation mechanism. *CELL*, 137(2):216–233.

[123] Kopan, R. and Ilagan, M. X. G. (2009b). The Canonical Notch Signaling Pathway: Unfolding the Activation Mechanism. *CELL*, 137(2):216–233.

[124] Koressaar, T. and Remm, M. (2007). Enhancements and modifications of primer design program Primer3. *Bioinformatics*, 23(10):1289–1291.

[125] Kotzot, D. (2004). Maternal uniparental disomy 14 dissection of the phenotype with respect to rare autosomal recessively inherited traits, trisomy mosaicism, and genomic imprinting. *Annales de genetique*, 47(3):251–260.

[126] Kouadjo, K. E., Nishida, Y., Cadrin-Girard, J. F., Yoshioka, M., and St-Amand, J. (2007). Housekeeping and tissue-specific genes in mouse tissues. *BMC Genomics*, 8(1):127.

[127] Krogh, T. N., Bachmann, E., Teisner, B., Skjødt, K., and Højrup, P. (1997). Glycosylation Analysis and Protein Structure Determination of Murine Fetal Antigen 1 (mFA1). *European Journal of Biochemistry*, 244(2):334–342.

[128] Kuscu, C., Arslan, S., Singh, R., Thorpe, J., and Adli, M. (2014). Genome-wide analysis reveals characteristics of off-target sites bound by the Cas9 endonuclease. *Nature biotechnology*, 32(7):677–683.

[129] Laborda, J., Sausville, E. A., Hoffman, T., and Notario, V. (1993). dlk, a putative mammalian homeotic gene differentially expressed in small cell lung carcinoma and neuroendocrine tumor cell line. *Journal of Biological Chemistry*, 268(6):3817–3820.

[130] Lamichhaney, S., Berglund, J., Almén, M. S., Maqbool, K., Grabherr, M., Martinez-Barrio, A., Promerová, M., Rubin, C.-J., Wang, C., Zamani, N., Grant, B. R., Grant, P. R., Webster, M. T., and Andersson, L. (2015). Evolution of Darwin's finches and their beaks revealed by genome sequencing. *Nature*, 518(7539):371–375.

[131] Lander, E. S., Linton, L. M., Birren, B., Nusbaum, C., Zody, M. C., Baldwin, J., Devon, K., Dewar, K., Doyle, M., FitzHugh, W., Funke, R., Gage, D., Harris, K., Heaford, A., Howland, J., Kann, L., Lehoczky, J., LeVine, R., McEwan, P., McKernan, K., Meldrim, J., Mesirov, J. P., Miranda, C., Morris, W., Naylor, J., Rosetti, M., Santos, R., Sheridan, A., Sougnez, C., Stange-Thomann, N., Stojanovic, N., Subramanian, A., Wyman, D., Rogers, J., Sulston, J., Ainscough, R., Beck, S., Bentley, D., Burton, J., Clee, C., Carter, N., Coulson, A., Deadman, R., Deloukas, P., Dunham, A., Dunham, I., Durbin, R., French, L., Grafham, D., Gregory, S., Hubbard, T., Humphray, S., Hunt, A., Jones, M., Lloyd, C., McMurray, A., Matthews, L., Mercer, S., Milne, S., Mullikin, J. C., Mungall, A., Plumb, R., Ross, M., Shownkeen, R., Sims, S., Waterston, R. H., Wilson, R. K., Hillier, L. W., McPherson, J. D., Marra, M. A., Mardis, E. R., Fulton, L. A., Chinwalla, A. T., Pepin, K. H., Gish, W. R., Chissoe, S. L., Wendl, M. C., Delehaunty, K. D., Miner, T. L., Delehaunty, A., Kramer, J. B., Cook, L. L., Fulton, R. S., Johnson, D. L., Minx, P. J., Clifton, S. W., Hawkins, T., Branscomb, E., Predki, P., Richardson, P., Wenning, S., Slezak, T., Doggett, N., Cheng, J. F., Olsen, A., Lucas, S., Elkin, C., Uberbacher, E., Frazier, M., Gibbs, R. A., Muzny, D. M., Scherer, S. E., Bouck, J. B., Sodergren, E. J., Worley, K. C., Rives, C. M., Gorrell, J. H., Metzker, M. L., Naylor, S. L., Kucherlapati, R. S., Nelson, D. L., Weinstock, G. M., Sakaki, Y., Fujiyama, A., Hattori, M., Yada, T., Toyoda, A., Itoh, T., Kawagoe, C., Watanabe, H., Totoki, Y., Taylor, T., Weissenbach, J., Heilig, R., Saurin, W., Artiguenave, F., Brottier, P., Bruls, T., Pelletier, E., Robert, C., Wincker, P., Smith, D. R., Doucette-Stamm, L., Rubenfield, M., Weinstock, K., Lee, H. M., Dubois, J., Rosenthal, A., Platzer, M., Nyakatura, G., Taudien, S., Rump, A., Yang, H., Yu, J., Wang, J., Huang, G., Gu, J., Hood, L., Rowen, L., Madan, A., Qin, S., Davis, R. W., Federspiel, N. A., Abola, A. P., Proctor, M. J., Myers, R. M., Schmutz, J., Dickson, M., Grimwood, J., Cox, D. R., Olson, M. V., Kaul, R., Raymond, C., Shimizu, N., Kawasaki, K., Minoshima, S., Evans, G. A., Athanasiou, M., Schultz, R., Roe, B. A., Chen, F., Pan, H., Ramser, J., Lehrach, H., Reinhardt, R., McCombie, W. R., de la Bastide, M., Dedhia, N., Blöcker, H., Hornischer, K., Nordsiek, G., Agarwala, R., Aravind, L., Bailey, J. A., Bateman, A., Batzoglou, S., Birney, E., Bork, P., Brown, D. G., Burge,

C. B., Cerutti, L., Chen, H. C., Church, D., Clamp, M., Copley, R. R., Doerks, T., Eddy, S. R., Eichler, E. E., Furey, T. S., Galagan, J., Gilbert, J. G., Harmon, C., Hayashizaki, Y., Haussler, D., Hermjakob, H., Hokamp, K., Jang, W., Johnson, L. S., Jones, T. A., Kasif, S., Kaspryzk, A., Kennedy, S., Kent, W. J., Kitts, P., Koonin, E. V., Korf, I., Kulp, D., Lancet, D., Lowe, T. M., McLysaght, A., Mikkelsen, T., Moran, J. V., Mulder, N., Pollara, V. J., Ponting, C. P., Schuler, G., Schultz, J., Slater, G., Smit, A. F., Stupka, E., Szustakowski, J., Thierry-Mieg, D., Thierry-Mieg, J., Wagner, L., Wallis, J., Wheeler, R., Williams, A., Wolf, Y. I., Wolfe, K. H., Yang, S. P., Yeh, R. F., Collins, F., Guyer, M. S., Peterson, J., Felsenfeld, A., Wetterstrand, K. A., Patrinos, A., Morgan, M. J., de Jong, P., Catanese, J. J., Osoegawa, K., Shizuya, H., Choi, S., Chen, Y. J., Szustakowki, J., and International Human Genome Sequencing Consortium (2001). Initial sequencing and analysis of the human genome. *Nature*, 409(6822):860–921.

[132] Larkin, M. A., Blackshields, G., Brown, N. P., Chenna, R., McGettigan, P. A., McWilliam, H., Valentin, F., Wallace, I. M., Wilm, A., Lopez, R., Thompson, J. D., Gibson, T. J., and Higgins, D. G. (2007). Clustal W and Clustal X version 2.0. *Bioinformatics*, 23(21):2947–2948.

[133] Larsen, J. B., Jensen, C. H., Schrøder, H. D., Teisner, B., Bjerre, P., and Hagen, C. (1996). Fetal antigen 1 and growth hormone in pituitary somatotroph cells. *Lancet (London, England)*, 347(8995):191.

[134] Lee, K., Villena, J. A., Moon, Y. S., Kim, K.-H., Lee, S., Kang, C., and Sul, H. S. (2003). Inhibition of adipogenesis and development of glucose intolerance by soluble preadipocyte factor-1 (Pref-1). *Journal of Clinical Investigation*, 111(4):453–461.

[135] Lee, S. H., Rhee, M., Yang, H. K., Ha, H. S., Lee, J. H., Kwon, H. S., Park, Y. M., Yim, H. W., Kang, M. I., Lee, W. C., Son, H. Y., and Yoon, K. H. (2015a). Serum preadipocyte factor 1 concentrations and risk of developing diabetes: a nested case-control study. *Diabetic Medicine*, pages n/a–n/a.

[136] Lee, Y.-h., Yun, M. R., Kim, H. M., Jeon, B. H., Park, B.-C., Lee, B.-W., Kang, E. S., Lee, H. C., Park, Y. W., and Cha, B.-S. (2015b). Exogenous administration of DLK1 ameliorates hepatic steatosis and regulates gluconeogenesis via activation of AMPK. *International journal of obesity (2005)*.

[137] Li, J., Sun, Y., and Chen, J. (2018). Identification of Critical Genes and miRNAs Associated with the Development of Parkinson's Disease. *Journal of Molecular Neuroscience*, 65(4):527–535.

[138] Li, L., Forman, S. J., and Bhatia, R. (2005). Expression of DLK1 in hematopoietic cells results in inhibition of differentiation and proliferation. *Oncogene*, 24(27):4472–4476.

[139] Li, X., Ito, M., Zhou, F., Youngson, N., Zuo, X., Leder, P., and Ferguson-Smith, A. C. (2008). A maternal-zygotic effect gene, Zfp57, maintains both maternal and paternal imprints. *Developmental Cell*, 15(4):547–557.

[140] Lin, S.-P., Youngson, N., Takada, S., Seitz, H., Reik, W., Paulsen, M., Cavaille, J., and Ferguson-Smith, A. C. (2003). Asymmetric regulation of imprinting on the maternal and paternal chromosomes at the Dlk1-Gtl2 imprinted cluster on mouse chromosome 12. *Nature Genetics*, 35(1):97–102.

[141] Litzky, J. F., Deyssenroth, M. A., Everson, T. M., Lester, B. M., Lambertini, L., Chen, J., and Marsit, C. J. (2018). Prenatal exposure to maternal depression and anxiety on imprinted gene expression in placenta and infant neurodevelopment and growth. *Pediatric research*, 83(5):1075–1083.

[142] Lizio, M., Harshbarger, J., Shimoji, H., Severin, J., Kasukawa, T., Sahin, S., Abugessaisa, I., Fukuda, S., Hori, F., Ishikawa-Kato, S., Mungall, C. J., Arner, E., Baillie, J. K., Bertin, N., Bono, H., de Hoon, M., Diehl, A. D., Dimont, E., Freeman, T. C., Fujieda, K., Hide, W., Kaliyaperumal, R., Katayama, T., Lassmann, T., Meehan, T. F., Nishikata, K., Ono, H., Rehli, M., Sandelin, A., Schultes, E. A., 't Hoen, P. A. C., Tatum, Z., Thompson, M., Toyoda, T., Wright, D. W., Daub, C. O., Itoh, M., Carninci, P., Hayashizaki, Y., Forrest, A. R. R., Kawaji, H., and FANTOM consortium (2015). Gateways to the FANTOM5 promoter level mammalian expression atlas. *Genome Biology*, 16:22.

[143] López-Terrada, D., Gunaratne, P. H., Adesina, A. M., Pulliam, J., Hoang, D. M., Nguyen, Y., Mistretta, T.-A., Margolin, J., and Finegold, M. J. (2009). Histologic subtypes of hepatoblastoma are characterized by differential canonical Wnt and Notch pathway activation in DLK+ precursors. *Human pathology*, 40(6):783–794.

[144] Lottrup, G., Nielsen, J. E., Skakkebæk, N. E., Juul, A., and Rajpert-De Meyts, E. (2015). Abundance of DLK1, differential expression of CYP11B1, CYP21A2 and MC2R, and lack of INSL3 distinguish testicular adrenal rest tumours from Leydig cell tumours. *European journal of endocrinology*, 172(4):491–499.

[145] Luo, J.-H., Ren, B., Keryanov, S., Tseng, G. C., Rao, U. N. M., Monga, S. P., Strom, S., Demetris, A. J., Nalesnik, M., Yu, Y. P., Ranganathan, S., and Michalopoulos, G. K. (2006). Transcriptomic and genomic analysis of human hepatocellular carcinomas and hepatoblastomas. *Hepatology (Baltimore, Md.)*, 44(4):1012–1024.

[146] Lykke-Andersen, J. and Bennett, E. J. (2014). Protecting the proteome: Eukaryotic cotranslational quality control pathways. *The Journal of Cell Biology*, 204(4):467–476.

[147] Lynch, M. and Conery, J. S. (2000). The evolutionary fate and consequences of duplicate genes. *Science*.

[148] Mašek, J. and Andersson, E. R. (2017). The developmental biology of genetic Notch disorders. *Development*, 144(10):1743–1763.

[149] Mattapallil, M. J., Wawrousek, E. F., Chan, C.-C., Zhao, H., Roychoudhury, J., Ferguson, T. A., and Caspi, R. R. (2012). The Rd8 mutation of the Crb1 gene is present in vendor lines of C57BL/6N mice and embryonic stem cells, and confounds ocular induced mutant phenotypes. *Investigative Opthalmology & Visual Science*, 53(6):2921–2927.

[150] Mei, B., Zhao, L., Chen, L., and Sul, H. S. (2002). Only the large soluble form of preadipocyte factor-1 (Pref-1), but not the small soluble and membrane forms, inhibits adipocyte differentiation: role of alternative splicing. *Biochemical Journal*, 364(Pt 1):137–144.

[151] Miller, A. J. and Cole, S. E. (2014). Multiple Dlk1 splice variants are expressed during early mouse embryogenesis. *The International Journal of Developmental Biology*, 58(1):65–70.

[152] Mirshekar-Syahkal, B., Haak, E., Kimber, G. M., van Leusden, K., Harvey, K., O'Rourke, J., Laborda, J., Bauer, S. R., de Bruijn, M. F. T. R., Ferguson-Smith, A. C., Dzierzak, E., and Ottersbach, K. (2013). Dlk1 is a negative regulator of emerging hematopoietic stem and progenitor cells. *Haematologica*, 98(2):163–171.

[153] Miyajima, A., Tanaka, M., and Itoh, T. (2014). Stem/progenitor cells in liver development, homeostasis, regeneration, and reprogramming. *Cell Stem Cell*, 14(5):561–574.

[154] Miyaoka, Y., Tanaka, M., Imamura, T., Takada, S., and Miyajima, A. (2010). A novel regulatory mechanism for Fgf18 signaling involving cysteine-rich FGF receptor (Cfr) and delta-like protein (Dlk). *Development*, 137(1):159–167.

[155] Miyoshi, N., Kuroiwa, Y., Kohda, T., Shitara, H., Yonekawa, H., Kawabe, T., Hasegawa, H., Barton, S. C., Surani, M. A., Kaneko-Ishino, T., and Ishino, F. (1998). Identification of the Meg1/Grb10 imprinted gene on mouse proximal chromosome 11, a candidate for the Silver–Russell syndromegene. *Proceedings of the National Academy of Sciences of the United States of America*, 95(3):1102–1107.

[156] Møller, N. and Jørgensen, J. O. L. (2009). Effects of growth hormone on glucose, lipid, and protein metabolism in human subjects. *Endocrine reviews*, 30(2):152–177.

[157] Monsalve, E., García-Gutiérrez, M., Navarrete, F., Giner, S., Laborda, J., and Manzanares, J. (2014). Abnormal Expression Pattern of Notch Receptors, Ligands, and Downstream Effectors in the Dorsolateral Prefrontal Cortex and Amygdala of Suicidal Victims. *Molecular Neurobiology*, 49(2):957–965.

[158] Moon, Y. S., Smas, C. M., Lee, K., Villena, J. A., Kim, K.-H., Yun, E. J., and Sul, H. S. (2002). Mice lacking paternally expressed Pref-1/Dlk1 display growth retardation and accelerated adiposity. *Molecular and Cellular Biology*, 22(15):5585–5592.

[159] Moore, G. E., Ishida, M., Demetriou, C., Al-Olabi, L., Leon, L. J., Thomas, A. C., Abu-Amero, S., Frost, J. M., Stafford, J. L., Chaoqun, Y., Duncan, A. J., Baigel, R., Brimioulle, M., Iglesias-Platas, I., Apostolidou, S., Aggarwal, R., Whittaker, J. C., Syngelaki, A., Nicolaides, K. H., Regan, L., Monk, D., and Stanier, P. (2015). The role and interaction of imprinted genes in human fetal growth. *Philosophical transactions of the Royal Society of London. Series B, Biological sciences*, 370(1663):20140074.

[160] Moore, K. A., Pytowski, B., Witte, L., Hicklin, D., and Lemischka, I. R. (1997). Hematopoietic activity of a stromal cell transmembrane protein containing epidermal growth factor-like repeat motifs. *Proceedings of the National Academy of Sciences*, 94(8):4011–4016.

[161] Moreno-Mateos, M. A., Vejnar, C. E., Beaudoin, J.-D., Fernandez, J. P., Mis, E. K., Khokha, M. K., and Giraldez, A. J. (2015). CRISPRscan: designing highly efficient sgRNAs for CRISPR-Cas9 targeting in vivo. *Nature methods*, 12(10):982–988.

[162] Mortensen, S. B., Jensen, C. H., Schneider, M., Thomassen, M., Kruse, T. A., Laborda, J., Sheikh, S. P., and Andersen, D. C. (2012). Membrane-Tethered Delta-Like 1 Homolog (DLK1) Restricts Adipose Tissue Size by Inhibiting Preadipocyte Proliferation. *Diabetes*, 61(11):2814–2822.

[163] Naegele, M. and Martin, R. (2014). The good and the bad of neuroinflammation in multiple sclerosis. *Handbook of clinical neurology*, 122:59–87.

[164] Nakahara, J., Maeda, M., Aiso, S., and Suzuki, N. (2011). Current Concepts in Multiple Sclerosis: Autoimmunity Versus Oligodendrogliopathy. *Clinical Reviews in Allergy & Immunology*, 42(1):26–34.

[165] Nueda, M. L., Baladrón, V., García-Ramírez, J. J., Sánchez-Solana, B., Ruvira, M. D., Rivero, S., Ballesteros, M.-Á., Monsalve, E. M., Díaz-Guerra, M. J. M., Ruiz-Hidalgo, M. J., and Laborda, J. (2007a). The Novel Gene EGFL9/Dlk2, Highly Homologous to Dlk1, Functions as a Modulator of Adipogenesis. *Journal of Molecular Biology*, 367(5):1270–1280.

[166] Nueda, M. L., Baladrón, V., Sánchez-Solana, B., Ballesteros, M.-Á., and Laborda, J. (2007b). The EGF-like protein dlk1 inhibits notch signaling and potentiates adipogenesis of mesenchymal cells. *Journal of Molecular Biology*, 367(5):1281–1293.

[167] Nueda, M. L., Naranjo, A.-I., Baladrón, V., and Laborda, J. (2014). The proteins DLK1 and DLK2 modulate NOTCH1-dependent proliferation and oncogenic potential of human SK-MEL-2 melanoma cells. *BBA - Molecular Cell Research*, 1843(11):2674–2684.

[168] Ohno, N., Izawa, A., Hattori, M., Kageyama, R., and Sudo, T. (2001). dlk inhibits stem cell factor-induced colony formation of murine hematopoietic progenitors: Hes-1-independent effect. *Stem cells (Dayton, Ohio)*, 19(1):71–79.

[169] Orchard, S., Ammari, M., Aranda, B., Breuza, L., Briganti, L., Broackes-Carter, F., Campbell, N. H., Chavali, G., Chen, C., del Toro, N., Duesbury, M., Dumousseau, M., Galeota, E., Hinz, U., Iannuccelli, M., Jagannathan, S., Jimenez, R., Khadake, J., Lagreid, A., Licata, L., Lovering, R. C., Meldal, B., Melidoni, A. N., Milagros, M., Peluso, D., Perfetto, L., Porras, P., Raghunath, A., Ricard-Blum, S., Roechert, B., Stutz, A., Tognolli, M., van Roey, K., Cesareni, G., and Hermjakob, H. (2014). The MIntAct project–IntAct as a common curation platform for 11 molecular interaction databases. *Nucleic Acids Research*, 42(Database issue):D358–63.

[170] Pacifici, R. (2007). T cells and post menopausal osteoporosis in murine models. *Arthritis research & therapy*, 9(2):102.

[171] Papin, J. and Subramaniam, S. (2004). Bioinformatics and cellular signaling. *Current opinion in biotechnology*, 15(1):78–81.

[172] Park, H. C. (2003). Delta-Notch signaling regulates oligodendrocyte specification. *Development*, 130(16):3747–3755.

[173] Perry, J. R. B., Day, F., Elks, C. E., Sulem, P., Thompson, D. J., Ferreira, T., He, C., Chasman, D. I., Esko, T., Thorleifsson, G., Albrecht, E., Ang, W. Q., Corre, T., Cousminer, D. L., Feenstra, B., Franceschini, N., Ganna, A., Johnson, A. D., Kjellqvist, S., Lunetta, K. L., McMahon, G., Nolte, I. M., Paternoster, L., Porcu, E., Smith, A. V., Stolk, L., Teumer, A., Tšernikova, N., Tikkanen, E., Ulivi, S., Wagner, E. K., Amin, N., Bierut, L. J., Byrne, E. M., Hottenga, J.-J., Koller, D. L., Mangino, M., Pers, T. H., Yerges-Armstrong, L. M., Hua Zhao, J., Andrulis, I. L., Anton-Culver, H., Atsma, F., Bandinelli, S., Beckmann, M. W., Benitez, J., Blomqvist, C., Bojesen, S. E., Bolla, M. K.,

Bonanni, B., Brauch, H., Brenner, H., Buring, J. E., Chang-claude, J., Chanock, S., Chen, J., Chenevix-Trench, G., Collée, J. M., Couch, F. J., Couper, D., Coviello, A. D., Cox, A., Czene, K., D'adamo, A. P., Davey Smith, G., De Vivo, I., Demerath, E. W., Dennis, J., Devilee, P., Dieffenbach, A. K., Dunning, A. M., Eiriksdottir, G., Eriksson, J. G., Fasching, P. A., Ferrucci, L., Flesch-Janys, D., Flyger, H., Foroud, T., Franke, L., Garcia, M. E., García-Closas, M., Geller, F., de Geus, E. E. J., Giles, G. G., Gudbjartsson, D. F., Gudnason, V., Guénel, P., Guo, S., Hall, P., Hamann, U., Haring, R., Hartman, C. A., Heath, A. C., Hofman, A., Hooning, M. J., Hopper, J. L., Hu, F. B., Hunter, D. J., Karasik, D., Kiel, D. P., Knight, J. A., Kosma, V.-M., Kutalik, Z., Lai, S., Lambrechts, D., Lindblom, A., Mägi, R., Magnusson, P. K., Mannermaa, A., Martin, N. G., Masson, G., McArdle, P. F., McArdle, W. L., Melbye, M., Michailidou, K., Mihailov, E., Milani, L., Milne, R. L., Nevanlinna, H., Neven, P., Nohr, E. A., Oldehinkel, A. J., Oostra, B. A., Palotie, A., Peacock, M., Pedersen, N. L., Peterlongo, P., Peto, J., Pharoah, P. D. P., Postma, D. S., Pouta, A., Pylkäs, K., Radice, P., Ring, S., Rivadeneira, F., Robino, A., Rose, L. M., Rudolph, A., Salomaa, V., Sanna, S., Schlessinger, D., Schmidt, M. K., Southey, M. C., Sovio, U., Stampfer, M. J., Stöckl, D., Storniolo, A. M., Timpson, N. J., Tyrer, J., Visser, J. A., Vollenweider, P., Völzke, H., Waeber, G., Waldenberger, M., Wallaschofski, H., Wang, Q., Willemsen, G., Winqvist, R., Wolffenbuttel, B. H. R., Wright, M. J., Australian Ovarian Cancer Study, GENICA Network, kConFab, LifeLines Cohort Study, InterAct Consortium, Early Growth Genetics (EGG) Consortium, Boomsma, D. I., Econs, M. J., Khaw, K.-T., Loos, R. J. F., Mccarthy, M. I., Montgomery, G. W., Rice, J. P., Streeten, E. A., Thorsteinsdottir, U., van Duijn, C. M., Alizadeh, B. Z., Bergmann, S., Boerwinkle, E., Boyd, H. A., Crisponi, L., Gasparini, P., Gieger, C., Harris, T. B., Ingelsson, E., Jarvelin, M.-R., Kraft, P., Lawlor, D., Metspalu, A., Pennell, C. E., Ridker, P. M., Snieder, H., Sørensen, T. I. A., Spector, T. D., Strachan, D. P., Uitterlinden, A. G., Wareham, N. J., Widen, E., Zygmunt, M., Murray, A., Easton, D. F., Stefansson, K., Murabito, J. M., and Ong, K. K. (2014). Parent-of-origin-specific allelic associations among 106 genomic loci for age at menarche. *Nature*, 514(7520):92–97.

[174] Peters, J. and Beechey, C. (2004). Identification and characterisation of imprinted genes in the mouse. *Briefings in Functional Genomics & Proteomics*, 2(4):320–333.

[175] Popp, M. W. and Maquat, L. E. (2016). Leveraging Rules of Nonsense-Mediated mRNA Decay for Genome Engineering and Personalized Medicine. *CELL*, 165(6):1319–1322.

[176] Puertas-Avendaño, R. A., González-Gómez, M. J., Ruvira, M. D., Ruiz-Hidalgo, M. J., Morales-Delgado, N., Laborda, J., Díaz, C., and Bello, A. R. (2011). Role of the non-canonical notch ligand delta-like protein 1 in hormone-producing cells of the adult male mouse pituitary. *Journal of Neuroendocrinology*, 23(9):849–859.

[177] Qi, S., Yan, Y., Wen, Y., Li, J., Wang, J., Chen, F., Tang, X., Shang, G., Xu, Y., and Wang, R. (2017). The effect of delta-like 1 homologue on the proliferation and odontoblastic differentiation in human dental pulp stem cells. *Cell Proliferation*, 50(3):e12335.

[178] Qi, S., Zhu, X., Wang, X., Chen, F., Yan, Y., Shang, G., and Chen, W. (2018). Role of protein delta homolog 1 in the proliferation and differentiation of ameloblasts. *Molecular medicine reports*, 17(3):3537–3544.

[179] Qi, Y., Zhang, Y., Zhang, F., Baller, J. A., Cleland, S. C., Ryu, Y., Starker, C. G., and Voytas, D. F. (2013). Increasing frequencies of site-specific mutagenesis and gene targeting in Arabidopsis by manipulating DNA repair pathways. *Genome Research*, 23(3):547–554.

[180] Raggatt, L. J. and Partridge, N. C. (2010). Cellular and Molecular Mechanisms of Bone Remodeling. *Journal of Biological Chemistry*, 285(33):25103–25108.

[181] Raghunandan, R., Ruiz-Hidalgo, M., Jia, Y., Ettinger, R., Rudikoff, E., Riggins, P., Farnsworth, R., Tesfaye, A., Laborda, J., and Bauer, S. R. (2008a). Dlk1 influences differentiation and function of B lymphocytes. *Stem cells and development*, 17(3):495–507.

[182] Raghunandan, R., Ruiz-Hidalgo, M., Jia, Y., Ettinger, R., Rudikoff, E., Riggins, P., Farnsworth, R., Tesfaye, A., Laborda, J., and Bauer, S. R. (2008b). Dlk1 influences differentiation and function of B lymphocytes. *Stem cells and development*, 17(3):495–507.

[183] Rhee, M., Lee, S.-H., Kim, J.-W., Ham, D.-S., Park, H.-S., Yang, H. K., Shin, J.-Y., Cho, J.-H., Kim, Y.-B., Youn, B.-S., Sul, H. S., and Yoon, K.-H. (2016). Preadipocyte factor 1 induces pancreatic ductal cell differentiation into insulin-producing cells. *Scientific reports*, 6:23960.

[184] Rice, P., Longden, I., and Bleasby, A. (2000). EMBOSS: the European Molecular Biology Open Software Suite. *Trends in Genetics*, 16(6):276–277.

[185] Rivero, S., Díaz-Guerra, M. J. M., Monsalve, E. M., Laborda, J., and García-Ramírez, J. J. (2012). DLK2 Is a Transcriptional Target of KLF4 in the Early Stages of Adipogenesis. *Journal of Molecular Biology*, 417(1-2):36–50.

[186] Rivero, S., Ruiz-García, A., Díaz-Guerra, M. J. M., Laborda, J., and García-Ramírez, J. J. (2011). Characterization of a proximal Sp1 response element in the mouse Dlk2 gene promoter. *BMC molecular biology*, 12(1):52.

[187] Rocha, S. T. d., Edwards, C. A., Ito, M., Ogata, T., and Ferguson-Smith, A. C. (2008). Genomic imprinting at the mammalian Dlk1-Dio3 domain. *Trends in Genetics*, 24(6):306–316.

[188] Rodríguez, P., Higueras, M. A., González-Rajal, A., Alfranca, A., Fierro-Fernández, M., García-Fernández, R. A., Ruiz-Hidalgo, M. J., Monsalve, M., Rodríguez-Pascual, F., Redondo, J. M., de la Pompa, J. L., Laborda, J., and Lamas, S. (2012). The non-canonical NOTCH ligand DLK1 exhibits a novel vascular role as a strong inhibitor of angiogenesis. *Cardiovascular Research*, 93(2):232–241.

[189] Ruiz-Hidalgo, M. J., Gubina, E., Tull, L., Baladrón, V., and Laborda, J. (2002). dlk modulates mitogen-activated protein kinase signaling to allow or prevent differentiation. *Experimental Cell Research*, 274(2):178–188.

[190] Sakajiri, S., O'kelly, J., Yin, D., Miller, C. W., Hofmann, W. K., Oshimi, K., Shih, L.-Y., Kim, K.-H., Sul, H. S., Jensen, C. H., Teisner, B., Kawamata, N., and Koeffler, H. P. (2005). Dlk1 in normal and abnormal hematopoiesis. *Leukemia*, 19(8):1404–1410.

[191] Samulewicz, S. J., Seitz, A., Clark, L., and Heber-Katz, E. (2002). Expression of preadipocyte factor-1(Pref-1), a delta-like protein, in healing mouse ears. *Wound repair and regeneration : official publication of the Wound Healing Society [and] the European Tissue Repair Society*, 10(4):215–221.

[192] Sánchez-Solana, B., Nueda, M. L., Ruvira, M. D., Ruiz-Hidalgo, M. J., Monsalve, E. M., Rivero, S., García-Ramírez, J. J., Díaz-Guerra, M. J. M., Baladrón, V., and Laborda, J. (2011). The EGF-like proteins DLK1 and DLK2 function as inhibitory non-canonical ligands of NOTCH1 receptor that modulate each other's activities. *BBA - Molecular Cell Research*, 1813(6):1153–1164.

[193] Sanlaville, D. (2000). Maternal uniparental heterodisomy of chromosome 14: chromosomal mechanism and clinical follow up. *Journal of medical genetics*, 37(7):525–528.

[194] Scheer, N., Groth, A., Hans, S., and Campos-Ortega, J. A. (2001). An instructive function for Notch in promoting gliogenesis in the zebrafish retina. *Development*, 128(7):1099–1107.

[195] Schluter, D. (2000). *The Ecology of Adaptive Radiation*. OUP Oxford.

[196] Schmidt, R., Strähle, U., and Scholpp, S. (2013). Neurogenesis in zebrafish - from embryo to adult. *Neural development*, 8(1):3.

[197] Schneider, G., Bowser, M. J., Shin, D.-M., Barr, F. G., and Ratajczak, M. Z. (2014). The paternally imprinted DLK1-GTL2 locus is differentially methylated in embryonal and alveolar rhabdomyosarcomas. *International journal of oncology*, 44(1):295–300.

[198] Schober, A., Nazari-Jahantigh, M., Wei, Y., Bidzhekov, K., Gremse, F., Grommes, J., Megens, R. T. A., Heyll, K., Noels, H., Hristov, M., Wang, S., Kiessling, F., Olson, E. N., and Weber, C. (2014). MicroRNA-126-5p promotes endothelial proliferation and limits atherosclerosis by suppressing Dlk1. *Nature Medicine*, 20(4):368–376.

[199] Schuster-Gossler, K., Cordes, R., and Gossler, A. (2007). Premature myogenic differentiation and depletion of progenitor cells cause severe muscle hypotrophy in Delta1 mutants. *Proceedings of the National Academy of Sciences*, 104(2):537–542.

[200] Segovia, S. A., Vickers, M. H., Harrison, C. J., Patel, R., Gray, C., and Reynolds, C. M. (2018). Maternal High-Fat and High-Salt Diets Have Differential Programming Effects on Metabolism in Adult Male Rat Offspring. *Frontiers in Nutrition*, 5:341.

[201] Seitz, H., Royo, H., Bortolin, M.-L., Lin, S.-P., Ferguson-Smith, A. C., and Cavaille, J. (2004). A large imprinted microRNA gene cluster at the mouse Dlk1-Gtl2 domain. *Genome Research*, 14(9):1741–1748.

[202] Sellers, Z. P., Schneider, G., Maj, M., and Ratajczak, M. Z. (2018). Analysis of the Paternally-Imprinted DLK1-MEG3 and IGF2-H19 Tandem Gene Loci in NT2 Embryonal Carcinoma Cells Identifies DLK1 as a Potential Therapeutic Target. *Stem Cell Reviews*, 138(3):351–14.

[203] Shamis, Y., Cullen, D. E., Liu, L., Yang, G., Ng, S.-F., Xiao, L., Bell, F. T., Ray, C., Takikawa, S., Moskowitz, I. P., Cai, C.-L., Yang, X., and Li, X. (2015). Maternal and zygotic Zfp57 modulate NOTCH signaling in cardiac development. *Proceedings of the National Academy of Sciences of the United States of America*, 112(16):E2020–9.

[204] Shin, S., Choi, Y. M., Suh, Y., and Lee, K. (2015). Delta-like 1 homolog (DLK1) inhibits proliferation and myotube formation of avian QM7 myoblasts. *Comparative biochemistry and physiology. Part B, Biochemistry & molecular biology*, 179:37–43.

[205] Shin, S., Han, J. Y., and Lee, K. (2010). Cloning of avian Delta-like 1 homolog gene: the biallelic expression of Delta-like 1 homolog in avian species. *Poultry science*, 89(5):948–955.

[206] Shin, S., Suh, Y., Zerby, H. N., and Lee, K. (2014). Membrane-bound delta-like 1 homolog (Dlk1) promotes while soluble Dlk1 inhibits myogenesis in C2C12 cells. *FEBS letters*, 588(7):1100–1108.

[207] Sigrist, C. J. A., Cerutti, L., Hulo, N., Gattiker, A., Falquet, L., Pagni, M., Bairoch, A., and Bucher, P. (2002). PROSITE: A documented database using patterns and profiles as motif descriptors. *Briefings in Bioinformatics*, 3(3):265–274.

[208] Singh, P., Schimenti, J. C., and Bolcun-Filas, E. (2015a). A mouse geneticist's practical guide to CRISPR applications. *Genetics*.

[209] Singh, S., Rajput, Y. S., Barui, A. K., Sharma, R., and Grover, S. (2015b). Expression of developmental genes in brown fat cells grown in vitro is linked with lipid accumulation. *In vitro cellular & developmental biology. Animal*.

[210] Six, E., Ndiaye, D., Laâbi, Y., Brou, C., Gupta-Rossi, N., Israël, A., and Logeat, F. (2003). The Notch ligand Delta1 is sequentially cleaved by an ADAM protease and gamma-secretase. *Proceedings of the National Academy of Sciences*, 100(13):7638–7643.

[211] Smas, C. M., Chen, L., and Sul, H. S. (1997). Cleavage of membrane-associated pref-1 generates a soluble inhibitor of adipocyte differentiation. *Molecular and Cellular Biology*, 17(2):977–988.

[212] Smas, C. M., Green, D., and Sul, H. S. (1994). Structural characterization and alternate splicing of the gene encoding the preadipocyte EGF-like protein pref-1. *Biochemistry*, 33(31):9257–9265.

[213] Smas, C. M. and Sul, H. S. (1993). Pref-1, a protein containing EGF-like repeats, inhibits adipocyte differentiation. *CELL*, 73(4):725–734.

[214] Smith, C., Gore, A., Yan, W., Abalde-Atristain, L., Li, Z., He, C., Wang, Y., Brodsky, R. a., Zhang, K., Cheng, L., and Ye, Z. (2014). Whole-genome sequencing analysis reveals high specificity of CRISPR/Cas9 and TALEN-based genome editing in human iPSCs. *Cell Stem Cell*, 15(1):12–13.

[215] Smith, C. L., Blake, J. A., Kadin, J. A., Richardson, J. E., Bult, C. J., and Mouse Genome Database Group (2018). Mouse Genome Database (MGD)-2018: knowledgebase for the laboratory mouse. *Nucleic Acids Research*, 46(D1):D836–D842.

[216] Song, Y., Willer, J. R., Scherer, P. C., Panzer, J. A., Kugath, A., Skordalakes, E., Gregg, R. G., Willer, G. B., and Balice-Gordon, R. J. (2010). Neural and Synaptic Defects in slytherin, a Zebrafish Model for Human Congenital Disorders of Glycosylation. *PLoS ONE*, 5(10):e13743.

[217] Stelzer, Y., Wu, H., Song, Y., Shivalila, C. S., Markoulaki, S., and Jaenisch, R. (2016). Parent-of-Origin DNA Methylation Dynamics during Mouse Development. *CellReports*, 16(12):3167–3180.

[218] Stothard, P. (2000). The sequence manipulation suite: JavaScript programs for analyzing and formatting protein and DNA sequences. *BioTechniques*, 28(6):1102–1104.

[219] Stridh, P., Ruhrmann, S., Bergman, P., Thessén Hedreul, M., Flytzani, S., Beyeen, A. D., Gillett, A., Krivosija, N., Öckinger, J., Ferguson-Smith, A. C., and Jagodic, M. (2014). Parent-of-Origin Effects Implicate Epigenetic Regulation of Experimental Autoimmune Encephalomyelitis and Identify Imprinted Dlk1 as a Novel Risk Gene. *PLoS Genetics*, 10(3):e1004265–17.

[220] Strogantsev, R., Krueger, F., Yamazawa, K., Shi, H., Gould, P., Goldman-Roberts, M., McEwen, K., Sun, B., Pedersen, R., and Ferguson-Smith, A. C. (2015). Allele-specific binding of ZFP57 in the epigenetic regulation of imprinted and non-imprinted monoallelic expression. *Genome Biology*, 16(1):112.

[221] Sunkin, S. M., Ng, L., Lau, C., Dolbeare, T., Gilbert, T. L., Thompson, C. L., Hawrylycz, M., and Dang, C. (2013). Allen Brain Atlas: an integrated spatio-temporal portal for exploring the central nervous system. *Nucleic Acids Research*, 41(Database issue):D996–D1008.

[222] Szklarczyk, D., Franceschini, A., Wyder, S., Forslund, K., Heller, D., Huerta-Cepas, J., Simonovic, M., Roth, A., Santos, A., Tsafou, K. P., Kuhn, M., Bork, P., Jensen, L. J., and von Mering, C. (2015). STRING v10: protein-protein interaction networks, integrated over the tree of life. *Nucleic Acids Research*, 43(Database issue):D447–52.

[223] Takada, S., Tevendale, M., Baker, J., Georgiades, P., Campbell, E., Freeman, T., Johnson, M. H., Paulsen, M., and Ferguson-Smith, A. C. (2000). Delta-like and gtl2 are reciprocally expressed, differentially methylated linked imprinted genes on mouse chromosome 12. *Current Biology*, 10(18):1135–1138.

[224] Takahashi, I., Takahashi, T., Utsunomiya, M., Takada, G., and Koizumi, A. (2005). Long-Acting Gonadotropin-Releasing Hormone Analogue Treatment for Central Precocious Puberty in Maternal Uniparental Disomy Chromosome 14. *The Tohoku journal of ...*, 207(4):333–338.

[225] Tanimizu, N., Nishikawa, M., Saito, H., Tsujimura, T., and Miyajima, A. (2003). Isolation of hepatoblasts based on the expression of Dlk/Pref-1. *Journal of Cell Science*, 116(9):1775–1786.

[226] Temple, I. K., Shrubb, V., Lever, M., Bullman, H., and Mackay, D. J. G. (2007). Isolated imprinting mutation of the DLK1/GTL2 locus associated with a clinical presentation of maternal uniparental disomy of chromosome 14. *Journal of medical genetics*, 44(10):637–640.

[227] The UniProt Consortium (2017). UniProt: the universal protein knowledgebase. *Nucleic Acids Research*, 45(D1):D158–D169.

[228] Tolman, K. G. and Dalpiaz, A. S. (2007). Treatment of non-alcoholic fatty liver disease. *Therapeutics and Clinical Risk Management*, 3(6):1153–1163.

[229] Tomkins, D. J., Roux, A. F., Waye, J., Freeman, V. C., Cox, D. W., and Whelan, D. T. (1996). Maternal uniparental isodisomy of human chromosome 14 associated with a paternal t(13q14q) and precocious puberty. *European Journal of Human Genetics*, 4(3):153–159.

[230] Tornehave, D., Jansen, P., Teisner, B., Rasmussen, H. B., Chemnitz, J., and Moscoso, G. (1993). Fetal antigen 1 (FA1) in the human pancreas: cell type expression, topological and quantitative variations during development. *Anatomy and Embryology*, 187(4):335–341.

[231] Tornehave, D., Jensen, C. H., Teisner, B., and Larsson, L.-I. (1996). FA1 immunoreactivity in endocrine tumours and during development of the human fetal pancreas; negative correlation with glucagon expression. *Histochemistry and Cell Biology*, 106(6):535–542.

[232] Traustadóttir, G. Á., Jensen, C. H., Thomassen, M., Beck, H. C., Mortensen, S. B., Laborda, J., Baladrón, V., Sheikh, S. P., and Andersen, D. C. (2016). Evidence of non-canonical NOTCH signaling: Delta-like 1 homolog (DLK1) directly interacts with the NOTCH1 receptor in mammals. *Cellular signalling*, 28(4):246–254.

[233] Tsubaki, M., Kato, C., Manno, M., Ogaki, M., Satou, T., Itoh, T., Kusunoki, T., Tanimori, Y., Fujiwara, K., Matsuoka, H., and Nishida, S. (2007). Macrophage inflammatory protein-1alpha (MIP-1alpha) enhances a receptor activator of nuclear factor kappaB ligand (RANKL) expression in mouse bone marrow stromal cells and osteoblasts through MAPK and PI3K/Akt pathways. *Molecular and Cellular Biochemistry*, 304(1-2):53–60.

[234] Tsukamoto, H. (2015). Metabolic reprogramming and cell fate regulation in alcoholic liver disease. *Pancreatology : official journal of the International Association of Pancreatology (IAP) ... [et al.]*, 15(4 Suppl):S61–5.

[235] Van de Peer, Y., Taylor, J. S., Braasch, I., and Meyer, A. (2001). The ghost of selection past: rates of evolution and functional divergence of anciently duplicated genes. *Journal of Molecular Evolution*, 53(4-5):436–446.

[236] Van Limpt, V. A. E., Chan, A. J., Van Sluis, P. G., Caron, H. N., Van Noesel, C. J. M., and Versteeg, R. (2003). High delta-like 1 expression in a subset of neuroblastoma cell lines corresponds to a differentiated chromaffin cell type. *International journal of cancer. Journal international du cancer*, 105(1):61–69.

[237] Vandesompele, J., De Preter, K., Pattyn, F., Poppe, B., Van Roy, N., De Paepe, A., and Speleman, F. (2002). Accurate normalization of real-time quantitative RT-PCR data by geometric averaging of multiple internal control genes. *Genome Biology*, 3(7):RESEARCH0034.

[238] Vasyutina, E., Lenhard, D. C., and Birchmeier, C. (2007). Notch function in myogenesis. *Cell Cycle*.

[239] Veres, A., Gosis, B. S., Ding, Q., Collins, R., Ragavendran, A., Brand, H., Erdin, S., Cowan, C. A., Talkowski, M. E., and Musunuru, K. (2014). Low incidence of off-target mutations in individual CRISPR-Cas9 and TALEN targeted human stem cell clones detected by whole-genome sequencing. *Cell Stem Cell*, 15(1):27–30.

[240] Villanueva, C., Jacquier, S., and de Roux, N. (2012). DLK1 Is a Somato-Dendritic Protein Expressed in Hypothalamic Arginine-Vasopressin and Oxytocin Neurons. *PLoS ONE*, 7(4):e36134.

[241] Villena, J. A., Choi, C. S., Wang, Y., Kim, S., Hwang, Y.-J., Kim, Y.-B., Cline, G., Shulman, G. I., and Sul, H. S. (2008). Resistance to high-fat diet-induced obesity but exacerbated insulin resistance in mice overexpressing preadipocyte factor-1 (Pref-1): a new model of partial lipodystrophy. *Diabetes*, 57(12):3258–3266.

[242] Vuocolo, T., Pearson, R., Campbell, P., and Tellam, R. L. (2003). Differential expression of Dlk-1 in bovine adipose tissue depots. *Comparative biochemistry and physiology. Part B, Biochemistry & molecular biology*, 134(2):315–333.

[243] Waddell, J. N., Zhang, P., Wen, Y., Gupta, S. K., Yevtodiyenko, A., Schmidt, J. V., Bidwell, C. A., Kumar, A., and Kuang, S. (2010). Dlk1 Is Necessary for Proper Skeletal Muscle Development and Regeneration. *PLoS ONE*, 5(11):e15055.

[244] Wagner, A. (2002). Selection and gene duplication: a view from the genome. *Genome Biology*, 3(5):reviews1012.

[245] Wallace, C., Smyth, D. J., Maisuria-Armer, M., Walker, N. M., Todd, J. A., and Clayton, D. G. (2009). The imprinted DLK1-MEG3 gene region on chromosome 14q32.2 alters susceptibility to type 1 diabetes. *Nature Genetics*, 42(1):68–71.

[246] Wang, Y., Lee, K., Moon, Y. S., Ahmadian, M., Kim, K.-H., Roder, K., Kang, C., and Sul, H. S. (2015). Overexpression of Pref-1 in pancreatic islet β-cells in mice causes hyperinsulinemia with increased islet mass and insulin secretion. *Biochemical and Biophysical Research Communications*, 461(4):630–635.

[247] Wang, Y. and Sul, H. S. (2006). Ectodomain Shedding of Preadipocyte Factor 1 (Pref-1) by Tumor Necrosis Factor Alpha Converting Enzyme (TACE) and Inhibition of Adipocyte Differentiation. *Molecular and Cellular Biology*, 26(14):5421–5435.

[248] Wang, Y. and Sul, H. S. (2009). Pref-1 regulates mesenchymal cell commitment and differentiation through Sox9. *Cell Metabolism*, 9(3):287–302.

[249] Wang, Y., Zhao, L., Smas, C., and Sul, H. S. (2010). Pref-1 interacts with fibronectin to inhibit adipocyte differentiation. *Molecular and Cellular Biology*, 30(14):3480–3492.

[250] Weidman, J., Maloney, K., and Jirtle, R. (2006). Comparative phylogenetic analysis reveals multiple non-imprinted isoforms of opossum Dlk1. *Mammalian Genome*, 17(2):157–167.

[251] Weitzmann, M. N. and Pacifici, R. (2006). Estrogen regulation of immune cell bone interactions. *Annals of the New York Academy of Sciences*, 1068(1):256–274.

[252] Wermter, A.-K., Scherag, A., Meyre, D., Reichwald, K., Durand, E., Nguyen, T. T., Koberwitz, K., Lichtner, P., Meitinger, T., Schäfer, H., Hinney, A., Froguel, P., Hebebrand, J., and Brönner, G. (2008). Preferential reciprocal transfer of paternal/maternal DLK1 alleles to obese children: first evidence of polar overdominance in humans. *European Journal of Human Genetics*, 16(9):1126–1134.

[253] Westerlind, H., Ramanujam, R., Uvehag, D., Kuja-Halkola, R., Boman, M., Bottai, M., Lichtenstein, P., and Hillert, J. (2014). Modest familial risks for multiple sclerosis: a registry-based study of the population of Sweden. *Brain : a journal of neurology*, 137(Pt 3):770–778.

[254] Xu, W., Wang, Y., Zhao, H., Fan, B., Guo, K., Cai, M., and Zhang, S. (2018). Delta-like 2 negatively regulates chondrogenic differentiation. *Journal of cellular physiology*, 233(9):6574–6582.

[255] Yanai, H., Nakamura, K., Hijioka, S., Kamei, A., Ikari, T., Ishikawa, Y., Shinozaki, E., Mizunuma, N., Hatake, K., and Miyajima, A. (2010). Dlk-1, a cell surface antigen on foetal hepatic stem/progenitor cells, is expressed in hepatocellular, colon, pancreas and breast carcinomas at a high frequency. *The Journal of Biochemistry*, 148(1):85–92.

[256] Yevtodiyenko, A. and Schmidt, J. V. (2006). Dlk1 expression marks developing endothelium and sites of branching morphogenesis in the mouse embryo and placenta. *Developmental Dynamics*, 235(4):1115–1123.

[257] Yin, D., Xie, D., Sakajiri, S., Miller, C. W., Zhu, H., Popoviciu, M. L., Said, J. W., Black, K. L., and Koeffler, H. P. (2006). DLK1: increased expression in gliomas and associated with oncogenic activities. *Oncogene*, 25(13):1852–1861.

[258] Zacharioudaki, E. and Bray, S. J. (2014). Tools and methods for studying Notch signaling in Drosophila melanogaster. *Methods (San Diego, Calif.)*, 68(1):173–182.

[259] Zaucker, A., Mercurio, S., Sternheim, N., Talbot, W. S., and Marlow, F. L. (2013). notch3 is essential for oligodendrocyte development and vascular integrity in zebrafish. *Disease Models & Mechanisms*, 6(5):1246–1259.

[260] Zhang, H., Nøohr, J., Jensen, C. H., Petersen, R. K., Bachmann, E., Teisner, B., Larsen, L. K., Mandrup, S., and Kristiansen, K. (2003). Insulin-like growth factor-1/insulin bypasses Pref-1/FA1-mediated inhibition of adipocyte differentiation. *Journal of Biological Chemistry*, 278(23):20906–20914.

[261] Zhang, J. and Jiao, J. (2015). Molecular Biomarkers for Embryonic and Adult Neural Stem Cell and Neurogenesis. *BioMed research international*, 2015(1):727542–14.

[262] Zhu, N.-L., Asahina, K., Wang, J., Ueno, A., Lazaro, R., Miyaoka, Y., Miyajima, A., and Tsukamoto, H. (2012). Hepatic stellate cell-derived delta-like homolog 1 (DLK1) protein in liver regeneration. *The Journal of biological chemistry*, 287(13):10355–10367.

A Appendix

A.1 Sequences used in evolutionary analysis

A.1.1 Protein sequences used for DLK1

Human DLK1

MTATEALLRVLLLLLAFGHSTYGAECFPACNPQNGFCEDDNVCRCQPGWQGPLCDQCVT-
SPGCLHGLCGEPGQCICTDGWDGELCDRDVRACSSAPCANNGTCVSLDDGLYECSCAP-
GYSGKDCQKKDGPCVINGSPCQHGGTCVDDEGRASHASCLCPPGFSGNFCEIVANSCTP-
NPCENDGVCTDIGGDFRCRCPAGFIDKTCSRPVTNCASSPCQNGGTCLQHTQVSYECLCK-
PEFTGLTCVKKRALSPQQVTRLPSGYGLAYRLTPGVHELPVQQPEHRILKVSMKELNKK-
TPLLTEGQAICFTILGVLTSLVVLGTVGIVFLNKCETWVSNLRYNHMLRKKKNLLLQYNS-
GEDLAVNIIFPEKIDMTTFSKEAGDEEI

Mouse DLK1

MIATGALLRVLLLLLAFGHSTYGAECDPPCDPQYGFCEADNVCRCHVGWEGPLCDKCV-
TAPGCVNGVCKEPWQCICKDGWDGKFCEIDVRACTSTPCANNGTCVDLEKGQYECSCTPGF-
SGKDCQHKAGPCVINGSPCQHGGACVDDEGQASHASCLCPPGFSGNFCEIVAATNSCTP-
NPCENDGVCTDIGGDFRCRCPAGFVDKTCSRPVSNCASGPCQNGGTCLQHTQVSFECLCKPPFMG-
PTCAKKRGASPVQVTHLPSGYGLTYRLTPGVHELPVQQPEQHILKVSMKELNKSTPLL-
TEGQAICFTILGVLTSLVVLGTVAIVFLNKCETWVSNLRYNHMLRKKKNLLLQYNSGEELAVNI-
IFPEKIDMTTFNKEAGDEEI

Cow DLK1

MAATAALLPALLLLLAFGRSAHGAECFPACHPENGFCDDDSVCRCQPGWQGPLCDQCVTF-
PGCVNGLCVEPWQCICKDGWDGHLCDLDIRACTSTPCANNGTCLNLDDGQYECSCAPGF-
SGKDCQEMDGPCVVNGSPCQHGGSCVDDEGRAPHAVCLCPPGFSGNFCEIVTNSCIP-
NPCENQGICTDIGGDFRCRCPAGFMDKTCSRPVNTCTSEPCLNGGTCLQHSQVSFECLCK-
PAFTGPRCGRKRAAGPQQVTRLPSGYGLTYRLTPGVHELPVPQPEHRVLKVSMKELNKST-

PLLSEGQAICFTILGVLTSLVVLGTMGIVFLNKCEAWVSNLRYNHMLRKKKNLLLHYNS-
GEELAVNIVFPEKIDMTTFTKEAGEEEI

Dog DLK1

MTATAALLPVLLLLLAFGHSVHGAECFPACHPQNGFCEDDNVCRCQPGWQGPLCDQCVTF-
PGCVNGLCVEPWQCICDDGWDGNLCDIDIRACASAPCANNGTCVNLDASHYECSCAPGF-
SGKDCQKKDGPCVINGSPCQHGGSCVDDEGRASHASCLCPPGFSGNFCEIVANSCTPN-
PCENQGICTDIGGDFRCRCPAGFVDKTCSRPVSNCASDPCLNGGTCLQHTQVRYECLCK-
PEFTGPICGRKRAPSPQQVTRLPSGYGLTYRLTPGVHELPVPQPEHRILKVSMKELHKNT-
PLLSEGQAICFTILGVLTSLVVLGTMGIVFLNKCEAWLSNLRYNRMLRQKKNLLLHYNS-
GEDLA VNIIFPEKIDMTTFSKEAGEDDI

Elephant shrew DLK1

MIVTAVLPRVLLLLLAFGHSTHGDDTNCSPACHPVHGSCEDDNVCRCQPGWQGPLCD-
HCVPFPGCVNGICFEPWQCVCNQGWEGHLCDIDARPCSSNPCANNATCENLEVGGYK-
CACVPGFQGDRCEEKRPGPCVINGSPCQHGGTCVDDEGRASHASCLCPPGFSGIFCEIVAN-
SCTPNPCENDGVCTDIGGDFRCRCPPGFIDKTCSRQVTSCASSPCLNGATCLQHGQVSYE-
CLCKPDFTGPTCAKRRAAGPPQSSLPSSYGLTYRLTPGVPQPEHRILKVSMKEFNKSSPIFTEGQAVCFTI
GVLTGLVVLATVGIIFINKCEAWVSSLRYSHMLRKKKSLLLQASSGEDLAVNIIFPEKIHMT-
TFNKEAGEEEI

Nine banded armadillo DLK1

MTATGALLPVLWLLLAFGPRAHGADCYPPCHPLNGFCDDDDVCRCHPGWDGPQCND-
CLPDPECVNGICYDEPGQCVCDDGWDGKFCDIDTRACISGPCANNGTCVNIEKGHYTC-
SCPPGYSGRVCEKKIGPCVVNGSPCQHGGTCVDDEGRASHASCLCPPGYSGNFCEILAASCVP-
NPCENNGVCTDIGGDFRCRCPPGFVDKTCSRPVTLCSSSPCQNGGTCLPHSQVSYECLCKPGFT-
GLTCAKKRPSGAQQVTRVPSGYGLTYRLTPGVHELPVPQPEHRILKVSMKELNRSEPLLSEGQAICFTVL
GVLTGLVVLGTVGIVFLNKCEAWVSNLRYGHLLRKKKNLLLHYNSGEDLAVNIIFPEKID-
MATFSREAGEDDV

Opossum DLK1

MFALGSFLLLCLLGPPFGFFSALGLECEVDCHRDRGICEKDLCRCRPGWQGPLCNECVTF-
PGCLHGSCSLPWQCICEDGWIGSLCDIDLQLCAAKPCPKNGTCTASEEGGSSCSCAPSSS-
GRNCHFKEGPCVINGSPCQNGGACIDDNGLASYTSCLCPDGFSGNFCELNMNSCDPN-
PCENGGMCTDIGGDFHCRCPLGFMDKTCGRPVGDHCASGPCEHGGTCVPQARGGFE-

CLCKPEFSGPTCNHGHPNHSHPGPKTKRGPGLSDQFVPETQGRIATHQPSHRMLKITM-
RELTKNSKPLLNESQAICFTILGVLTCLVVLGTISIVFFNKCEVWLSNAKYSRLLRKKKN-
LLLRYSNGDEHTINIILPEKMNLKSYSKCLNEI

Tammar wallaby DLK1

MFAPGSWLLLCVLGPPLCFFSALGLECEVDCHPDRGICDKDQCRCRPGWQGPLCNECVPF-
PGCLHGSCSLPWQCICEDGWIGSLCDIDLQLCAAKPCHKNGTCTGSEEGGSSCSCVPGSS-
GRNCHLKEGPCVINGSPCQNGGACIDDNGLASYTSCLCPEGFSGNFCELNMNSCVPN-
PCENGGVCTDIGGDFRCRCPLGFMDKTCSRRVGDHCASGPCEHGGTCVPHARGGFE-
CLCRPEFSGPTCNHGHPGTKTKRDPGLADQLPPETQGKIATHQPNHRMLKITMRELTKN-
SKPLLNESQAICFTILGVLTCLVVLGTVSIVFFNKCEVWLSNAKYSRLLRKKKNLLLRYS-
NGDEHTINIILPEKMNLKSYSKCLNEI

Tasmanian devil DLK1

MFAPESLLLLCVLGSPFCFFSALGLECEVSCHPDRGICDKDQCRCRPGWQGPLCNECVSF-
PGCLHGICSLPWQCICEDGWIGSLCDIDLQLCAAKSCHKNGTCTGSEESGSRCSCAPGSS-
GRNCRFKEGPCVINGSPCQNGGACIDENGLASYTSCLCPEGFSGNFCELDMNSCVPN-
PCENGGVCTDIGGDFRCRCPLGFMDKTCSQHVVDHCASGPCEHGGTCVPHARGGFE-
CLCRPEFSGPTCNHGHPNHSHPGTKTKRGPGLPDQFSPETQGRLAAHQPNHRMLKITM-
RELTKNSKPLLNESQAICFTILGVLTCLVVLGTISIVFFNKCEIWLSNAKYSRLLRKKKNSLL-
RYSNGDEHTINIILPEKMNLKSYSQCLNEI

Platypus DLK1

MEGSAEPRLLCAFLLPLALSAAAQGIACKPGCHPTNGFCANPNECRCQPGWRGPLCTE-
CIPFPGCLHGGCTLPWQCVCQEGWVGSLCDIDTHPCSATPCTNNSTCIETGDGGYVCLCGPGFT-
GKNCHLRKGPCIINGSPCQNGGACVDGDGSAPHASCLCPSGFTGHFCELDADDCHPN-
PCAHGGACTDIGRDFRCHCPTGFTGKSCGRRLPACLDSVGGPGLECVCPHGLSGPTC-
AHFGHNSTGPSRSPERGEGPGDPPAQEALRGASGHHQERRVLKISLKEVIRHADPWLSH-
SQVTCLIVLGLLTCLVVLGTTAIVFYSKCETWLANAKYSRLLRKKKRRLMTSNNGETLSVNI-
IFPEKVKLTSYSTCSAAM

Chicken DLK1

MRLRAAGLLGCCCCCCCLLPLVLPAAPGVSCKAGCHPVNGFCEFPSECRCLPGWQGAL-
CNQCVPFPGCLHGSCVKPWQCICEEGWVGSLCDIDIQPCSAKPCTNNSTCIETGDGGY-
ICLCAQGFTGKNCHLRKGPCIINGSPCQNGGTCIDDNGFAPHASCLCPSGFAGNFCEIDRD-

DCESNPCENGGTCTDIGAGFSCLCPHGYTGKLCSSRVTFCASDPCENGGTCKEHPQG-
GFKCICKPEFVGATCKHASKNTSLSAVNIGTKNMQNYKIPPKAHHRSVHQEHEILKITMKE-
TIQNADLLLSKSQVICFVVLGLLTCLVVLGTTGIVFFSKCEMWLANAKYSHLLRKKKN-
FLLKSSNGENLSVNIIFPEKIKLTNYTKNYTAI

Anole lizard DLK1

MHLCLWRGLCALLLACLPLAQGTDCKPGCHPVNGFCEVSNECRCRSGWQGPLCDQCIPF-
PGCLHGTCVKAWQCMCEEGWIGSHCDTDVHPCASKPCTSNSSTCVETGNGGYICLCA-
EGYTGKSCHMKKGPCIVNGSPCQHGGTCVDDDGSAPHASCLCLPGFTGNFCEIDIDD-
CEPNPCENGGTCTDIGRGFHCHCPMGFSGALCSSHVSACTSNPCQNGGICRVHPSRGFE-
CRCKPHFVGVTCASADRNKSLNGEVKHRLNHHSHMRVHHKPVHAQEREVLTIKETIEN-
RQPFLNKNQMICFMVLGLLTCLVVLGTTGIIFFSKFERWLANAKYSQLVRKERDDFLKA-
NEGENLSVKIIFPDQTEE

Chinese soft shell turtle DLK1

MDFRAATLNCCCFALVLPVSQGVACKPGCHPVNGFCEVPSECRCQPGWQGALCNQCVPF-
PGCVHGSCAKPWQCVCEEGWVGSLCDIDIHPCSSKPCTNNATCIETGDGGYICLCAKGFT-
GKNCHLKKGPCIINGSPCQNGGTCVDDNGFSAHASCLCLPSFSGNFCEIDIDDCEPNPCD-
NGGTCTDIGRGFNCHCPIGYMGQSCNSHVLFCASSPCENGGTCHEHPGGRFECLCKPE-
FVGVTCTYPSRNTSLHGMNTEAKTGQRYNLPPNAHPKSAHHQEHKVLKITMKETIQN-
TEPLLNKSQLICFIVLGLLTCLVVLGTTAIVFFSKCEIWLANAKYSHLLRKKKNCFLQSNNGENLSVNI-
IFPEKIKLTNYTKNYTDI

Western clawed frog DLK1

MELTASCILCLFLSRFITTETKEIACMPGCHPVNGFCESQGECRCRTGWKGQFCDQCIPF-
PACMHGSCTKPWQCICEEGWVGSLCDIDVHPCAAKPCSSNSTCIETGDGGYICLCSLGYT-
GKNCLLKKGPCSTNGSPCQNGGKCTDNNGFASYASCQCPPGFIGNYCEIQIDIDDCNPN-
PCRNGGSCTDIGSGFHCHCPLGFSGQFCNDLTPLCSSNPCANGGTCYQIGEKFQCFCQP-
KYTGTTCSFPHRNMSLHLYERRNSLPSYHKSPQHEVLKITVKETIQNVDPLLNKSQVIC-
FIVLGLLTCLIVLITTGIVFFSKCETWFANAKYSRLLRKKKNIYMQRSRGEDRDVKIIFPEGVK-
FEDCCRDYAST

Ceolacanth DLK1

MEGTVIPLSCVAVVSESDLILYYRIDCKPGCHSVNGYCEKPGECRCNEGWRGALCNKCVRF-
PGCLHGSCNKPWQCVCEEGWVGSLCDIDIHPCAVRPCANNSTCIETRDGGYICVCAQ-

GYTGKNCHQKKGPCYTSGSPCQNGGTCVDGNGFAHYTSCMCPPGFTGDFCEIRNND-
CNPSPCENGGVCTNIGSEISCLCPSGYIGPSCSTRVIACLSDPCENGGTCLEHPGGRFNCI-
CKPEFVGDICSHLKRNMSRFVMNTEVKHKQHHNLHPNVFHKSTHQQEHEVLKITLKETVQHS-
GILLNKSQVICFIVLGLLTCLVVLVTTGIVFFSKCEMWLANAKYSHLIRKQRNRFMKSNS-
GEELSVNIIFPEKIKLTNYSKSYTSI

Zebrafish DLK1

MSVLLRLGFCFLLLFCCAAAQGPDCGAGCHRHHGFCEQSGECRCKSGWRGAVCDQCVP-
SADCVHGWCESPGECICESGWSGARCDRDVRPCSSQPCSADSRCVDAAGGRGHVCI-
CTATHCRTEETHCTVNGSLCQNGGSCVSSSSSFNTSSSSSNTSSSPSSSSSSSCLCPAGFT-
GSLCELQSAVCKSSVCVNGGRCVRRGLSYRCVCARRFSGSSCERHRPRVKAPQQHHTALHK-
PLETPGALASRSQLICFSVLALLTVLVVLGSTAIVFFQRCEVWMANVRYRQLVAQQRELIQDQATVNI
ILPEKIKLSSYSRHYTSI

Medaka DLK1

MMMHLIWVVFILSVAGMVKGWECSAGCSPENGFCERQGKCRCKPGWEGENCDRCIPF-
PGCLHGSCEKAWQCICKEGWVGSLCDQDTRLCSSRPCSSNATCVETGEGGYMCICPQGFAGKD-
CHLKKQLCLENGSPCQNGGTCVDASGSAASPFCSCPSGFSGDFCEIGVDSCQPNPCLNYGNCTNHGI
SGFTCNDSTSSSSCAGRPCSNSGTCVRQLDGTFQCVCQKGFAGPTCSLRHRPKSRNKLL-
GARPVEHHMLALAPQHYSLPAHAFHKLLKPPDRDLLKITLKETVHSSGVLVTHGQLICFGM-
LALLTCLVILGTTGIVLFGRCETWLANAKYSQLVRQQREHLLREVGSPSQEEPEHSVNI-
ILPEKIRLSSFGRHYTSI

Australian ghost shark DLK1

MAHHSAASVLVVSLLLPLLTGTRTQGTECKPDCHPLHGFCQDTGECRCQSGWQGDL-
CDQCTPIPGCLHGSCTKPWQCCCEEGWSGILCDTAPHTCSSEHPCANNSTCIESEGGGYR-
CICGEEFTGNHCQLRKGNFCINGSLCQNGGSCIDGNGFGSQASCLCLKGFTGVLCETK-
ISDCDSNPCANNGTCTDLVSGYSCLCPLGFTGGSCDYLITSCLSHPCKNGGTCHDLPEG-
GFDCACLPGYEAETCHEHISSKHDTKQNISKHVRVSWVRHGKLFNPPLHAFHKPTHHQGNEM-
LKITVKETIHTSNSLLNRSQVICFVMLGLLTCLVILGTTLIIFFSKCKMWMANAKYRQYL-
RKQKNHFLNDEETSVKIIFPDMSKLTNYRKSYISM

A.1.2 Protein sequences used for DLK2

Human DLK2

MPSGCRCLHLVCLLCILGAPGQPVRADDCSSHCDLAHGCCAPDGSCRCDPGWEGLHCER-
CVRMPGCQHGTCHQPWQCICHSGWAGKFCDKDEHICTTQSPCQNGGQCMYDGGGEY-
HCVCLPGFHGRDCERKAGPCEQAGSPCRNGGQCQDDQGFALNFTCRCLVGFVGARCEVN-
VDDCLMRPCANGATCLDGINRFSCLCPEGFAGRFCTINLDDCASRPCQRGARCRDRVHDFD-
CLCPSGYGGKTCELVLPVPDPPTTVDTPLGPTSAVVVPATGPAPHSAGAGLLRISVKEVVR-
RQEAGLGEPSLVALVVFGALTAALVLATVLLTLRAWRRGVCPPGPCCYPAPHYAPACQDQEC-
QVSMLPAGLPLPRDLPPEPGKTTAL

Mouse DLK2

MPSGCRCLNLVCLLCILGATSQPARADDCSSHCDLAHGCCAPDGSCRCDPGWEGLHCER-
CVRMPGCQHGTCHQPWQCICHSGWAGKFCDKDEHICTSQSPCQNGGQCVYDGGGEY-
HCVCLPGFHGRGCERKAGPCEQAGFPCRNGGQCQDNQGFALNFTCRCLAGFMGAHCEVN-
VDDCLMRPCANGATCIDGINRFSCLCPEGFAGRFCTINLDDCASRPCQRGARCRDRVHDFDYL-
CPSGYGGKTCELVLPAPEPASVGTPQMPTSAVVVPATGPAPHSAGAGLLRISVKEVVR-
RQESGLGESSLVALVVFGSLTAALVLATVLLTLRAWRRGICPTGPCCYPAPHYAPARQDQEC-
QVSMLPAGFPLSPDLPPEPGKTTAL

Cow DLK2

MPSGCRCLHLVCLLCILGAPVKPARGNDCSSLCDLAHGCCAPDGSCRCDPGWEGLHCER-
CVRMPGCQHGTCHQPWQCICHTGWAGKFCDKDEHICTTQSPCRNGGQCVYDGGGDY-
HCVCPPGFHGRDCERKAGPCEQAGSPCRNGGQCQDDQGFALNFTCRCLAGFMGARCEVN-
VDDCLMRPCANGATCLDGINRFSCLCPEGFTGRFCTINLDDCASRPCQRGARCRDRVHDFD-
CLCPSGYGGKTCELVLPVPGPAATADSPPGPTLAVLVPATGPIPHSAGAGLLRISVKEVVR-
RQEAGLGEPSLVAVVVFGAVTAALVLSTVLLTLRAWRRGFCPPGPCCYPAPHYAPARQDQEC-
QVSMLPTGLPLPPDLPPEPGKTTAL

Dog DLK2

MPSGCRCLHLVCLLCILGAPVQPAGADDCSSHCDLAHGCCAPDGSCRCDPGWEGLHCER-
CVRMPGCQHGTCHQPWQCICHSGWAGKFCDKDEHICTTQNPCRNGGQCVYDGGGEY-
HCVCPPSFHGHDCERKSGPCEQAGSPCRNGGQCQDDQGFALNFTCRCLVGFVGSRCEVN-
VDDCLMRPCANGATCLDGINRFSCLCPEGFAGRFCTVNLDDCASRPCQRGARCRDRVHDFD-
CLCPSGYGGKTCELILPVSEPATIVDIPLGTTSALAVPATGPVPHSVGAGLLRISVKEVVR-

RQEAGLGVSSLVAVVVFGALTTALVLSTMLLTLRAWRRGVCPPGPCCYPAPHYAPACQDQEC-
QVSMLPAGLPLSPDLPPEPGKTTAL

Elephant DLK2

MPSGCRCLHLVCLLCILGPPGQPARADDCSSHCDLAHGCCAPDGSCRCDPGWEGLHCER-
CVRMPGCQHGTCHQPWQCICHSGWAGKFCDKDEHICTTQSPCQNGGQCMYDGGGEY-
HCVCPPGFHGHDCERKAGPCEQAGSPCQNGGQCQDNQGFALNFTCRCLAGFVGARCEVN-
VDDCLMRPCANGATCLDGINRFSCLCPEGFAGRFCTINLDDCASHPCQRGARCRDRVHDFD-
CLCPSGYGGKTCELVLPVPDPFTTADLPLGPTSAVVVPTTGPVPHSAGAGLLRISVKEVVR-
RQEAALAESSLVAVVVFGALTAALVLATGLLTLRAWRRGVRPPGPCCYPIPHYAPARQDQEC-
QVSMLPAGLPLPPDLPGEPGKTTAL

Opossum DLK2

MPSGCRCLQLVSLLWILGASGQPTHADDCSSHCDLAHGCCEPDGTCRCDPGWEGLHCE-
QCVRMPGCQHGTCHQPWQCICSNGWAGKFCDKDEHICTKQPPCQNGGKCVYEGDGEY-
HCVCPPGFHGHNCERKTGPCEHAGSPCRNGGQCQDDQGFAENFTCRCLAGFVGPRCEVN-
VDDCLMRPCANGATCHDGINRFSCHCPKGFAGRFCTVNLDDCASRPCQHGARCRDRVHDFD-
CLCPDGFGGKTCEIVLPALDLPTEPDSAPGPTPAAVVPFTVPAPFSVGAGLLRISVKEVVR-
RQEAGIGDSSLIVLFIFGAITITGVFGTGLVIFWVRRHGHCPTGPCCCPYHQYAPPPERHDQEC-
QVSMLPAGISPPPDFPSELGKTTAL

Tasmanian devil DLK2

MPHGCRCLQLVSLLWILGASGQPTPANDCSSHCDLAHGCCEPDGTCRCDPGWEGLHCER-
CVRMPGCQHGTCHQPWQCICHNGWAGKFCDKDEHICTKQPPCQNGGKCVYEGDGEY-
HCVCPPGFHGHNCERKTGPCEHAGSPCRNGGQCQDDQGFAKNFTCRCLAGFVGPRCEVN-
VDDCLMRPCANGATCHDGINRFSCHCPEGFAGRFCTINLDDCASRPCQHGARCRDRVHDFD-
CLCPDGYGGKTCEIALPALDLPTEPESAAGSTPAAVVPFTVPAPFSVGAGLLRISVKEVVR-
RQEAGLGESSLLVLVIFGVLTATLVLTTGLLIFWAWCHGHCPAGLCCYPFRQYAIPPEQHDQEC-
QVSMLPAGISPPPGSPPEPGKTTAL

Chicken DLK2

MLRSFCLQLMSLLWILLAHHQLAQGDDCSEHCNLAHGSCDQDGKCRCDPGWEGDYCEECVRMPG
CLHGTCHQPWQCICHSGWAGKFCDKDVHICEHQSPCQNGAQCIYDRDGDYSCLCPEGFHGKD-
CEMKAGPCEKAGSPCKNGGQCQDENGFATNFTCRCLAGFVGALCEHDVDDCLMRPCAN-
GATCHDGINRFSCQCQVGFEGRFCTININDCASQPCKNGAKCYDRINDYDCLCSDRFT-

GKTCEISIPEPTWAPPYHPANHESSWAMRSTTSEMPEVTQPEPVRTAVTGRRVANHSEKVPGGGLLK-
ISVKEVVTQRDSGLSEAQLVTVLVFGVLTAVLVLITVLLILRNWQRGRQRSNWCQSPSQAARK-
LQDQECQVGMLNTVLIEPRKTTEL

Anole lizard DLK2

MLRSFYLQLMSLLWILVAHHHFTQGDDCSDHCNLAHGSCEDGKCRCDPGWDGASCE-
QCVRMLGCIHGTCHQPWQCICQSGWAGKFCDKDVHICEHQPPCQNGAECIYDRDGEYSCLCLEEFHGE
CELKTGPCEKSGFPCKNGGLCQDKNGFASNYTCKCLAGFTGAHCEIDVDDCLMQPCAN-
GATCLDGMNRFSCQCQAGFEGRFCTINIDDCANQPCRNGAKCYDRINDFDCLCPEGFVGK-
TCELPAPEPTWVTAFEPGHKDNDNAVTSIDPWTAQSDPARTAVTGKRITNYSEKSNGGGLLISVKEVVTQ
GLSQSQLILLLVFGLLTMLLVFVTVLMVLLKNWQRGNQRCQSPSQSARKLQDQECQVGML-
STVLIEPRKTTEL

Chinese soft shell turtle DLK2

MLRSFCLQLMSLVWILLAHHHLAQGDDCSEHCNLAHGSCDQDGKCRCDPGWEGEYCE-
QCVRMPSCLHGTCHQPWQCICHNGWAGKFCDKDVHICEHNPPCQNGAGCVYDGDGEYSCLC-
SEGFHGKDCERKTGPCEKAGFPCRNGGQCQDENGFAKNFTCRCLAGFVGALCEEDVD-
DCLMRPCANGAICQDGINRFSCQCQVGFEGRFCTININDCASHPCKNGAKCYDRINDFD-
CVCPEGFTGKTCEASAPEPTWVPFYLSANKENNDALKSTTSEYLWVTQPEPVRTVVT-
GKRVANHSEKASGGGLLKISVKEVVTQRDTGLSESQLVTVLVFGTLTAALVLVTILLML-
RNWQRGRRRSNWCQSPSQAARKLQEQECQMGMLNTVMVEPRKTTEL

Zebrafish DLK2

MKLAVVLLLCGCCVLFKHNCEAQVLFSSEETSPTPSASNCTCEIGHGKCAENGDCRCDPG-
WGGPMCDDCVRMPGCVHGTCHQPWQCSCMDGWAGRFCDKDVYVCSRQQPCHNGATCELS-
DSGDYSCLCPEGFHGRDCELKAGPCQKTKSPCKNGGLCEDLGGYAPELSCRCLAGFT-
GARCETNMDDCLMRPCANGATCLDGVNRFSCLCPAGFTGRFCTINLDDCASQPCLNG-
GRCIDRVSNFQCVCPLGFTGRTCELVSPTKSPLKAEHNPNMTLKPSHWTTPSGGEERL-
LKITFRTPAGGEGLSEFQLIVLLVLGGMTLAVVGLTAALVLRGYFQDRSASCQCRPAHRTQRKHSQQECE
ISFLQSPEKKRLNTDVI

Medaka DLK2

MAPVRAEGVLLLLSCWFVLHIQSSAGQGSDCSCNMTNSRCDESGICRCDPGWEGEHC-
DRCVLMPGCVHGSCQQPWQCTCEPGWGGRFCDKDLSVCSNQQPCRNGATCAMKDS-
GDFTCLCPQGYHGHLCQRKSGPCHQIRSPCKNGGLCEDADGFAADLTCRCLAGFTGS-

FCETDIDDCLLKPCANDAICLDGINRFSCICPSGFTGRFCTVNLDDCASQPCLNGGRCLD-
LAGGFRCICQLGYMGNTCEMSLSSPNWTTKGEKGKGKRSSNITQHGNRLMKVTVSDR-
GIASLSDIQLIVVVVLGGVTLVAVALTSGLVLWGRCQNCSYTAGWSPPCSQGAERSRRRGQSETQQC-
QISFLNSVEPQKKLNLEAV

Coelacanth DLK2

MRPSGRPALQLLHFVWMLLLQRPVRGADCKSSCNLAHGRCDVNGDCRCDPGWEGDSCER-
CVRMPGCLHGTCHQPWQCICLSGWAGRFCDKDVHICEHQRPCQNSARCINDREGDYSCVCPDGFH
PCELAGSPCQNGGTCLDNNGYADAFACRCLAGFVGDLCELDVDDCLMRPCANGATCHDG-
INRFSCKCPAGFEGRFCTSNLDDCASQPCRNGGKCYDRVNDFDCVCPEGYAGKSCATVLEPQREE-
QVQTAPRNAQRVNYFTPESATQVPPQGTRPQPIGKPDAARRKGNQSEALSGERRAGGLLK-
ISVKEVVAQEESGLAETRFVILAVFGACTLLLALVTATLVLWSHWQGRPSSEAQRPDSAS-
RPEKKQLNAEEYESHLPLRHNQLTQKLNSFDVL

Australian ghost shark DLK2

MRGIRDWGLPLWGLACFLCSPSMAAGAEDVQCNPGCNLLHGRCESSECRCDPGWEGEL-
CERCVRSPGCVHGTCHQPWQCICQTDWAGRFCDKDIHACTHQQPCQNGGSCFDTGEGE-
HWCSCPDGFYGKNCELRAGPCTKSRSPCKNGGTCLDRDGFADTLTCRCLAGFVGPRCEED-
VDDCLMRPCANGATCRDGVNRFSCICPQGFEGRFCTVNWDDCTSGPCQNGGRCYDR-
VADFDCVCLKGYSGKTCSLPVPQWRKERPALSRRDPGITIPQPDHATRQGLAALPAASP-
TQPVREQERLLKVEVKELLSEPSSALAHSQIVGLSVFGALTALLVSVTVVVMLLCRRQEEP-
SRKPPRSGERGQAEGAISFLQPPAPESRKELYLDLM

Ciona DLK2

MSIKLILLLCSVAIGLAVGKPTDTTTCPSRCNLSHGFCNPRQQCTCFPGWEGPECNQCSTLIG-
CLHGSCDRPGQCNCDVGWGGRKCDRDLQYCERHRPCRNGATCINNLLGGFKCICPT-
GLTGTTCQETATTTPPITPRSGGKPRCSNGGTCIRGNAELGCESCRCPTGFTGQLCEQIVRM-
CVMRPCANGGKCQDVIGNFRCDCAHGYRGRYCTEDINECTVLGRHACENGGTCVN-
RFGGYTCACSDGYYGSRCQSKIIQIQARVTTTVKPTTTTTTTTTTEATTTKSTTETLKEIVVVPN-
LKKPFRKNIKVTHIVRQVEVETSNGDMTFIRDVVDHQGPNSAENEAQSSVTTVQALT-
FAFLGVAIALFIGIVIFMWIHCSKKGRNLRQRCTGESPTEETPMNENSREPSIVKTRHASYSP-
PQYVLEECQPKPGYPMRSVALPSDDREPIDCLYVALPNNSTPDVASMANRVLNSPSLPAY

A.1.3 Coding sequences used for *Dlk1*

Human *Dlk1*

ATGACCGCGACCGAAGCCCTCCTGCGCGTCCTCTTGCTCCTGCTGGCTTTCGGCCACAGCAC-
CTATGGGGCTGAATGCTTCCCGGCCTGCAACCCCCAAAATGGATTCTGCGAGGATGA-
CAATGTTTGCAGGTGCCAGCCTGGCTGGCAGGGTCCCCTTTGTGACCAGTGCGTGAC-
CTCTCCCGGCTGCCTTCACGGACTCTGTGGAGAACCCGGGCAGTGCATTTGCACCGACG-
GCTGGGACGGGGAGCTCTGTGATAGAGATGTTCGGGCCTGCTCCTCGGCCCCCTGT-
GCCAACAACGGGACCTGCGTGAGCCTGGACGATGGCCTCTATGAATGCTCCTGTGC-
CCCCGGGTACTCGGGAAAGGACTGCCAGAAAAAGGACGGGCCCTGTGTGATCAACG-
GCTCCCCCTGCCAGCACGGAGGCACCTGCGTGGATGATGAGGGCCGGGCCTCCCAT-
GCCTCCTGCCTGTGCCCCCCTGGCTTCTCAGGCAATTTCTGCGAGATCGTGGCCAACAGCT-
GCACCCCCAACCCATGCGAGAACGACGGCGTCTGCACTGACATTGGGGGCGACTTC-
CGCTGCCGGTGCCCAGCCGGCTTCATCGACAAGACCTGCAGCCGCCCGGTGACCAACT-
GCGCCAGCAGCCCGTGCCAGAACGGGGGCACCTGCCTGCAGCACACCCAGGTGAGC-
TACGAGTGTCTGTGCAAGCCCGAGTTCACAGGTCTCACCTGTGTCAAGAAGCGCGCGCT-
GAGCCCCCAGCAGGTCACCCGTCTGCCCAGCGGCTATGGGCTGGCCTACCGCCTGAC-
CCCTGGGGTGCACGAGCTGCCGGTGCAGCAGCCGGAGCACCGCATCCTGAAGGTGTC-
CATGAAAGAGCTCAACAAGAAAACCCCTCTCCTCACCGAGGGCCAGGCCATCTGCTTCAC-
CATCCTGGGCGTGCTCACCAGCCTGGTGGTGCTGGGCACTGTGGGTATCGTCTTCCT-
CAACAAGTGCGAGACCTGGGTGTCCAACCTGCGCTACAACCACATGCTGCGGAAGAA-
GAAGAACCTGCTGCTTCAGTACAACAGCGGGGAGGACCTGGCCGTCAACATCATCTTC-
CCCGAGAAGATCGACATGACCACCTTCAGCAAGGAGGCCGGCGACGAGGAGATCTAA

Mouse *Dlk1*

ATGATCGCGACCGGAGCCCTCCTGCGCGTCCTCTTGCTCCTGCTGGCTTTCGGCCACAGCAC-
CTATGGGGCTGAATGCGACCCACCCTGTGACCCCCAGTATGGATTCTGCGAGGCTGA-
CAATGTCTGCAGGTGCCATGTTGGCTGGGAGGGTCCCCTCTGTGACAAGTGTGTAACT-
GCCCCTGGCTGTGTCAATGGAGTCTGCAAGGAACCATGGCAGTGCATCTGCAAGGATG-
GCTGGGACGGGAAATTCTGCGAAATAGACGTTCGGGCTTGCACCTCAACCCCCTGCGC-
CAACAATGGAACTTGCGTGGACCTGGAGAAAGGCCAGTACGAATGCTCCTGCACAC-
CTGGGTTCTCTGGAAAGGACTGCCAGCACAAGGCTGGGCCCTGCGTGATCAATGGTTCTC-
CCTGCCAGCACGGAGGCGCCTGCGTGGATGATGAGGGCCAGGCCTCGCATGCTTC-
CTGCCTGTGCCCCCCTGGCTTCTCAGGCAACTTCTGTGAGATCGTAGCCGCAACCAACAGCT-
GTACCCCTAACCCATGCGAGAACGATGGCGTCTGCACCGACATCGGGGGTGACTTC-
CGTTGCCGCTGCCCAGCTGGATTCGTCGACAAGACCTGCAGCCGCCCGGTGAGCAACT-

GCGCCAGTGGCCCGTGCCAGAACGGGGGCACCTGCCTCCAGCACACCCAGGTGAGCTTC-
GAGTGTCTGTGCAAGCCCCCGTTCATGGGTCCCACGTGCGCGAAGAAGCGCGGGGC-
TAGCCCCGTGCAGGTCACCCACCTGCCCAGCGGCTATGGGCTCACCTACCGCCTGAC-
CCCCGGGGTGCACGAGCTGCCTGTTCAGCAGCCCGAGCAACACATCCTGAAGGTGTC-
CATGAAAGAGCTCAACAAGAGTACCCCTCTCCTCACCGAGGGACAGGCCATCTGCTTCAC-
CATCCTGGGCGTGCTCACCAGCCTGGTGGTGCTGGGCACCGTGGCCATCGTCTTTCT-
CAACAAGTGCGAAACCTGGGTGTCCAACCTGCGCTACAACCACATGCTTCGCAAGAA-
GAAGAACCTCCTGTTGCAGTATAACAGCGGCGAGGAGCTGGCGGTCAATATCATCTTC-
CCCGAGAAGATTGACATGACCACTTTCAACAAGGAGGCTGGTGATGAGGAGATCTAA

Cow *Dlk1*

ATGGCCGCGACCGCAGCCCTCCTGCCCGCCCTCTTGCTCCTGCTGGCTTTCGGCCGCAGT-
GCCCATGGAGCTGAATGCTTCCCGGCCTGCCACCCTGAAAATGGATTCTGCGACGAT-
GACAGTGTGTGCAGGTGCCAGCCTGGCTGGCAGGGTCCCCTGTGTGACCAGTGCGT-
GACCTTTCCCGGCTGTGTGAACGGCCTCTGCGTGGAGCCATGGCAGTGCATCTGCAAG-
GACGGCTGGGACGGACACCTCTGTGACCTAGACATCCGGGCTTGCACCTCGACCC-
CCTGCGCCAACAACGGCACCTGCCTGAACCTCGATGACGGCCAGTACGAGTGCTC-
CTGCGCCCCCCGGGTTCTCAGGAAAGGATTGTCAGGAAATGGATGGGCCCTGCGTG-
GTGAATGGCTCGCCCTGCCAGCACGGAGGCAGCTGCGTGGACGATGAGGGCCGGGC-
CCCCCACGCTGTCTGCCTGTGCCCCCCTGGCTTCTCGGGCAACTTCTGCGAGATCGT-
GACCAACAGCTGCATCCCCAACCCGTGCGAGAACCAGGGCATCTGCACCGACATCGGGGGT-
GACTTCCGCTGCCGTTGCCCCGCCGGCTTCATGGACAAGACCTGCAGCCGCCCGGT-
GAACACCTGCACCAGCGAGCCGTGCCTCAACGGCGGCACCTGCCTGCAGCACTCCCAGGT-
GAGCTTCGAGTGTCTGTGCAAGCCCGCGTTCACCGGCCCCCGGTGTGGCCGGAAGCGCGCG-
GCGGGCCCCCAGCAGGTCACCCGTCTGCCCAGCGGTTACGGGCTGACCTACCGCCT-
GACCCCCGGGGTGCACGAGCTGCCGGTGCCGCAGCCCGAGCACCGCGTCCTGAAG-
GTGTCCATGAAGGAGCTCAACAAGAGCACTCCGCTCCTCTCCGAGGGACAGGCCATCT-
GCTTCACCATCCTGGGCGTGCTCACCAGCCTGGTGGTCCTGGGCACCATGGGCATCGTCTTC-
CTCAACAAGTGCGAGGCCTGGGTGTCCAATCTGCGCTACAACCACATGTTGCGCAA-
GAAGAAGAACCTGCTGCTGCACTACAACAGCGGGGAGGAGCTGGCCGTCAACATCGTCTTC-
CCGGAGAAGATCGACATGACCACCTTCACCAAGGAGGCCGGCGAGGAGGAGATCTGA

Dog *Dlk1*

ATGACCGCGACCGCAGCCCTCCTGCCCGTCCTCTTGCTCCTGCTGGCCTTCGGCCACAGT-
GTCCATGGAGCTGAATGCTTCCCGGCCTGCCACCCCCAAAATGGATTCTGCGAGGAT-
GACAATGTTTGCAGGTGCCAGCCTGGCTGGCAGGGTCCCCTGTGTGACCAGTGCGT-

GACCTTTCCCGGCTGTGTTAACGGACTCTGCGTGGAACCCTGGCAGTGCATTTGTGAC-
GACGGCTGGGACGGCAACCTGTGCGACATAGACATCCGGGCCTGTGCCTCGGCCC-
CCTGCGCCAACAATGGCACCTGCGTGAACCTCGATGCCAGCCACTACGAGTGCTCCT-
GCGCCCCTGGGTTCTCGGGCAAGGACTGTCAGAAGAAGGACGGGCCCTGCGTGAT-
CAATGGTTCCCCCTGCCAGCACGGAGGCAGCTGCGTGGATGATGAGGGCCGGGCCTC-
CCATGCCTCCTGCCTGTGCCCCCCTGGCTTCTCAGGCAATTTCTGCGAGATCGTGGC-
CAACAGCTGCACCCCCAACCCGTGCGAGAACCAGGGCATCTGTACGGACATCGGGGGC-
GACTTCCGCTGCCGATGCCCCGCCGGCTTCGTGGACAAGACCTGCAGCCGCCCCGT-
GAGCAACTGCGCCAGCGACCCGTGCCTCAACGGGGGCACCTGCCTGCAGCACACCCAGGT-
GAGGTACGAGTGTCTGTGCAAGCCCGAGTTCACAGGCCCCATCTGTGGCCGGAAGCGT-
GCCCCGAGCCCCCAGCAGGTCACCCGTCTGCCCAGCGGGTACGGGCTGACCTACCGC-
CTGACCCCCGGGGTGCACGAGCTGCCGGTGCCCCAGCCCGAGCACCGCATCCTCAAG-
GTGTCCATGAAGGAGCTCCACAAGAACACCCCCCTCCTCTCCGAGGGCCAGGCCATCT-
GCTTCACCATCCTGGGCGTGCTGACCAGTCTGGTGGTGCTGGGCACCATGGGCATCGTCTTC-
CTCAACAAGTGCGAGGCCTGGCTGTCCAACCTGCGCTACAACCGCATGCTGCGCCA-
GAAGAAGAACCTCCTGCTGCACTACAACAGCGGGGAGGACCTGGCCGTCAACATCATCTTC-
CCCGAGAAGATCGACATGACCACCTTCAGCAAGGAGGCTGGCGAGGACGACATCTAA

Elephant shrew *Dlk1*

ATGATCGTGACCGCAGTCCTCCCGCGCGTCCTCCTGCTCCTGCTGGCCTTCGGCCACAGCAC-
CCATGGTGATGATACTAACTGCTCCCCGGCCTGTCACCCGGTCCACGGGTCCTGCGAG-
GATGACAACGTTTGCAGATGTCAGCCCGGCTGGCAGGGCCCCCTGTGTGACCACTGCG-
TACCATTTCCTGGCTGTGTCAATGGGATTTGCTTCGAGCCCTGGCAGTGTGTTTGCAAC-
CAAGGCTGGGAGGGACACCTTTGTGACATAGATGCGCGCCCTTGCAGCTCCAACCC-
CTGTGCCAACAACGCCACCTGCGAGAACCTGGAGGTCGGAGGCTACAAGTGCGCCT-
GCGTCCCTGGCTTCCAAGGGGACCGCTGTGAGGAGAAGCGCCCCGGGCCCTGCGT-
CATCAATGGCTCCCCGTGCCAGCACGGAGGCACGTGCGTGGACGATGAGGGCCGGGC-
CTCCCACGCCTCCTGCCTGTGCCCCCCTGGCTTCTCAGGCATCTTCTGCGAGATTGTG-
GCCAACAGCTGCACCCCCAATCCGTGCGAGAATGATGGTGTCTGCACCGACATTGGGGGC-
GACTTCCGCTGCCGCTGCCCACCCGGCTTCATCGACAAGACTTGCAGCCGCCAGGT-
GACCAGCTGCGCCAGCAGCCCCTGCCTGAACGGGGCCACCTGCCTGCAGCACGGCCAGGT-
GAGCTACGAGTGTCTGTGCAAGCCCGACTTCACAGGGCCCACTTGTGCCAAGAGGCGGGCG-
GCGGGGCCCCCGCAGAGCAGCCTGCCCAGCAGCTACGGGCTCACCTACCGCCTGAC-
CCCCGGGGTGCCACAGCCCGAGCACCGCATCCTCAAGGTGTCCATGAAGGAGTTCAA-
CAAGAGCTCCCCCATTTTCACCGAGGGGCAGGCCGTCTGCTTCACCATCCTGGGCGT-
GCTCACCGGCCTGGTGGTGCTGGCCACCGTGGGCATCATCTTCATCAACAAGTGCGAG-

GCCTGGGTGTCCAGTCTACGCTACAGCCACATGCTCCGGAAGAAGAAGAGCCTTCT-
GCTGCAGGCCAGCAGCGGCGAGGACCTGGCGGTCAACATCATCTTCCCGGAGAAAATC-
CACATGACCACCTTCAACAAGGAGGCGGGCGAGGAGGAGATCTGA

Nine banded armadillo *Dlk1*

ATGACCGCGACCGGAGCCCTCCTGCCCGTCCTCTGGCTCCTGCTGGCCTTCGGCCCCAGGGC-
CCATGGAGCTGATTGCTACCCGCCTTGCCACCCCTTAAACGGATTCTGCGACGATGAC-
GACGTTTGCAGGTGCCATCCTGGCTGGGATGGCCCCCAGTGCAACGACTGCCTGC-
CCGATCCCGAATGTGTCAATGGAATCTGCTACGACGAGCCTGGGCAGTGCGTGTGC-
GATGATGGCTGGGACGGAAAGTTCTGCGACATAGACACCCGGGCTTGCATCTCCGGC-
CCCTGCGCCAACAACGGGACCTGCGTCAACATCGAGAAAGGCCACTACACGTGCTC-
CTGTCCCCCTGGCTACTCGGGGCGGGTCTGCGAGAAGAAGATCGGCCCCTGCGTG-
GTCAACGGCTCCCCTTGCCAGCACGGAGGCACCTGCGTGGACGACGAGGGCCGGGC-
CTCCCACGCCTCCTGCCTGTGCCCCCCGGGCTACTCGGGCAATTTCTGCGAGATCCTG-
GCCGCCAGCTGCGTGCCCAACCCCTGCGAGAACAACGGCGTCTGCACCGACATCG-
GCGGCGACTTCCGCTGCCGCTGCCCGCCCGGCTTCGTCGACAAGACCTGCAGCCGC-
CCGGTGACCCTGTGCTCCAGCAGCCCCTGCCAGAACGGGGGCACCTGCCTGCCGCACTC-
CCAGGTGAGCTACGAGTGTCTGTGCAAGCCCGGGTTCACGGGCCTCACCTGCGCCAA-
GAAGCGGCCGTCCGGCGCCCAGCAGGTCACCCGCGTGCCCAGCGGCTACGGGCTGAC-
CTACCGCCTGACGCCGGGGGTGCACGAGCTGCCCGTGCCGCAGCCCGAGCACCGCATC-
CTCAAGGTGTCCATGAAGGAGCTCAACCGCAGCGAGCCGCTGCTCAGCGAGGGCCAGGC-
CATCTGCTTCACCGTCCTCGGCGTGCTCACCGGCCTCGTGGTGCTGGGCACGGTGGGCATCGTCT
CTCAACAAGTGCGAGGCCTGGGTGTCCAACCTGCGCTACGGCCACCTGCTGCGCAA-
GAAGAAGAACCTGCTGCTGCACTACAACAGCGGCGAGGACCTCGCGGTCAACATCATCTTC-
CCCGAGAAGATCGACATGGCCACCTTCAGCAGGGAGGCCGGCGAGGACGACGTCTGA

Opossum *Dlk1*

ATGTTCGCCTTGGGATCCTTTCTGCTGTTGTGCCTTCTTGGGCCACCTTTTGGCTTCTTCTCT-
GCGCTAGGCCTTGAATGTGAGGTGGACTGTCACCGGGATAGAGGAATCTGTGAAAAG-
GACCTGTGTAGGTGTCGACCTGGTTGGCAGGGACCCCTGTGCAATGAGTGTGTTAC-
CTTTCCTGGTTGCCTACATGGAAGTTGTTCTCTTCCCTGGCAATGTATCTGTGAGGATG-
GCTGGATTGGGAGCCTCTGTGATATAGATCTCCAGCTGTGTGCTGCCAAGCCCTGC-
CCCAAGAATGGGACATGCACTGCTTCTGAAGAAGGTGGTTCCAGCTGCTCTTGTGC-
CCCAAGCTCTTCAGGAAGAAACTGTCATTTTAAGGAAGGACCTTGTGTTATTAATG-
GTTCTCCCTGCCAGAATGGAGGCGCTTGCATTGATGACAATGGCCTTGCTTCTTACAC-
CTCCTGCTTATGCCCAGATGGCTTCTCTGGCAACTTCTGTGAGCTGAACATGAACAGCT-

GTGACCCGAATCCATGTGAGAATGGAGGTATGTGCACTGACATTGGTGGGGACTTTCATTGTCGCT-
GTCCACTGGGGTTCATGGACAAGACTTGTGGTCGACCTGTGGGGGACCATTGTGCCAGTG-
GCCCCTGTGAGCATGGGGGTACTTGTGTGCCTCAAGCCAGAGGAGGCTTTGAATGC-
CTCTGCAAACCAGAATTCTCTGGACCCACTTGTAACCATGGCCACCCAAACCATAGC-
CACCCAGGACCCAAGACCAAGAGGGGTCCTGGGCTGTCTGACCAATTTGTCCCTGA-
GACTCAGGGCAGGATTGCCACCCATCAGCCCAGTCACAGAATGCTAAAGATCACCAT-
GAGGGAACTGACCAAGAATAGCAAACCTCTACTTAATGAAAGCCAGGCCATCTGCTTCAC-
CATCCTGGGGGTTCTGACATGCCTGGTTGTGCTGGGCACCATCAGCATTGTTTTCTTCAA-
CAAGTGTGAGGTGTGGCTCTCCAATGCCAAGTACAGTCGTCTCCTCCGTAAAAAAAA-
GAATTTGCTCCTCAGGTACAGCAATGGGGATGAGCATACCATTAACATCATCTTACCT-
GAGAAGATGAATCTGAAATCCTACAGTAAGTGCTTGAATGAGATATGA

Tammar wallaby *Dlk1*

ATGTTCGCCCCGGGATCCTGGTTGCTGTTGTGCGTTCTTGGGCCACCTCTTTGCTTCTTCTCT-
GCTCTAGGCCTGGAATGTGAGGTGGACTGTCACCCAGACAGAGGAATCTGTGACAAG-
GACCAGTGTAGATGTCGACCTGGTTGGCAGGGACCCTTGTGCAATGAGTGTGTGCC-
CTTTCCTGGCTGTCTACATGGAAGTTGTTCCCTGCCCTGGCAATGTATCTGTGAGGATG-
GCTGGATCGGAAGTCTCTGTGACATAGATCTCCAGTTGTGTGCTGCCAAACCCTGT-
CACAAGAATGGGACATGCACTGGTTCTGAAGAAGGTGGCTCCAGCTGTTCTTGTGTTC-
CTGGCTCTTCAGGAAGAAACTGTCATTTGAAGGAAGGACCTTGTGTTATTAATGGTTCTC-
CCTGTCAAAATGGAGGAGCTTGCATTGATGACAATGGTCTTGCCTCCTATACCTCCT-
GCTTGTGCCCAGAAGGCTTTTCTGGCAACTTCTGCGAACTGAACATGAACAGCTGT-
GTCCCAAATCCATGTGAGAATGGAGGTGTGTGCACTGACATTGGTGGGGACTTCCGTTGTCGCT-
GTCCGCTGGGGTTCATGGATAAGACTTGCAGCCGACGTGTGGGGGACCATTGTGCCAGTG-
GTCCCTGTGAGCATGGGGGTACCTGTGTGCCTCATGCCAGAGGAGGCTTTGAATGC-
CTCTGTCGACCAGAATTCTCTGGGCCCACTTGTAACCATGGCCACCCAGGAACCAA-
GACCAAGAGAGATCCTGGGCTAGCTGACCAACTTCCCCCTGAGACTCAGGGTAAGATTGC-
TACCCATCAACCCAACCACAGAATGCTGAAGATCACCATGAGGGAGTTGACCAAGAACAGTAAAC-
CTCTGCTTAATGAAAGCCAGGCCATCTGCTTCACCATCCTTGGGGTTCTGACGTGC-
CTAGTTGTCCTGGGCACTGTTAGCATTGTGTTCTTCAACAAGTGTGAGGTGTGGCTCTC-
CAATGCCAAGTACAGCCGTCTCCTTCGTAAAAAAAAGAACTTGCTTCTCAGATACAGCAATG-
GTGATGAGCACACCATTAACATCATCTTACCTGAGAAGATGAATCTGAAATCCTACAGTAAGT-
GCCTGAATGAGATATGA

Tasmanian devil *Dlk1*

ATGTTCGCCCCGGaATCCTtGcTGCTaTTGTGCGTTCTTGGGtCACCTtTTTGCTTCTTCTCT-
GCTCTAGGCCTGGAATGTGAGGTcagCTGTCACCCgGACAGAGGAATCTGTGACAAG-
GACCAGTGTAGgTGTCGACCTGGTTGGCAGGGACCCcTGTGCAATGAGTGTGTttCCTTTC-
CTGGCTGTCTACATGGAAtcTGTTCCCTGCCaTGGCAATGTATCTGTGAGGATGGCTG-
GATCGGAAGTCTCTGTGAtatagATCTCCAaTTGTGTGCTGCCAAAtCCTGcCACAAGAATGGGA-
CATGCACTGGcTCTGAgGAAaGTGGCTCCAGaTGTTCTTGTGccCCaGGCTCTTCAGGAA-
GAAACTGTCGTTTtAAGGAAGGACCTTGTGTaATTAATGGTTCTCCCTGcCAgAATGGAG-
GAGCTTGCATTGATGAaAATGGcCTTGCCTCCTATACCTCCTGCTTGTGtCCgGAgGGCTTCTCTG-
GCAACTTtTGtGAAtTGGACATGAAtAGCTGTGTCCCtAATCCATGTGAGAATGGAGGT-
GTGTGCACaGACATCGGTGGGGACTTtCGcTGTCGCTGcCCGCTGGGGTTCATGGACAA-
GACcTGCAGCCaACaTGTGGtGGACCAcTGTGCCAGTGGcCCCTGTGAGCATGGGGGTAC-
CTGTGTcCCTCATGCCAGAGGAGGtTTTGAATGCCTCTGTaGACCAGAATTCTCTGGc-
CCtACTTGTAACCATGGCCACccgaaccatagccacCCAGGAACCAAGACCAAGAGgGgTCCTGGGCTtc-
CTGACCAAtTTtCCCCTGAGACTCAGGGTAgGcTTGCcgCtCATCAgCCCAACCACAGAAT-
GCTGAAaATCACCATGAGGGAGTTGACtAAGAACAGTAAACCTCTGCTTAATGAAAGC-
CAaGCCATCTGCTTCACtattcTGGGtGTTCTGACaTGtCTgGTTGTCCTGGGCACcaTaAG-
CATcGTGTTCTTCAACAAGTGTGAGaTaTGGCTCTCCAATGCCAAGTACAGCCGTCTC-
CTTCGTAAAAAAAAGAACTcaCTTCTCAGgTACAGCAATGGTGATGAGCAtACCATTAA-
CATCATCTTACCTGAGAAaATGAATCTGAAATCCTACAGTcAGTGCCTGAATGAGATATGA

Platypus *Dlk1*

ATGGAGGGGTCGGCGGAGCCTCGACTGCTCTGCGCCTTCCTCCTGCCCCTCGCCCTCTC-
CGCCGCTGCCCAAGGAATTGCTTGTAAGCCAGGATGTCACCCTACAAATGGATTCT-
GTGCCAACCCCAATGAGTGCAGATGTCAACCAGGATGGAGGGGCCCTCTCTGCACT-
GAATGCATTCCCTTTCCAGGGTGCCTGCACGGCGGATGTACCCTCCCCTGGCAGTGT-
GTCTGTCAAGAAGGCTGGGTTGGAAGTCTGTGTGACATAGATACTCACCCTTGCTCT-
GCAACGCCCTGCACCAACAACTCCACCTGCATCGAGACAGGAGATGGTGGCTATGTCT-
GCTTGTGTGGCCCAGGGTTTACAGGGAAAAACTGCCATCTTAGGAAAGGGCCCTG-
TATTATTAATGGCTCTCCCTGCCAGAACGGCGGTGCCTGCGTGGACGGCGACGGCTCG-
GCCCCCCACGCCTCCTGCCTGTGCCCCAGTGGCTTCACCGGTCATTTCTGTGAGCTTGACGCT-
GATGACTGCCACCCCAACCCGTGCGCCCACGGCGGTGCCTGCACCGACATCGGCCGGGACTTC-
CGCTGCCATTGCCCCACCGGCTTCACGGGCAAGTCCTGTGGCCGCCGGCTCCCAGC-
CTGCCTGGACTCTGTGGGCGGGCCCGGACTCGAGTGTGTCTGCCCCCATGGCCTCTC-
CGGCCCGACGTGCGCCCACTTTGGCCACAACTCCACTGGGCCATCCAGGAGCCCG-

GAACGTGGGGAAGGGCCCGGAGACCCTCCGGCCCAGGAGGCCCTCCGTGGGGCATCTG-
GCCATCACCAGGAGCGCCGCGTCCTGAAGATCTCCCTGAAGGAGGTGATTCGACACGCA-
GACCCGTGGCTCAGCCACAGCCAGGTGACCTGCCTCATCGTCCTCGGTTTACTGAC-
CTGCCTGGTGGTGCTGGGGACAACAGCTATCGTCTTTTACTCCAAGTGTGAGACGTG-
GCTCGCCAACGCCAAGTACAGCCGCCTCTTGCGCAAGAAGAAGCGCCGCCTAATGACTTC-
GAACAATGGCGAGACTCTCTCCGTCAACATCATATTCCCAGAAAAGGTCAAATTGAC-
TAGCTACAGCACGTGCTCCGCTGCCATGTAA

Chicken *Dlk1*

ATGAGGCTGCGCGCCGCCGGGCTCCTCGGCTGCTGCTGCTGCTGCTGCCTTCT-
GCCCCTCGTCCTCCCCGCCGCCCCAGGTGTGAGCTGTAAAGCTGGCTGCCACCCAGT-
GAATGGATTTTGTGAATTTCCCAGTGAATGCAGGTGTCTGCCTGGTTGGCAGGGCGCTCTCT-
GCAATCAGTGTGTCCCTTTTCCTGGGTGCTTGCACGGCAGCTGTGTCAAACCCTGGCAGT-
GCATCTGTGAGGAGGGCTGGGTTGGCAGCCTCTGTGACATAGATATTCAGCCGTGCTCT-
GCAAAGCCCTGCACCAATAACTCAACATGCATAGAGACTGGTGATGGAGGATATATTTGTTTGT-
GTGCCCAGGGATTTACAGGAAAAAACTGCCATCTCAGGAAAGGACCATGTATTATTAATG-
GCTCTCCCTGCCAGAATGGAGGAACATGCATTGATGACAATGGTTTTGCACCCCAT-
GCTTCCTGTCTATGCCCTTCTGGTTTTGCTGGAAATTTCTGTGAAATAGATAGGGAT-
GACTGTGAATCCAACCCATGTGAAAATGGAGGAACGTGCACAGATATTGGTGCAGGTTTCAGCT-
GTTTATGTCCCCATGGCTATACAGGAAAGCTCTGCAGCAGCCGTGTCACATTCTGTG-
CAAGTGACCCATGTGAGAATGGAGGAACATGCAAAGAACATCCACAGGGAGGATTCAAAT-
GCATCTGTAAGCCAGAATTTGTTGGTGCCACCTGCAAACATGCCAGCAAAAACACAAGTCTTTCT-
GCTGTGAATATCGGCACAAAGAACATGCAGAATTACAAGATACCCCCAAAAGCTCAT-
CACAGATCAGTGCATCAAGAACATGAAATCCTGAAAATAACAATGAAAGAAACAATC-
CAAAATGCAGATCTCTTGCTCAGTAAAAGTCAAGTGATATGTTTTGTGGTACTGGGAT-
TACTTACTTGTCTTGTAGTTTTGGGTACAACTGGGATTGTATTTTTTTCAAAGTGTGAAAT-
GTGGTTGGCTAATGCCAAATATAGTCATCTCCTGCGCAAGAAAAAGAACTTTCTTCT-
GAAGTCTAGCAATGGGGAAAACCTTTCTGTTAATATTATCTTCCCAGAGAAAATCAAATTGAC-
GAATTACACCAAGAACTACACTGCCATCTAG

Anole lizard *Dlk1*

ATGCATCTCTGCCTCTGGCGCGGGCTCTGCGCCCTTCTCCTCGCTTGCCTCCCTCTCGC-
CCAAGGAACTGATTGCAAACCTGGTTGCCATCCAGTGAATGGGTTTTGTGAAGTTTCAAAT-
GAATGCAGATGTCGATCTGGTTGGCAAGGCCCTCTGTGTGATCAATGTATCCCATTC-
CCTGGTTGCTTGCATGGGACCTGTGTCAAAGCATGGCAGTGCATGTGTGAAGAAGGGTG-
GATTGGCAGCCACTGTGATACAGATGTTCATCCCTGTGCTTCAAAACCATGTACAAG-

TAACTCAAGCACATGTGTAGAGACAGGCAATGGTGGCTACATTTGTTTGTGTGCTGAAG-
GATATACGGGAAAAAGCTGCCATATGAAAAAGGGACCCTGCATAGTTAATGGCTCAC-
CTTGTCAGCATGGAGGAACCTGTGTGGATGATGATGGATCTGCGCCTCATGCTTCCT-
GCCTGTGCCTTCCTGGGTTTACTGGAAATTTTTGTGAAATCGATATTGATGACTGTGAGC-
CAAACCCATGTGAAAATGGGGGCACATGCACAGATATCGGCAGAGGCTTCCACTGC-
CACTGCCCAATGGGGTTCAGCGGGGCTTTGTGCAGCAGCCATGTGTCAGCCTGTAC-
TAGCAACCCCTGTCAAAATGGTGGGATTTGTCGTGTGCACCCCAGCAGAGGTTTTGAGT-
GTCGCTGCAAACCCCATTTTGTTGGTGTTACCTGTGCTTCTGCTGACAGAAACAAGAGTCT-
GAATGGGGAGGTTAAACATAGGTTAAATCATCACTCCCATATGAGAGTTCACCACAAAC-
CTGTTCACGCCCAGGAACGGGAGGTCTTGACCATCAAAGAGACGATTGAAAACCGTCAGC-
CTTTTCTCAATAAGAACCAAATGATCTGCTTTATGGTTCTGGGCTTGCTGACATGCCTTGTTGTTC-
TAGGTACAACCGGGATTATCTTTTTTTCCAAATTTGAAAGGTGGCTGGCCAATGCCAAG-
TATAGCCAACTGGTCCGCAAGGAGAGAGATGATTTTCTGAAAGCAAATGAAGGTGA-
GAACCTCTCAGTGAAGATAATCTTTCCAGATCAAACTGAGGAATGA

Chinese soft shell turtle *Dlk1*

ATGGATTTCCGGGCTGCCACTTTAAACTGCTGCTGCTTTGCCCTCGTCCTCCCCGTTAGC-
CAAGGTGTTGCTTGTAAACCTGGCTGCCACCCAGTGAATGGATTTTGTGAAGTTCCCAGT-
GAATGCAGGTGTCAACCTGGGTGGCAAGGAGCTCTCTGTAATCAGTGTGTTCCTTTTC-
CTGGTTGTGTGCATGGCAGCTGTGCCAAACCATGGCAGTGTGTCTGTGAAGAAGGATGGGTTG-
GCAGCCTTTGTGATATAGATATTCATCCATGTTCTTCAAAACCCTGCACCAATAATGCAA-
CATGCATAGAGACTGGAGATGGTGGATATATTTGTTTGTGCGCCAAAGGATTTACAGGAAAAAACT
GCCATCTGAAAAAAGGGCCCTGCATTATTAATGGCTCTCCCTGTCAGAATGGGGGAA-
CATGTGTTGATGATAATGGATTTTCAGCTCATGCCTCCTGTTTGTGCCTTCCAAGTTTTTCTG-
GCAATTTTTGTGAAATAGATATAGATGACTGTGAACCCAACCCATGTGACAATGGAG-
GAACATGCACGGATATTGGTAGAGGCTTCAACTGCCATTGCCCTATTGGCTATATGGGCCAGTC-
CTGCAACAGCCATGTCCTATTCTGTGCTAGCAGCCCATGTGAGAATGGAGGAACAT-
GTCATGAGCATCCTGGAGGAAGATTTGAATGTCTTTGTAAGCCAGAATTTGTTGGTGT-
GACCTGTACCTATCCCAGCAGAAACACAAGTCTCCATGGCATGAATACAGAGGCCAAAACTGGGC
GAGGTATAATCTACCCCCAAATGCTCATCCCAAGTCAGCTCATCACCAAGAACATAAAGTCTTGAA
CAATGAAAGAAACAATCCAAAACACAGAGCCCTTGCTTAATAAAAGTCAATTGATAT-
GCTTCATTGTTCTGGGCTTGCTTACATGTCTTGTTGTGTTGGGTACAACTGCAATTG-
TATTTTTCTCCAAATGTGAAATATGGCTTGCTAATGCCAAATATAGCCATCTCCTACG-
CAAGAAGAAGAATTGTTTTCTTCAATCTAACAATGGGGAAAACCTTTCAGTTAACATAATTTTC-
CCAGAGAAGATCAAACTTACTAACTACACTAAGAACTATACTGACATTTAG

Western clawed frog *Dlk1*

ATGGAGTTAACTGCCTCGTGCATTCTGTGCCTGTTTCTGTCTCGCTTCATAACCACA-
GAGACTAAAGAAATCGCCTGCATGCCTGGCTGCCATCCAGTAAATGGGTTTTGTGAAAGT-
CAAGGAGAATGCAGGTGTCGTACCGGCTGGAAAGGACAATTCTGTGATCAATGTATC-
CCATTTCCTGCTTGTATGCATGGGAGCTGTACAAAACCATGGCAGTGCATCTGTGAA-
GAAGGATGGGTTGGAAGCCTCTGTGATATAGATGTTCACCCGTGTGCAGCCAAGCC-
CTGCTCCAGCAACTCTACCTGCATCGAAACGGGGGATGGTGGATACATTTGCTTGT-
GCTCTCTGGGGTATACAGGAAAAAACTGTCTTCTTAAAAAGGGACCCTGCAGTACAAATG-
GATCTCCCTGTCAGAATGGAGGCAAATGCACAGACAACAATGGCTTTGCATCGTAT-
GCCTCTTGTCAGTGTCCCCCTGGTTTTATTGGTAATTATTGTGAAATACAAATAGATATTGAC-
GATTGCAACCCCAATCCTTGCAGAAATGGTGGAAGCTGCACAGACATTGGATCAGGATTTCACT-
GTCATTGCCCTTTGGGGTTTTCTGGGCAGTTCTGTAATGATCTCACCCCACTGTGCAGTAG-
CAATCCATGTGCAAACGGTGGGACGTGTTATCAGATAGGAGAGAAATTCCAGTGTTTTTGTCAGC-
CCAAATATACAGGAACTACTTGCTCTTTTCCCCATAGAAACATGAGCTTACACCTATAT-
GAGAGAAGAAATAGTCTGCCTTCATATCATAAATCTCCACAACATGAAGTACTTAAAAT-
TACAGTCAAAGAGACTATTCAAAATGTGGACCCACTCCTTAACAAAAGTCAGGTTATCT-
GTTTTATTGTGTTAGGGCTACTGACCTGTCTCATTGTCCTCATTACCACGGGGATTGT-
GTTCTTTTCTAAGTGCGAGACATGGTTTGCCAATGCCAAATATAGCCGTCTTTTAAGAAA-
GAAAAAGAACATTTACATGCAAAGAAGTCGAGGAGAGGACCGTGATGTCAAAATAATATTC-
CCAGAAGGAGTTAAGTTTGAAGACTGCTGCAGGGATTATGCTTCTACATAA

Coelacanth *Dlk1*

ATGGAAGGTACTGTAATCCCTTTATCTTGTGTTGCTGTGGTTTCTGAAAGTGATCTCATTCTC-
TATTACAGGATTGATTGTAAACCTGGCTGCCACTCAGTGAATGGATACTGTGAAAAAC-
CTGGAGAATGCAGATGCAACGAGGGTTGGCGGGGAGCACTCTGCAACAAATGTGTTCGTTTC-
CCTGGTTGCCTGCATGGTAGCTGCAACAAACCCTGGCAGTGTGTTTGTGAGGAAGGGTGGGTGGGC
CTCTGTGACATAGATATCCACCCTTGTGCTGTCAGACCCTGTGCCAACAACTCAACTTG-
TATAGAAACCAGAGATGGTGGATACATCTGTGTATGTGCACAGGGATATACAGGAAAAAACT-
GCCACCAGAAAAAAGGACCTTGTTACACCAGTGGCTCTCCTTGCCAAAATGGAGGAACTTGT-
GTTGATGGAAATGGATTTGCTCACTATACTTCATGTATGTGCCCTCCTGGGTTCACTG-
GTGATTTCTGTGAAATACGTAACAATGACTGTAACCCCAGTCCTTGTGAAAATGGTG-
GAGTTTGCACAAATATTGGCTCTGAAATCAGTTGCCTTTGTCCTAGTGGGTATATTG-
GCCCATCTTGCAGCACCCGTGTGATCGCGTGTCTCAGTGACCCCTGTGAAAATGGAG-
GAACATGTCTTGAGCATCCAGGAGGGAGGTTCAACTGTATCTGCAAACCAGAATTTGTTG-
GAGATATTTGCAGTCATTTGAAAAGAAACATGAGTAGATTTGTCATGAACACAGAAGT-

GAAACACAAGCAGCATCACAATCTGCATCCTAATGTTTTTCATAAATCCACACACCAA-
CAAGAGCATGAAGTGTTGAAGATCACATTGAAAGAAACTGTACAGCACTCTGGTATTT-
TACTCAATAAGAGTCAAGTGATTTGCTTCATTGTACTGGGTTTACTTACGTGCCTTGTTGTCTTG-
GTCACAACCGGGATTGTGTTTTTCTCCAAGTGTGAGATGTGGCTTGCCAATGCCAAAT-
ACAGTCACCTTATACGCAAGCAGAGAAACCGTTTTATGAAGTCTAACAGTGGGGAA-
GAACTCTCTGTGAACATAATTTTCCCTGAAAAAATAAAACTGACCAACTACAGTAA-
GAGTTATACATCTATCTAA

Zebrafish *Dlk1*

ATGAGTGTGCTTCTCCGGCTCGGGTTTTGCTTTCTGCTGCTCTTCTGCTGCGCTGCT-
GCTCAAGGTCCAGACTGTGGAGCTGGATGTCACCGACACCACGGGTTCTGTGAGCAGTCTG-
GAGAATGCAGGTGCAAGTCTGGCTGGCGAGGCGCAGTGTGTGATCAGTGTGTTCC-
CTCAGCTGACTGTGTTCACGGCTGGTGTGAATCTCCCGGCGAGTGTATCTGTGAGTC-
CGGCTGGAGCGGCGCGCGCTGCGATCGAGATGTTCGTCCGTGTTCATCGCAGCCCT-
GCTCTGCAGACTCCAGATGTGTGGACGCTGCAGGAGGACGAGGACACGTCTGCATCT-
GCACTGCTACACACTGCCGCACGGAGGAGACACACTGCACAGTCAACGGATCTCTCT-
GCCAGAATGGAGGCTCCTGTGTGTCCAGTAGCTCCTCCTTCAACACATCTAGCTCCTC-
CTCCAACACTAGCTCCTCCCCCAGCTCCTCTAGCTCCTCCTCCTGCCTCTGTCCGGCTGGGTTCAC
GTTCTCTCTGTGAGCTCCAGTCTGCCGTGTGTAAGTCCAGTGTGTGTGTGAATGGCGGGC-
GATGCGTCCGGCGTGGTCTCTCCTACAGGTGTGTGTGCGCGCGCCGCTTCAGCGGGT-
CATCGTGCGAGCGACACAGGCCCAGAGTAAAAGCGCCACAGCAGCACCACACAGCACTC-
CACAAGCCGCTGGAGACCCCCGGCGCTCTGGCGTCCCGCAGTCAGCTCATCTGCTTCTC-
CGTCCTGGCTCTCCTCACGGTCCTCGTGGTCCTGGGCTCCACCGCTATCGTCTTCTTCCAGCGCT-
GCGAGGTCTGGATGGCCAACGTGAGGTACAGGCAGCTGGTGGCGCAGCAGAGGGAGCT-
GATCCAGGACCAGGCCACCGTGAACATCATCCTGCCTGAGAAGATCAAGCTGAGCAGC-
TACAGCAGACACTACACCTCCATCTGA

Medaka *Dlk1*

ATGATGATGCATCTGATCTGGGTGGTCTTCATTCTTAGTGTGGCAGGCATGGTAAAAG-
GCTGGGAATGCAGCGCAGGGTGCAGTCCAGAAAATGGGTTTTGTGAGAGGCAGGGGAAGT-
GCAGGTGCAAACCTGGGTGGGAAGGAGAGAACTGTGACCGGTGCATTCCCTTCCCTG-
GATGTCTGCACGGCTCATGTGAAAAGGCATGGCAGTGTATCTGCAAAGAGGGCTGGGTGGGCAG
CTGTGTGACCAAGATACCCGCCTGTGCTCATCCAGGCCGTGTTCCAGCAACGCCAC-
CTGCGTAGAGACGGGAGAGGGAGGATACATGTGTATCTGTCCTCAAGGCTTTGCTG-
GAAAAGACTGCCATTTGAAGAAGCAACTCTGCCTGGAGAATGGCTCCCCTTGTCA-
GAATGGAGGCACATGTGTGGACGCTAGTGGCTCAGCCGCATCCCCTTTCTGTTCCT-

GTCCCTCTGGGTTTTCCGGAGACTTCTGTGAGATCGGTGTTGACAGCTGCCAGCCTAAC-
CCCTGCCTCAACTATGGCAATTGTACAAACCACGGCCTCACGTTCACGTGTGTCTGTC-
CACCGGGCTTCTCGGGTTTCACCTGCAACGACAGCACCAGCAGCTCCTCCTGTGCTG-
GCAGGCCCTGTTCCAACAGCGGGACATGTGTCCGTCAGCTTGATGGAACGTTCCAGT-
GTGTCTGCCAGAAAGGGTTTGCGGGTCCAACTTGTTCTCTGCGTCACAGACCAAA-
GAGCAGAAACAAACTGCTTGGTGCTAGACCGGTGGAGCACCACATGCTCGCCCTAGC-
CCCCCAACACTACTCTCTGCCCGCCCACGCCTTTCACAAGCTGCTTAAACCTCCCGATA-
GAGACCTGCTGAAGATCACCCTGAAGGAGACTGTCCACTCCTCTGGCGTTCTTGTCACT-
CACGGTCAGCTCATCTGCTTCGGCATGCTGGCCTTGCTCACCTGCCTGGTTATTCTAG-
GCACGACGGGAATAGTTTTATTTGGCCGCTGCGAGACGTGGCTGGCCAATGCCAAG-
TACAGCCAGCTTGTTCGACAGCAACGGGAACACCTGCTGAGAGAAGTCGGAAGCC-
CGAGCCAAGAAGAGCCGGAGCACTCGGTAAACATCATCCTGCCAGAGAAGATTAGACTCTCCAGCT
GACACTACACCTCAATCTGA

Australian ghost shark *Dlk1*

ATGGCTCATCACTCCGCAGCCTCTGTGCTGGTGGTCAGTCTCCTGTTACCGCTGCTCACTG-
GTACCCGGACTCAGGGGACTGAATGCAAACCCGACTGTCACCCACTGCATGGATTCT-
GCCAGGATACTGGGGAATGCAGGTGTCAGTCTGGCTGGCAGGGAGACTTGTGTGATCAGT-
GCACTCCCATTCCTGGCTGTTTACATGGGAGTTGCACAAAACCTTGGCAGTGCTGTTGT-
GAAGAGGGTTGGTCAGGCATCCTCTGCGACACAGCTCCCCACACCTGTTCCTCAGAA-
CACCCATGCGCTAACAATTCAACGTGTATAGAGAGTGAAGGAGGTGGCTACAGATG-
TATCTGTGGAGAGGAGTTTACAGGGAACCATTGCCAGCTCAGGAAAGGAAATTTCT-
GCATAAATGGGTCACTGTGTCAGAATGGAGGAAGTTGCATAGATGGTAATGGATTTG-
GATCCCAGGCTTCCTGCCTGTGCTTGAAGGGTTTTACTGGGGTCTTGTGTGAGACCAAAATCAGT-
GACTGTGACTCTAATCCATGTGCAAACAATGGGACTTGCACAGACCTGGTTTCTGGC-
TACAGCTGCCTCTGTCCCCTTGGTTTTACTGGCGGATCTTGCGATTATCTAATCACATC-
CTGCCTTAGTCATCCATGCAAGAATGGAGGCACTTGCCATGATCTTCCTGAGGGGGGTTTTGATTGCC
CATGCTTGCCTGGTTATGAAGCAGAAACCTGTCACGAGCATATCTCTTCTAAACATGAT-
ACAAAGCAAAACATATCCAAGCACGTGAGAGTAAGTTGGGTCAGACATGGCAAGCTTTTCAATC-
CACCGCTGCATGCCTTTCACAAGCCCACCCACCATCAAGGTAATGAGATGCTGAAGAT-
CACCGTCAAAGAAACCATCCACACATCGAATTCCCTGCTCAACAGAAGTCAAGTCATCT-
GCTTTGTCATGCTTGGATTGCTGACTTGTCTCGTGATCCTGGGAACGACACTGATCATCTTTTTCTC-
CAAGTGTAAAATGTGGATGGCAAATGCTAAATATCGTCAATACCTACGGAAACAAAAAAAT-
CACTTTCTCAACGACGAAGAGACTTCAGTCAAAATCATATTCCCGGACATGAGTAAATTGA-
CAAACTACAGGAAAAGTTACATCTCGATGTGA

A.1.4 Coding sequences used for *Dlk2*

Human *Dlk2*

atgcccagcggctgccgctgcctgcatctcgtgtgcctgttgtgcattctgggggctcccggtcagcctgtccgagccgatgactgcagctc-
ccactgtgacctggcccacggctgctgtgcacctgacggctcctgcaggtgtgacccgggctgggaggggctgcactgtgagcgct-
gtgtgaggatgcctggctgccagcacggtacctgccaccagccatggcagtgcatctgccacagtggctgggcaggcaagttctgtga-
caaagatgaacatatctgtaccacgcagtccccctgccagaatggaggccagtgcatgtatgacgggggcggtgagtaccattgtgt-
gtgcttaccaggcttccatgggcgtgactgcgagcgcaaggctggaccctgtgaacaggcaggctccccatgccgcaatggcgggcagt-
gccaggacgaccagggctttgctctcaacttcacgtgccgctgcttggtgggctttgtgggtgcccgctgtgaggtaaatgtggatgact-
gcctgatgcggccttgtgctaacggtgccacctgccttgacggcataaaccgcttctcctgcctctgtcctgagggctttgctggacgcttct-
gcaccatcaacctggatgactgtgccagccgcccatgccagagaggggcccgctgtcgggaccgtgtccacgacttcgactgcctct-
gccccagtggctatggtggcaagacctgtgagcttgtcttacctgtcccagacccccaaccacagtggacacccctctagggcccac-
ctcagctgtagtggtacctgccacggggccagccccccacagcgcaggggctggtctgctgcggatctcagtgaaggaggtggtgcg-
gaggcaagaggctgggctaggtgagcctagcttggtggccctggtggtgtttggggccctcactgctgccctggttctggctactgtgttgct-
gaccctgagggcctggcgccggggtgtctgcccccctggaccctgttgctaccctgccccacactatgctccagcgtgccaggaccaggagt-
gtcaggttagcatgctgccagcagggctccccctgccacgtgacttgccccctgagcctggaaagaccacagcactgtga

Mouse *Dlk2*

atgcccagcggctgccgctgcctaaatctcgtgtgcctgctgtgcatcctgggggcaaccagccagcctgccagagcggatgactgcagctc-
ccactgtgacctggcccacggctgctgcgctcctgacggctcctgcaggtgtgacccaggctgggaggggctgcactgtgagcgct-
gtgtgaggatgcctggctgccagcacggtacctgccaccagccctggcagtgcatctgccacagtggctgggcaggaaagttctgtga-
caaagatgagcacatctgtacctcacaatcaccctgccagaatggaggccagtgtgtgtatgacgggggtggtgagtaccactgtgtgt-
gcctgccaggcttccatggacgtggctgtgagcgcaaggctggaccttgtgagcaggcaggcttcccgtgccggaatggagggcagt-
gccaggacaaccagggttttgccctcaacttcacatgccgctgcttggcaggattcatgggtgcccactgtgaggtcaatgtggacgact-
gtctgatgcggccttgcgccaatggtgccacatgcattgatggcataaaccgcttttcctgcctctgtcctgagggcttcgctggacgcttct-
gcaccatcaacctggatgactgtgccagccgcccatgccagagaggggcccgctgcagggaccgtgtccatgactttgactacctgt-
gccccagtggctatggtggtaagacttgtgaacttgtcctacctgctccagagcctgcctcagtgggcaccccacaaatgcccacctcagct-
gtagttgtacctgccacggggccggcccctcacagtgcgggggcgggcctgctaaggatctcagtgaaggaggtggtacggaggcaa-
gagtctgggcttggtgaatctagcctggttgccctggtggtgtttgggtctctcactgctgcgctggtcctggccacggtgctgctgacc-
ctgagggcatggcgccgaggtatatgccccactggaccctgctgctacccagccccacactatgccccagctcggcaggatcaggagt-
gccaggttagcatgctgccagcggggttccctctgtccccagacctgccccctgagcctggtaagaccacagcgctgtga

Cow *Dlk2*

atgcccagcggctgccgctgcctacatctcgtttgcctgttgtgcatcctgggggcacccgtaaagcctgccagaggcaatgactgcagctc-
cctctgtgacctggctcacggctgctgcgcgcctgacggctcttgcaggtgtgacccaggctgggaggggctgcactgtgagcgctgt-

gtgagaatgcctggctgccagcacggtacctgtcaccagccctggcagtgcatctgtcacactggctgggcaggcaagttctgtgacaaa-
gatgaacacatctgtaccacgcagtccccctgccggaacggaggccagtgcgtgtatgacgggggcggtgattaccattgtgtgtgc-
ccaccaggcttccacgggcgtgattgtgagcgcaaggccggaccctgtgagcaggcaggctccccgtgccggaacggtgggcagt-
gccaggacgaccagggctttgccctcaacttcacctgccgctgcctggcgggcttcatgggtgcccgctgcgaggtgaatgtggatgact-
gtctgatgcggccctgtgctaacggcgccacatgcctggacggcatcaaccgcttctcctgcctctgccccgagggcttcaccgggcgcttct-
gcaccatcaacctggatgactgtgccagccgcccctgccagagaggggcccgctgtcgggaccgggtccacgactttgactgtctct-
gccccagcggctatggtggcaagacttgtgagctagtcttaccggtcccgggtcctgccgccacagcggacagccccccagggcc-
caccttggctgtgcttgtacctgccacggggcccatccctcacagcgcgggcgccgggctgctgcgcatctccgtgaaggaagtggt-
gcggcgacaggaggccgggctgggcgagcccagcctggtggccgtggtggtgtttggggccgtcactgccgccctggtcctgtccacg-
gtgttgctgaccctgagggcctggcgccggggcttctgtccccctggaccctgctgctaccctgccccacactacgccccagcacgccaggaccaggagt-
gtcaggttagcatgctgcccacggggctccctctgccgcctgacctgccccccgagcctgggaagaccaccgctctgtga

Dog *Dlk2*

atgcccagcggctgccgctgtctacatctcgtgtgcctgttgtgcatcctgggggcgcccgttcagcctgcgggagccgatgactgcagctc-
ccactgtgacctggcccacggctgctgtgcgcctgacggctcctgcaggtgtgacccaggctgggaagggctgcactgtgagcgct-
gcgtgagaatgcctggctgccagcatgggacctgccaccagccctggcagtgcatctgtcatagtggctgggcaggcaagttctgtga-
caaagatgagcacatctgtaccacacagaaccctgtcggaatggtggccagtgtgtctatgacgggggtggtgagtaccactgtgtgt-
gtccaccaagtttccatggacatgactgcgagcgcaagtctggaccctgtgaacaggcaggctccccatgccggaatggtgggcaat-
gccaggatgaccagggctttgctctcaacttcacctgccgctgtctggtaggctttgtgggttctcgttgtgaggtcaatgtagacgactgtct-
gatgcgaccttgtgccaatggcgccacctgcctggatggcataaaccgcttctcctgcctctgccctgagggctttgctggtcgcttctg-
cacagtcaacctggatgactgtgccagccgtccgtgccagagaggggcccgctgtcgggaccgcgtccatgactttgactgtctctgc-
cccagcggctatggcggcaagacctgcgagctcatcttaccggtctcagaacccgccaccatagtggacatccccttggggaccac-
ctcggctctggcagtacctgccacagggcctgtcccccacagcgtgggggcgggtctgctgcgcatctcagtgaaagaggtggtgcg-
gaggcaagaggctgggctaggtgtatctagcctggtggctgtggtggtctttggggccctcaccaccgccctggtcctgtccacaatgttgct-
gaccctgagggcctggcgccggggtgtatgccccctggaccctgttgctaccctgccccacactatgccccggcatgccaggaccaggagt-
gtcaggttagcatgctgccggcagggctccccctgtcacctgacctgccccctgagcctggaaagaccacagcactgtga

Elephant *Dlk2*

atgcccagcggctgccgctgcctacatctcgtgtgcctgttgtgcatcctggggccacccggtcagcctgcccgagcggatgactgcagctc-
ccactgtgatctggcccacggctgctgcgcgcctgacggctcctgcaggtgtgacccgggctgggaggggctgcactgcgagcgct-
gtgtgaggatgcctggctgccagcacggaacctgccaccagccctggcagtgcatctgccacagtggctgggcggggaagttctgt-
gacaaagatgagcacatctgtaccacacagtccccctgccagaacggaggccagtgcatgtatgacgggggcggtgagtaccactgt-
gtgtgcccaccaggtttccacgggcacgactgtgagcgcaaggctgggccctgtgagcaggcaggctccccatgccagaatggcgggcagt-
gccaggacaaccagggctttgccctgaacttcacatgccgctgcttggcaggatttgttggtgcccgctgtgaggtgaatgttgatgact-
gcctgatgaggccttgtgcaaacggcgccacctgccttgatggcataaaccgcttctcctgcctctgtcctgagggctttgctggacgcttct-
gcaccatcaacctggatgattgtgccagccacccatgccagagaggggcccgatgtcgggaccgcgtccatgactttgactgtctctgc-

cccagtggctatggcggcaagacttgtgagcttgtcttaccagttccagacccttcaccacggcggaccttcccctgggtcccacctcagct-
gtggtggtacccaccacggggccagttccccatagtgcaggggccggtttacttcggatctccgtgaaggaggtggtgcggagacaa-
gaggcggcgctggcggagtctagcctggtggccgtggtggtatttggggctctcactgctgccctggtcctggccactggattgctgac-
cctgagggcctggcgccggggtgtccgcccccctggaccctgttgctaccccattccacactatgccccagcacgccaggaccaggagt-
gtcaggttagcatgctgccagctgggcttcccctgccacctgacttgcccggtgagcccggaaagactacagcactgtga

Opossum *Dlk2*

atgcccagcggctgccgctgtctccagcttgtgtccctgctgtggatcctgggggcatccggacagcccacccatgctgatgactgtagttc-
ccactgtgatctggcccacggctgttgtgagcctgacggcacgtgcaggtgtgaccctggctgggagggattacactgtgagcaatgt-
gtcaggatgcctggctgccagcatgggacctgtcaccaaccctggcagtgtatctgcagtaatggctgggcaggcaaattctgtgacaaa-
gatgagcatatctgcaccaagcagccaccctgtcagaatggagggaagtgtgtctatgaaggggatggagaataccactgtgtgtgc-
ccaccaggcttccacgggcacaactgtgagcgcaagactgggccctgtgagcacgctggatctccttgccggaatggtgggcagtgc-
caagatgatcaaggcttcgcagagaactttacatgccgctgcttggcaggctttgtgggtccacgctgtgaggtcaatgtggatgactgc-
ctaatgaggccctgtgccaatggtgccacctgtcatgacggcatcaaccgcttctcctgccactgccccaaaggctttgctggccgattct-
gcactgtcaacctggatgactgtgccagccgaccgtgccagcatggtgcccgctgccgggaccgagtccatgactttgattgcctctgc-
cctgatggctttgggggcaagacatgtgagattgttctcccagccctggacctgcctacagagccagacagtgcccctggacccacc-
cctgcagccgtggttcctttcacagtaccagccccttcagtgtgggcgcagggctactgaggatctcagtgaaggaggtagtacggc-
gacaagaggcagggataggggattcaagcctgattgttttgttcatatttggggccatcactattactggggtctttggcacagggctggt-
gatttttgggtacgacgccatggccactgccccactgggccttgctgctgcccttatcaccagtatgccccacccctgagcgacatgaccaggagt-
gccaggtcagcatgctcccggctgggatctcccctccacctgacttcccatctgagcttggcaagaccacggcattgtga

Tasmanian devil *Dlk2*

atgccccacggttgccgctgcctccagctcgtgtctctactctggatcctgggggcatccggacagcccacccctgccaatgattgtagttc-
ccattgtgatctggcccacggctgctgtgagccagacggcacttgcagatgtgaccctggctgggagggactacactgtgagcgctgt-
gtcaggatgcctggttgccaacatggcacttgtcaccaaccctggcagtgtatctgccataatggctgggctggcaaattctgtgacaaa-
gatgagcacatctgcaccaagcagccgccctgccagaacggagggaagtgtgtgtatgaggggatggggagtaccactgcgtgt-
gcccaccaggttttcacgggcataactgtgagcgcaagactgggccctgtgagcatgctgggtccccttgccggaatggtgggcaat-
gccaagatgatcaaggctttgcgaagaacttcacatgccgctgcttggcaggctttgtggggccacgctgtgaagtcaacgtggatgact-
gcctaatgaggccgtgtgccaatggtgccacctgtcatgatggcatcaaccgcttctcctgccactgtcctgaaggctttgctggccgcttct-
gtactatcaacctggatgactgtgccagccgcccatgccagcatggtgcccgctgccgggaccgtgtccatgacttcgattgcctctgc-
cctgatggctatgggggcaagacatgtgagattgccctcccagccctggacctccctacggagccagagagtgctgctggatccactc-
ctgcagctgtggttcctttcacggtaccagccccttcagcgtgggggcagggctgctgcggatctcagtgaaggaggtagtaaggc-
gacaggaggcaggcctaggggagtcaagcctgcttgtgttagtgatatttggggtcctcactgccaccctggtccttaccacagggct-
gctgatcttttgggcatggtgccatggccactgccctgctgggctctgctgctaccctttttcgccaatatgccatacccccgagcagcat-
gaccaggagtgccaggtcagcatgctccctgccggaatctcccctccacctggctccccacctgagcctggcaagaccacagcact-
gtga

Chicken *Dlk2*

atgctcaggagcttctgccttcagctcatgtccttgctttggatcctcttggcccatcaccagcttgcccaaggtgatgactgcagcgagcact-
gcaatctggcccacggcagctgcgaccaggatgggaagtgcaggtgtgacccaggctgggagggcgactactgtgaggagtgcg-
tacgcatgccgggctgcctccatgggacctgccaccagccctggcagtgcatctgtcacagcggctgggccggcaagttctgcgacaag-
gatgtccacatctgcgaacatcagtcaccatgccagaatggggctcagtgcatctacgaccgagatggggactactcctgcctgtgtcca-
gagggcttccatgggaaggactgtgagatgaaggcaggaccatgtgagaaggcagggtctccatgcaagaacgggggacagtgtcaa-
gatgaaaatggctttgccaccaacttcacctgccggtgccttgctggcttcgtgggggctctctgtgagcacgacgtggatgactgcct-
gatgcggccctgcgccaacggtgccacctgccatgatggcatcaaccgcttctcctgccagtgccaggtgggcttcgaggggcgtttct-
gcaccatcaacatcaacgactgcgccagccagccctgcaaaaacggggccaagtgctatgaccgcatcaatgactatgactgcttgt-
gttctgaccgtttcactggcaaaacctgtgagatctccatccctgaacccacctgggctccccctaccaccctgcgaaccacgagagcagctgggc-
gatgaggagcaccaccagcgagatgcccgaggtgacacagccagagcccgtgaggactgcggttacggggcggcgcgtggccaac-
cacagtgagaaagtgccaggaggagggttgttaaaaatctctgtgaaggaggtggtgacccaaagggactcggggctgagcgaagc-
ccagctggtgacagtgctggtgttcggggtgctgacggcggtgctggtcctcatcaccgtcctgctcatcctgaggaactggcagaggggc-
cgacagcggtcgaactggtgccaaagcccttcgcaggctgccaggaagctccaagatcaggagtgccaggtgggcatgttaaacacg-
gtcctgatcgagcccaggaaaacaacagagctgtga

Anole lizard *Dlk2*

ATGCTCAGGAGCTTCTATCTTCAGCTCATGTCCTTGCTTTGGATCCTGGTGGCCCAT-
CACCATTTTACCCAAGGTGATGACTGTAGCGACCATTGTAATTTGGCTCACGGCAGCT-
GTGAAGATGGCAAATGCAGATGTGACCCAGGCTGGGATGGGGCATCTTGTGAGCAGT-
GTGTGAGGATGCTGGGCTGTATCCATGGAACATGCCACCAACCCTGGCAATGTATCT-
GTCAAAGTGGCTGGGCCGGCAAGTTCTGTGACAAAGATGTGCACATTTGTGAGCACCAGC-
CTCCATGTCAAAATGGAGCCGAGTGCATCTATGATCGTGATGGCGAATATTCATGCCT-
GTGCCTTGAAGAATTCCATGGGAAGGACTGCGAGCTGAAGACAGGGCCATGTGAGAAGTCAGGGTT
CATGCAAGAATGGTGGGCTGTGCCAGGATAAGAATGGCTTTGCTAGCAACTACACCT-
GCAAGTGCCTTGCTGGCTTCACTGGTGCGCATTGCGAGATTGATGTAGATGACTGC-
CTGATGCAGCCCTGTGCCAATGGTGCCACCTGCCTCGATGGCATGAACCGTTTCTC-
CTGCCAATGCCAGGCTGGTTTTGAAGGCCGTTTCTGCACTATCAACATTGATGACTGT-
GCCAACCAGCCTTGCAGAAATGGGGCCAAGTGTTATGACCGCATCAATGATTTTGATTGCT-
TATGCCCTGAGGGCTTTGTTGGCAAGACCTGTGAGCTCCCTGCACCAGAACCAACATGGGT-
TACTGCATTTGAGCCTGGTCACAAGGACAATGATAATGCTGTGACCAGTATTGACCCTTG-
GACAGCCCAGTCTGATCCTGCAAGGACTGCAGTTACTGGGAAAAGAATCACTAACTACAGT-
GAGAAATCAAATGGGGGAGGGCTCCTCATCTCTGTGAAAGAGGTGGTGACCCAGCAGGACTCGGG
TAAGCCAATCGCAGCTGATTTTACTGCTGGTGTTTGGCCTGCTCACTATGCTTTTGGTCTTTG-
TAACTGTCTTGATGGTGCTGCTCAAGAACTGGCAGAGAGGGAATCAGAGGTGCCA-

GAGCCCATCCCAGTCTGCAAGGAAACTTCAGGACCAAGAGTGTCAAGTGGGAATGT-
TAAGTACAGTCTTGATAGAACCCAGGAAAACAACAGAGCTGTAA

Chinese soft shell turtle *Dlk2*

ATGCTCAGAAGTTTCTGTCTTCAGCTCATGTCCTTGGTTTGGATCCTCTTGGCCCAT-
CATCATCTTGCCCAAGGTGATGACTGCAGTGAGCACTGTAACCTGGCCCACGGCTC-
CTGTGACCAGGACGGCAAGTGCAGGTGTGACCCAGGCTGGGAAGGAGAATATTGC-
GAGCAGTGTGTGCGGATGCCGAGCTGTCTCCATGGTACATGCCATCAGCCGTGGCAAT-
GCATCTGTCACAATGGCTGGGCTGGCAAGTTCTGTGACAAAGATGTACACATTTGC-
GAACACAACCCCCCCTGCCAGAATGGGGCTGGATGCGTCTACGATGGGGACGGGGAG-
TATTCCTGCCTGTGTTCTGAGGGCTTTCATGGAAAGGACTGTGAGCGGAAGACAGGGC-
CATGTGAAAAGGCAGGGTTTCCGTGCAGGAATGGTGGGCAGTGCCAGGACGAGAACG-
GCTTTGCTAAGAACTTCACCTGCAGGTGCCTGGCTGGCTTTGTCGGTGCCCTCTGT-
GAGGAGGATGTAGATGATTGCCTGATGCGCCCCTGTGCCAATGGTGCCATCTGCCAGGACG-
GTATCAACCGCTTTTCCTGCCAGTGCCAGGTGGGCTTTGAGGGGCGTTTTTGCACCAT-
CAACATCAACGACTGTGCCAGCCACCCGTGCAAAAATGGGGCAAAGTGTTACGATCG-
CATCAATGATTTTGACTGCGTGTGTCCTGAGGGTTTTACTGGCAAAACGTGTGAGGC-
CTCTGCTCCGGAACCGACCTGGGTCCCCTTCTACCTTTCTGCTAACAAGGAGAACAAT-
GATGCTCTGAAAAGCACAACCAGCGAGTATCTCTGGGTTACGCAGCCCGAGCCAGTCAGGACT-
GTGGTTACTGGAAAGCGGGTTGCCAACCACAGTGAGAAAGCCAGTGGGGGAGGGCT-
GTTGAAAATTTCTGTGAAAGAGGTGGTGACCCAGCGGGACACAGGGTTGAGTGAGTC-
CCAGCTGGTGACCGTGCTGGTCTTTGGGACACTCACAGCCGCACTGGTCCTGGTGAC-
CATACTGTTAATGCTGCGGAACTGGCAGAGAGGGCGTCGGAGGTCAAACTGGTGC-
CAAAGCCCCTCACAGGCTGCAAGGAAGCTCCAGGAACAAGAATGTCAAATGGGCAT-
GTTAAATACAGTCATGGTAGAGCCCAGGAAGACAACAGAGCTGTGA

Coelacanth *Dlk2*

ATGAGACCCAGCGGACGGCCTGCTCTTCAGCTCCTGCATTTCGTCTGGATGCTGTTGCTCCAGCG
CCTGTCCGAGGTGCAGACTGCAAGTCTAGCTGTAACCTGGCCCACGGCCGCTGTGAT-
GTCAACGGAGATTGCAGGTGTGACCCCGGCTGGGAGGGAGACAGCTGTGAACGCT-
GTGTGCGGATGCCCGGCTGCCTTCATGGCACGTGCCACCAACCGTGGCAGTGTATTTGTTTGAGT
GATGGGCTGGCAGATTTTGTGATAAGGATGTGCACATCTGCGAGCACCAGCGTCCGT-
GTCAGAACAGCGCCCGCTGCATCAACGACCGGGAGGGCGATTACTCCTGCGTCTGC-
CCCGACGGCTTCCACGGCAAGAACTGCGAGGTGAAGAGGGGCCCGTGCGAACTCGCAGGATCTG
CGTGTCAAAATGGCGGCACCTGCTTGGACAACAACGGCTACGCTGACGCTTTTGC-
CTGTCGCTGCCTGGCTGGCTTCGTTGGTGACCTCTGTGAGCTCGATGTGGATGACT-

GCCTGATGCGCCCCTGCGCCAACGGTGCCACCTGCCATGACGGCATCAACCGCTTCTC-
CTGCAAGTGCCCGGCGGGCTTCGAGGGGCGCTTCTGCACCAGCAACTTGGACGACT-
GTGCCTCCCAGCCGTGCCGCAATGGCGGCAAATGCTACGACCGGGTGAACGACTTTGATTGCGTCT-
GCCCCGAAGGCTACGCGGGTAAATCCTGCGCCACGGTCTTGGAACCACAGCGGGAA-
GAGCAAGTGCAAACGGCCCCCAGGAATGCCCAGCGCGTCAACTATTTTACACCCGAAAGT-
GCCACCCAGGTCCCTCCGCAAGGAACTCGCCCTCAGCCCATCGGTAAGCCCGACGCT-
GCCAGGCGGAAGGGCAATCAGTCAGAGGCATTAAGCGGTGAGCGGCGAGCAGGAGGGCT-
GTTGAAAATCTCAGTGAAGGAGGTGGTGGCACAGGAGGAGTCGGGGCTGGCGGA-
GACCCGTTTCGTCATCCTGGCCGTCTTTGGCGCCTGCACGCTGCTCCTGGCCTTGGT-
GACGGCCACTCTGGTCCTGTGGAGCCACTGGCAGGGAAGGCCAAGCAGTGAGGCTCAGCGC-
CCGGACTCCGCCTCCAGACCAGAGAAGAAGCAGCTCAACGCGGAGGAATATGAGAGC-
CACCTCCCACTGAGACATAACCAGCTAACCCAAAAACTCAACAGCTTTGATGTCTTATAA

Zebrafish *Dlk2*

ATGAAACTCGCTGTCGTTCTGCTGCTCTGTGGCTGCTGTGTGCTGTTTAAACACAACT-
GTGAAGCTCAAGTTTTATTTTCCTCAGAAGAAACGTCTCCGACTCCATCAGCCAGTAACT-
GCACGTGTGAAATTGGCCACGGAAAATGTGCCGAAAATGGCGACTGCAGGTGTGATC-
CGGGATGGGGCGGGCCGATGTGTGACGACTGTGTTCGGATGCCCGGATGTGTCCACG-
GCACCTGTCATCAGCCCTGGCAGTGCTCCTGCATGGACGGGTGGGCAGGAAGATTCT-
GCGACAAAGATGTTTACGTGTGCTCCAGACAGCAGCCGTGTCATAACGGGGCCACTTGT-
GAACTGAGTGACTCTGGAGATTATAGCTGCTTGTGTCCTGAAGGCTTCCACGGCCGGGACT-
GTGAACTCAAAGCTGGGCCCTGCCAAAAGACCAAATCTCCCTGCAAGAACGGCGGTCT-
GTGTGAGGATCTGGGTGGTTACGCTCCAGAACTGTCCTGTCGATGCCTTGCAGGATTCAC-
CGGTGCCCGCTGCGAGACCAACATGGATGACTGCCTGATGCGCCCCTGTGCCAACG-
GTGCCACCTGTTTGGACGGCGTGAATCGTTTTTCCTGCCTGTGCCCTGCCGGATTCACAGGACGTTT
GCACCATCAACCTGGACGACTGCGCCAGCCAACCCTGCCTAAACGGAGGACGCTG-
CATAGATCGAGTCTCCAACTTCCAGTGCGTCTGCCCTCTAGGATTCACCGGGAGAACTTGC-
GAGTTGGTATCTCCAACCAAATCTCCGCTTAAAGCTGAACACAACCCAAACATGACGCT-
GAAGCCCTCCCATTGGACGACTCCAAGCGGAGGCGAGGAACGCCTGCTTAAGATCACTTT-
TAGAACTCCAGCCGGTGGAGAAGGGCTGTCGGAGTTTCAGCTCATCGTTCTGCTGGTTT-
TAGGTGGGATGACGCTGGCTGTAGTGGGATTAACAGCTGCTCTGGTGCTTCGCGGGTATTTCCAGGA
CGATCGGCTAGCTGTCAGTGCAGACCGGCTCACCGGACGCAGAGGAAACATTCGCAACAGGAGT-
GCAAGATCAGTTTCCTCCAATCTCCGGAGAAGAAGAGGCTGAACACTGATGTTATT-
TAG

Medaka *Dlk2*

ATGGCGCCGGTCCGAGCTGAAGGCGTCCTGTTGCTCCTGAGCTGCTGGTTTGTCCTC-
CACATCCAGTCATCAGCAGGTCAAGGAAGTGACTGCAGCTGCAACATGACCAACAGTCGCT-
GTGATGAGTCTGGAATATGCAGGTGTGACCCTGGCTGGGAAGGTGAACACTGCGATCGCT-
GCGTGCTCATGCCTGGCTGTGTGCACGGCTCCTGCCAGCAGCCATGGCAGTGCACAT-
GTGAGCCTGGATGGGGGGGGCGATTCTGTGACAAAGATCTTAGCGTGTGCTCAAATCAGCAGC-
CATGCCGGAATGGTGCCACCTGTGCAATGAAGGACAGCGGAGATTTTACTTGTCTGT-
GTCCACAAGGCTATCATGGCCACCTGTGCCAACGAAAGTCGGGGCCATGTCATCAAATCAGGTCT
CCTGTAAAAATGGTGGCCTTTGTGAAGACGCTGATGGTTTTGCTGCAGATCTTACCT-
GCCGCTGTCTGGCGGGTTTCACTGGATCGTTTTGCGAGACAGACATAGACGACTGTCT-
GTTGAAGCCATGCGCCAACGACGCCATCTGCCTGGATGGCATCAATCGGTTCTCAT-
GCATCTGTCCCAGTGGCTTCACTGGACGCTTCTGCACCGTCAACCTGGACGACTGT-
GCTAGTCAGCCCTGCCTGAATGGCGGCCGCTGCCTAGACCTTGCGGGGGGCTTTCGCT-
GTATATGTCAGCTGGGTTACATGGGAAACACCTGTGAGATGTCGCTCAGCAGCCCCAACTG-
GACCACAAAGGGGGAGAAGGGAAAAGGCAAAAGAAGCAGCAACATCACTCAACATGGGAACA-
GACTGATGAAGGTGACAGTGAGCGACCGTGGAATAGCCAGCCTCTCGGACATTCAGCT-
TATTGTTGTCGTGGTTCTGGGGGGAGTGACTTTGGTAGCGGTGGCACTAACGAGTG-
GTTTGGTGCTGTGGGGCCGTTGCCAAAACTGTAGTTACACCGCCGGCTGGTCACCGC-
CATGCTCTCAAGGAGCCGAGAGGAGCAGACGGCGAGGACAGAGTGAAACACAGCAAT-
GCCAGATCAGCTTTCTGAACTCGGTAGAACCACAGAAGAAGTTAAATTTGGAGGCT-
GTTTAA

Australian ghost shark *Dlk2*

ATGAGAGGGATCAGAGACTGGGGACTTCCACTGTGGGGCTTGGCCTGTTTTTTGTGCTCGC-
CCAGCATGGCCGCAGGTGCAGAAGACGTGCAGTGTAATCCTGGTTGTAACCTATTA-
CATGGTCGCTGTGAGTCAAGCGAATGCAGGTGTGATCCCGGCTGGGAGGGGGAGCT-
GTGTGAACGTTGTGTCCGTTCTCCGGGCTGTGTGCACGGCACCTGTCACCAACCCTG-
GCAATGCATCTGTCAGACTGACTGGGCTGGACGATTCTGTGACAAGGACATTCATGCTTG-
CACCCACCAGCAGCCGTGCCAGAATGGTGGGAGCTGCTTCGACACAGGCGAGGGC-
GAGCACTGGTGCTCGTGTCCGGATGGTTTCTATGGGAAGAACTGTGAGCTGCGGGCAGGAC-
CCTGCACTAAGTCCAGGTCTCCCTGTAAGAATGGTGGGACGTGCTTGGACCGGGACG-
GTTTTGCGGACACGCTCACCTGTCGTTGCTTGGCTGGCTTTGTGGGGCCGAGGTGC-
GAAGAGGACGTCGACGACTGCCTGATGCGTCCATGTGCCAATGGTGCCACCTGCCGGGATG-
GAGTGAACCGTTTCTCTTGCATATGCCCACAGGGCTTTGAAGGCCGCTTCTGCACCGT-
CAACTGGGACGATTGTACCAGCGGTCCATGCCAGAATGGTGGTCGGTGCTATGACCGGGTG-

GCCGACTTTGATTGCGTCTGTCTTAAAGGCTACTCTGGGAAGACCTGCTCTTTACCT-
GTCCCTCAGTGGAGGAAGGAGCGGCCAGCGCTGAGCCGCCGAGATCCTGGGATTAC-
CATTCCTCAGCCAGACCATGCCACTCGGCAGGGATTGGCAGCGTTACCCGCTGCCAGC-
CCCACACAGCCCGTGCGGGAACAGGAGAGGCTGCTGAAGGTGGAGGTGAAGGAGCT-
GCTGTCAGAACCCAGCTCAGCACTAGCCCACAGCCAGATAGTCGGCCTGAGTGTGTTCGGGGC-
CTTGACGGCACTGCTGGTCTCAGTGACGGTCGTTGTGATGCTCTTGTGCCGGCGGCAA-
GAAGAGCCCTCCCGCAAGCCCCCCCGATCGGGAGAGAGGGGCCAAGCTGAGGGGGC-
CATTAGCTTCCTACAACCCCCTGCTCCCGAGAGCAGGAAGGAGCTTTATCTTGATCTAAT-
GTAG

A.1.5 Alignments of DLK1 (close-up view)

A.1.6 Alignments of DLK2 (close-up view)

A.2 *In situ* hybridisation sense controls

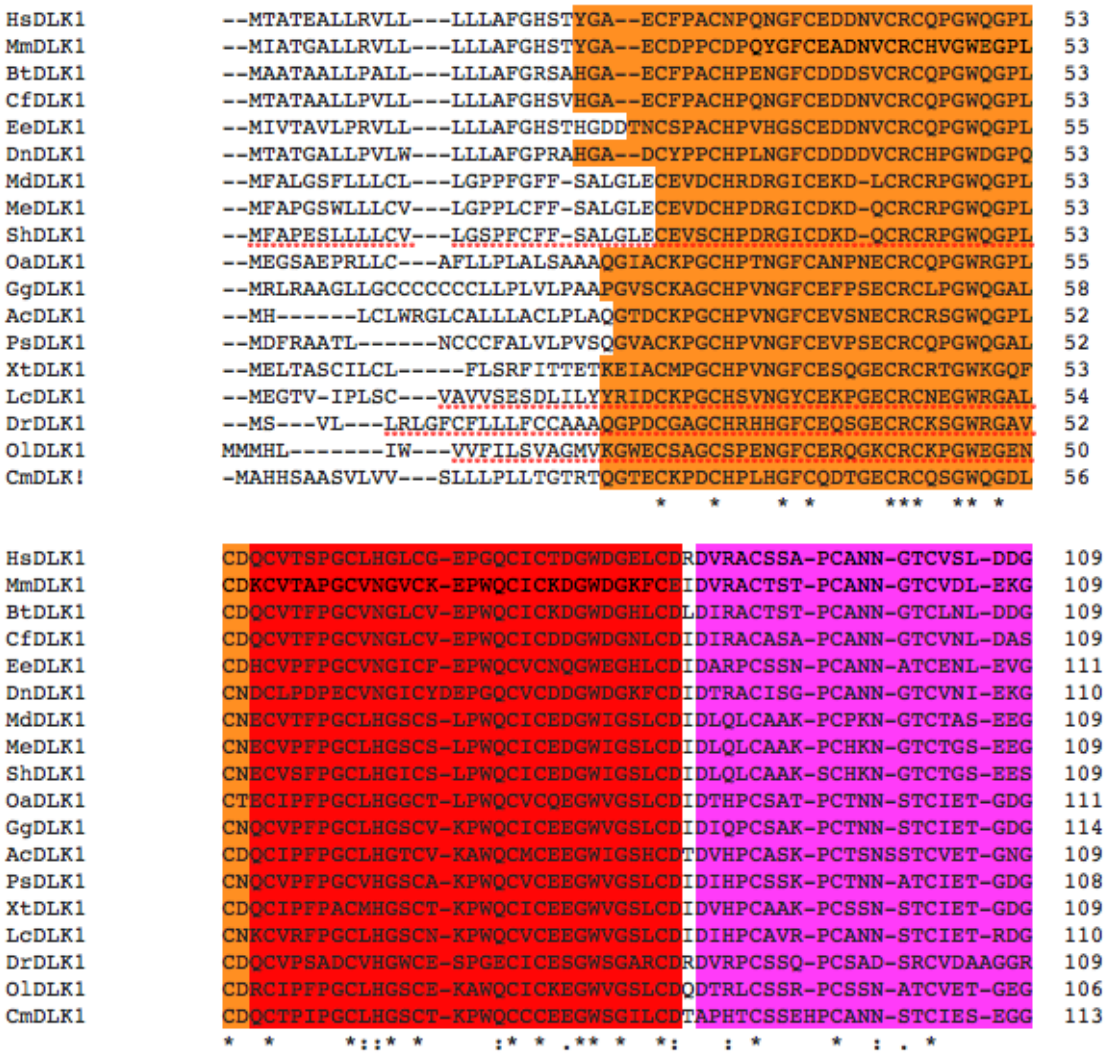

Fig. A.1 **Close up of alignments of DLK1 protein sequences across various vertebrates in section 2.3 part 1**

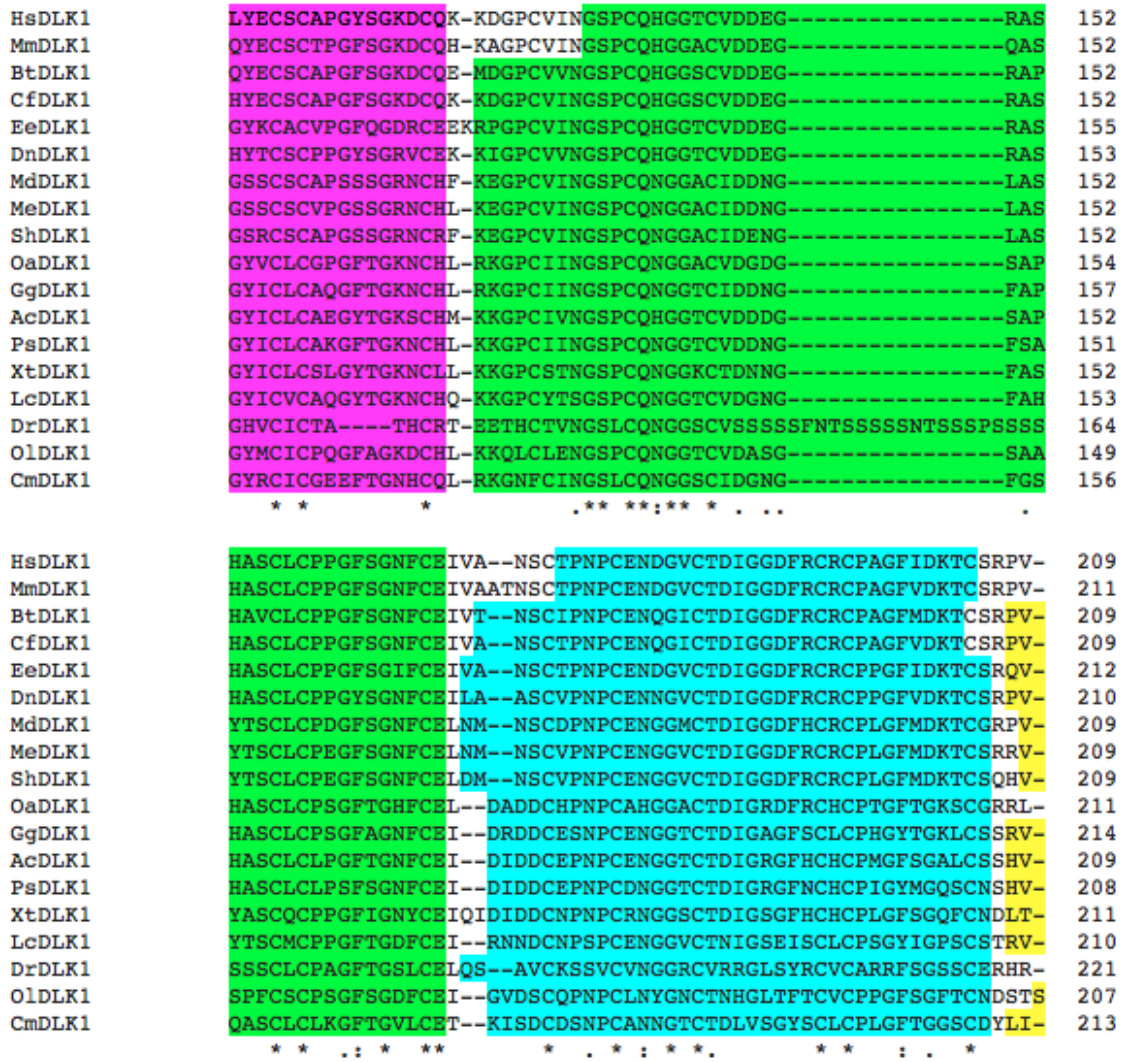

Fig. A.2 **Close up of alignments of DLK1 protein sequences across various vertebrates in section 2.3 part 2**

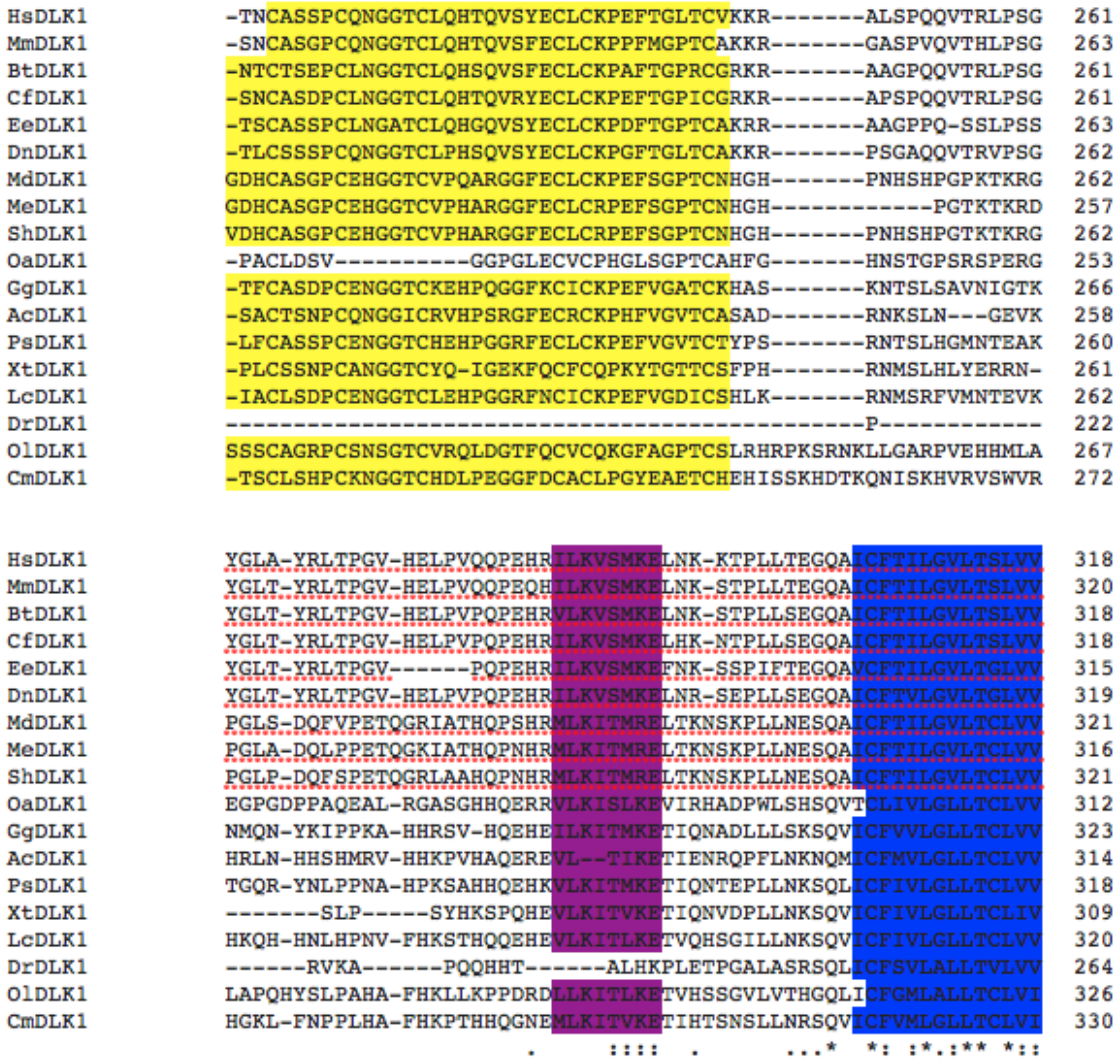

Fig. A.3 **Close up of alignments of DLK1 protein sequences across various vertebrates in section 2.3 part 3**

```
HsDLK1          LGTVGIVFLNKCETWVSNLRYNHMLRKKKNLLLQY-----NSGEDLAVNIIFPEKIDMTT  373
MmDLK1          LGTVAIVFLNKCETWVSNLRYNHMLRKKKNLLLQY-----NSGEELAVNIIFPEKIDMTT  375
BtDLK1          LGTMGIVFLNKCEAWVSNLRYNHMLRKKKNLLLHY-----NSGEELAVNIVFPEKIDMTT  373
CfDLK1          LGTMGIVFLNKCEAWLSNLRYNRMLRQKKNLLLHY-----NSGEDLAVNIIFPEKIDMTT  373
EeDLK1          LATVGIIFINKCEAWVSSLRYSHMLRKKKSLLLQA-----SSGEDLAVNIIFPEKIHMTT  370
DnDLK1          LGTVGIVFLNKCEAWVSNLRYGHLLRKKKNLLLHY-----NSGEDLAVNIIFPEKIDMAT  374
MdDLK1          LGTISIVFFNKCEVWLSNAKYSRLLRKKKNLLLRY-----SNGDEHTINIILPEKMNLKS  376
MeDLK1          LGTVSIVFFNKCEVWLSNAKYSRLLRKKKNLLLRY-----SNGDEHTINIILPEKMNLKS  371
ShDLK1          LGTISIVFFNKCEIWLSNAKYSRLLRKKKNSLLRY-----SNGDEHTINIILPEKMNLKS  376
OaDLK1          LGTTAIVFYSKCETWLANAKYSRLLRKKKRRLMTS-----NNGETLSVNIIFPEKVKLTS  367
GgDLK1          LGTTGIVFFSKCEMWLANAKYSHLLRKKKNFLLKS-----SNGENLSVNIIFPEKIKLTN  378
AcDLK1          LGTTGIIFFSKFERWLANAKYSQLVRKERDDFLKA-----NEGENLSVKIIFPDQTEE--  367
PsDLK1          LGTTAIVFFSKCEIWLANAKYSHLLRKKKNCFLQS-----NNGENLSVNIIFPEKIKLTN  373
XtDLK1          LITTGIVFFSKCETWFANAKYSRLLRKKKNIYMQR-----SRGEDRDVKIIFPEGVKFED  364
LcDLK1          LVTTGIVFFSKCEMWLANAKYSHLIRKQRNRFMKS-----NSGEELSVNIIFPEKIKLTN  375
DrDLK1          LGSTAIVFFQRCEVWMANVRYRQLVAQQRELIQD----------QATVNIILPEKIKLSS  314
OlDLK1          LGTTGIVLFGRCETWLANAKYSQLVRQQREHLLREVGSPSQEEPEHSVNIILPEKIRLSS  386
CmDLK1          LGTTLIIFFSKCKMWMANAKYRQYLRKQKNHFLN--------DEETSVKIIFPDMSKLTN  382
                * :  *::  : : *.:. :* : : :::                 ::*::*:

HsDLK1          FSKEAGDEEI 383
MmDLK1          FNKEAGDEEI 385
BtDLK1          FTKEAGEEEI 383
CfDLK1          FSKEAGEDDI 383
EeDLK1          FNKEAGEEEI 380
DnDLK1          FSREAGEDDV 384
MdDLK1          YSKCLNEI-- 384
MeDLK1          YSKCLNEI-- 379
ShDLK1          YSQCLNEI-- 384
OaDLK1          YSTCSAAM-- 375
GgDLK1          YTKNYTAI-- 386
AcDLK1          ---------- 367
PsDLK1          YTKNYTDI-- 381
XtDLK1          CCRDYAST-- 372
LcDLK1          YSKSYTSI-- 383
DrDLK1          YSRHYTSI-- 322
OlDLK1          FGRHYTSI-- 394
CmDLK1          YRKSYISM-- 390
```

Fig. A.4 **Close up of alignments of DLK1 protein sequences across various vertebrates in section 2.3 part 4**

Fig. A.5 **Close up of alignments of DLK2 protein sequences across various vertebrates in section 2.3 part 1**

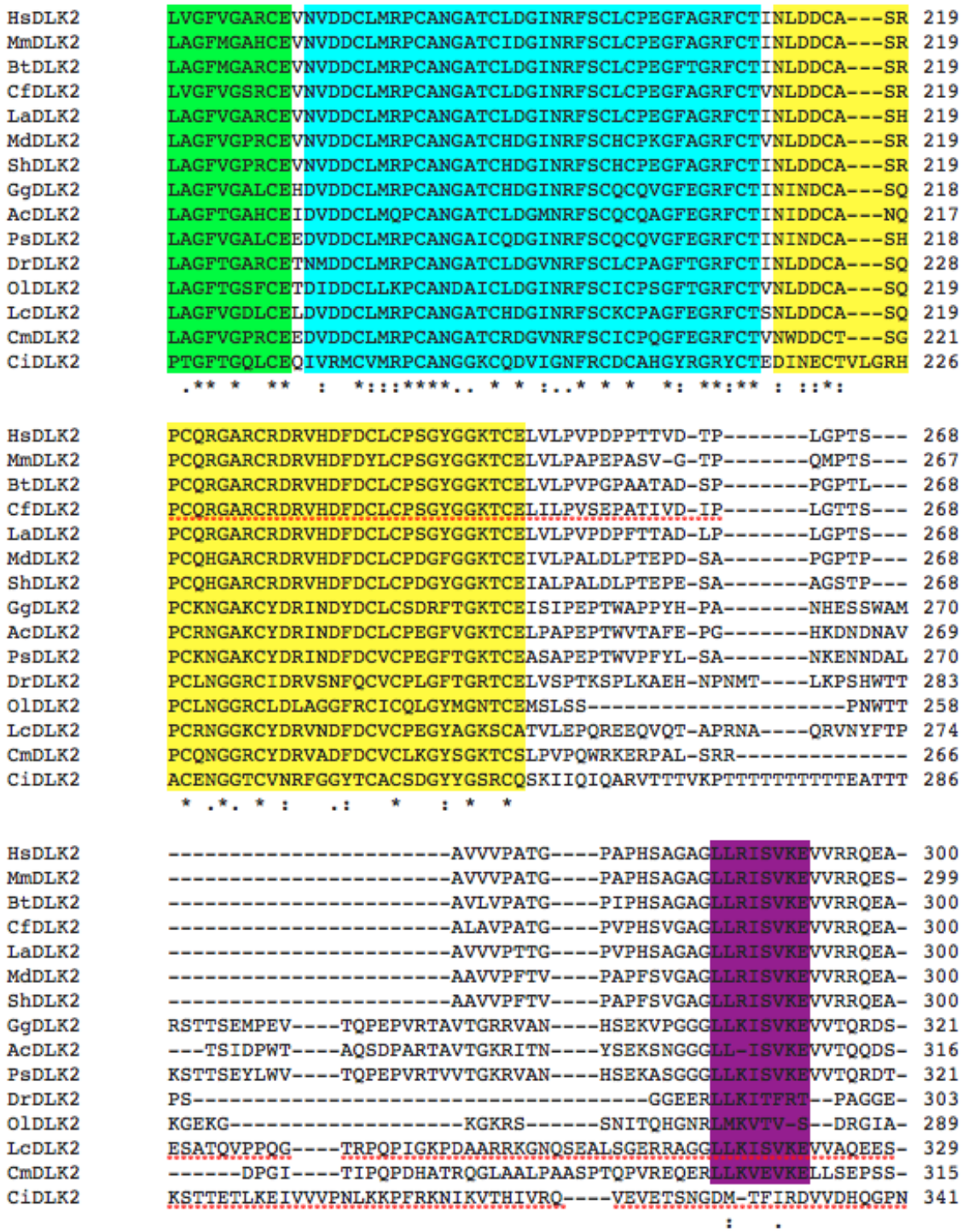

Fig. A.6 **Close up of alignments of DLK2 protein sequences across various vertebrates in section 2.3 part 2**

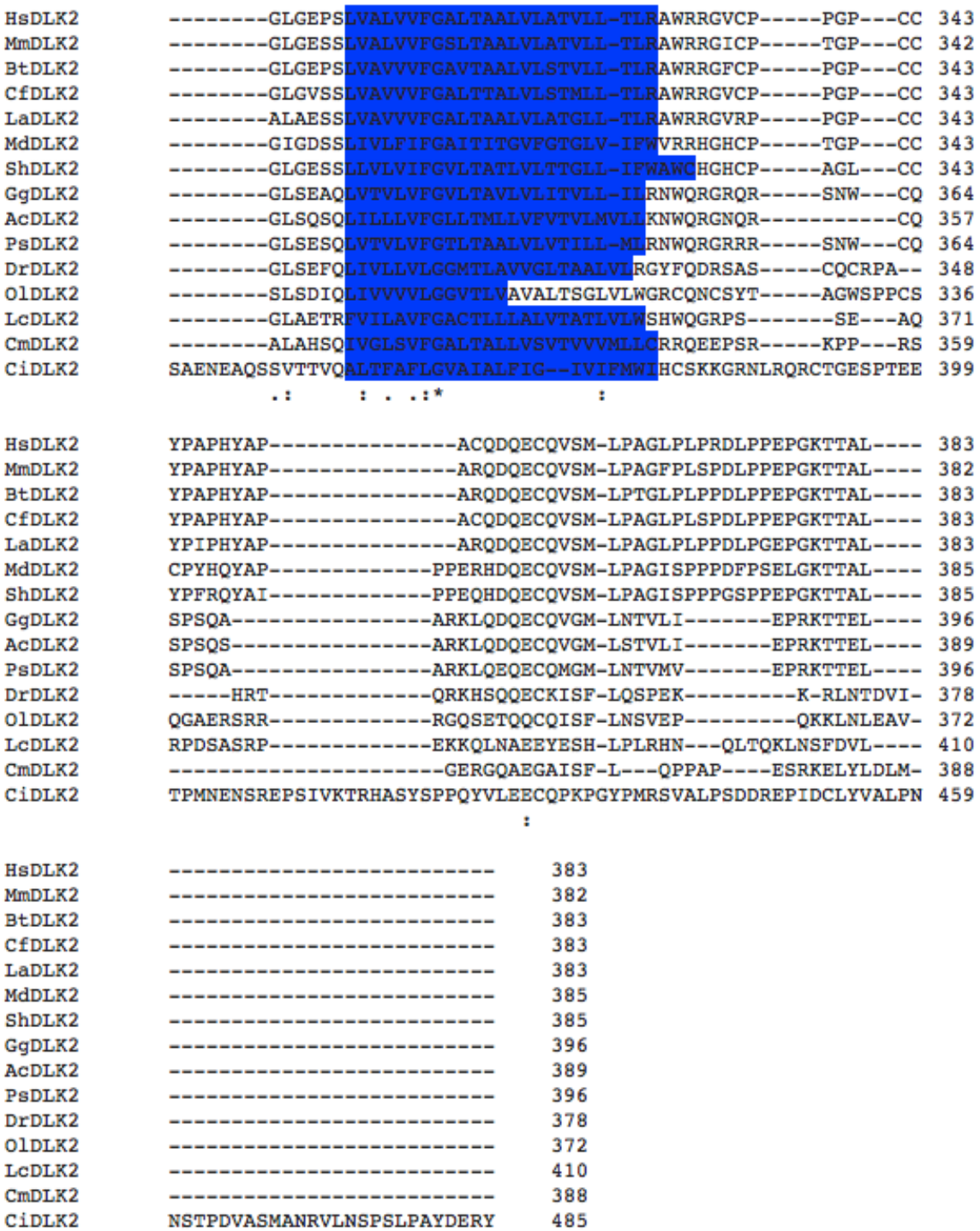

Fig. A.7 **Close up of alignments of DLK2 protein sequences across various vertebrates in section 2.3 part 3**

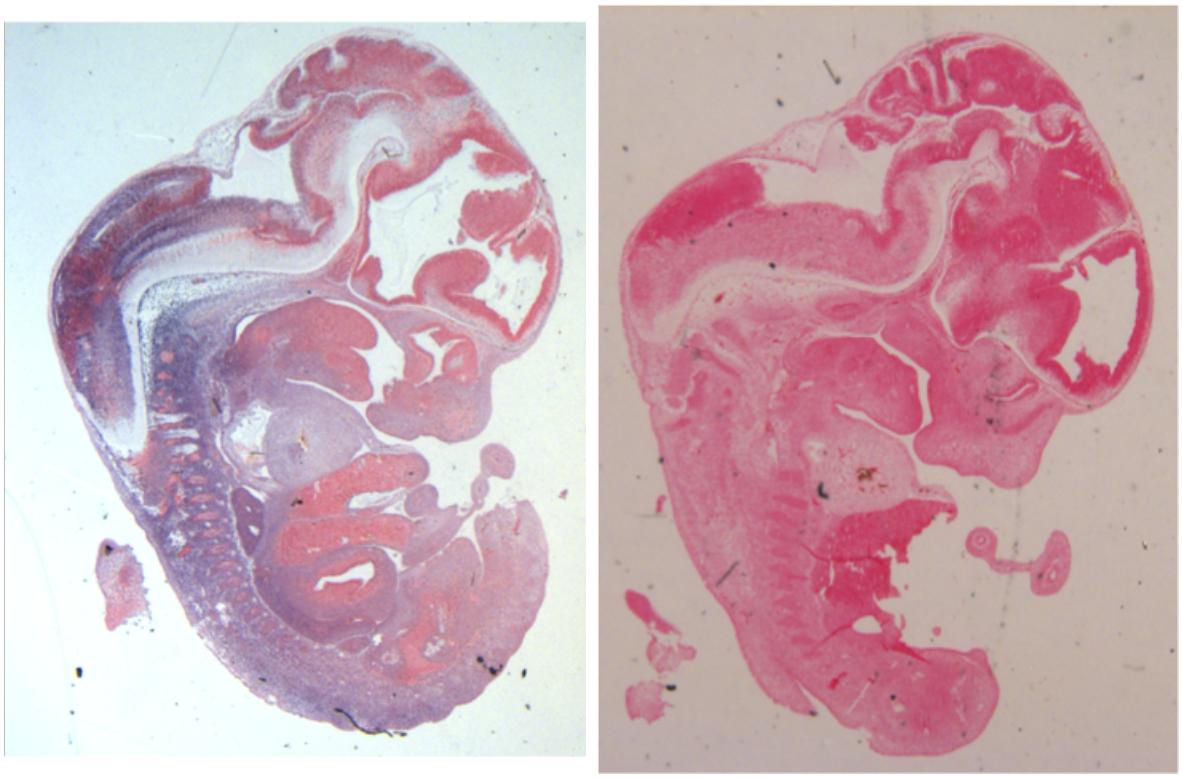

(a) Antisense

(b) Sense

Fig. A.8 **Antisense and sense *Dlk2* ISH on e12.5 wild-type embryos (N=3)**

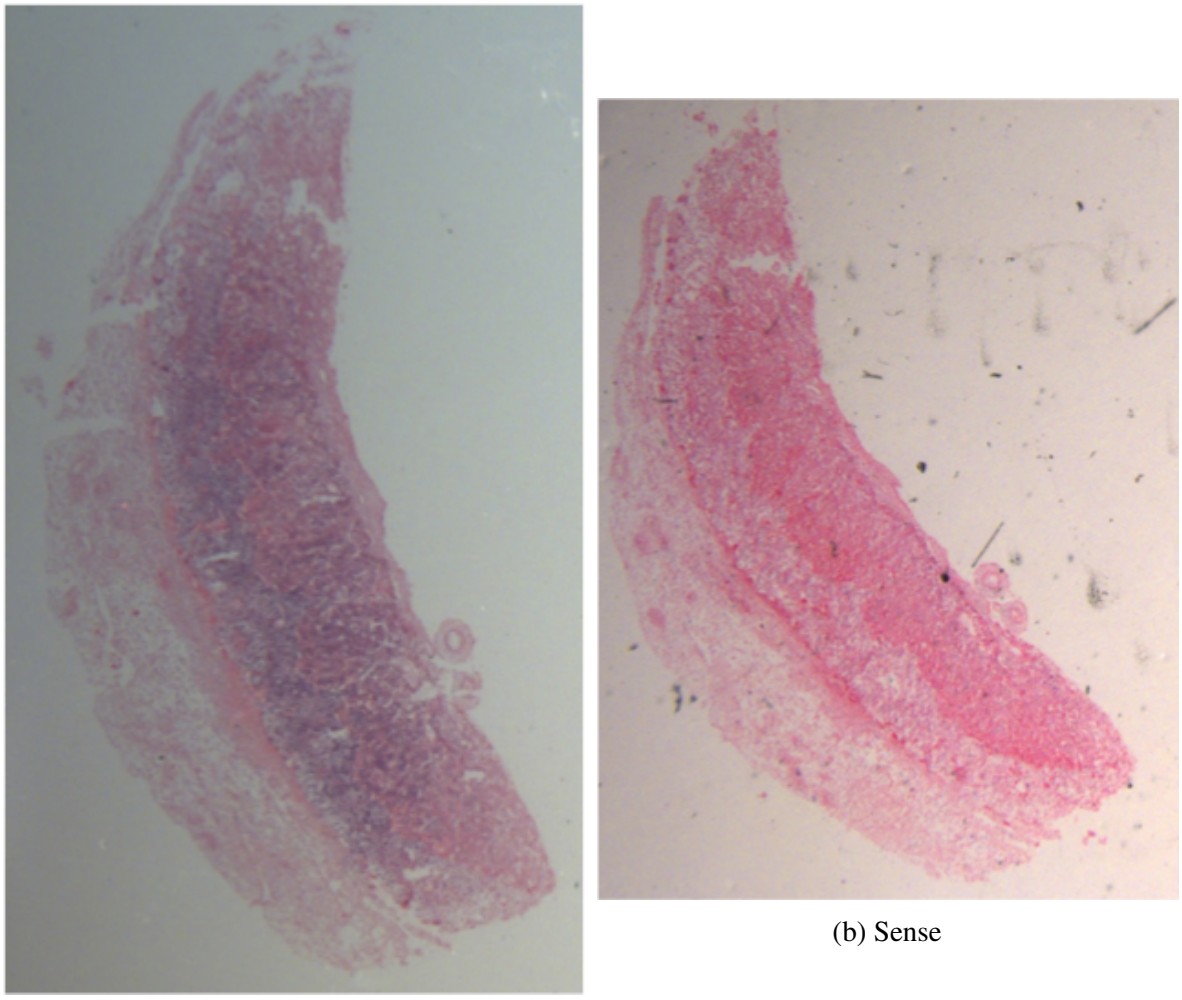

(a) Antisense

(b) Sense

Fig. A.9 **Antisense and sense *Dlk2* ISH on e12.5 wild-type placentae (N=3)**

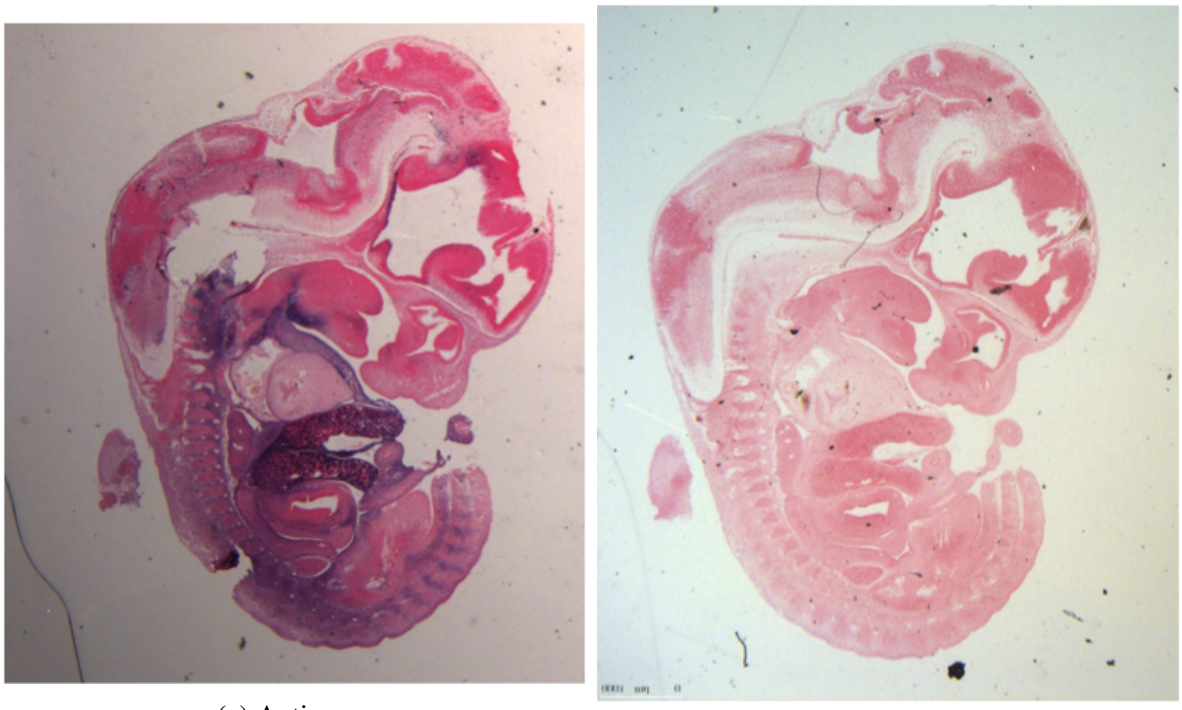

(a) Antisense

(b) Sense

Fig. A.10 **Antisense and sense *Dlk1* ISH on e12.5 wild-type embryos (N=2)**

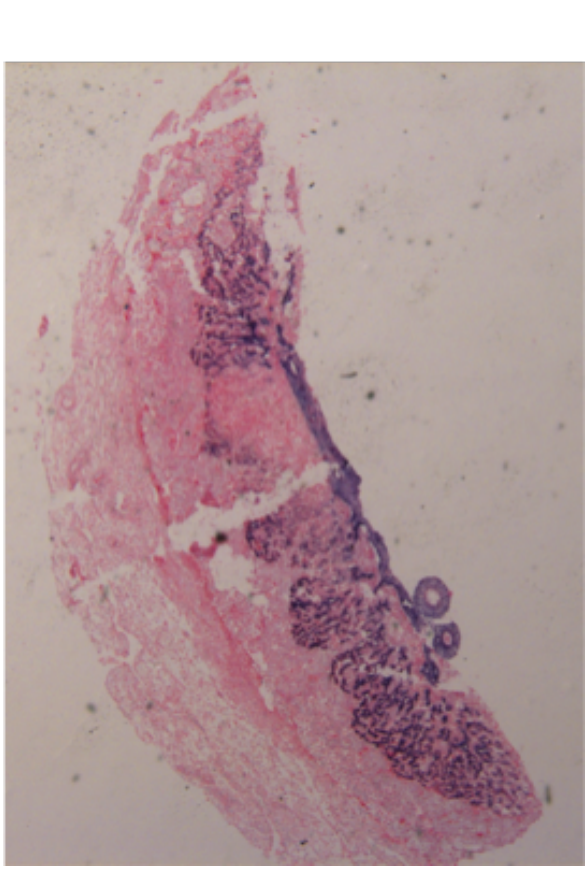

(a) Antisense

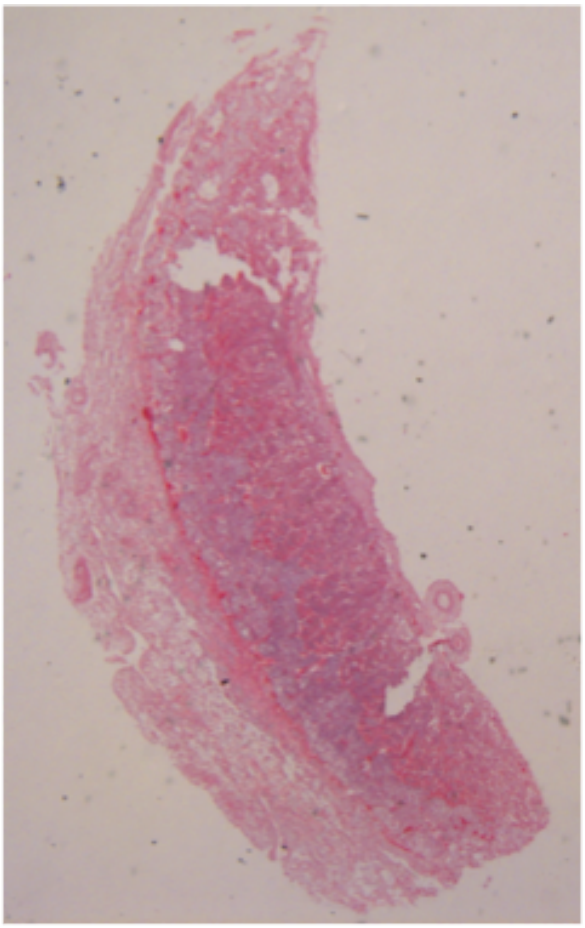

(b) Sense

Fig. A.11 **Antisense and sense *Dlk1* ISH on e12.5 wild-type placentae (N=2)**

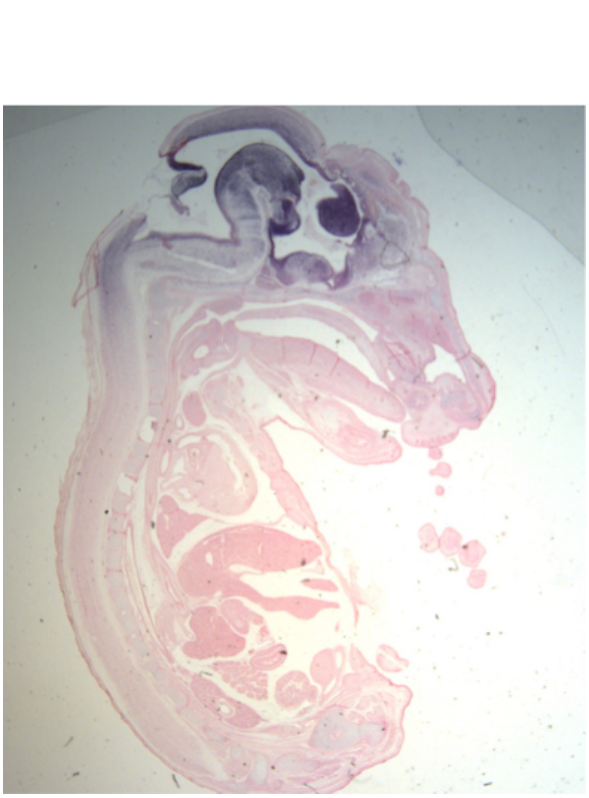

(a) Antisense

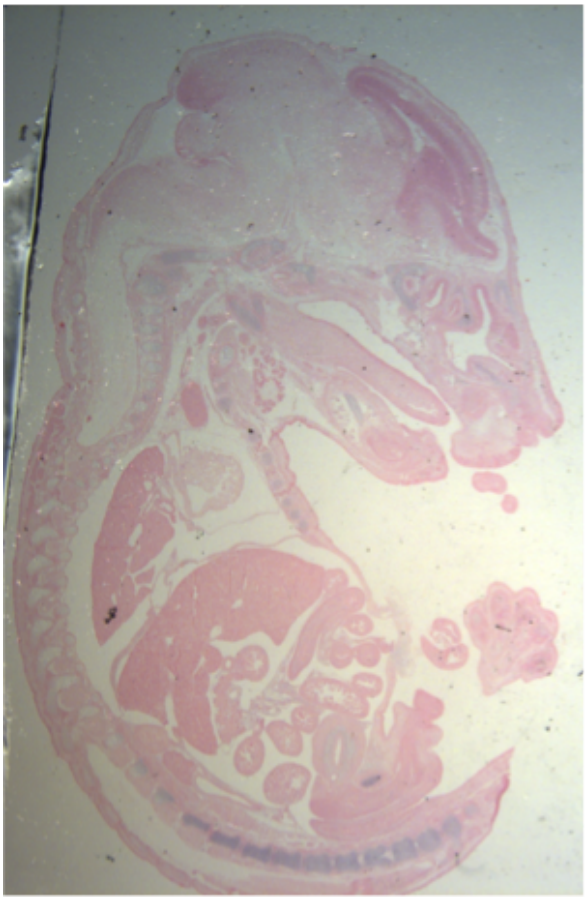

(b) Sense

Fig. A.12 **Antisense and sense *Dlk2* ISH on e14.5 wild-type embryos (N=4)**

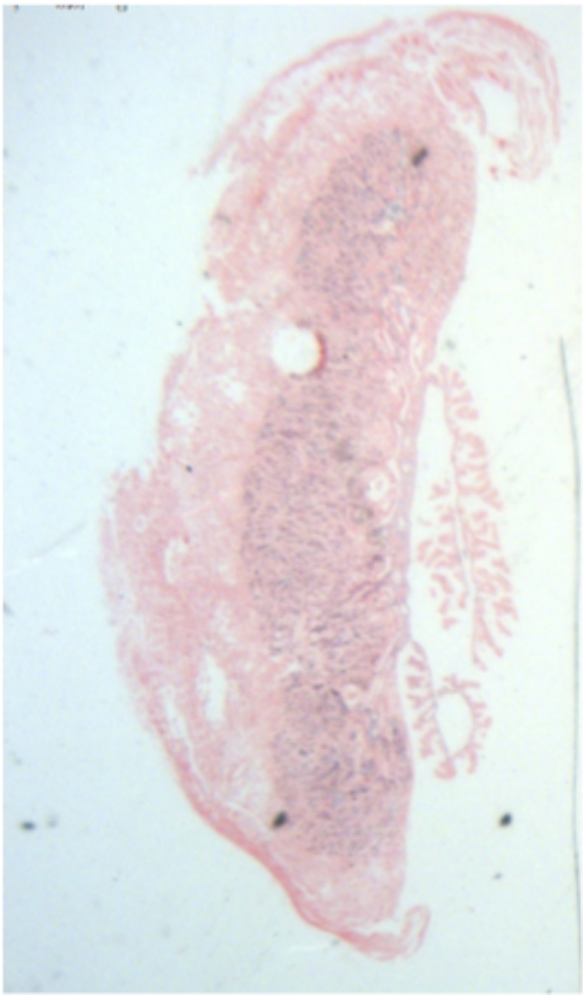

(a) Antisense

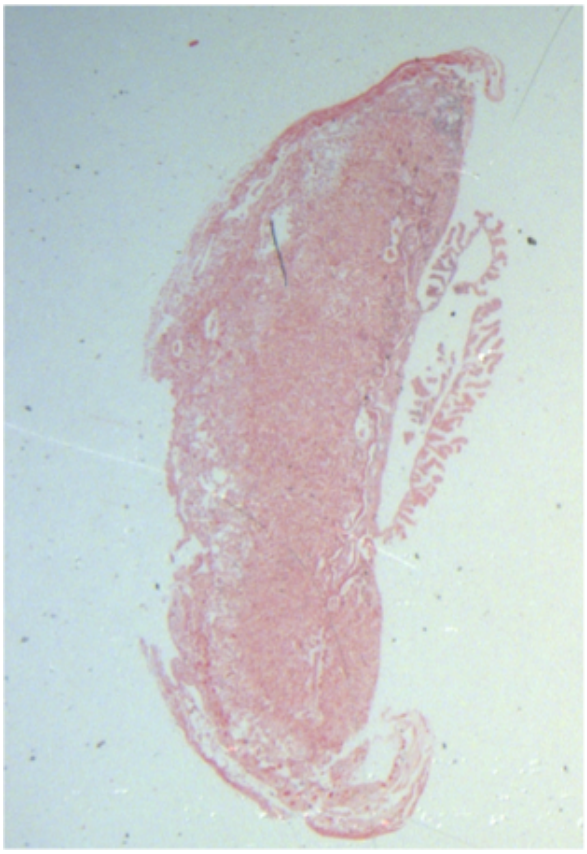

(b) Sense

Fig. A.13 **Antisense and sense *Dlk2* ISH on e14.5 wild-type placentae (N=2)**

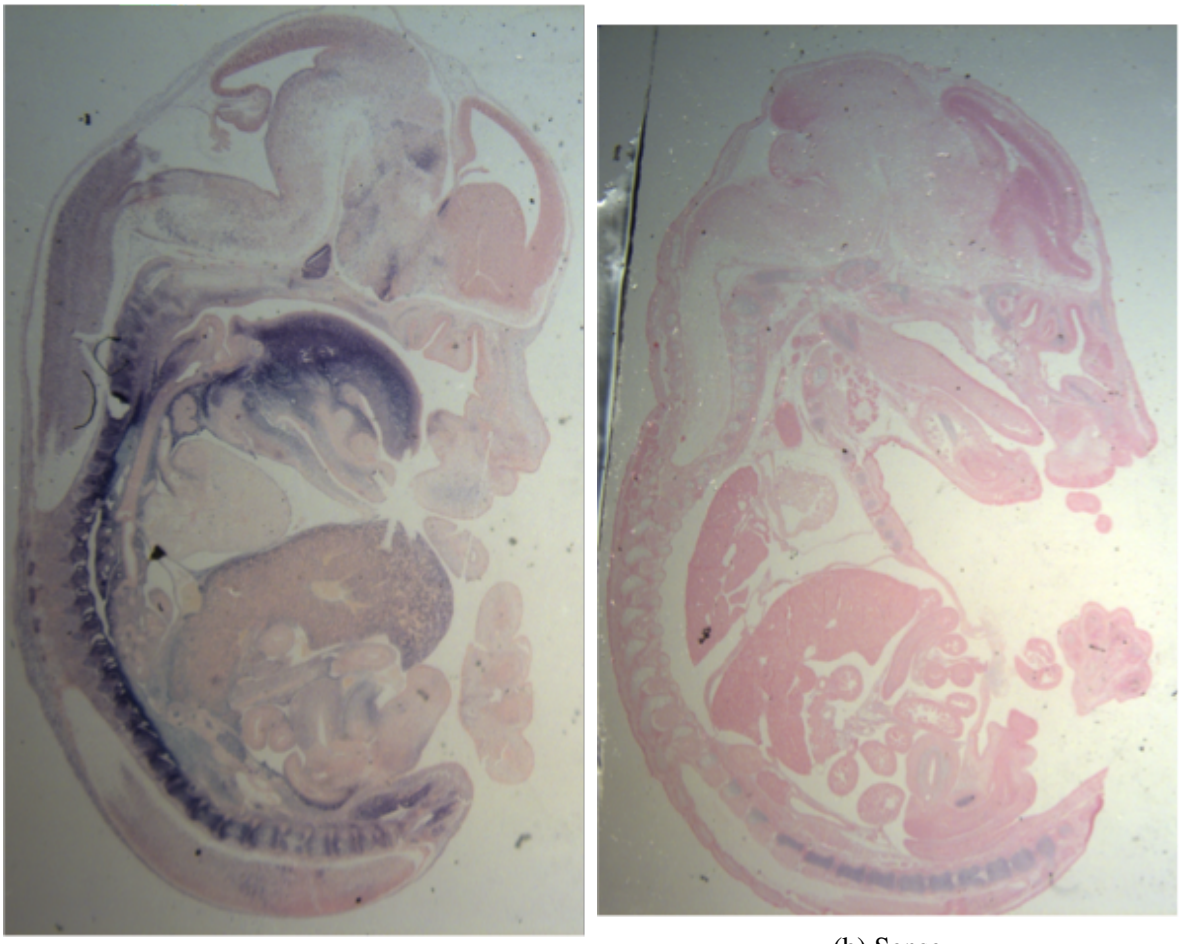

(a) Antisense

(b) Sense

Fig. A.14 **Antisense and sense *Dlk1* ISH on e14.5 wild-type embryos (N=4)**

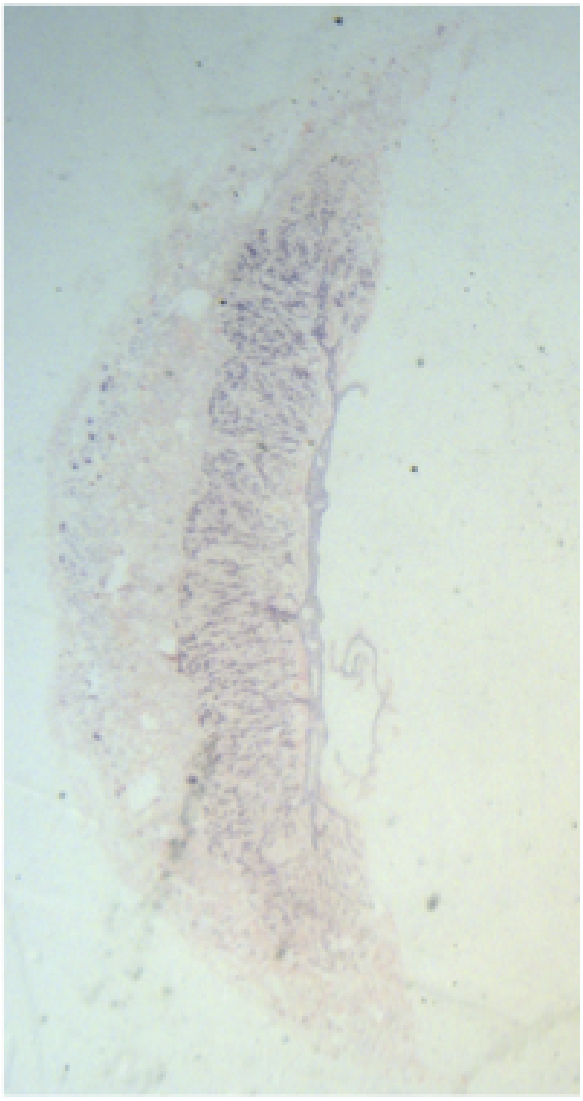

(a) Antisense

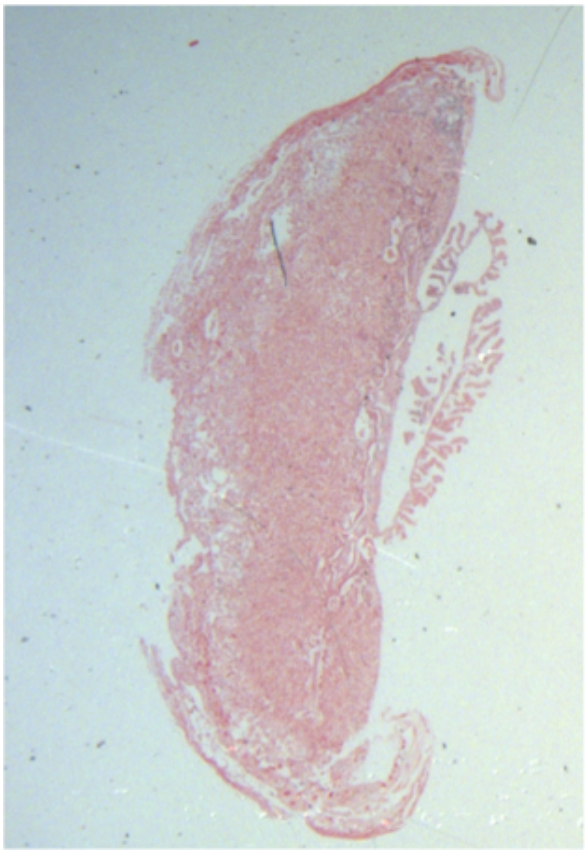

(b) Sense

Fig. A.15 **Antisense and sense *Dlk1* ISH on e14.5 wild-type placentae (N=3)**

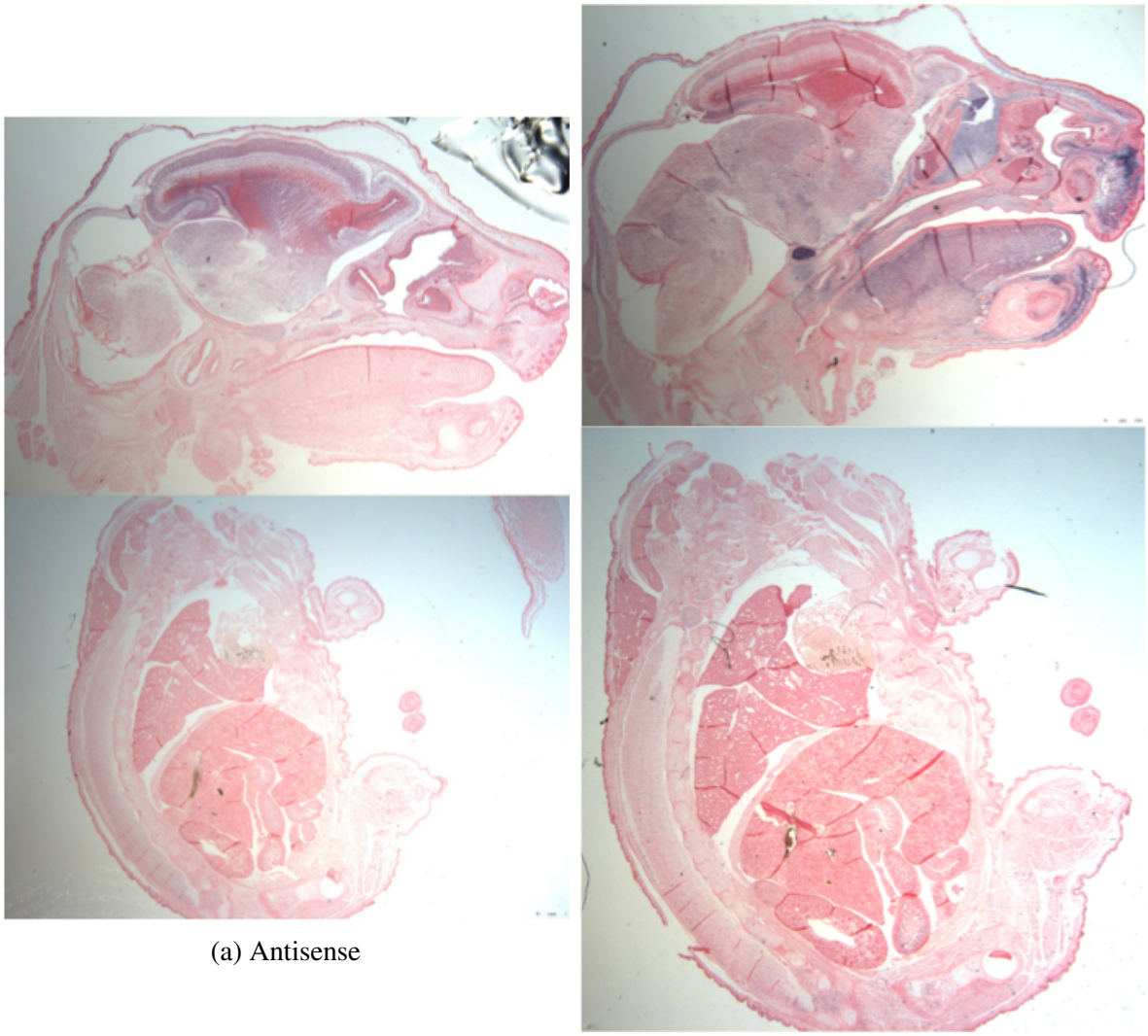

(a) Antisense

(b) Sense

Fig. A.16 **Antisense and sense *Dlk2* ISH on e16.5 wild-type embryos (N=1)**

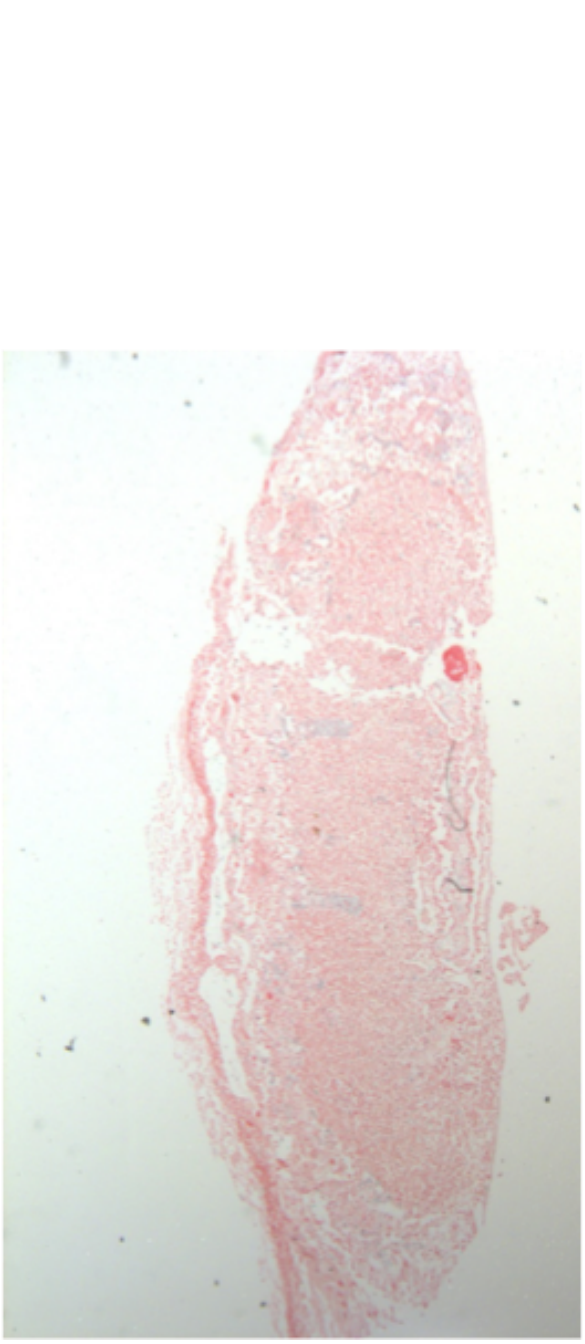

(a) Antisense

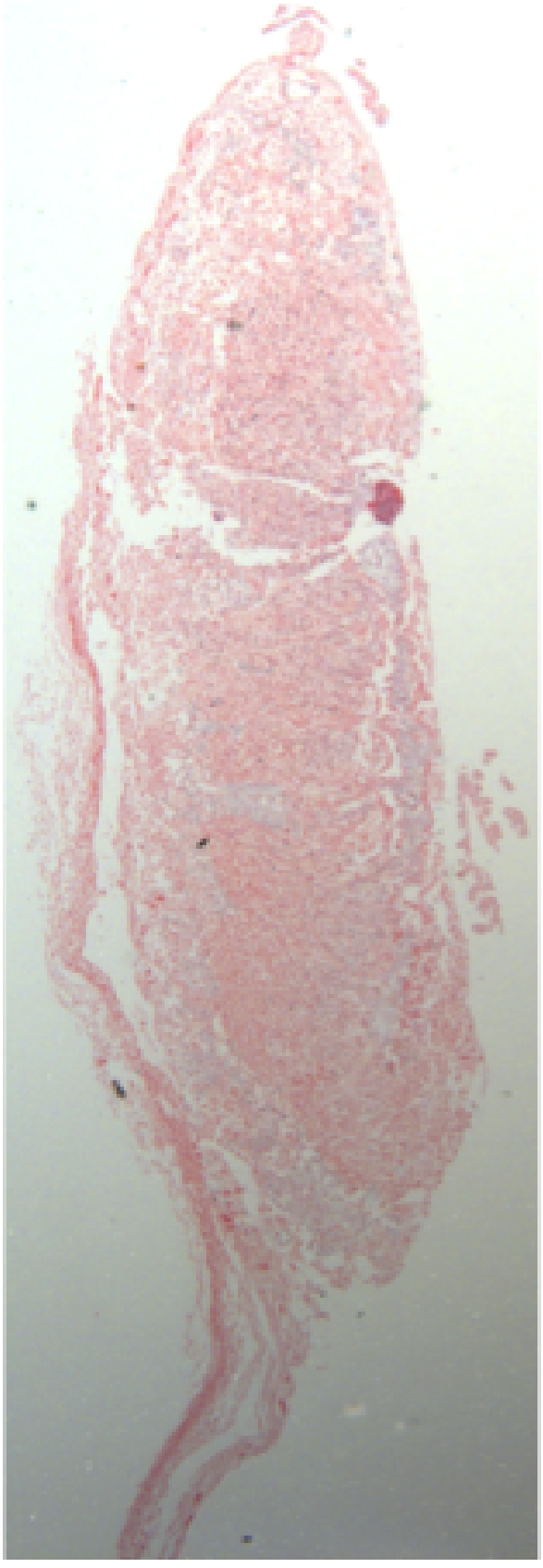

(b) Sense

Fig. A.17 **Antisense and sense *Dlk2* ISH on e16.5 wild-type placentae (N=1)**

A.3 DNA sequences of CRISPR generated *Dlk2* mutants

DLK2 exon5 13bp del

ATGCCCAGCGGCTGCCGCTGCCTAAATCTCGTGTGCCTGCTGTGCATCCTGGGGGGCAACCAGCCAGG
CTGCCAGAGCGGATGACTGCAGCTCCCACTGTGACCTGGCCCACGGCTGCTGCGCTC-
CTGACGGCTCCTGCAGGTGTGACCCAGGCTGGGAGGGGCTGCACTGTGAGCGCTGT-
GTGAGGATGCCTGGCTGCCAGCACGGTACCTGCCACCAGCCCTGGCAGTGCATCTGC-
CACAGTGGCTGGGCAGGAAAGTTCTGTGACAAAGATGAGCACATCTGTACCTCACAAT-
CACCCTGCCAGAATGGAGGCCAGGGGGTGGTGAGTACCACTGTGTGTGCCTGCCAGGCTTC-
CATGGACGTGGCTGTGAGCGCAAGGCTGGACCTTGTGAGCAGGCAGGCTTCCCGT-
GCCGGAATGGAGGGCAGTGCCAGGACAACCAGGGTTTTGCCCTCAACTTCACATGC-
CGCTGCTTGGCAGGATTCATGGGTGCCCACTGTGAGGTCAATGTGGACGACTGTCT-
GATGCGGCCTTGCGCCAATGGTGCCACATGCATTGATGGCATAAACCGCTTTTCCTGC-
CTCTGTCCTGAGGGCTTCGCTGGACGCTTCTGCACCATCAACCTGGATGACTGTGCCAGC-
CGCCCATGCCAGAGAGGGGCCCGCTGCAGGGACCGTGTCCATGACTTTGACTGCCT-
GTGCCCCAGTGGCTATGGTGGTAAGACTTGTGAACTTGTCCTACCTGCTCCAGAGC-
CTGCCTCAGTGGGCACCCCACAAATGCCCACCTCAGCTGTAGTTGTACCTGCCACGGGGC-
CGGCCCCTCACAGTGCGGGGGCGGGCCTGCTAAGGATCTCAGTGAAGGAGGTGGTACG-
GAGGCAAGAGTCTGGGCTTGGTGAATCTAGCCTGGTTGCCCTGGTGGTGTTTGGGTCTCT-
CACTGCTGCGCTGGTCCTGGCCACGGTGCTGCTGACCCTGAGGGCATGGCGCCGAG-
GTATATGCCCCACTGGACCCTGCTGCTACCCAGCCCCACACTATGCCCCAGCTCGGCAGGATCAGGAG
GCCAGGTTAGCATGCTGCCAGCGGGGTTCCCTCTGTCCCCAGACCTGCCCCCTGAGC-
CTGGTAAGACCACAGCGCTGTGA

DLK2 exon5 2bp del

ATGCCCAGCGGCTGCCGCTGCCTAAATCTCGTGTGCCTGCTGTGCATCCTGGGGGGCAACCAGCCAGG
CTGCCAGAGCGGATGACTGCAGCTCCCACTGTGACCTGGCCCACGGCTGCTGCGCTC-
CTGACGGCTCCTGCAGGTGTGACCCAGGCTGGGAGGGGCTGCACTGTGAGCGCTGT-
GTGAGGATGCCTGGCTGCCAGCACGGTACCTGCCACCAGCCCTGGCAGTGCATCTGC-
CACAGTGGCTGGGCAGGAAAGTTCTGTGACAAAGATGAGCACATCTGTACCTCACAAT-
CACCCTGCCAGAATGGAGGCCAGTGTGTGTATGGGGGGTGGTGAGTACCACTGTGT-
GTGCCTGCCAGGCTTCCATGGACGTGGCTGTGAGCGCAAGGCTGGACCTTGTGAGCAGGCAGGCTT
CCGTGCCGGAATGGAGGGCAGTGCCAGGACAACCAGGGTTTTGCCCTCAACTTCA-
CATGCCGCTGCTTGGCAGGATTCATGGGTGCCCACTGTGAGGTCAATGTGGACGACT-
GTCTGATGCGGCCTTGCGCCAATGGTGCCACATGCATTGATGGCATAAACCGCTTTTC-

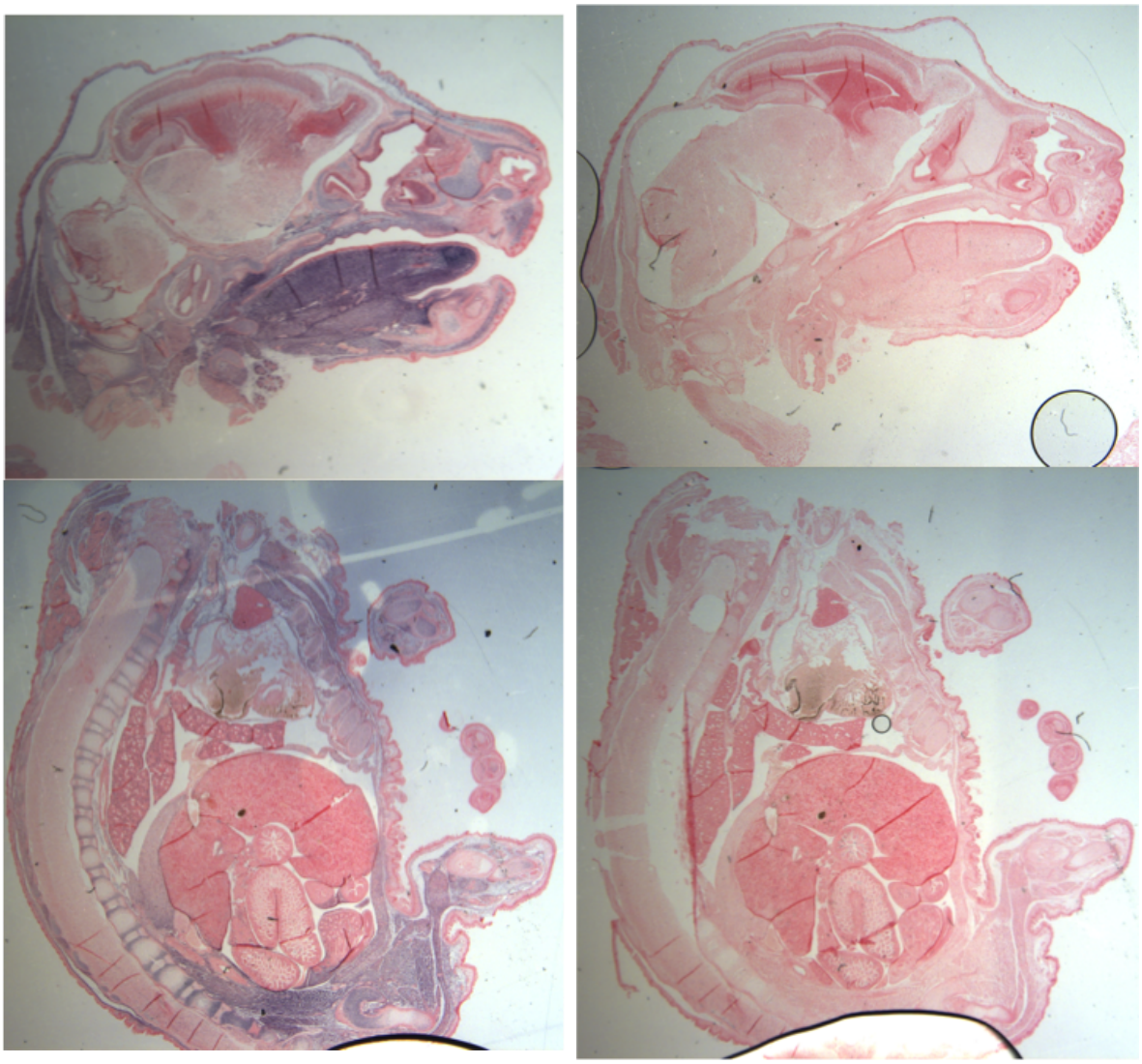

(a) Antisense

(b) Sense

Fig. A.18 **Antisense and sense *Dlk1* ISH on e16.5 wild-type embryos (N=1)**

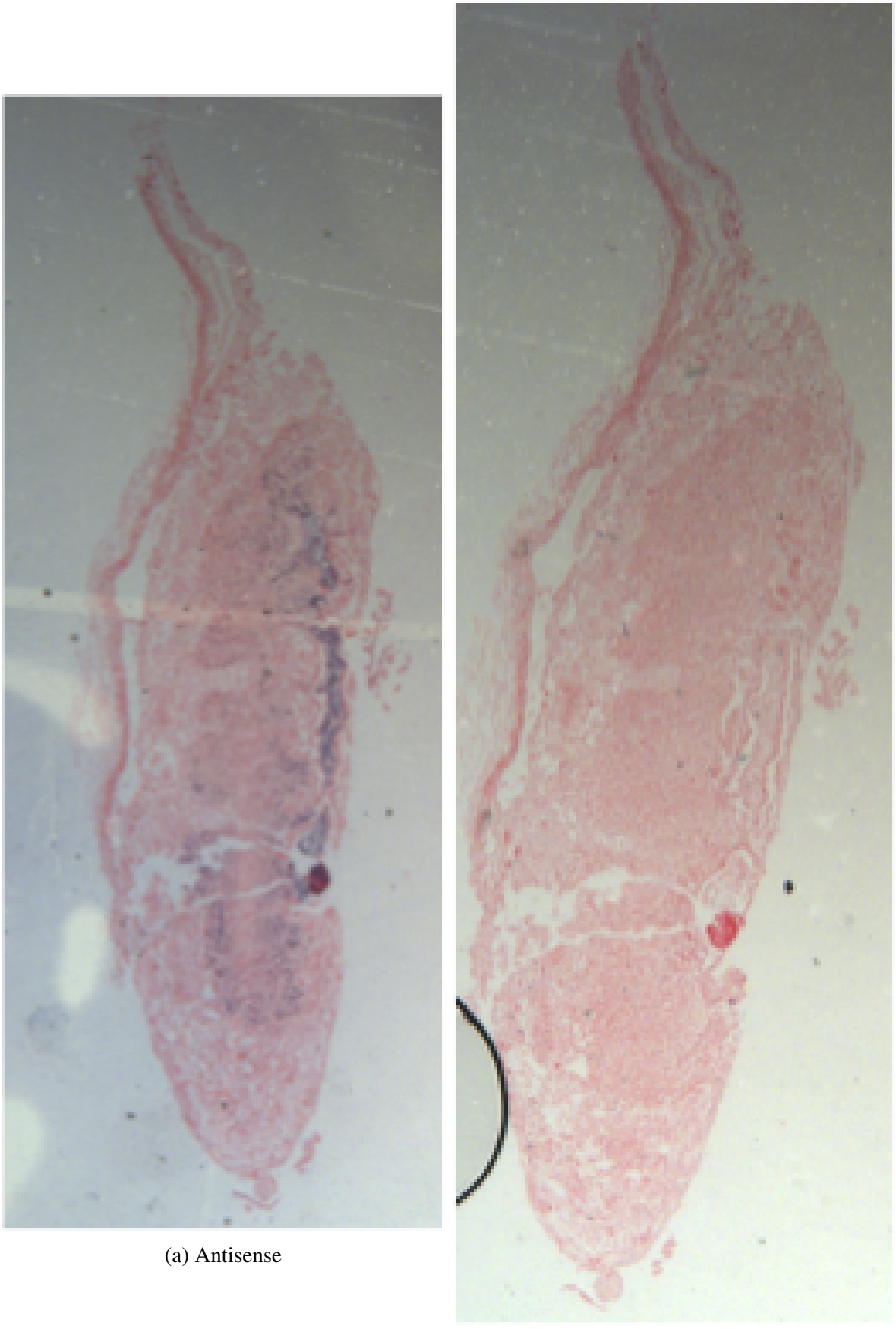

(a) Antisense

(b) Sense

Fig. A.19 **Antisense and sense *Dlk1* ISH on e16.5 wild-type placentae (N=1)**

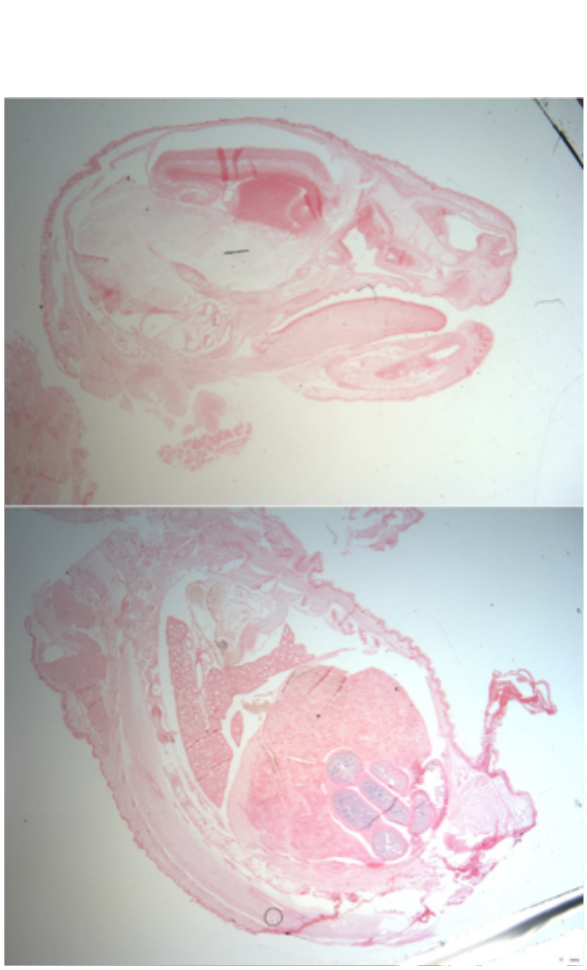

(a) Antisense

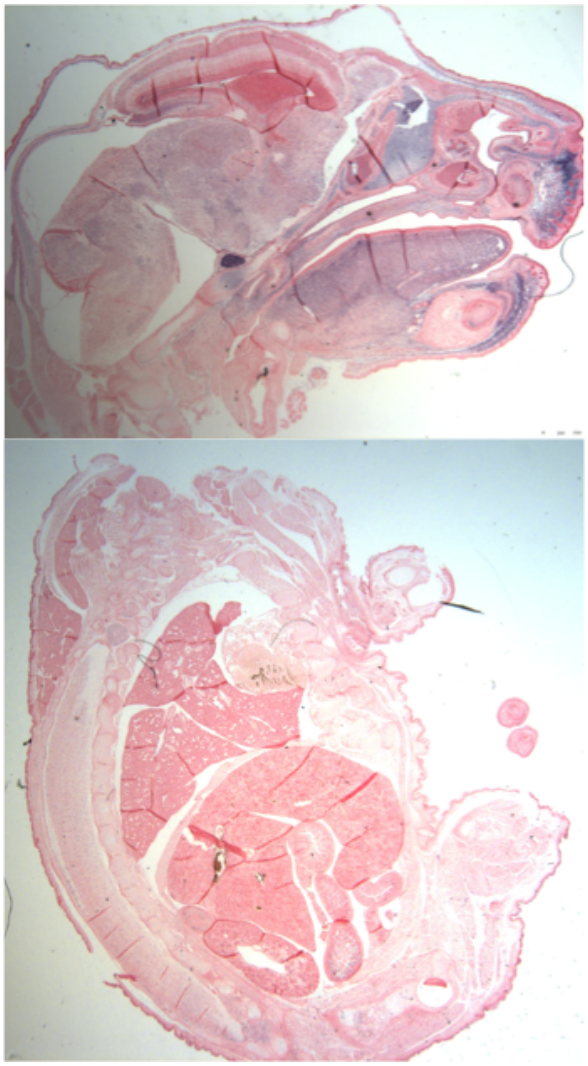

(b) Sense

Fig. A.20 **Antisense and sense *Dlk2* ISH on e18.5 wild-type embryos (N=3)**

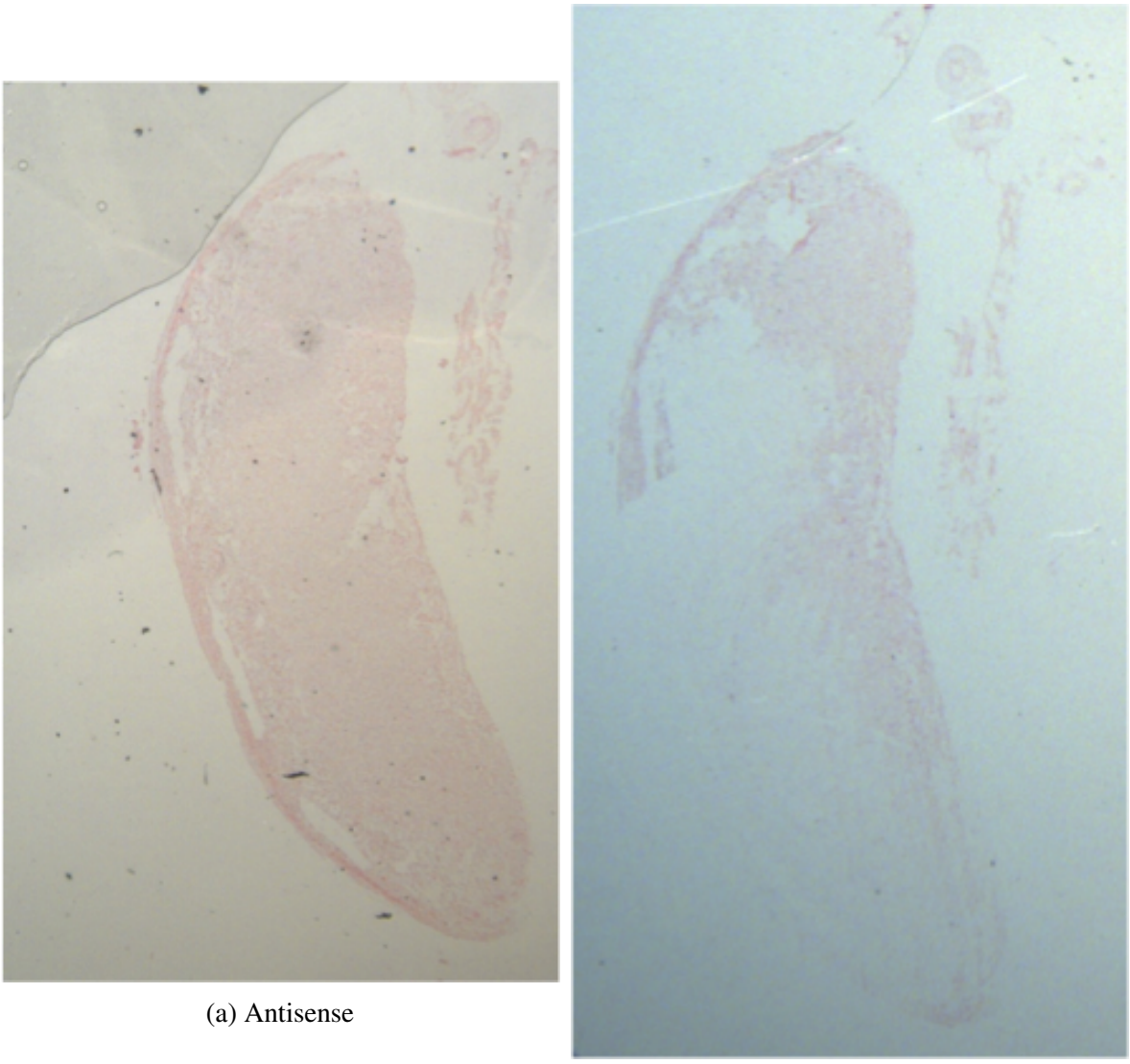

(a) Antisense

(b) Sense

Fig. A.21 **Antisense and sense *Dlk2* ISH on e18.5 wild-type placentae (N=3)**

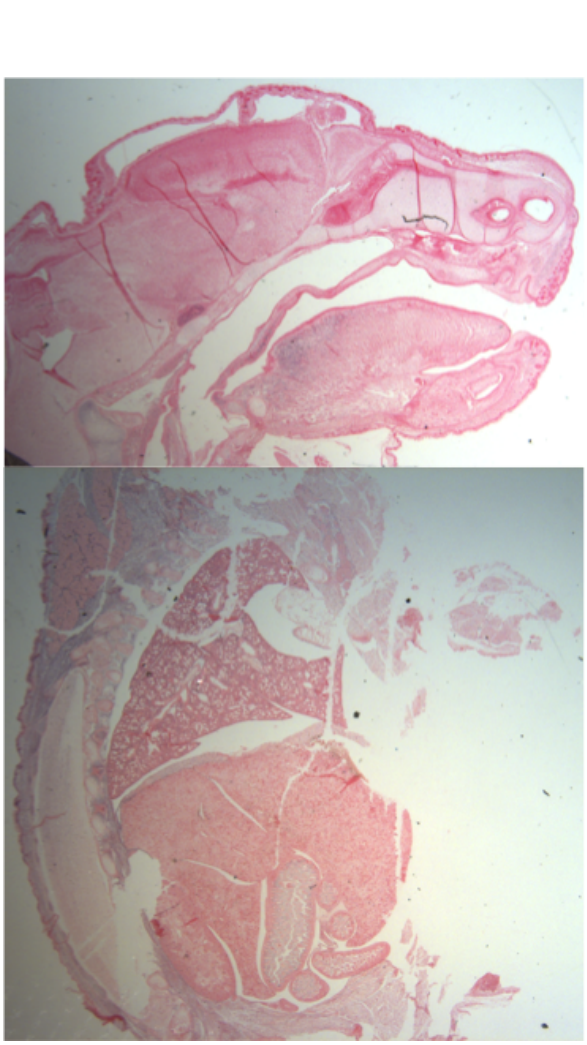

(a) Antisense

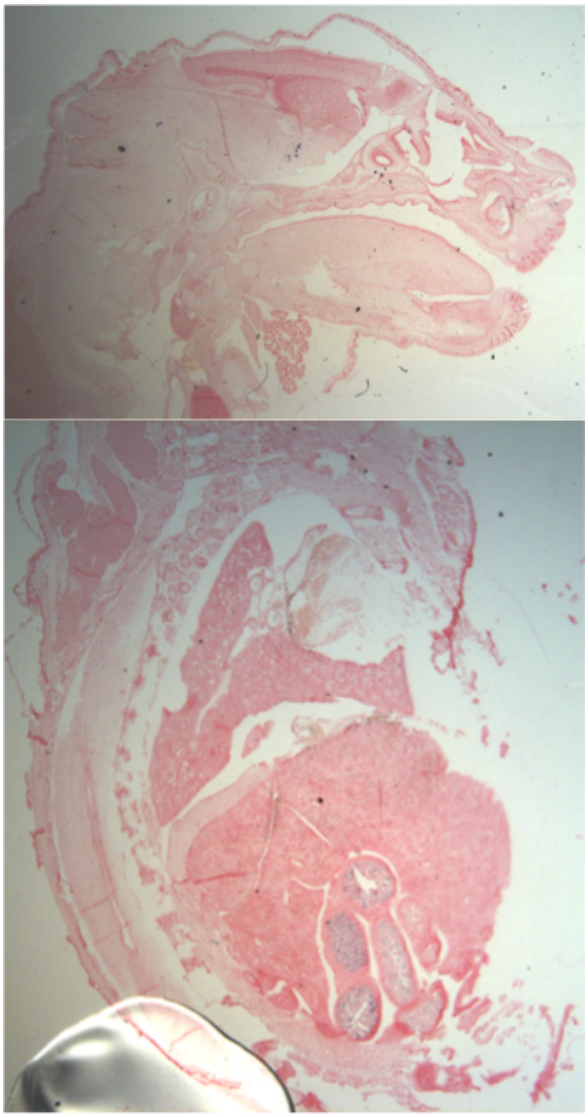

(b) Sense

Fig. A.22 **Antisense and sense *Dlk1* ISH on e18.5 wild-type embryos (N=2)**

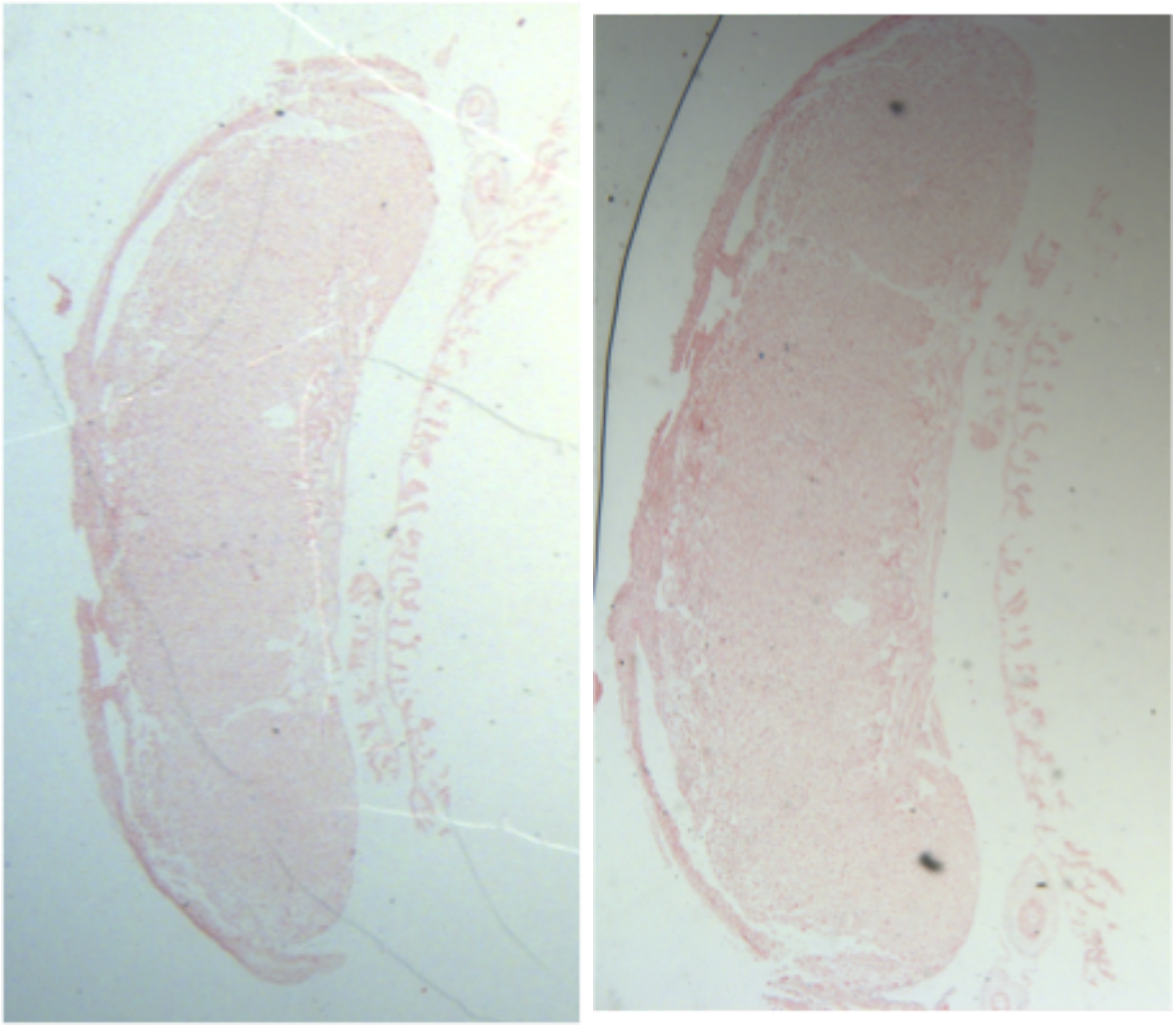

(a) Antisense

(b) Sense

Fig. A.23 **Antisense and sense *Dlk1* ISH on e18.5 wild-type placentae (N=2)**

CTGCCTCTGTCCTGAGGGCTTCGCTGGACGCTTCTGCACCATCAACCTGGATGACT-
GTGCCAGCCGCCCATGCCAGAGAGGGGCCCGCTGCAGGGACCGTGTCCATGACTTTGACT-
GCCTGTGCCCCAGTGGCTATGGTGGTAAGACTTGTGAACTTGTCCTACCTGCTCCA-
GAGCCTGCCTCAGTGGGCACCCCACAAATGCCCACCTCAGCTGTAGTTGTACCTGC-
CACGGGGCCGGCCCCTCACAGTGCGGGGGCGGGCCTGCTAAGGATCTCAGTGAAG-
GAGGTGGTACGGAGGCAAGAGTCTGGGCTTGGTGAATCTAGCCTGGTTGCCCTGGTG-
GTGTTTGGGTCTCTCACTGCTGCGCTGGTCCTGGCCACGGTGCTGCTGACCCTGAGGGCATG-
GCGCCGAGGTATATGCCCCACTGGACCCTGCTGCTACCCAGCCCCACACTATGCCCCAGCTCG-
GCAGGATCAGGAGTGCCAGGTTAGCATGCTGCCAGCGGGGTTCCCTCTGTCCCCAGAC-
CTGCCCCCTGAGCCTGGTAAGACCACAGCGCTGTGA

DLK2 exon5 INDEL

ATGCCCAGCGGCTGCCGCTGCCTAAATCTCGTGTGCCTGCTGTGCATCCTGGGGGCAACCAGCCA
CTGCCAGAGCGGATGACTGCAGCTCCCACTGTGACCTGGCCCACGGCTGCTGCGCTC-
CTGACGGCTCCTGCAGGTGTGACCCAGGCTGGGAGGGGCTGCACTGTGAGCGCTGT-
GTGAGGATGCCTGGCTGCCAGCACGGTACCTGCCACCAGCCCTGGCAGTGCATCTGC-
CACAGTGGCTGGGCAGGAAAGTTCTGTGACAAAGATGAGCACATCTGTACCTCACAAT-
CACCCTGCCAGAATGGAGGCCAGTGTGTGTATGGGGGGGGGTGAGTACCACTGTGT-
GTGCCTGCCAGGCTTCCATGGACGTGGCTGTGAGCGCAAGGCTGGACCTTGTGAGCAGGCAGGG
CCGTGCCGGAATGGAGGGCAGTGCCAGGACAACCAGGGTTTTGCCCTCAACTTCA-
CATGCCGCTGCTTGGCAGGATTCATGGGTGCCCACTGTGAGGTCAATGTGGACGACT-
GTCTGATGCGGCCTTGCGCCAATGGTGCCACATGCATTGATGGCATAAACCGCTTTTC-
CTGCCTCTGTCCTGAGGGCTTCGCTGGACGCTTCTGCACCATCAACCTGGATGACT-
GTGCCAGCCGCCCATGCCAGAGAGGGGCCCGCTGCAGGGACCGTGTCCATGACTTTGACT-
GCCTGTGCCCCAGTGGCTATGGTGGTAAGACTTGTGAACTTGTCCTACCTGCTCCA-
GAGCCTGCCTCAGTGGGCACCCCACAAATGCCCACCTCAGCTGTAGTTGTACCTGC-
CACGGGGCCGGCCCCTCACAGTGCGGGGGCGGGCCTGCTAAGGATCTCAGTGAAG-
GAGGTGGTACGGAGGCAAGAGTCTGGGCTTGGTGAATCTAGCCTGGTTGCCCTGGTG-
GTGTTTGGGTCTCTCACTGCTGCGCTGGTCCTGGCCACGGTGCTGCTGACCCTGAGGGCATG-
GCGCCGAGGTATATGCCCCACTGGACCCTGCTGCTACCCAGCCCCACACTATGCCCCAGCTCG-
GCAGGATCAGGAGTGCCAGGTTAGCATGCTGCCAGCGGGGTTCCCTCTGTCCCCAGAC-
CTGCCCCCTGAGCCTGGTAAGACCACAGCGCTGTGA

DLK2 exon5 73bp del

ATGCCCAGCGGCTGCCGCTGCCTAAATCTCGTGTGCCTGCTGTGCATCCTGGGGGCAACCAGCCA
CTGCCAGAGCGGATGACTGCAGCTCCCACTGTGACCTGGCCCACGGCTGCTGCGCTC-

CTGACGGCTCCTGCAGGTGTGACCCAGGCTGGGAGGGGCTGCACTGTGAGCGCTGT-
GTGAGGATGCCTGGCTGCCAGCACGGTACCTGCCACCAGCCCTGGCAGTGCATCTGC-
CACAGTGGCTGGGCAGGAAAGTTCTGTGACAAAGATGAGCACATCTGTACCTCACAAT-
CACCCTGCCAGAATGGAGGCCAGTGTGTGGACCTTGTGAGCAGGCAGGCTTCCCGT-
GCCGGAATGGAGGGCAGTGCCAGGACAACCAGGGTTTTGCCCTCAACTTCACATGC-
CGCTGCTTGGCAGGATTCATGGGTGCCCACTGTGAGGTCAATGTGGACGACTGTCT-
GATGCGGCCTTGCGCCAATGGTGCCACATGCATTGATGGCATAAACCGCTTTTCCTGC-
CTCTGTCCTGAGGGCTTCGCTGGACGCTTCTGCACCATCAACCTGGATGACTGTGCCAGC-
CGCCCATGCCAGAGAGGGGCCCGCTGCAGGGACCGTGTCCATGACTTTGACTGCCT-
GTGCCCCAGTGGCTATGGTGGTAAGACTTGTGAACTTGTCCTACCTGCTCCAGAGC-
CTGCCTCAGTGGGCACCCCACAAATGCCCACCTCAGCTGTAGTTGTACCTGCCACGGGGC-
CGGCCCCTCACAGTGCGGGGGCGGGCCTGCTAAGGATCTCAGTGAAGGAGGTGGTACG-
GAGGCAAGAGTCTGGGCTTGGTGAATCTAGCCTGGTTGCCCTGGTGGTGTTTGGGTCTCT-
CACTGCTGCGCTGGTCCTGGCCACGGTGCTGCTGACCCTGAGGGCATGGCGCCGAG-
GTATATGCCCCACTGGACCCTGCTGCTACCCAGCCCCACACTATGCCCCAGCTCGGCAGGATCAGGA
GCCAGGTTAGCATGCTGCCAGCGGGGTTCCCTCTGTCCCCAGACCTGCCCCCTGAGC-
CTGGTAAGACCACAGCGCTGTGA

DLK2 exon5 12bp del

ATGCCCAGCGGCTGCCGCTGCCTAAATCTCGTGTGCCTGCTGTGCATCCTGGGGGCAACCAGCCAGC
CTGCCAGAGCGGATGACTGCAGCTCCCACTGTGACCTGGCCCACGGCTGCTGCGCTC-
CTGACGGCTCCTGCAGGTGTGACCCAGGCTGGGAGGGGCTGCACTGTGAGCGCTGT-
GTGAGGATGCCTGGCTGCCAGCACGGTACCTGCCACCAGCCCTGGCAGTGCATCTGC-
CACAGTGGCTGGGCAGGAAAGTTCTGTGACAAAGATGAGCACATCTGTACCTCACAAT-
CACCCTGCCAGAATGGAGGCCAGTGTGTGTATGAGTACCACTGTGTGTGCCTGCCAGGCTTC-
CATGGACGTGGCTGTGAGCGCAAGGCTGGACCTTGTGAGCAGGCAGGCTTCCCGT-
GCCGGAATGGAGGGCAGTGCCAGGACAACCAGGGTTTTGCCCTCAACTTCACATGC-
CGCTGCTTGGCAGGATTCATGGGTGCCCACTGTGAGGTCAATGTGGACGACTGTCT-
GATGCGGCCTTGCGCCAATGGTGCCACATGCATTGATGGCATAAACCGCTTTTCCTGC-
CTCTGTCCTGAGGGCTTCGCTGGACGCTTCTGCACCATCAACCTGGATGACTGTGCCAGC-
CGCCCATGCCAGAGAGGGGCCCGCTGCAGGGACCGTGTCCATGACTTTGACTGCCT-
GTGCCCCAGTGGCTATGGTGGTAAGACTTGTGAACTTGTCCTACCTGCTCCAGAGC-
CTGCCTCAGTGGGCACCCCACAAATGCCCACCTCAGCTGTAGTTGTACCTGCCACGGGGC-
CGGCCCCTCACAGTGCGGGGGCGGGCCTGCTAAGGATCTCAGTGAAGGAGGTGGTACG-
GAGGCAAGAGTCTGGGCTTGGTGAATCTAGCCTGGTTGCCCTGGTGGTGTTTGGGTCTCT-
CACTGCTGCGCTGGTCCTGGCCACGGTGCTGCTGACCCTGAGGGCATGGCGCCGAG-

GTATATGCCCCACTGGACCCTGCTGCTACCCAGCCCCACACTATGCCCCAGCTCGGCAGGATCAGC
GCCAGGTTAGCATGCTGCCAGCGGGGTTCCCTCTGTCCCCAGACCTGCCCCCTGAGC-
CTGGTAAGACCACAGCGCTGTGA

DLK2 exon5 84bp del

ATGCCCAGCGGCTGCCGCTGCCTAAATCTCGTGTGCCTGCTGTGCATCCTGGGGGCAACCAGCCA
CTGCCAGAGCGGATGACTGCAGCTCCCACTGTGACCTGGCCCACGGCTGCTGCGCTC-
CTGACGGCTCCTGCAGGTGTGACCCAGGCTGGGAGGGGCTGCACTGTGAGCGCTGT-
GTGAGGATGCCTGGCTGCCAGCACGGTACCTGCCACCAGCCCTGGCAGTGCATCTGC-
CACAGTGGCTGGGCAGGAAAGTTCTGTGACAAAGATGAGCACATCTGTACCTCACAAT-
CACCCTGCCAGAATGGAGGCCAGTGTGTGTAGGCAGGCTTCCCGTGCCGGAATGGAGGGCAGT-
GCCAGGACAACCAGGGTTTTGCCCTCAACTTCACATGCCGCTGCTTGGCAGGATTCATGGGT-
GCCCACTGTGAGGTCAATGTGGACGACTGTCTGATGCGGCCTTGCGCCAATGGTGC-
CACATGCATTGATGGCATAAACCGCTTTTCCTGCCTCTGTCCTGAGGGCTTCGCTGGACGCTTCT-
GCACCATCAACCTGGATGACTGTGCCAGCCGCCCATGCCAGAGAGGGGCCCGCTGCAGGGAC-
CGTGTCCATGACTTTGACTGCCTGTGCCCCAGTGGCTATGGTGGTAAGACTTGTGAACTTGTC-
CTACCTGCTCCAGAGCCTGCCTCAGTGGGCACCCCACAAATGCCCACCTCAGCTGTAGTTG-
TACCTGCCACGGGGCCGGCCCCTCACAGTGCGGGGGCGGGCCTGCTAAGGATCTCAGT-
GAAGGAGGTGGTACGGAGGCAAGAGTCTGGGCTTGGTGAATCTAGCCTGGTTGCC-
CTGGTGGTGTTTGGGTCTCTCACTGCTGCGCTGGTCCTGGCCACGGTGCTGCTGAC-
CCTGAGGGCATGGCGCCGAGGTATATGCCCCACTGGACCCTGCTGCTACCCAGCCC-
CACACTATGCCCCAGCTCGGCAGGATCAGGAGTGCCAGGTTAGCATGCTGCCAGCGGGGTTC-
CCTCTGTCCCCAGACCTGCCCCCTGAGCCTGGTAAGACCACAGCGCTGTGA

DLK2 exon3 1G INS

ATGCCCAGCGGCTGCCGCTGCCTAAATCTCGTGTGCCTGCTGTGCATCCTGGGGGCAACCAGCCA
CTGCCAGAGCGGATGACTGCAGCTCCCACTGTGACCTGGCCCACGGGCTGCTGCGCTC-
CTGACGGCTCCTGCAGGTGTGACCCAGGCTGGGAGGGGCTGCACTGTGAGCGCTGT-
GTGAGGATGCCTGGCTGCCAGCACGGTACCTGCCACCAGCCCTGGCAGTGCATCTGC-
CACAGTGGCTGGGCAGGAAAGTTCTGTGACAAAGATGAGCACATCTGTACCTCACAAT-
CACCCTGCCAGAATGGAGGCCAGTGTGTGTATGACGGGGGTGGTGAGTACCACTGT-
GTGTGCCTGCCAGGCTTCCATGGACGTGGCTGTGAGCGCAAGGCTGGACCTTGTGAGCAGGCAG
CCGTGCCGGAATGGAGGGCAGTGCCAGGACAACCAGGGTTTTGCCCTCAACTTCA-
CATGCCGCTGCTTGGCAGGATTCATGGGTGCCCACTGTGAGGTCAATGTGGACGACT-
GTCTGATGCGGCCTTGCGCCAATGGTGCCACATGCATTGATGGCATAAACCGCTTTTC-
CTGCCTCTGTCCTGAGGGCTTCGCTGGACGCTTCTGCACCATCAACCTGGATGACT-

GTGCCAGCCGCCCATGCCAGAGAGGGGCCCGCTGCAGGGACCGTGTCCATGACTTTGACT-
GCCTGTGCCCCAGTGGCTATGGTGGTAAGACTTGTGAACTTGTCCTACCTGCTCCA-
GAGCCTGCCTCAGTGGGCACCCCACAAATGCCCACCTCAGCTGTAGTTGTACCTGC-
CACGGGGCCGGCCCCTCACAGTGCGGGGGCGGGCCTGCTAAGGATCTCAGTGAAG-
GAGGTGGTACGGAGGCAAGAGTCTGGGCTTGGTGAATCTAGCCTGGTTGCCCTGGTG-
GTGTTTGGGTCTCTCACTGCTGCGCTGGTCCTGGCCACGGTGCTGCTGACCCTGAGGGCATG-
GCGCCGAGGTATATGCCCCACTGGACCCTGCTGCTACCCAGCCCCACACTATGCCCCAGCTCG-
GCAGGATCAGGAGTGCCAGGTTAGCATGCTGCCAGCGGGGTTCCCTCTGTCCCCAGAC-
CTGCCCCCTGAGCCTGGTAAGACCACAGCGCTGTGA

DLK2 exon3 2G INS

ATGCCCAGCGGCTGCCGCTGCCTAAATCTCGTGTGCCTGCTGTGCATCCTGGGGGCAACCAGCCAGC
CTGCCAGAGCGGATGACTGCAGCTCCCACTGTGACCTGGCCCACGGGGCTGCTGCGCTC-
CTGACGGCTCCTGCAGGTGTGACCCAGGCTGGGAGGGGCTGCACTGTGAGCGCTGT-
GTGAGGATGCCTGGCTGCCAGCACGGTACCTGCCACCAGCCCTGGCAGTGCATCTGC-
CACAGTGGCTGGGCAGGAAAGTTCTGTGACAAAGATGAGCACATCTGTACCTCACAAT-
CACCCTGCCAGAATGGAGGCCAGTGTGTGTATGACGGGGGTGGTGAGTACCACTGT-
GTGTGCCTGCCAGGCTTCCATGGACGTGGCTGTGAGCGCAAGGCTGGACCTTGTGAGCAGGCAGGC
CCGTGCCGGAATGGAGGGCAGTGCCAGGACAACCAGGGTTTTGCCCTCAACTTCA-
CATGCCGCTGCTTGGCAGGATTCATGGGTGCCCACTGTGAGGTCAATGTGGACGACT-
GTCTGATGCGGCCTTGCGCCAATGGTGCCACATGCATTGATGGCATAAACCGCTTTTC-
CTGCCTCTGTCCTGAGGGCTTCGCTGGACGCTTCTGCACCATCAACCTGGATGACT-
GTGCCAGCCGCCCATGCCAGAGAGGGGCCCGCTGCAGGGACCGTGTCCATGACTTTGACT-
GCCTGTGCCCCAGTGGCTATGGTGGTAAGACTTGTGAACTTGTCCTACCTGCTCCA-
GAGCCTGCCTCAGTGGGCACCCCACAAATGCCCACCTCAGCTGTAGTTGTACCTGC-
CACGGGGCCGGCCCCTCACAGTGCGGGGGCGGGCCTGCTAAGGATCTCAGTGAAG-
GAGGTGGTACGGAGGCAAGAGTCTGGGCTTGGTGAATCTAGCCTGGTTGCCCTGGTG-
GTGTTTGGGTCTCTCACTGCTGCGCTGGTCCTGGCCACGGTGCTGCTGACCCTGAGGGCATG-
GCGCCGAGGTATATGCCCCACTGGACCCTGCTGCTACCCAGCCCCACACTATGCCCCAGCTCG-
GCAGGATCAGGAGTGCCAGGTTAGCATGCTGCCAGCGGGGTTCCCTCTGTCCCCAGAC-
CTGCCCCCTGAGCCTGGTAAGACCACAGCGCTGTGA

DLK2 exon3 16bp del

ATGCCCAGCGGCTGCCGCTGCCTAAATCTCGTGTGCCTGCTGTGCATCCTGGGGGCAACCAGCCAGC
CTGCCAGAGCGGATGACTGCAGCTCCCACTGTGACCTGGCCCTGACGGCTCCTGCAGGT-
GTGACCCAGGCTGGGAGGGGCTGCACTGTGAGCGCTGTGTGAGGATGCCTGGCTGCCAGCACG-

GTACCTGCCACCAGCCCTGGCAGTGCATCTGCCACAGTGGCTGGGCAGGAAAGTTCT-
GTGACAAAGATGAGCACATCTGTACCTCACAATCACCCTGCCAGAATGGAGGCCAGT-
GTGTGTATGACGGGGGTGGTGAGTACCACTGTGTGTGCCTGCCAGGCTTCCATGGACGTG-
GCTGTGAGCGCAAGGCTGGACCTTGTGAGCAGGCAGGCTTCCCGTGCCGGAATGGAGGGCAGT-
GCCAGGACAACCAGGGTTTTGCCCTCAACTTCACATGCCGCTGCTTGGCAGGATTCATGGGT-
GCCCACTGTGAGGTCAATGTGGACGACTGTCTGATGCGGCCTTGCGCCAATGGTGC-
CACATGCATTGATGGCATAAACCGCTTTTCCTGCCTCTGTCCTGAGGGCTTCGCTGGACGCTTCT-
GCACCATCAACCTGGATGACTGTGCCAGCCGCCCATGCCAGAGAGGGGCCCGCTGCAGGGAC-
CGTGTCCATGACTTTGACTGCCTGTGCCCCAGTGGCTATGGTGGTAAGACTTGTGAACTTGTC-
CTACCTGCTCCAGAGCCTGCCTCAGTGGGCACCCCACAAATGCCCACCTCAGCTGTAGTTG-
TACCTGCCACGGGGCCGGCCCCTCACAGTGCGGGGGCGGGCCTGCTAAGGATCTCAGT-
GAAGGAGGTGGTACGGAGGCAAGAGTCTGGGCTTGGTGAATCTAGCCTGGTTGCC-
CTGGTGGTGTTTGGGTCTCTCACTGCTGCGCTGGTCCTGGCCACGGTGCTGCTGAC-
CCTGAGGGCATGGCGCCGAGGTATATGCCCCACTGGACCCTGCTGCTACCCAGCCC-
CACACTATGCCCCAGCTCGGCAGGATCAGGAGTGCCAGGTTAGCATGCTGCCAGCGGGGTTC-
CCTCTGTCCCCAGACCTGCCCCCTGAGCCTGGTAAGACCACAGCGCTGTGA

DLK2 exon3 1C INS

ATGCCCAGCGGCTGCCGCTGCCTAAATCTCGTGTGCCTGCTGTGCATCCTGGGGGCAACCAGCCA
CTGCCAGAGCGGATGACTGCAGCTCCCACTGTGACCTGGCCCACGCGCTGCTGCGCTC-
CTGACGGCTCCTGCAGGTGTGACCCAGGCTGGGAGGGGCTGCACTGTGAGCGCTGT-
GTGAGGATGCCTGGCTGCCAGCACGGTACCTGCCACCAGCCCTGGCAGTGCATCTGC-
CACAGTGGCTGGGCAGGAAAGTTCTGTGACAAAGATGAGCACATCTGTACCTCACAAT-
CACCCTGCCAGAATGGAGGCCAGTGTGTGTATGACGGGGGTGGTGAGTACCACTGT-
GTGTGCCTGCCAGGCTTCCATGGACGTGGCTGTGAGCGCAAGGCTGGACCTTGTGAGCAGGCAG
CCGTGCCGGAATGGAGGGCAGTGCCAGGACAACCAGGGTTTTGCCCTCAACTTCA-
CATGCCGCTGCTTGGCAGGATTCATGGGTGCCCACTGTGAGGTCAATGTGGACGACT-
GTCTGATGCGGCCTTGCGCCAATGGTGCCACATGCATTGATGGCATAAACCGCTTTTC-
CTGCCTCTGTCCTGAGGGCTTCGCTGGACGCTTCTGCACCATCAACCTGGATGACT-
GTGCCAGCCGCCCATGCCAGAGAGGGGCCCGCTGCAGGGACCGTGTCCATGACTTTGACT-
GCCTGTGCCCCAGTGGCTATGGTGGTAAGACTTGTGAACTTGTCCTACCTGCTCCA-
GAGCCTGCCTCAGTGGGCACCCCACAAATGCCCACCTCAGCTGTAGTTGTACCTGC-
CACGGGGCCGGCCCCTCACAGTGCGGGGGCGGGCCTGCTAAGGATCTCAGTGAAG-
GAGGTGGTACGGAGGCAAGAGTCTGGGCTTGGTGAATCTAGCCTGGTTGCCCTGGTG-
GTGTTTGGGTCTCTCACTGCTGCGCTGGTCCTGGCCACGGTGCTGCTGACCCTGAGGGCATG-
GCGCCGAGGTATATGCCCCACTGGACCCTGCTGCTACCCAGCCCCACACTATGCCCCAGCTCG-

GCAGGATCAGGAGTGCCAGGTTAGCATGCTGCCAGCGGGGTTCCCTCTGTCCCCAGAC-
CTGCCCCCTGAGCCTGGTAAGACCACAGCGCTGTGA

DLK2 exon2 INDEL

ATGCCCAGCGGCTGCCtaatttcagtgtggTCCTGGGGGCAACCAGCCAGCCTGCCAGAGCG-
GATGACTGCAGCTCCCACTGTGACCTGGCCCACGGCTGCTGCGCTCCTGACGGCTC-
CTGCAGGTGTGACCCAGGCTGGGAGGGGCTGCACTGTGAGCGCTGTGTGAGGATGC-
CTGGCTGCCAGCACGGTACCTGCCACCAGCCCTGGCAGTGCATCTGCCACAGTGGCTGGGCAGGAA
GTGACAAAGATGAGCACATCTGTACCTCACAATCACCCTGCCAGAATGGAGGCCAGT-
GTGTGTATGACGGGGGTGGTGAGTACCACTGTGTGTGCCTGCCAGGCTTCCATGGACGTG-
GCTGTGAGCGCAAGGCTGGACCTTGTGAGCAGGCAGGCTTCCCGTGCCGGAATGGAGGGCAGT-
GCCAGGACAACCAGGGTTTTGCCCTCAACTTCACATGCCGCTGCTTGGCAGGATTCATGGGT-
GCCCACTGTGAGGTCAATGTGGACGACTGTCTGATGCGGCCTTGCGCCAATGGTGC-
CACATGCATTGATGGCATAAACCGCTTTTCCTGCCTCTGTCCTGAGGGCTTCGCTGGACGCTTCT-
GCACCATCAACCTGGATGACTGTGCCAGCCGCCCATGCCAGAGAGGGGCCCGCTGCAGGGAC-
CGTGTCCATGACTTTGACTGCCTGTGCCCCAGTGGCTATGGTGGTAAGACTTGTGAACTTGTC-
CTACCTGCTCCAGAGCCTGCCTCAGTGGGCACCCCACAAATGCCCACCTCAGCTGTAGTTG-
TACCTGCCACGGGGCCGGCCCCTCACAGTGCGGGGGCGGGCCTGCTAAGGATCTCAGT-
GAAGGAGGTGGTACGGAGGCAAGAGTCTGGGCTTGGTGAATCTAGCCTGGTTGCC-
CTGGTGGTGTTTGGGTCTCTCACTGCTGCGCTGGTCCTGGCCACGGTGCTGCTGAC-
CCTGAGGGCATGGCGCCGAGGTATATGCCCCACTGGACCCTGCTGCTACCCAGCCC-
CACACTATGCCCCAGCTCGGCAGGATCAGGAGTGCCAGGTTAGCATGCTGCCAGCGGGGTTC-
CCTCTGTCCCCAGACCTGCCCCCTGAGCCTGGTAAGACCACAGCGCTGTGA

DLK2 exon2 70bp del

ATGCCCAGCGGCTGCCCCCAGGGATTGGGTCCCGGCTCTCCTCAGCCGTCCTCGCTG-
GCACGTTGACCTCTGCTGGCTAGAGACGGCACTGCAACCGCTCCGTTCCATAGGGA-
GAGATCTATAAGTGCTCTCTTTGGAATGGGACGCTCGTCCGTGCCCATGAGTCCATCT-
GACTACTGAAACCTCTGCCAAGTCCCGCGCCTGGGAAGTCAGACTCGGACCCAGACT-
CACACCCACTACACCAATCTCTTTCAGCGGATGACTGCAGCTCCCACTGTGACCTG-
GCCCACGGCTGCTGCGCTCCTGACGGCTCCTGCAGGTGTGACCCAGGCTGGGAGGGGCT-
GCACTGTGAGCGCTGTGTGAGGATGCCTGGCTGCCAGCACGGTACCTGCCACCAGC-
CCTGGCAGTGCATCTGCCACAGTGGCTGGGCAGGAAAGTTCTGTGACAAAGATGAG-
CACATCTGTACCTCACAATCACCCTGCCAGAATGGAGGCCAGTGTGTGTATGACGGGGGTG-
GTGAGTACCACTGTGTGTGCCTGCCAGGCTTCCATGGACGTGGCTGTGAGCGCAAG-
GCTGGACCTTGTGAGCAGGCAGGCTTCCCGTGCCGGAATGGAGGGCAGTGCCAGGA-

CAACCAGGGTTTTGCCCTCAACTTCACATGCCGCTGCTTGGCAGGATTCATGGGTGC-
CCACTGTGAGGTCAATGTGGACGACTGTCTGATGCGGCCTTGCGCCAATGGTGCCA-
CATGCATTGATGGCATAAACCGCTTTTCCTGCCTCTGTCCTGAGGGCTTCGCTGGACGCTTCT-
GCACCATCAACCTGGATGACTGTGCCAGCCGCCCATGCCAGAGAGGGGCCCGCTGCAGGGAC-
CGTGTCCATGACTTTGACTGCCTGTGCCCCAGTGGCTATGGTGGTAAGACTTGTGAACTTGTC-
CTACCTGCTCCAGAGCCTGCCTCAGTGGGCACCCCACAAATGCCCACCTCAGCTGTAGTTG-
TACCTGCCACGGGGCCGGCCCCTCACAGTGCGGGGGCGGGCCTGCTAAGGATCTCAGT-
GAAGGAGGTGGTACGGAGGCAAGAGTCTGGGCTTGGTGAATCTAGCCTGGTTGCC-
CTGGTGGTGTTTGGGTCTCTCACTGCTGCGCTGGTCCTGGCCACGGTGCTGCTGAC-
CCTGAGGGCATGGCGCCGAGGTATATGCCCCACTGGACCCTGCTGCTACCCAGCCC-
CACACTATGCCCCAGCTCGGCAGGATCAGGAGTGCCAGGTTAGCATGCTGCCAGCGGGGTTC-
CCTCTGTCCCCAGACCTGCCCCCTGAGCCTGGTAAGACCACAGCGCTGTGA

A.4 Protein sequences of CRISPR generated *Dlk2* mutants

DLK2 exon5 13bp del

MPSGCRCLNLVCLLCILGATSQPARADDCSSHCDLAHGCCAPDGSCRCDPGWEGLHCER-
CVRMPGCQHGTCHQPWQCICHSGWAGKFCDKDEHICTSQSPCQNGGQGVVSTTVCAC-
QASMDVAVSARLDLVSRQASRAGMEGSARTTRVLPSTSHAAAWQDSWVPTVRSMWTTV

DLK2 exon5 2bp del

MPSGCRCLNLVCLLCILGATSQPARADDCSSHCDLAHGCCAPDGSCRCDPGWEGLHCER-
CVRMPGCQHGTCHQPWQCICHSGWAGKFCDKDEHICTSQSPCQNGGQCVYGGW

DLK2 exon5 INDEL

MPSGCRCLNLVCLLCILGATSQPARADDCSSHCDLAHGCCAPDGSCRCDPGWEGLHCER-
CVRMPGCQHGTCHQPWQCICHSGWAGKFCDKDEHICTSQSPCQNGGQCVYGGG

DLK2 exon5 73bp del

MPSGCRCLNLVCLLCILGATSQPARADDCSSHCDLAHGCCAPDGSCRCDPGWEGLHCER-
CVRMPGCQHGTCHQPWQCICHSGWAGKFCDKDEHICTSQSPCQNGGQCVDLVSRQAS-
RAGMEGSARTTRVLPSTSHAAAWQDSWVPTVRSMWTTV

DLK2 exon5 12bp del

MPSGCRCLNLVCLLCILGATSQPARADDCSSHCDLAHGCCAPDGSCRCDPGWEGLHCER-
CVRMPGCQHGTCHQPWQCICHSGWAGKFCDKDEHICTSQSPCQNGGQCVYEYHCV-
CLPGFHGRGCERKAGPCEQAGFPCRNGGQCQDNQGFALNFTCRCLAGFMGAHCEVN-
VDDCLMRPCANGATCIDGINRFSCLCPEGFAGRFCTINLDDCASRPCQRGARCRDRVHDFD-
CLCPSGYGGKTCELVLPAPEPASVGTPQMPTSAVVVPATGPAPHSAGAGLLRISVKEVVR-
RQESGLGESSLVALVVFGSLTAALVLATVLLTLRAWRRGICPTGPCCYPAPHYAPARQDQEC-
QVSMLPAGFPLSPDLPPEPGKTTAL

DLK2 exon5 84bp del

MPSGCRCLNLVCLLCILGATSQPARADDCSSHCDLAHGCCAPDGSCRCDPGWEGLHCER-
CVRMPGCQHGTCHQPWQCICHSGWAGKFCDKDEHICTSQSPCQNGGQCV

DLK2 exon3 1G INS

MPSGCRCLNLVCLLCILGATSQPARADDCSSHCDLAHGLLRS

DLK2 exon3 2G INS

MPSGCRCLNLVCLLCILGATSQPARADDCSSHCDLAHGAAALLTAPAGVTQAGRGCTVSAV

DLK2 exon3 16bp del

MPSGCRCLNLVCLLCILGATSQPARADDCSSHCDLALTAPAGVTQAGRGCTVSAV

DLK2 exon3 1C INS

MPSGCRCLNLVCLLCILGATSQPARADDCSSHCDLAHALLRS

Dlk2 exon2 INDEL

MPSGCLISVWSWGQPASLPERMTAAPTVTWPTAAALLTAPAGVTQAGRGCTVSAV

DLK2 exon2 70bp del

MPSGCPQGLGPGSPQPSSLAR

A.5 Sample sizes used to assess postnatal weights of *Dlk2* mutant mice

Postnatal day	DK1G females	DK1G males	DK1C females	DK16 females	DK16 males	DK73 females	DK73 males	DK13 females	DK13 males
3								0H, 1W	4H, 2W
4				4H, 3W	1H, 1W				
5			4H, 1W	2H, 2W	2H, 2W				
7	2H, 1W	1H, 1W	4H, 2W	6H, 5W	3H, 3W	1H, 0W	1H, 2W	3H, 6W	3H, 4W
8	3H, 1W	1H, 1W		1H, 1W	2H, 2W	3H, 2W	3H, 4W	3H, 3W	6H, 4W
9								3H,2H	2H, 0W
14	5H, 2W	2H, 2W	4H, 2W	7H, 6W	5H, 5W	4H, 2W	4H, 6W	4H, 4W	6H, 4W
21	2H, 1W	1H, 1W		4H, 3W	1H, 1W	1H, 1W	3H, 4W	4H, 4W	4H, 3W
28	5H, 2W	2H, 2W		5H, 4W	3H, 3W	3H, 1W	1H, 2W	3H, 4W	4H, 1W
35	2H, 1W	1H, 1W		5H, 4W	3H, 3W		3H, 4W	6H, 6W	8H, 4W
42	2H, 1W	1H, 1W		4H, 3W	1H, 1W		2H, 2W	3H, 2W	4H, 3W
49	3H, 1W	1H, 1W					2H, 2W	3H, 2W	2H, 0W
56	3H, 1W	1H, 1W					2H, 2W		

Table A.1 **Sample sizes of each genotype (each time point) where postnatal weights were assessed in figure 6.5**

Blank cells — time point not assessed for that genotype or timepoint. Acronyms used: H — heterozygotes, W — wild-types

Postnatal day	DK1G females	DK1G males	DK1C females	DK1C males	DK73 females	DK73 males	DK13 females	DK13 males
3	2H, 2H, 0W	1Hm, 2H, 0W						0Hm, 2H, 1W
5							0Hm, 1H, 1W	0Hm, 1H, 0W
6					1Hm, 1H, 2W	1Hm, 1H, 0W		
7							0Hm, 1H, 1W	0Hm, 1H, 0W
9	2H, 2H, 0W	1Hm, 2H, 0W			1Hm, 1H, 2W	1Hm, 1H, 0W		0Hm, 2H, 1W
12	2H, 2H, 0W	1Hm, 2H, 0W	0Hm, 6H, 2W	1Hm, 0H, 1W	1Hm, 1H, 3W	4Hm, 4H, 1W		
15			0Hm, 6H, 2W	1Hm, 0H, 1W	1Hm, 1H, 3W	4Hm, 4H, 1W		0Hm, 2H, 1W
18	2H, 2H, 0W	1Hm, 2H, 0W	0Hm, 6H, 2W	1Hm, 0H, 1W	1Hm, 1H, 3W	4Hm, 4H, 1W		0Hm, 2H, 1W
21	2H, 2H, 0W	1Hm, 2H, 0W			1Hm, 1H, 1W	3Hm, 3H, 1W	0Hm, 1H, 1W	0Hm, 3H, 1W
24	2H, 2H, 0W	1Hm, 2H, 0W	0Hm, 6H, 3W	1Hm, 0H, 1W		1Hm, 2H, 1W		0Hm, 2H, 1W

Table A.2 (continued)

Postnatal day	DK1G females	DK1G males	DK1C females	DK1C males	DK73 females	DK73 males	DK13 females	DK13 males
27			0Hm, 6H, 3W	1Hm, 0H, 1W				
30			0Hm, 6H, 3W	1Hm, 0H, 1W	1Hm, 1H, 2W	1Hm, 1H, 0W	0Hm, 1H, 1W	0Hm, 3H, 1W
33					0Hm, 0H, 1W		2Hm, 1H, 0W	
36	2H, 2H, 0W	1Hm, 2H, 0W			1Hm, 1H, 2W		2Hm, 3H, 1W	0Hm, 1H, 1W
0Hm, 3H, 1W								
39			0Hm, 6H, 2W	1Hm, 0H, 1W	0Hm, 0H, 1W		2Hm, 1H, 1W	0Hm, 1H, 1W
0Hm, 1H, 0W								
42	2H, 2H, 0W	1Hm, 2H, 0W						
45			0Hm, 6H, 2W	1Hm, 0H, 1W				
48			0Hm, 6H, 3W	1Hm, 0H, 1W				

Table A.2 (continued)

Postnatal day	**DK1G females**	**DK1G males**	**DK1C females**	**DK1C males**	**DK73 females**	**DK73 males**	**DK13 females**	**DK13 males**
51			0Hm, 6H, 3W	1Hm, 0H, 1W			0Hm, 1H, 1W	0Hm, 1H, 0W
54			0Hm, 6H, 2W	1Hm, 0H, 1W				

Table A.2 **Sample sizes of each genotype (each time point) where postnatal weights were assessed in figure 6.6**

Blank cells — time point not assessed for that genotype or timepoint. Acronyms used: H — heterozygotes, Hm — homozygotes, W — wild-types

Postnatal day	DK73 N1 females	DK73 N1 males	DK73 N2 females	DK73 N2 males
3	0Hm, 3H, 0W	1Hm, 0H, 1W		
6	0Hm, 3H, 0W	1Hm, 0H, 2W	1Hm, 1H, 2W	1Hm, 1H, 0W
9	1Hm, 2H, 0W	1Hm, 3H, 3W	1Hm, 1H, 2W	1Hm, 1H, 0W
12			1Hm, 1H, 3W	4Hm, 4H, 1W
15	1Hm, 2H, 0W	1Hm, 3H, 1W	1Hm, 1H, 3W	4Hm, 4H, 1W
18	1Hm, 2H, 0W	1Hm, 3H, 1W	1Hm, 1H, 3W	4Hm, 4H, 1W
21	1Hm, 2H, 1W	1Hm, 1H, 3W	0Hm, 0H, 1W	3Hm, 3H, 1W
24	1Hm, 5H, 0W	1Hm, 3H, 3W		1Hm, 2H, 1W
27	1Hm, 2H, 1W	1Hm, 1H, 3W		
30	2Hm, 7H, 1W	2Hm, 4H, 6W	1Hm, 1H, 2W	1Hm, 1H, 0W
33	1Hm, 5H, 1W	1Hm, 1H, 5W	0Hm, 0H, 1W	2Hm, 1H, 0W
36	2Hm, 4H, 1W	2Hm, 4H, 4W	1Hm, 1H, 2W	2Hm, 3H, 1W
39	0Hm, 3H, 0W	0Hm, 0H, 2W	0Hm, 0H, 1W	2Hm, 1H, 1W
42	1Hm, 2H, 0W	1Hm, 3H, 1W		

Table A.3 **Sample sizes of each genotype (each time point) where postnatal weights were assessed in figure 6.7**

Blank cells — time point not assessed for that genotype or timepoint. Acronyms used: H — heterozygotes, Hm — homozygotes, W — wild-types